

AD/A-006 558

MODELING OF THE DESTRUCTIVE EFFECT OF  
EXPLOSIONS IN ROCKS

V. M. Komir, et al

Foreign Technology Division  
Wright-Patterson Air Force Base, Ohio

19 December 1974

DISTRIBUTED BY:

**NTIS**

**National Technical Information Service  
U. S. DEPARTMENT OF COMMERCE**

DOCUMENT CONTROL DATA - R & D

(Security classification of title, body of abstract and indexing annotation must be entered when the overall report is classified)

1. ORIGINATING ACTIVITY (Corporate author) Foreign Technology Division Air Force Systems Command U. S. Air Force	2a. REPORT SECURITY CLASSIFICATION Unclassified
	2b. GROUP

3. REPORT TITLE  
MODELING OF THE DESTRUCTIVE EFFECT OF EXPLOSIONS IN ROCKS

4. DESCRIPTIVE NOTES (Type of report and inclusive dates)  
Translation

5. AUTHOR (First name, middle initial, last name)  
V. M. Komir, L. M. Gevman, et. al.

6. REPORT DATE 1972	7a. TOTAL NO. OF PAGES 297	7b. NO. OF REFS 208
------------------------	-------------------------------	------------------------

8a. CONTRACT OR GRANT NO.  b. PROJECT NO  c.  d.	9a. ORIGINATOR'S REPORT NUMBER(S) FTD-HC-23-1564-74
	9b. OTHER REPORT NO(S) (Any other numbers that may be assigned this report)

10. DISTRIBUTION STATEMENT  
Approved for public release;  
distribution unlimited.

11. SUPPLEMENTARY NOTES	12. SPONSORING MILITARY ACTIVITY Foreign Technology Division Wright-Patterson AFB Ohio
-------------------------	--

13. ABSTRACT  
19, 08

Reproduced by  
NATIONAL TECHNICAL  
INFORMATION SERVICE  
US Department of Commerce  
Springfield, VA. 22151

PRICES SUBJECT TO CHANGE

## EDITED TRANSLATION

FTD-HC-23-1564-74

19 December 1974

MODELING OF THE DESTRUCTIVE EFFECT OF EXPLOSIONS  
IN ROCKS

By: V. M. Komir, L. M. Gevman, et.al.

English pages: 292

Source: Modelirovaniye Razrushayushchego Deystviya  
Vzryva v Gornyykh Porodakh, 1972, pp 1-213

Country of Origin: USSR

Translated under: F33657-72-D-0854

Requester: PDTM

Approved for public release;  
distribution unlimited.

THIS TRANSLATION IS A RENDITION OF THE ORIGINAL FOREIGN TEXT WITHOUT ANY ANALYTICAL OR EDITORIAL COMMENT. STATEMENTS OR THEORIES ADVOCATED OR IMPLIED ARE THOSE OF THE SOURCE AND DO NOT NECESSARILY REFLECT THE POSITION OR OPINION OF THE FOREIGN TECHNOLOGY DIVISION.

PREPARED BY:

TRANSLATION DIVISION  
FOREIGN TECHNOLOGY DIVISION  
WP-AFB, OHIO.

U. S. BOARD ON GEOGRAPHIC NAMES TRANSLITERATION SYSTEM

Block	Italic	Transliteration	Block	Italic	Transliteration
А а	<i>А а</i>	A, a	Р р	<i>Р р</i>	R, r
Б б	<i>Б б</i>	B, b	С с	<i>С с</i>	S, s
В в	<i>В в</i>	V, v	Т т	<i>Т т</i>	T, t
Г г	<i>Г г</i>	G, g	У у	<i>У у</i>	U, u
Д д	<i>Д д</i>	D, d	Ф ф	<i>Ф ф</i>	F, f
Е е	<i>Е е</i>	Ye, ye; E, e*	Х х	<i>Х х</i>	Kh, kh
Ж ж	<i>Ж ж</i>	Zh, zh	Ц ц	<i>Ц ц</i>	Ts, ts
З э	<i>З э</i>	Z, z	Ч ч	<i>Ч ч</i>	Ch, ch
И и	<i>И и</i>	I, i	Ш ш	<i>Ш ш</i>	Sh, sh
Й й	<i>Й й</i>	Y, y	Щ щ	<i>Щ щ</i>	Shch, shch
К к	<i>К к</i>	K, k	Ъ ъ	<i>Ъ ъ</i>	"
Л л	<i>Л л</i>	L, l	Ы ы	<i>Ы ы</i>	Y, y
М м	<i>М м</i>	M, m	Ь ь	<i>Ь ь</i>	'
Н н	<i>Н н</i>	N, n	Э э	<i>Э э</i>	E, e
О о	<i>О о</i>	O, o	Ю ю	<i>Ю ю</i>	Yu, yu
П п	<i>П п</i>	P, p	Я я	<i>Я я</i>	Ya, ya

\*ye initially, after vowels, and after ъ, ь; e elsewhere.  
 When written as *ë* in Russian, transliterate as *yë* or *ë*.  
 The use of diacritical marks is preferred, but such marks  
 may be omitted when expediency dictates.

\*\*\*\*\*

GRAPHICS DISCLAIMER

All figures, graphics, tables, equations, etc.  
 merged into this translation were extracted  
 from the best quality copy available.

## RUSSIAN AND ENGLISH TRIGONOMETRIC FUNCTIONS

Russian	English
sin	sin
cos	cos
tg	tan
ctg	cot
sec	sec
cosec	csc
sh	sinh
ch	cosh
th	tanh
cth	coth
sch	sech
csch	csch
arc sin	$\sin^{-1}$
arc cos	$\cos^{-1}$
arc tg	$\tan^{-1}$
arc ctg	$\cot^{-1}$
arc sec	$\sec^{-1}$
arc cosec	$\csc^{-1}$
arc sh	$\sinh^{-1}$
arc ch	$\cosh^{-1}$
arc th	$\tanh^{-1}$
arc cth	$\coth^{-1}$
arc sch	$\operatorname{sech}^{-1}$
arc csch	$\operatorname{csch}^{-1}$
—	
rot	curl
lg	log

## MODELING OF THE DESTRUCTIVE EFFECT OF EXPLOSIONS IN ROCKS

V.M. Komir, L.M. Gevman, V.S. Kravtsov, N.I. Myachina

### Foreword

At the basis of a fundamental scientific inquiry lies the process of reproducing in a logical manner on a small scale phenomena which are sometimes gigantic -- in other words, modeling. This process encompasses a huge amount of territory -- from the launching into space of a rocket to the mechanisms by which neurophysiological systems of the human organism operate. Modeling became a reliable instrument for investigating phenomena which were inaccessible by any other methods, and it became a highly simplified means for learning about the regularities in nature, a unique criterion for approving monumental engineering works and complex machines prior to realizing them in the form of concrete or metal, and an effective means of predicting the development of science and technology, and of establishing the general direction of scientific investigations.

The principle of modeling is not complicated -- it is the ability to reproduce effects which are similar to one another. The model may be an object possessing a different physical character than that of the object under study. In such a case it is mandatory that the requirement of identity of all relative quantitative characteristics be fulfilled. The sufficient criterion of similarity is the coincidence of dimensionless equations describing the object under study and its model.

The possibility of studying different sides of a phenomenon on the basis of its model is the expression of the philosophical principle of unity of the world. Even in phenomena which are in essence different there are general sides of the picture. In his work "Materialism and Empiriocriticism," V. I. Lenin makes this note: "The unity of nature is found in 'the striking similarity' of differential equations relating to different phenomenological areas."

---

<sup>1</sup> V. I. Lenin; Polnoye sobr. soch. (Complete Collected Works), Vol. 18, p. 306

Thus the mathematical generality of various phenomena predetermines the wide capabilities of modeling methods.

It is difficult to trace the origins of modeling, which apparently have been lost in the epoch of the building of the great pyramids and the first ships of antiquity. The history of modeling is more clearly traceable during the period under present review. Evidently the development of modeling may be divided into three stages: at first it was the attempt to build miniature prototypes of large scale production projects. Afterwards it was testing the reliability of monumental engineering works at the design state and, finally, modeling was formed into an independent scientific discipline, having a multi-faceted character.

It is known that knowledge about similarity began with I. Newton (1686 A.D.) and was developed by the French mathematician J. Bertran (1848 A.D.), who introduced the concept of the "Newton criterion." The English engineer W. Froud initiated a study of the sea-going qualities of ocean ships, and N. Ye. Zhukovskiy was the first to study the quality of airplanes with the help of models. M. V. Kirpichev and M. A. Mikheyev laid the foundations for thermal modeling. One of the first attempts at modeling in the sphere of mining is the works of M. Fayol, devoted to an investigation based on models of the phenomena of deformation and destruction of minerals in the process of mining. Creation of the scientific bases of modeling amplified a full circle of questions, which were solved by drawing upon data obtained from models.

At the present time a special value has been given to mathematical and physical modeling in the choice of rational systems for working beds of useful minerals, in the determination of optimum parameters for mineral-transport equipment, in the design of ventilation systems, in the construction of mining machines (electrical conductors, pneumatic, and hydraulic systems), etc. Application of the optical method of investigating the stressed state by models permitted one to solve many problems connected with the occurrence of pressure

in rocks, and this takes on an especially important significance with relation to increasing the depth of mineral works. The method of equivalent materials, proposed by Professor G. N. Kuznetsov, opened possibilities for studying by models the distribution of deformation and damage to rocks in the process of underground mining. The solution of problems related to mining was simplified through the use of centrifugal modeling, proposed by Professor G. I. Pokrovskiy. The method of centrifugal modeling was successfully utilized in the solution of a series of problems on the stability of banks and terraces in the construction of the Moscow canal and other corresponding construction projects where unique industrial explosions were carried out. This method is widely used in the investigation of the development of rock pressure.

Modeling of the disruptive action of explosions in the mountain mass, to which the present book is devoted, is relatively new and has yet been little studied. Direct study of industrial explosions is made difficult not only by the high pressures and temperatures, not only by the short time duration of the process, but also by the influence of subsidiary factors which are difficult to subject to detailed account. The modeling of an explosion permits one to limit the number of costly experiments in nature, maintain the identity of experimental conditions, and apply the results of laboratory experiments to natural objects.

An important side of the modeling of explosive action is its ponderable outcome in practice when embodied in complex mining construction problems. To the same class of problems belongs the production of effective and economical nuclear explosions for the moving of millions of tons of mountain rock in reckoned fractions of a second. In this connection it is fitting to mention the interesting publications of G. I. Pokrovskiy and A. A. Chernigovskiy pertaining to their investigation by modeling of the intensity of radioactive radiation as a function of the energy of a nuclear explosion, reported over ten years ago before the congress on world utilization of atomic energy. Unfortunately this direction in modeling, in spite of its

obvious future prospects, has not yet received the development it deserves. In the not too distant future the most appreciable results will be seen in the modeling of atomic explosions for opening rivers and building artificial channels and terraces. The enormous effect on the national economy may bring, in particular, the realization of the idea of an underground atomic explosion. In this case it is possible to construct dams owing to the intense seismic wave when the atomic charge is sufficiently removed due to the elimination of radioactive contamination of the body of the dam. No less practical is the wide application of massive directed explosions of ordinary explosive materials in hydraulic engineering construction. The large-scale scientific and engineering effect of the unique explosions for building the anti-erosion dam on the Malaya Alma Atinka River and the covering of the Terek and Vakhsh Rivers advances the problem of designing and realizing similar explosions in ever-increasing quantities as a candidate for the most important problems. An indispensable condition for realizing these projects must be the modeling of each explosion taking account of the concrete mineral engineering details.

It is inexcusable to bequeath to future generations overburden stripping by means of directed explosions of open-cut fields. The technological policy in effect today is that of constructing superdeep open mines whose annual yield is numbered in tens of millions of tons of useful minerals, and an ultimate depth of hundreds of meters may be still more economical and efficient, if the cutting of the trenches were realized with the aid of directed explosions. Substantiation of this was the successful driving of a slit trench in 1969 in the Dneprovsk GOK\* with the aid of an explosion. It deserves attention to note that interborehole retardation in the dispersed charges of the core were used in this experiment in order to control the movement of mountain rock on a front of about 100 meters.

---

\* mining and concentration kombinat.

The formulation of these and similar types of problems in design practice, taking account of the results of preliminary modeling experiments, will serve as a very clear example of the union of science and practice, as it frees considerable economic reserves in the mineral industry and it shortens the period for the introduction of new capacity.

In light of the above there has been a very sincere attempt on the part of the authors of the monograph here offered to analyze from a single point of view the diverse modeling methods which are in use in the investigation of the disruptive action of explosions in mineral rocks. In this book a thorough analysis has been carried out of the basic physical factors which determine the intensity of crushing of rock by an explosion and methods for determining the same are presented. The method proposed by the authors for accomplishing physical modeling of the wave phenomena in absorbing medium makes it possible to study under laboratory conditions the particulars of the propagation and damping of pressure pulses with differing characteristics and to establish the most effective prerequisites for obtaining a uniform crushing -- namely the creation of an optimum pressure field in the mass. A simple and original method is set forth in this book for evaluating the effectiveness of the method of controlling explosive energy when modeling on equivalent materials. (Up to recent times the method of equivalent materials was utilized only for studying the shape of the heap that was formed and the nature of the movement of rock mass.)

The wealth of factual material has made it possible to promote in this book a series of new ideas in the areas of study of the action of explosives on rock masses. Based on a statistical theory of crushing proposed by the authors new dimensionless criteria in the modeling of the disruptive action of explosions are worked out.

The ideas on modeling the action of explosions, concentrated in the monograph here offered to the reader, will serve as a stimulus toward

the search for new means in this most important methodological process and conceptual scheme for the phenomena of nature.

Academician N. V. Mel'nikov

## FROM THE AUTHORS

The modeling of processes occupies an evergrowing part of the task in scientific investigations, appearing in a number of cases as an indispensable link, its own kind of a general verification of a daring industrial experiment. It relates in full to a rapid acting process such as an explosion.

The monograph is devoted basically to a consideration of questions of modeling the explosive crushing of rock. A quantitative estimate in this area of explosive operations consists of billions of tons yearly of excavated rock broken up by explosions, and qualitatively it consists of the necessity of obtaining a uniform lumpiness on the bench of the mine, a fundamental prerequisite for utilizing a continuous technique in the extraction of hard excavated rock. In this work the basic principles of the process of breaking up mineral rocks by explosions are set forth, as well as the criteria for modeling this effect. Based on a statistical approach to the processes of explosive disintegration, dimensionless criteria are obtained which take account of the non-uniform structure of the materials.

The completion of this book was in considerable degree made possible by the advice, observations, and creative participation of academician N. V. Mel'nikov, and also Professors G. P. Demidyuk and G. I. Pokrovskiy, to whom we express our deepest gratitude.

## CHAPTER 1

### THE FUNDAMENTAL STATUS OF THE THEORY OF MODELING, SIMILARITY AND DIMENSIONALITY.

#### Modeling -- An Effective Method of Investigation

Modeling appeared at the dawn of civilization for the purpose of verifying technological solutions in the building of structures and the creation of mechanical devices. The necessity for modeling came as a result of lack of understanding of the behaviour of structures and devices in the process of their service and operation and of the absence of methods for calculating these. Until the theoretical bases of modeling were worked out, satisfactory results might be obtained only after drawn-out researches. In this connection even G. P. Galileo posed the question: "Why does a model in miniature perform perfectly, whereas a machine constructed in nature on the same model does not give the expected results?" Not a few cases are known where an incorrectly achieved model led to sad results in the construction of buildings and machines. The answer to Galileo's question took shape over the course of several centuries. I. Newton set the beginning to a scientific answer to this question, being the first to formulate the theorem of mechanical similarity in the book "The Mathematical Beginnings of Natural Philosophy," published in 1687. The working out of the scientific bases of modeling and the utilization of sound design methods made it possible to exclude erroneous solutions and deductions which had been obtained on the basis of investigations with models.

The first type of modeling which arose and which found application were various physical models in which the model and the object under study possess the same physical character. Physical modeling allows one to judge the behavior of an object on the basis of the results of studies on the models under the condition of their similarity. In this case the equations which describe the phenomena may be unknown or may be very difficult to solve. The model is constructed

in such a way that the equations describing the effect under study or the process with respect to the model and in nature might be known to be identical beforehand, i.e., the model should be a reduced copy of the object or should represent the same object, but should operate in other similar regimes. The foundation of physical modeling is the dimensionless theory which allows one to apply the results of an investigation of the model to the object.

The extension of the conception of processes and phenomena, and the use of the mathematical apparatus for describing them led to the development of mathematical modeling, which was based on the utilization of the identity of equations which describe the various physical effects. For instance, damped mechanical vibrations of a pendulum and the change in voltage and current in an electrical circuit containing capacitance, inductance, and resistance are described by the very same differential equations. The distribution of mechanical stresses in a medium and the distribution of electrical potential in a conductive solution, the heat flux and electrical current, gas permeability and hydrodynamic effects, the movement of air through mines, and the passage of current in corresponding electrical circuits -- here is far from a full list of pairs of phenomena; they are different in their physical nature and yet they are described by identical equations. The solution of these equations for one phenomenon may be employed in the study of another. To obtain the solution of the second equation it is necessary only to insert the corresponding variables and coefficients into the solution of the first.

The experimental investigation of one phenomenon may be replaced by the experimental study of another, and the results of the experiments may be extended to the second effect taking account of transition coefficients, the determination of which ordinarily does not cause any particular difficulties.

The development of mathematical modeling was the basis for the creation of electronic computing machines intended for the solution

of various equations. With the development of science and technology the necessity for modeling did not become superfluous. On the contrary, modeling is widely used as a method for scientific investigation, as a method which lightens the labors of human beings by rendering problems soluble which would not be solved using other methods.

According to the definition of academician L.I. Sednov (1965, page 64), "... modeling is a responsible scientific problem which has a general cognitive significance existing in principle, but it must be looked at only as a starting base for the main problem. The latter consists in the factual determination of the laws of nature, in finding the general properties and characteristics of various classes of phenomena, in the working out of experimental and theoretical methods for investigating and solving various problems, and finally in obtaining systematic materials, rules, and recommendations for solving concrete practical problems".

Notwithstanding the vigorous development of mathematical modeling, physical modeling has not lost its significance for the solution of the most difficult problems connected with the study of processes which depend on a great number of independent variables and which are described by complicated equations (for instance, in aerohydro-mechanics, hydraulic engineering construction, shipbuilding, airplane construction, mining, etc.).

In the historical plan one should point three most important steps in the development of modeling. The beginning of the first step is attributed to Isaac Newton with his formulation of the first theorem of mechanical similitude. Thereafter upon the course of a lengthy period of time the criteria of similitude of various mechanical systems and physical phenomena were established. It suffices to name the work of L. Euler who established the similitude criteria for ark constructions; J. Bertran who formulated the general properties of similar mechanical motions; V. L. Kirpichev (1874) who formulated the similitude conditions for elastic phenomena, and also

the works of other outstanding learned men. In the modeling of hydrodynamic effects a special position is occupied by the works of O. Reynolds, W. Froude and A. N. Krylov.

The second stage may be associated with the beginning of the twentieth century when the  $\Pi$ -theorem was formulated and proved; this is the fundamental theorem of the theory of similitude and dimensionality which describes the possibility of expressing physical laws in the form of dependencies between similitude criteria (dimensionless quantities) which characterize phenomena. In 1911 an instructor in the St. Petersburg Polytechnic Institute, A. O. Federam, published a work devoted to the proof of a theorem from which the  $\Pi$ -theorem follows as a result. Still earlier the  $\Pi$ -theorem was utilized in the works of the Kuchinsk Aerodynamic Institute, under the directorship of N. Ye. Zhukov. The proof of this theorem was published in works of the Kuchinsk Institute in 1912. Later a work by the American physicist E. Buckingham appeared (1914) which was devoted to this theorem. The second stage in the development of modeling is characterized by the general acceptance of this method of investigation into different branches of science. In fact not one branch of science and technology was left in which modeling would not be used for studying a variety of phenomena.

The third junction point in the history of modeling is the regular extension of the limits of a single experiment into a group of phenomena, an event which constitutes the content of the third theorem of similarity. The third theorem of similitude was formulated in 1931 by M. V. Kirpichev and A. A. Gukhman. A short statement of the third theorem of similitude may be set forth in the following way (Gukhman, 1963): "Similar phenomena are those which have the same conditions of single valueness and the same determining criteria". Determining criteria are formed from quantities which are independent of each other, which enter into the conditions of single valueness (geometrical relationships, physical parameters, marginal conditions: initial and boundary).

A special place in the history of modeling must be given to the creation of the first electronic model (the continuous action electronic computing machine). It would be difficult to overestimate the role of electronic analog machines in the enlargement of a circle of problems, which were being studied by the methods of mathematical modeling, through its adoption in various areas of science and technology. The groundwork of mathematical modeling was worked out by N. N. Pavlov (1922), who published his first work devoted to the theory of electrohydrodynamic analogs. In the work of S. A. Gershgorin (1925, 1929), L. I. Gutenmakher (1949), V. M. Glushkov (1964), and V. T. Kulik (1963), electronic modeling received further development, and on this basis analog computing machines were worked out.

Mathematical and physical modeling are widely employed in the investigation of explosive effects. Attention is given to questions of the modeling of the destructive effects in explosions in a series of works of noted scholars (Vlasov, 1962; Demidyuk, 1962; Mel'nikov 1964; Pokrovskiy, 1969). In modeling the various effects which take place in an explosion, various methods are employed. In the following chapters the basic methods of modeling phenomena which occur in an explosion will be considered. Considering the fact that physical modeling is widely applied in the study of the destructive effect of explosions, prior to consideration of the methods of modeling we will pause to discuss the basic positions held by the theories of dimensionality and of similitude.

### The Fundamental Position of the Theory of Dimensionality

When we refer to the measurement of a physical quantity what is understood is the comparison of that quantity with some quantity of similar physical nature, taken as unity. Every scalar quantity consists of an absolute number which indicates the number of units, and having the dimensionality of this unit. Units of measurement for various physical quantities, joined together on the basis of their internal consistency, form a system of units. At the present time

the international system of units (S.I.) has preferential usage; in this system the independent units of measurement -- mass (kilogram, kg), length (meter, m), time (second, sec), current (ampere, A), temperature (degrees Kelvin, K°), and lumirosity (candela, cd) -- are those chosen. The unit of plane angle -- radian -- and the unit of body angle -- steradian -- serve as supplementary units in the S.I. system.

Units of measurements of all the remaining magnitudes are expressed in terms of the units of measurement of the fundamental quantities in a well-defined manner. The expression for a derivative unit of measurement in terms of fundamental units of measurement is called the dimensionality. The dimensionality of a secondary quantity is found with the aid of a determining equation which functions by defining this quantity in mathematical form. The dimensionality is written down symbolically in the form of a formula in which the symbols for unit length is designated by [L], mass by [M], and time by [T]. One may speak of dimensionality only in reference to a definite system of measurement units. By making use of the determining equation one may establish the dimensionality of all physical quantities. In the following we will indicate dimensionality by taking the symbol for a quantity and enclosing it in square brackets. The determining equations for force may be taken to be Newton's Second Law:  $F = ma$ ; for energy and work:  $E = mv^2/2$ ,  $E = mgH$ ,  $A = Fl$ , etc. In the literature (Beklemishev, 1963; Burdun, 1963) one may find the dimensionalities of fundamental physical quantities in the S.I. system and the equations which may be utilized as determining equations.

Besides the S.I. system which we are considering there is a multitude of other systems of units. Some of these have been established on the scale of a number of countries and others have been established on a world-wide scale. There are systems in which the fundamental units differ only by a chosen scale factor, whereas others differ also in the fundamental quantities. For instance, in the engineering system of units, the fundamental

ones are taken to be the meter, kilogram force, and second. In contrast to the S.I. system the kilogram force rather than the kilogram mass is taken as a fundamental unit. The choice of fundamental units may be arbitrary, but they are subject to the requirement that they be single-valued independent functions of [M], [L], and [T]. In the theory of dimensionality it is shown (Alabuzhev, 1968) that the dimensionality formulas for physical quantities must have the form of monomials of factors raised to powers.

$$[\phi] = [M]^{\mu} [L]^{\lambda} [T]^{\tau}. \quad (1)$$

Thus, if we choose [X], [Y], [Z], to serve as fundamental units, then their dimensionalities are expressed in the following way:

$$[X] = [M]^{\mu_x} [L]^{\lambda_x} [T]^{\tau_x}, \quad (2)$$

$$[Y] = [M]^{\mu_y} [L]^{\lambda_y} [T]^{\tau_y}, \quad (3)$$

$$[Z] = [M]^{\mu_z} [L]^{\lambda_z} [T]^{\tau_z}. \quad (4)$$

The uniqueness of these functions is obvious since the dimensionality of each quantity in any system is specified uniquely. With the aid of not-too-complicated algebraic operations, it may be shown that all three quantities will be linearly independent if the following condition is satisfied

$$\Delta = \begin{vmatrix} \mu_x & \lambda_x & \tau_x \\ \mu_y & \lambda_y & \tau_y \\ \mu_z & \lambda_z & \tau_z \end{vmatrix} \neq 0. \quad (5)$$

From equation (5) it follows that for independent fundamental quantities one may choose: force, time, length ( $\Delta = -1$ ); force, mass, time ( $\Delta = 1$ ); force, mass, length ( $\Delta = -2$ ); mass, velocity, power ( $\Delta = -1$ ), force, density, time ( $\Delta = -4$ ). On the other hand

one is not permitted to choose for the independent units force, velocity and power ( $\Delta = 0$ ). Indeed power may be expressed in terms of velocity and force

$$N = Fv. \tag{6}$$

Mass, density and length ( $\Delta = 0$ ) are not independent, since

$$\rho = \frac{m}{l^3}. \tag{7}$$

The quantities  $[X]$ ,  $[Y]$ ,  $[Z]$  may be expressed in terms of fundamental units of any other system in which the fundamental units are known to be independent. By way of example let us express  $[X]$ ,  $[Y]$ ,  $[Z]$  in terms of the dimensionality of the fundamental units of the system -- force  $[F]$ , density  $[D]$ , time  $[T]$ :

$$[X] = F^{l_x} D^{d_x} T^{t_x}, \tag{8}$$

$$[Y] = F^{l_y} D^{d_y} T^{t_y}, \tag{9}$$

$$[Z] = F^{l_z} D^{d_z} T^{t_z}. \tag{10}$$

The quantities  $X$ ,  $Y$ ,  $Z$  will be independent if

$$\Delta = \begin{vmatrix} l_x & d_x & t_x \\ l_y & d_y & t_y \\ l_z & d_z & t_z \end{vmatrix} \neq 0. \tag{11}$$

Thus any three quantities will be independent if they can be expressed in terms of other quantities known to be independent and if at the same time condition (5) or (11) are satisfied, i.e., the determinant  $\Delta \neq 0$ .

A question which arises in this connection regards the acceptable number of fundamental units and the feasibility of using dependent quantities as fundamental units. It is not difficult to convince

oneself that the number of fundamental units may be arbitrary, both greater and less than 3. In order to remove the lack of correspondence between the dimensionalities of these dependent units one introduces supplementary dimensional physical constants, the number of which is equal to the number of dependent fundamental units. Let us take a look at a system of four fundamental quantities -- length, time, mass, and force. Let us suppose that force is a dependent quantity, but with equal justification any of the other quantities (force or mass, or time, or length) might be considered the dependent quantity. In this case Newton's equation should be written down in the form

$$F = kma \quad (12)$$

where F is force; m is mass; a is acceleration; k is a dimensional physical constant.

Inasmuch as the dimensionalities of F, m, a are chosen arbitrarily the constant k must have the dimensionality

$$[k] = [F]/([m][a]) = [F][M]^{-1}[L]^{-1}[T]^2.$$

The numerical values of the dimensional coefficients depend on the dimensionalities of the chosen quantities. For instance if the dimensionality of force is chosen to be kilograms of force, mass to be kilograms of mass, acceleration to be meters per second squared, then the quantity

$$k = 0.1021 \text{ g/N}$$

i.e., it represents the conversion factor for force from one system of units into the other. If three quantities are expressed in a different system of units, the coefficient k may be represented by the product of two factors, characterizing the conversion of two quantities into the system of units of the third. If all fundamental units are chosen in one system of units, then k equals one and is a dimensionless quantity, i.e., such a system automatically converts into a system with three fundamental units. A further

increase in the number of fundamental units leads to the appearance of new constants, similar to  $k$ . In the S.I. system there are two arbitrary fundamental units characterizing energy -- the joule and the degree Kelvin, a situation which gives rise to a physical constant  $r$  (the gas constant) with dimensionality  $m^2/\text{sec}^2\text{deg}$  ( $[R] = [L]^2[T]^{-2}[\theta]^{-1}$ ). If for the unit of heat we choose the calorie (also characterizing energy), then the necessity arises for still another physical constant -- the mechanical equivalent of heat  $I$ , which has the dimensionality joule per calorie. When the number of fundamental units is reduced the corresponding dimensional constants disappear.

Let us consider a system of units in which only two fundamental units are used -- length  $[L]$  and time  $[T]$ . In this case the determining equation for mass may be taken to be the law of universal gravitation

$$F = k_1 (mM)/r^2. \quad (13)$$

Taking the gravitational constant  $k_1$  as an absolute dimensionless constant and using the determining equation for force ( $F=ma$ ), we obtain the dimensionality of mass

$$[M] = [L]^3 [T]^{-2}. \quad (14)$$

Excluding length or time from the fundamental units we obtain a system of units in which there is one fundamental quantity. To serve as the determining equation we will use the equation from quantum mechanics

$$E = h\nu \quad (15)$$

where  $E$  is the quantum energy,  $\nu$  is the frequency of a radiator, and  $h$  is Planck's constant. If we take Planck's constant as an absolute dimensionless quantity equal to unity, we obtain

$$[E] = [T]^{-1}.$$

In turn

$$[E] = [M] [L]^2 [T]^{-2} = L^2 T^{-2}.$$

Because of the conditions for consistency of both dimensionalities for energy it follows that

$$L = T^2/s.$$

The dimensionalities of mass, length, or time in the systems of measurement under consideration depend on the chosen determining equation, and consequently, on the constant which is taken to serve as the absolute dimensionless constant. Thus, for instance, if for the determining equation for mass we take not the universal law of gravitation, but equation (15), and if for the absolute dimensionless quantity we had taken Planck's constant and not the gravitational constant, then the dimensionality of mass is expressed in terms of [L] and [T] in the following manner:

$$[M] = [T] \cdot [L]^{-2}. \quad (16)$$

As we see, the dimensionalities of mass in the relations (14) and (16) differ substantially. Therefore in converting to systems where the number of fundamental units is less than three, it must be indicated which constants are taken to be the absolute dimensionless quantities.

Excluding the last dimensional unit, we obtain a single universal system of units, based on the chosen physical constants. The introduction of such a system of units is equivalent to the complete removal of the concept of dimensionality, and the numerical values of all quantitative properties are unambiguously determined from their physical value.

In the system of units proposed by M. Planck, the gravitational constant, the velocity of light, Planck's constant, and Boltzmann's constant are dimensionless and equal to unity. In this case all physical quantities will have fully-determined units of measurement and not one of these will be able to be chosen arbitrarily. In Planck's system of units the unit of length is equal to  $4.02 \cdot 10^{-33}$  cm, mass --  $5.43 \cdot 10^{-5}$  g and time --  $1.34 \cdot 10^{-43}$  sec.

In Hartree's system of units the charge of the electron ( $e = 4.803 \cdot 10^{-10}$  CGSE units), the electron mass ( $m = 9.108 \cdot 10^{-29}$  g), the radius of the first bohr orbit of the hydrogen atom ( $r_0 = h^2/4\pi^2 m l^2 = 0.5292 \cdot 10^{-8}$  cm) and Planck's constant ( $\hbar = h/2\pi = 1.0544 \cdot 10^{-27}$  g.cm<sup>2</sup>/sec) are dimensionless and equal to unity. In this system the unit of time is equal to  $2.419 \cdot 10^{-17}$  sec. Utilization of Hartree's system of units permits freedom from superfluous numerical factors and simplification of some of the equations of quantum mechanics and atomic physics. Obviously such units are inconvenient for use in practice. Moreover, only in some of the equations do the dimensional coefficients disappear, since in regard to many other phenomena the chosen physical constants have only the remotest connection, for which reason these systems of units and those similar to them have not received wide usage.

Every physical phenomenon is determined by corresponding parameters. Therefore, in order to describe a phenomenon or a process it is necessary to determine the functional dependencies between the quantities which characterize the effect under study. The numerical values of these quantities, the determining parameter and the state of the system or the process depend on the units of measurement. Functional relationships which express the essence of the physical phenomena do not need to depend on the choice of the system of units. It is shown in the theory of dimensionality that every relationship between dimensional quantities may be replaced by a relationship between dimensionless quantities. A particular role in the theory of similarity is played by dimensionless complexes of quantities, the so-called dimensionless criteria, which represent the products of various powers of the determining dimensional quantities. It is

standard to designate the similarity criteria through the symbol  $\Pi$ . To serve as an example we will introduce several criteria; the homochronicity number  $vt/\ell = \Pi_V$  and Reynolds number  $\bar{v}\ell\rho/\mu = \Pi_R$  where  $v$  is velocity,  $t$  is time,  $\ell$  is linear dimension,  $\bar{v}$  is average flow velocity,  $\rho$  is density,  $\mu$  is the dynamic viscosity, and  $\Pi_V, \Pi_R$  are similarity criteria.

Without dwelling in the meantime on the physical determination the similarity criteria, let us solve a problem relating to the theory of dimensionality, and having to do with the number of independent similarity criteria which can be composed from  $n$  dimensional quantities. The independence of the similarity criteria means that not one of them can be a function of the rest, i.e., the relationship at this point

$$\Pi_i = \psi(\Pi_1, \Pi_2, \dots, \Pi_{m-1}); \quad i = 1, 2, 3, \dots, m. \quad (17)$$

cannot hold.

In the theory of dimensionality it is shown that the number of independent similarity criteria is determined by the number of dimensional quantities  $n$  and the number of fundamental independent units of measurement  $r$ .

$$m = n - r, \quad (18)$$

where  $m$  is the number of independent similarity criteria.

If  $n=r$ , i.e., the process is determined only by a fundamental independent dimensional quantity, then in general it is not possible to set up dimensionless similarity criteria. In fact, if the process is determined by length, time, mass, and force and they are chosen in order to serve as fundamental units, then it is not possible to form dimensionless similarity criteria from them. By excluding force from the fundamental units, for the same process we may set up one dimensionless criterion

$$\Pi_1 = \frac{[M][L][T]^{-2}}{[F]}. \quad (19)$$

In the case where force is chosen for a fundamental unit this complex

will not be dimensionless, but will carry the dimensionality of the coefficient  $k$  in Newton's equation. If we choose three fundamental units, then the dimensional coefficient  $k$  disappears and a dimensionless complex  $\Pi_1$  appears.

Passing to a system with two units of measurement (time, length), we may add to the first similarity criterion a second

$$\Pi_2 = \frac{[M][T]^2}{[L]^3}. \quad (20)$$

For this case the dimensional coefficient  $k_1$  disappears in the equation describing the law of universal gravitation, inasmuch as we have gone over from a system with three fundamental units to a system with two fundamental units. In the practical investigations it is possible to change the number of independent similitude criteria by means of making a change in the number of fundamental units and determining parameters. However, it must not be forgotten that the appearance (disappearance) of a new unit of measurement is accompanied by the appearance (disappearance) of a dimensional coefficient. This method is effective in a case where the dimensional coefficients which are appearing or disappearing do not enter into the determining parameters and the differential equations of the system. In the opposite case a change in the number of units of measurement leads to the same change in the number of system parameters

$$n-r = (n+d) - (r+d) = (n-d) - (r-d),$$

and the number of independent criteria will remain unchanged.

### Bases of the Theory of Similitude

Dimensional and similitude theory is the basic underlying the modeling of various processes and phenomena. Academician L. I. Sedov defines modeling in the following manner: "Modeling is a substitution of the study of an interesting natural phenomenon by the study of an analogous effect on a model of a smaller or larger

scale, usually under special laboratory conditions. The basic sense of modeling is comprised in the idea that from the results of experiments with models it should be possible to give the necessary answers about the nature of the effects and about various quantities which are connected with the phenomenon under natural conditions " (1965, page 54).

In order to make judgments on the behavior of an object in nature based on the data of measurements on a model, it is necessary as a preliminary step to prove that nature and the model are similar, i.e., subject to the same physical laws or are described by the same mathematical dependences. If this is proved in the general sense or if it is known as a result of more general physical laws which are obeyed by the phenomenon under study, then subsequently, in setting up a particular problem, one may dispense with the construction of equations to describe the effect and build models according to rules which are basic to the theory of similitude. Two phenomena are similar if by the specified characteristics of one it is possible to determine the characteristics of the other with the aid of a conversion scale. In the case of linear similitude the conversion scale is a constant, usually established by a calculation or by an experimental means. The numerical characteristics for two different but similar phenomena may be considered as the numerical characteristics of one and the same phenomenon, but expressed in a different system of units. The simplest and most typical example is that of geometrical similitude. With geometrical similarity of two objects the relationship between corresponding dimensions, determining the geometrical form of the objects, is a fixed quantity bearing the name of the geometrical scale. From the point of view of the material of the object and its position in space, geometrical similarity does not impose any limitations. Geometrical similarity establishes only the identity of form between the natural object and the model. The geometrical scale of the modeling is determined by the relation between any corresponding dimensions of the object and the model. In practical problems in the majority of cases there is no necessity for observance of similitude in all characteristics and parameters of the phenomenon. In a great number of cases it is sufficient to

observe similitude only for separate parameters which are of interest to the investigator. In this connection it is possible to separate out the most characteristic specific forms of physical similitude -- kinematic, material, and dynamic.

The modeling of mechanical motions is based on kinematic similitude which determines the similitude of mechanical movements. As is known, the position of the object of the investigation is determined by the coordinates of its points in space as a function of time or according to a law of motion. In the case of kinematic similitude the relation between coordinates of any analogous points in nature and in the model for like moments of time is the constant

$$\frac{x_i(t_n)}{x_{iM}(t_M)} = \frac{y_{in}(t_n)}{y_{iM}(t_M)} = \frac{z_{in}(t_n)}{z_{iM}(t_M)} = \lambda_l, \quad (21)$$

where  $x_{in}(t)$ ,  $y_{in}(t)$ ,  $z_{in}(t)$  are the coordinates of the  $i$ -point in nature as a function of time;  $x_{iM}(t_M)$ ,  $y_{iM}(t_M)$ ,  $z_{iM}(t_M)$  are the coordinates of the analogous model point as a function of time;  $t_n$  and  $t_M$  are the time base corresponding to nature and to the model;  $\lambda_l$  is the similitude coefficient for length.

Kinematic similitude permits one to determine all characteristics of motion in nature (velocity, acceleration) as the result of investigations on the model. The value of velocity is determined from the relationship

$$\frac{(v_x)_{in}}{(v_x)_{iM}} = \frac{dx_{in}/dt_n}{dx_{iM}/dt_M}. \quad (22)$$

Denoting the ratio  $t_n/t_M = \lambda_t$  and taking account of (21), let us transform equation (22)

$$\frac{(v_x)_{in}}{(v_x)_{iM}} = \frac{\lambda_l}{\lambda_t} = \lambda_v, \quad (23)$$

where  $\lambda_t$  is the similitude coefficient for time (time scale);  $\lambda_v$  is the similitude coefficient of velocity (velocity scale). Usually, the similitude coefficient of time is specified in the initial premises or is determined experimentally.

By analogy, it is possible to write

$$\frac{(v_y)_{in}}{(v_y)_{iM}} = \frac{(v_z)_{in}}{(v_z)_{iM}} = \frac{\lambda_l}{\lambda_l} = \lambda_v. \quad (24)$$

The acceleration scale is also expressed in terms of the initial similitude coefficient

$$\lambda_a = \frac{a_{in}(t_n)}{a_{iM}(t_M)} = \frac{dv_{in}/dt_n}{dv_{iM}/dt_M} = \frac{\lambda_v}{\lambda_l} = \frac{\lambda_l}{\lambda_l^2}. \quad (25)$$

However with kinematic similitude it is not permissible to say anything about stresses in the system elements. In order to study the force and energy characteristics of processes on models and to apply the results of these investigations to nature, in addition to the conditions of kinematic similitude it is necessary to guarantee material similitude for points of the system

$$\frac{m_{in}}{m_{iM}} = \lambda_m = \text{const}, \quad (26)$$

where  $m_{in}$  is the mass of the  $i$ -point in nature;  $m_{iM}$  is the mass of the analogous model point;  $\lambda_m$  is the similitude coefficient for mass.

In the case of dynamic similitude the connection between force and work in nature and in the model is expressed in terms of the similitude coefficient of length, mass, and time

$$\frac{F_{in}}{F_{iM}} = \frac{m_{in} a_{in}}{m_{iM} a_{iM}} = \lambda_m \lambda_a = \frac{\lambda_m \lambda_l}{\lambda_l^2} = \lambda_F, \quad (27)$$

$$\frac{A_{in}}{A_{iM}} = \frac{F_{in} l_{in}}{F_{iM} l_{iM}} = \lambda_F \lambda_l = \frac{\lambda_m \lambda_l^2}{\lambda_l^2} = \lambda_A, \quad (28)$$

where  $F_{in}$  is the value of the force applied to the  $i$ -point in nature;  $F_{iM}$  is the value of the force applied to the analogous model point;  $\lambda_F$  is the similitude coefficient of force (force scale);  $A_{in}$  is the work produced in the motion of the  $i$ -point in nature;  $A_{iM}$  is the work produced in the motion of the analogous model point;  $\lambda_A$  is the similitude coefficient of work.

The combination of dynamic and kinematic similitude is called mechanical similitude. In mechanical similitude the system of corresponding similitude coefficients of the various quantities may be obtained from the formulas of dimensionality if in place of the dimensionality of a quantity we substitute into the formulas the corresponding coefficient of similitude.

$$[v] = \frac{[L]}{[T]}, \quad \lambda_v = \frac{\lambda_l}{\lambda_t}, \quad (29)$$

$$[A] = \frac{[M][L]}{[T]^2}; \quad \lambda_A = \frac{\lambda_m \lambda_l^2}{\lambda_t^2}, \quad (30)$$

i.e., in place of [A], [M], [L], [T] the similitude coefficients  $\lambda_A, \lambda_m, \lambda_l, \lambda_t$  are substituted in a corresponding manner. The similitude coefficients for other quantities (force, acceleration, and others) may be obtained in an analogous manner.

Having considered some of the particular cases, let us set up the rules for converting from a model to nature for the general similitude case. Such rules may be formulated on the basis of a theorem regarding necessary and sufficient conditions for similitude, which appears as a result of the  $\Pi$ -theorem.

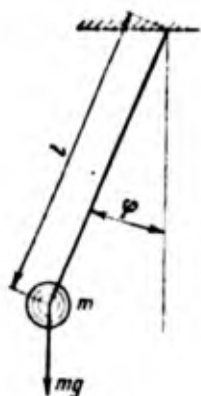
If a phenomenon is determined by  $n$  parameters (a part of these may be non-dimensional, some may be physical dimensional constants), but the dimensionalities of the parameter variables and the physical constants are expressed in terms of  $r$  basic units of measurement ( $r \leq n$ ), then from  $n$  quantities one may set up no more than  $n - r$  independent dimensionless combinations or similitude criteria. All non-dimensional characteristics of the effect may be considered as functions of the  $n - r$  independent dimensionless combinations which have been composed from the determining parameters. The theorem concerning the necessary and sufficient conditions for similitude may be formulated in the following manner (Sedov, 1965,

page 55). "A necessary and sufficient condition for similarity of two phenomena will be the constancy of the numerical values of dimensionless combinations forming the base." By the term base in the above sentence is meant the system of independent dimensionless quantities which determine all basic parameters of the effect or process.

Taking account of the fact that these dimensionless combinations are the similitude criteria, the theorem may be put into a different formulation -- the necessary and sufficient condition for similarity of two phenomena will be equality of any two corresponding similitude criteria for these phenomena. In fulfilling the similitude conditions for calculating the characteristics in nature from data on the dimensional characteristics on the model it is necessary to know the similitude coefficients for all corresponding quantities. The similitude coefficients of the basic dimensional quantities are specified arbitrarily or are determined from the conditions of the experiment. The similitude coefficients for the remaining dimensional quantities may be easily determined from the formulas of dimensionality for each of these in the same way as this was done in relation (29).

Investigations and determinations of the functional dependencies between the parameters of the process or the effect in a series of cases may be significantly simplified if we use the very important theorem of similitude known by the name  $\Pi$ -theorem: "The functional dependence between quantities characterizing a given process may be represented in the form of a dependence between the similitude criteria composed from them". If the process is characterized by  $n$  dimensional quantities and  $s$  non-dimensional quantities, of which  $r$  quantities are fundamental dimensional ones, then it is possible to set up  $n+s-r$  independent dimensionless complexes. Making use of the  $\Pi$ -theorem, one may reduce the number of quantities which must be related by a functional dependence. This makes it possible in many cases to simplify the problem and to decrease the number of experimental measurements. To serve as an example we might take a look at the classical problem of the motion of a

pendulum. A mathematical pendulum (Figure 1) can be visualized as a heavy material point, suspended on a weightless inextensible string, the other end of which is fastened securely. The motion of the pendulum is characterized by the quantities:  $l$  - length of the pendulum;  $t$  - time;  $m$  - mass of the load;  $g$  - acceleration of free-fall;  $\varphi$  - angle of inclination of the string from the vertical.



In the absence of damping forces the problem of the motion of a pendulum reduces to solution of the equations

$$d^2\varphi/dt^2 = -(g/l) \sin \varphi, \quad (31)$$

$$m (d\varphi/dt)^2 l = N - mg \cdot \cos \varphi \quad (32)$$

where

$$t = 0: \quad \varphi = \varphi_0; \quad d\varphi/dt = 0, \quad (33)$$

Figure 1  
Diagram of a  
Mathematical  
Pendulum

where  $N$  is the tension in the string.

From the equations and from the initial conditions it follows that for the determining parameters one may take the following system:

$$t, l, g, m, \varphi_0.$$

In this manner one may express all the remaining quantities in terms of these parameters

$$\varphi = \varphi(t, \varphi_0, l, g, m), \quad (34)$$

$$N = mg/l, (t, \varphi_0, l, g, m). \quad (35)$$

From equation (18) it follows that from the five determining parameters, in light of the three independent units of measurement, one may set up two dimensionless complexes:

$$\varphi_0, \quad t \sqrt{\frac{g}{l}}.$$

By virtue of the  $\Pi$ -theorem, equations (34) and (35) may be written in the form

$$\varphi = \varphi_1 \left( \varphi_0, t \sqrt{\frac{g}{l}} \right), \quad (36)$$

$$N = mg f_1 \left( \varphi_0, t \sqrt{\frac{g}{l}} \right). \quad (37)$$

From the dependencies (36) and (37) it follows that the law of motion of the pendulum does not depend on the mass of the load, but the tension in the string is proportional to the mass of the load.

For the period of oscillation it is not difficult to obtain

$$T = \sqrt{\frac{l}{g}} f_2(\varphi_0), \quad (38)$$

where  $f_2(\varphi_0)$  is a function of the maximum angle of inclination, determined by calculation or by experiment.

Experimental investigations are significantly simplified since it is necessary only to determine the dependence between  $\varphi_0$  and  $T$ , rather than studying its dependence on five parameters. Thus it is established that the motion of other pendulums will be similar, if their values of  $t \cdot \sqrt{\frac{g}{l}}$ ,  $\varphi_0$  are the same.

Linear similitude is widely utilized in the modeling of various mechanics problems. However in the description of complicated non-stationary processes the similitude coefficient may be a function of some parameter. According to the accepted terminology in this case the similitude coefficient would be called a function

of the non-linear similitude transformation of the corresponding parameter. In the given case the similitude will be non-linear, inasmuch as it is based on non-linear transformations of the quantities which characterize the effect under study. Non-linear similitude usually holds in a case where a model which has the same mathematical description as does nature is difficult to realize. For instance, in the physical modeling of strained and deformed states it is difficult to prepare a model with the physical parameters of the medium changing according to a well-defined law. In this case the problem may be solved with the aid of a model in which the processes are described by equations different from the mathematical description of nature, but the correspondence between the same quantities of nature and of the model are established with the aid of non-linear similitude. The basic circumstances of non-linear similitude were worked out by V. A. Venikov (1966), A. A. Gukhman (1946, 1963), A. G. Nazarov (1965), G. Ye. Pukhov (1963), and by other investigators. The ideas of non-linear similitude were employed by the authors in a series of works (Drukovanyy, 1965; 1968) for the modeling of destruction processes in an explosion. When statistical damage series are employed non-linear similitude turns out to be the only realistic possibility for creating a model of the destructive process. In this case the similarity of macroscopic phenomena may be established on the basis of the similarity of micro processes.

In practice when modeling complicated processes which depend on many parameters, one often resorts to an approximate similarity. In this case one does not account for parameters which are insignificant in comparison with the others in their effect on the ultimate results of the process. Depending on which parameters are being studied in the modeling of the effect, it pays to establish the degree of influence of the other factors, in order to sort out the first order and neglect the second-order effects. The successfulness of approximate modeling in general depends on the degree of justification for neglecting some factors with respect to the others. In approximate modeling no small value should be placed on the evaluation of tolerable error, a step which is also not

possible without studying the effect of the separate factors on the process being studied.

One of the methods of overcoming the difficulties of modeling is an adherence to affine similarity instead of geometric. As a common example of affine similarity we might submit the similarity of two ellipses having a different geometrical scale for their coordinate axes. Although in the given case the geometrical forms of the figures are the same, for similar points on the ellipsis (for the same angle  $\varphi$ ) the ratio of the radius vectors is not a constant quantity. Another example of affine geometrical bodies is provided by two circular cylinders for which the ratio of the diameters is not equal to the ratio of heights, i.e.,  $d_1/d_2 \neq h_1/h_2$ . Such a situation is encountered in practice in the modeling of an explosion in deep bore holes of comparatively small diameter. In this case if we are to observe geometric similarity the diameter of the bore holes may turn out to be smaller than the critical diameter of the charge and in order to assure a stable detonation, it is necessary to resort to an increase in the diameter of the charge without changing its height, i.e., a resort to affine similarity.

The methods of non-linear, approximate affine and statistical similarity is still not used on a sufficiently wide scale in the modeling of effects in mining, especially in the area of the modeling of the crushing effects of an explosion. In light of the great possibilities of non-linear, approximate and affine similarity, the most serious attention should be given to the prospects and the inevitable development of these methods as applied to problems in mining, where one is bound to run into processes and phenomena which are highly complicated and little understood.

THE MODELING OF EXPLOSIVE ACTION IN A SOLID MEDIUM

Basic Parameters Characterizing the Effect of an Explosion  
in a Solid Medium

An explosion in a solid, brittle medium is characterized by a diversity of processes and effects taking place. By the term effect (or phenomenon) and processes making up an effect let us agree to understand the aggregate of changes occurring in the system. Each change in the state of a system, taking place in space and in time, is caused by one or by a series of processes. As these processes proceed the quantities which characterize the state of the system change. These quantities will be called the parameters of the process in the following. In turn the parameters are a function of one or several variables, affecting the character of the process taking place. The elements of which the system is comprised are characterized by their parameters, the so-called system parameters. Starting from the definitions just taken, let us characterize the action of an explosion in a solid medium.

Explosive action in a solid medium is accompanied by the following basic phenomena:

- 1) detonation of the charge;
- 2) discharge of the products of detonation;
- 3) mechanical interaction of the detonation product with the surrounding medium;
- 4) a propagation of pressure waves in the medium;
- 5) destruction of the surrounding medium;
- 6) displacement of the destroyed material and scattering of the debris.

If we consider the effect of a detonation of an elongated cylindrical charge in a bore hole, the system will be the charge of explosive material which is about to undergo a change of state. This change of state of the system is governed by the process of chemical reaction,

in the process of which quantities characterizing the state of the system are changed: temperature, density, pressure, volume of the reacting explosive material, the velocity of particle movement in the shock wave, and the velocity of sound in the detonation products (DP). These quantities are the parameters of the process. The system itself (the charge of the explosive material) is characterized by the elements: charge diameter, length, density of charge packing, velocity of detonation, and specific energy of the explosive material.

Taking a look at the effect of discharging the detonation products, it is appropriate to take as the system the detonation products in the bore hole that undergo a change of state in the process of the discharge. The parameters of the process are the discharge velocity, density of escaping products, pressure, and DP temperature. The parameters of the system are: the bore hole diameter, the initial density, temperature, pressure and volume of the detonation products, and the friction coefficient of their motion.

Upon interaction of the detonation product with the surrounding medium the state of the two interacting systems is changed -- mainly the surrounding medium and the detonation products. Therefore, the parameters of the process characterize the state of both the medium and of the detonation products. The change in state of the medium arises as a consequence of the change in value of stresses at the contact with the charge, the value and direction of the displacement velocity of the particles, and the density of the medium. The change in state of the DP is caused by a change in pressure, density, velocity, and direction of the DP motion prior to encounter with the surrounding medium and after interaction with the wall of the charging chamber. The parameters of the medium will be the material density, the velocity of propagation of pressure waves, the acoustic rigidity, and the shock compressibility of the material. The parameters which determine the DP state are the initial velocity and direction of motion, the pressure, density, velocity of sound in the DP, and the detonation velocity. Furthermore, the parameter which characterizes the interaction of the two systems is the angle of incidence of the shock wave with the bore hole wall.

The phenomenon of propagation of a pressure wave is accompanied by a change in stress at various points in the medium. The system in such a case is the medium, changing its state of stress. As the pressure waves are propagated, the following quantities which characterize the state of the system (medium) undergo a change: the value of the stresses and the deformation of the medium at a point, the position of the pressure wave front, the stress at the wave front, the density of the medium at a point, and its temperature. The parameters of the system are the propagation velocity of pressure waves, the coefficient of dissipative losses, the initial density of the medium, the modulus of elasticity, the Poisson coefficient, the porosity, and the dynamic compressibility.

The phenomenon of the shattering of a brittle material is characterized by a disturbance of the continuity of the medium. The system is comprised of the medium, which is changing its state, though this change differs substantially from that being considered, because the continuity of the medium is being upset. The destruction process is characterized by the following parameters: a change in the stress field, the dimensions of cracks about to grow at a given moment, and the growth rate of the cracks. To the parameters of the system we should relate the hardness of the material, the modulus of elasticity, the propagation velocity of the disturbing action, the energy capacity of the process of destruction, and the distribution of microcracks in size and direction.

The movement of rock and the dispersion of fragments is explained in terms of a displacement of the rock mass in space. The parameters of the process are the acceleration, velocity and direction of motion, and dispersion of the fragments. The parameters of the system are the mass of separate fragments, and the coefficients characterizing the resistance to motion of the massif and to the dispersion of fragments.

The system parameters may have a substantial influence on the course of the processes, even if they themselves do not change during the

process. For example, in the investigation of a process of detonation the charge diameter is a system parameter. If the charge diameter is greater than the critical value, the detonation is propagated with each charge having the nominal velocity. For a charge diameter smaller than critical, the detonation is propagated with decreasing velocity and thereafter generally comes to a halt. As we can see, the system parameter, which in a given case is the charge diameter, has a telling effect on the course of the process. At the same time a change in the charge diameter within wide limits (greater than critical) has no effect on the course of the process. As our second example we might mention the plastic and brittle shattering of a material upon application of an impulsive load. The parameters of the system, in this case the properties of the material and the characteristics of the load, determine the course of the process -- brittle or plastic shattering. Thus, the parameters of the system in a series of cases determine the basic particulars of the way in which the process takes place.

At the present stage in the development of the exterior damage, and in the development of methods of investigation, and given contemporary knowledge about the processes which take place in an explosion and in destruction of materials, it is not possible to guarantee the similarity of all phenomena in the modeling of the explosive action in a solid medium, and in practice it is not necessary to do so. It is sufficient to provide a similarity for the separate effects which are interesting to us. We will decide on a detailed treatment of the process of destruction of mineral rocks in an explosion. All parameters of the system and the process of destruction will be grouped in the following manner: parameters characterizing the physical and mechanical properties of the medium, the explosive loading, and the characteristics of the process of destruction itself.

In describing the processes which take place in the medium during an explosion various diagrammatic schemes are used for the explosion. The most successful, having become one of the most classical, is the diagram for explosive action proposed by Professor G. I. Pokrovskiy

(1957). According to this scheme for the explosion of an explosive charge occurring instantaneously, a compression load is excited in the surrounding medium (Figure 2), which is propagated in all directions from the charge with a single velocity. When the compression wave reaches a free surface it is reflected, transforming into a rarefaction wave. For an ideally elastic medium the rarefaction wave may be considered as a wave which is propagated from the virtual image center of the explosion, if we take the free surface as the surface of specular reflection (in analogy with the optical effect). In the case of an ideal elastic medium the stresses in the rarefaction wave at the free surface are equal in magnitude to the stresses in the compression wave upon approach to the surface. Moreover, as the pressure in the charging chamber falls away from the walls, a rarefaction wave also begins to propagate. The indicated types of disturbances in the medium are the reasons for the determined character of the damage (Figure 3). The volume in which destruction takes place, caused by the compression wave, depends on the durability of the arc and on the pressure in the charging chamber. If the pressure caused by the explosion of the charge exceeds the limit of the durability of the rock with respect to crushing, then in the zone closest to the charge the rock is crushed and collapses. As the stresses decrease further and further the destruction process takes on a different character. Disruption of the continuity of the material occurs by means of the formation of separate cracks, which propagate along radii from the charge. The appearance of radial cracks is explained by the presence of tangential tensile stresses, which exceed the limit of durability of the material toward rupture. If the tensile stresses in the reflected rarefaction wave exceed the limit of durability of the rock toward rupture then at the free surface splintering effects are observed. Analogous splintering effects may arise around the charging chamber when the rarefaction wave emerges (See Figure 3). The diagram for explosive action set forth in the works of G. I. Pokrovskiy permit one to determine the factors which influence the destruction process, and to establish the diversity of forms for the process of destruction.

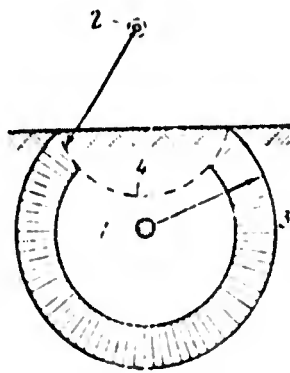


Figure 2. Diagram for the propagation of stress waves in a medium upon explosion of a charge near a free surface (according to G.I. Pokrovskiy). 1 - explosive charge; 2 - center of the dilatation wave front; 3 - a compression wave; 4 - dilatation wave.

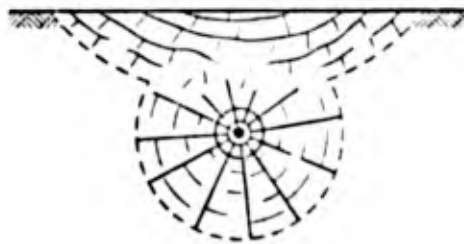


Figure 3. Nature of damage to a medium in the explosion of a charge near a free surface (according to G. I. Pokrovskiy).

In view of the difficulties which arise in the modeling of an explosive effect, observance of the similitudes for separate phenomena and parameters is ordinarily the rule. The most typical phenomena and parameters in an explosion are the stress field, the crushing and the ejection of material, the zone of scattering of fragments, the loading of the rock mass, and the degree of its compaction.

In the modeling of each of the enumerated parameters and phenomena various methods are employed, taking account of the various factors and obeying the various similitude criteria. In this connection use is made both of mathematical modeling with application of the model of an absolutely incompressible medium, as well as physical

modeling with the use of centrifugal modeling methods, applying equivalent materials and obeying the energetic, thermodynamic and other types of similitudes. Several methods may be utilized in the modeling of some of the phenomena which arise in an explosion, just as separate effects may be modeled by several methods.

### Bases for Physical Modeling of Elastic Wave Phenomena in an Explosion

In modeling the parameters of stress field arising in a medium at the time of explosion, various methods are used depending on the assumptions made. With regard to the charge assumptions are made pertaining to its form (point, spherical, cylindrical) and the instantaneousness of detonation. It is presumed that the explosive action is determined only by the charge energy  $E_0$ . With respect to the medium several different assumptions are made. The most widely used models for the medium are: 1) a continuous medium with density  $\rho$ , the compressibility of which is a specified function of pressure; 2) an absolutely elastic medium, characterized by a density  $\rho$ , a modulus of elasticity  $E$ , and a Poisson ratio  $\nu$ ; 3) an elastic medium with inelastic aftereffect, caused by dissipative losses.

The continuous medium model is utilized in the description of explosive processes in liquids and in gases, whereas the shear modulus is equal to zero. For brittle materials the model of such a medium is employed in calculating the pressure parameters at the front of strong shock waves where cohesive forces may be neglected in comparison with the stresses developed. The model of an ideally elastic medium has been more widely adopted, since it allows one to determine the stress field parameters with greater accuracy without having to take account of dissipative losses.

Let us consider the propagation of a one-dimensional elastic expansion wave. By a one-dimensional wave we understand a wave whose displacement on the wave front occurs only in the direction of one coordinate axis.

As shown in the work of Chou Pie Chi and Koenig (1966), the equation describing the stress wave parameters may be written down in

the form

$$\frac{\partial^2 u}{\partial r^2} + K \frac{\partial}{\partial r} \left( \frac{u}{r} \right) = \frac{1}{c^2} \frac{\partial^2 u}{\partial t^2}, \quad (39)$$

where  $u(r, t)$  is the radial displacement as a function of distance and time;  $r$  is the radial coordinate;  $c$  is the velocity of a longitudinal stress wave,  $K$  is a coefficient depending on the type of waves. For plain waves  $K$  equals 0, for cylindrical waves  $K$  equals 1, and for spherical  $K$  equals 2. Inasmuch as the equation describing the process is well-known, for specified initial and boundary conditions we may establish the similitude criteria for modeling the dynamic stress field which arise at the time of explosion. Let us take a look at the explosions of a cylindrical charge ( $K = 1$ ) with radius  $r_0$  in an unbounded ( $r_0 \leq r < \infty$ ) homogeneous ideally elastic medium. In specifying the initial conditions we say that at the initial moment in time ( $t = 0$ ) the medium is not loaded, i.e., the displacement velocity and the stresses at the initial moment are equal to zero. For the boundary conditions we take  $\sigma_0 = f_0(r_0, t)$  and  $v_0(r_0, 0) = 0$ , i.e., at the wall of the charging chamber the load varies according to a specified law. The displacement velocity at the initial moment is equal to zero, but afterwards it is determined by the nature of the applied charge and the properties of the medium.

From equation (39), with the specified initial and boundary conditions, it follows that the process of wave propagation and the stress field characteristics are determined by the following parameters:  $c, v, u, r, t, E, \sigma, \nu, \rho$ . In choosing (time, length, mass) for the fundamental three units of measurement in accordance with the  $\Pi$ -theorem, one may set up  $n-r$  independent similitude criteria. In the given case the number of parameters  $n = 9$ , the number of units of measurement  $r = 3$ , and the number of independent similitude criteria  $m = 6$

$$\begin{aligned} \Pi_1 &= v; & \Pi_2 &= \frac{E}{\sigma}; & \Pi_3 &= \frac{r}{u}; \\ \Pi_4 &= \frac{u}{c \cdot t}; & \Pi_5 &= \frac{\nu}{\rho r^2}; & \Pi_6 &= \frac{E}{\rho c^2}. \end{aligned} \quad (40)$$

From the similitude criteria it follows that the Poisson ratio must be the same for the materials of the model and of nature. The remaining five similitude criteria are functions of six parameters. This implies that the relationships among the three independent parameters of nature and of the model may be chosen arbitrarily. To serve as the arbitrarily chosen relationship we may take

$$\frac{r_n}{r_m} = \lambda_l \quad \text{Geometrical scale;}$$

$$\frac{\rho_r}{\rho_m} = \lambda_\rho \quad \text{Density Scale;}$$

$$\frac{t_n}{t_m} = \lambda_t \quad \text{Time Scale.}$$

Similitude criteria (40) permit one to express the scales of other parameters in terms of the chosen  $\lambda_l, \lambda_\rho, \lambda_t$

$$E_n/\sigma_n = E_m/\sigma_m.$$

From this it follows that

$$\frac{\rho_n c_n^2}{\rho_n v_n^2} = \frac{\rho_m c_m^2}{\rho_m v_m^2}, \quad \frac{v_n}{r_n} = \frac{c_n}{c_m} = \lambda_v.$$

i.e., the scale of wave propagation velocity and the scale of displacement velocity in the wave must be the same. It is not difficult to show that when the Poisson ratios are the same the scale of the transverse wave propagation velocity is equal to the scale of the longitudinal wave propagation velocity ( $\lambda_v$ ).

From the relation

$$r_n/u_n = r_M/u_M$$

It follows that  $u_n/u_M = r_n/r_M = \lambda_\rho$ . Thus the geometric scale, chosen for the model must be preserved as far as the ratio of displacement values is concerned.

From the relationship

$$\frac{v_n}{v_n t_n} = \frac{v_M}{v_M t_M}$$

we determine the velocity scale, expressing it in terms of the known scale

$$\frac{v_n}{v_M} = \frac{r_n t_n}{r_M t_M}$$

whence

$$\lambda_v = \frac{v_n}{v_M} = \frac{v_n t_M}{v_M t_n} = \frac{\lambda_l}{\lambda_t}, \quad \lambda_v = \frac{\lambda_l}{\lambda_t}. \quad (41)$$

From the relation

$$\frac{\sigma_n}{\rho_n v_n^2} = \frac{\sigma_M}{\rho_M v_M^2}$$

we determine the stress scale

$$\lambda_\sigma = \frac{\sigma_n}{\sigma_M} = \frac{\rho_n v_n^2}{\rho_M v_M^2} = \lambda_\rho \lambda_v^2. \quad (42)$$

Consequently the scales of all parameters which characterize an elastic wave loading are expressed in terms of three arbitrarily chosen scales. It is essential that any independent three scales may be chosen arbitrarily. However it is not permissible to choose the dependent scale  $\lambda_\ell$ ,  $\lambda_t$  or  $\lambda_\rho$ ,  $\lambda_v$ , and  $\lambda_\sigma$ , since if that were done conditions (41) or (42) would be violated.

In choosing  $\lambda_\ell$ ,  $\lambda_t$ , and  $\lambda_\rho$  for the arbitrary scales, difficulties arise in attempting to observe the scales of density and propagation velocity of the elastic oscillation. Therefore it is more convenient to choose arbitrarily the model material, an action which is equivalent to the arbitrary choice of velocity and density scales. Having decided on a geometric scale, it is possible to determine the time and stress scales by formulas (41) and (42). In the particular case where the materials of nature and the model are the same  $\lambda_\rho = 1$  and  $\lambda_v = 1$ . From relations (42) and (41) it follows that  $\lambda_\sigma = 1$ , but  $\lambda_t = \lambda_\ell$ , i.e., the time scale must be equal to the geometric scale. This implies that a similar time period for the model is  $\lambda_\ell$  times smaller than in nature. For the same moment of time the distance over which a wave is propagated must be  $\lambda_\ell$  times smaller for the model than for nature, by virtue of geometric similarity.

Inasmuch as the wave propagation velocity is the same, similitude for the explosive action zone dimensions is obtained only on account of the introduction of the wave propagation time scale. The time duration of loading, determined by the initial conditions at the point of loading, must change in correspondence with this proportionately to the geometrical scale. The similitude criteria of elastic wave phenomena, first obtained by G. N. Ivakin (1956), is used in the modeling of various phenomena which occur in an explosion. In the works of Ivakin similarity of elastic wave phenomena is utilized for the modeling of seismic operations in lumpy-inhomogeneous ideal media, each of which consists of  $n$  isotropic layers, having arbitrary forms (Figure 4). The boundary conditions are written down in the form of equality of the displacement and stress vectors on all possible boundaries of the medium

under consideration. The similitude criteria obtained permit one to employ modeling for studying the principles of seismic wave propagation and elastic wave movement in an explosion taking place in a solid quarry rock.

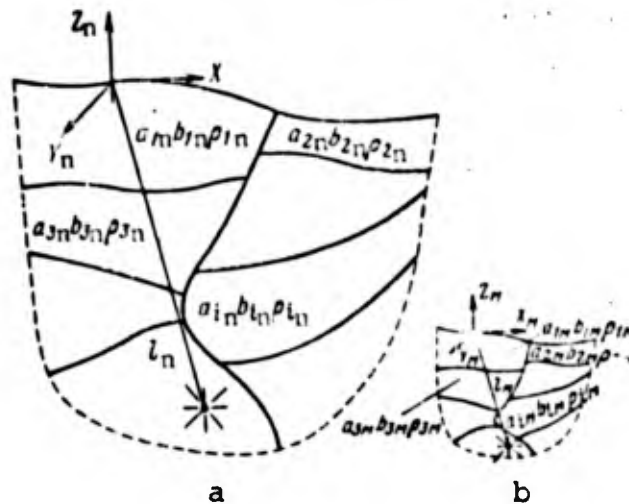


Figure 4. A diagram of the lumpy-inhomogeneous ideal medium model. (a) - nature; (b) - model.

In the propagation of stress waves in real media one must take account of the change in amplitude as a result of dissipative losses. In order to preserve similarity in the transient oscillations it is mandatory that the damping on some wavelengths in both nature and in the model are the same. The spatial damping coefficient of the wave for a fixed moment in time may be represented in the form  $e^{-\alpha x}$ , where  $\alpha = \omega/2cQ$  -- the amplitude absorption coefficient. The quantity  $1/Q = 2\alpha/\omega$  is the dimensionless damping coefficient. In order to obey similarity in processes connected with damping it is necessary that

$$Q_n = Q_m. \quad (43)$$

If  $\alpha$  is a fixed quantity, then from condition (43) it follows that

$$\frac{\alpha_n}{\alpha_m} = \frac{c_m \omega_n}{c_n \omega_m} = \frac{1}{\lambda_1}$$

i.e., the amplitude absorption coefficient in the model must be  $\lambda_l$  times larger. Therefore, in the modeling processes concerning the damping of stress waves, the material of nature (where  $\lambda_l$  is not equal to one) may not be used in the preparation of the model if the amplitude absorption coefficient does not depend on frequency. However, as is shown by studies in real materials, the amplitude absorption coefficient is a function of frequency. For the majority of solid state materials the amplitude absorption coefficient is proportional to frequency and the value of Q remains a constant. Values of Q for some solid materials are presented in Table 1 (according to data in Fizicheskaya akustika, (1963)). In these materials observance of similarity in damping processes is guaranteed when using the material of nature for the model ( $Q_n = Q_M$ ).

TABLE 1  
VALUES OF THE DIMENSIONLESS DAMPING COEFFICIENT  
FOR SOME MATERIALS

<u>Material</u>	<u>Q'</u>	<u>Frequency Region</u>	<u>Type of Excitation</u>
Pottsville Sandstone	7	100-900 Hz	Compression Impulses
Tyrro-Argillaceous Shale	23	50-450 Hz	Compression Waves
	10	20-125 Hz	Transverse Waves
Loose Martite Ore	12	300-500 Hz	Compression Waves
Ferrosilicate Shale	13	400-1000 Hz	"
Magnetic Hematite	53	600-1500 Hz	"
Silicate Shale	22	450-900 Hz	"
Granite (Quincy)	100	140-1600 Hz	Longitudinal Resonance
	150-200	140-1600 Hz	Flexing Resonance
Amherst Sandstone	52	930-12800 Hz	Longitudinal Resonance
Hanton Limestone	65	2800-10600 Hz	"
Sylvan Argillaceous Shale	73	3,4-12.8 kHz	"
Granite (Westerley)	79	50-400 kHz	Rayleigh Wave Impulses
Solenhofen Limestone	110	3-15 MHz	Compression Impulses
	190	3-9 MHz	Transverse Impulses
Soda-Lime Glass	1450	5,6-6,1 kHz	Longitudinal Resonance
	1340	3,6-64 kHz	Transverse Resonance

TABLE 1 (cont.)

<u>Material</u>	<u>Q'</u>	<u>Frequency Region</u>	<u>Type of Excitation</u>
Fused Silica	44500	5-15 MHz	Transverse Impulses
Copper	2180	2,5-30 kHz	Longitudinal Resonance
	4380	3,0-30 kHz	Transverse Resonance
Lead	36	1,6-15 kHz	Longitudinal Resonance
	34	1,0-9,0 kHz	Transverse Resonance
Steel	5000	5-10 Hz	Longitudinal Resonance
Aluminum	200000	1-200 kHz	"

Sometimes (water-saturated rocks) the amplitude absorption coefficient is proportional to the square of the frequency, and the damping coefficient  $1/Q$  is proportional to frequency. In Figure 5 the dependence of the damping coefficient on frequency is presented for sandstone with varying degrees of water saturation ("Physical Acoustics, 1968). The dependence of  $Q$  on frequency may be expressed in the following manner.

$$\frac{1}{Q} = \frac{1}{Q_0} + \omega k, \quad (44)$$

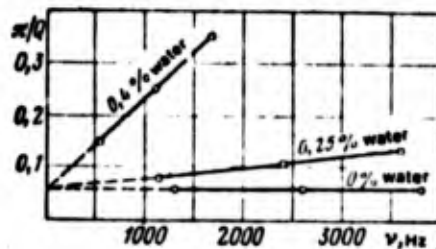


Figure 5. The logarithmic decrement of damping for sandstone with varying water contents.

$Q_0$  is the damping coefficient for  $\omega = 0$ . The value of  $Q_0$  is constant and is numerically equal to the damping coefficient in the dry material;  $k$  is a coefficient characterizing the dependence of absorption on frequency. Numerically  $k$  is equal to the tangent of the angle of inclination of the straight line  $1/Q = f(\omega)$  to

the axis of the abscissa. The value of  $k$  depends on the degree of water saturation of the rock.

From condition (44) it follows that

$$\frac{1}{Q_{nn}} + \omega_n k = \frac{1}{Q_{mm}} + \omega_m k_m. \quad (44A)$$

Equation (44A) allows one to establish similarity in damping processes for water saturated rocks. From condition (44) it is not difficult to find that

$$Q_{nn} = Q_{mm}, \quad \omega_n k_n = \omega_m k_m. \quad (45)$$

Hence

$$\frac{k_n}{k_m} = \frac{\omega_m}{\omega_n} = \lambda_t, \quad (46)$$

i.e., the value of  $Q$  for the dry material in nature and for the model must be the same, that the tangent of the angle of inclination of the straight line  $k$ , which characterizes the dependence of  $Q$  on frequency, in the material of the model must be  $\lambda_t$  times smaller than in nature. Taking account of the dependence of  $k$  on the degree of water saturation, modeling of damping processes and observance of the similitude conditions (45) and (46) may be attained by using as the model material the material of nature with the corresponding degree of water saturation. Providing the specified moisture content for the model under laboratory conditions does not cause any particular difficulties.

As a rule, when studying the action of an explosion in nature, it is necessary to solve volume problems. The complexity of preparing

volume models and the laboriousness of carrying out experimental investigations on such models induced investigators to replace volume models with plane models which represented layers which were cut out of the volume model. The transition to plane models demands that the formulation of such experiments be put on a sound basis. In some works (Vlasov, 1966) the feasibility and legitimacy of modeling volume problems on plane models is subjected to doubt on the basis of the difference in charge state of the material. The replacement of volume models with the corresponding plane models is equivalent to a replacement of the plane deformation by a plane charge state. In the work of G. N. Kuznetsov (1968) it is shown that in the majority of cases the error introduced by changing the charged state does not exceed 10%, i.e., it lies within the limits of measurement error or experimental investigation. Taking a look at deformations in the case of the plane charge state

$$\begin{aligned} \epsilon_{xx} &= \frac{1}{E} (\sigma_{xx} - \nu \sigma_{yy}), & \epsilon_{yy} &= \frac{1}{E} (\sigma_{yy} - \nu \sigma_{xx}), \\ \epsilon_{xy} &= \frac{2(1-\nu)}{E} \sigma_{xy} \end{aligned} \quad (47)$$

and of the plane deformation

$$\begin{aligned} \epsilon_{xx} &= \frac{1}{E} [(1-\nu^2) \sigma_{xx} - \nu(1+\nu) \sigma_{yy}], \\ \epsilon_{yy} &= \frac{1}{E} [(1-\nu^2) \sigma_{yy} - \nu(1-\nu) \sigma_{xx}], \\ \epsilon_{xy} &= \frac{2(1+\nu)}{E} \sigma_{xy}, \end{aligned} \quad (48)$$

by means of substituting

$$E = \frac{E}{1-\nu^2}, \quad \nu = \frac{\nu}{1-\nu}.$$

we bring equation (48) into a form analogous to equation (47), where  $E$  and  $\nu$  are elastic constants for the same material under conditions of plane deformation. Thus, a change in the charged state in the plane model is identical to a replacement of its elastic constants  $E$  and  $\nu$  by  $E'$  and  $\nu'$ . A change in the indicated constants leads to a change in the longitudinal wave propagation velocity  $c$  in the material. If we determine the ratio of two velocities - the longitudinal wave velocity  $c$ , calculated from the constants  $E$  and  $\nu$ , for a plane deformation, and the longitudinal wave velocity  $c'$ , calculated from the constants  $E'$  and  $\nu'$  for the generalized plane charged state,

$$\frac{c}{c'} = \sqrt{\frac{(1-\nu)^2}{1-2\nu}}, \quad (49)$$

We find that upon a change in the Poisson ratio  $\nu$  from 0.15 to 0.33 the ratio (49) changes from 1.02 to 1.10. Taking account of the fact that the errors in the remaining dynamic parameters are determined only by the measurement error in the stress wave propagation velocity, we come to the conclusion that it is possible to apply modeling of elastic wave motions in a three dimensional space with plane models.

Thus, in modeling the seismic action of explosions similarity of both elastic wave phenomena and damping processes of the seismic oscillations are not difficult to attain if the material of nature is used for the model material. However, in order to obtain quantitative dependences it is necessary to assure similarity of the explosive loading. In attempting to fulfill this condition, difficulties arise as the result of an insufficiency of experimental data on the parameters of shock waves originating at the charge-medium boundary for various constructions of the charges and types of explosive materials. Special attention should be given to similarity of explosive loading in the transition from volume models to the plane model since, along with other factors, in this case the conditions of the discharge of detonation products is substan-

tially changed, and effects relating to the whole charge are changed by effects relating to its parts.

Bases of Mathematical Modeling of Elastic Wave Motions Originating in An Explosion

The physical essence of the connection between mechanical and electrical fields is comprised in the fact that processes in these fields conform to the generalized laws of Newton, Ohm, and Kirchhoff, these laws being in actuality the manifestation of the laws of the conservation of energy and the continuity theorem. Translation of these laws into mathematical language leads to characteristic differential equations, and since these laws are applicable to mechanical and electrical systems, the corresponding differential equations are similar in form. The solution to the problem of propagation of stress waves turns out to be functions of continuously changing variables of the coordinate and time. A wave equation in the form

$$\frac{\partial^2 u}{\partial x^2} + \frac{\partial^2 u}{\partial y^2} + \frac{\partial^2 u}{\partial z^2} = \frac{1}{c^2} \frac{\partial^2 u}{\partial t^2} \quad (50)$$

may not be modeled, inasmuch as it is exceedingly difficult to build an analog with continuously changing properties. Therefore, the left-hand side of the equation is replaced by a finite difference approximation. In order to establish the physical sense of a finite difference approximation, let us write down the wave equation in the following form:

$$\frac{\partial^2 u}{\partial x^2} E + \frac{\partial^2 u}{\partial y^2} E + \frac{\partial^2 u}{\partial z^2} E = \frac{E}{c^2} \frac{\partial^2 u}{\partial t^2} = \rho \frac{\partial^2 u}{\partial t^2}, \quad (51)$$

where E is the modulus of elasticity of the material; ρ is the density of the material.

The second derivative with respect to coordinate  $x$  in the left-hand part of the equation represents the ratio of the difference between the first derivatives at two neighboring points to the distance between them, under the condition that this distance approaches zero.

$$\frac{\partial^2 u}{\partial x^2} = \lim_{\Delta x \rightarrow 0} \frac{\left(\frac{\partial u}{\partial x}\right)_{1'} - \left(\frac{\partial u}{\partial x}\right)_{2'}}{x_{1'} - x_{2'}}, \quad (52)$$

where

$$\Delta x = x_{1'} - x_{2'} = x_1 - x_0 = x_0 - x_2.$$

The first derivative  $du/dx$  in the first approximation may be considered as the ratio of displacement at two neighboring points to the distance between those points (Figure 6).

$$\left(\frac{\partial u}{\partial x}\right)_{1'} \approx \frac{u_1 - u_0}{\Delta x}, \quad \left(\frac{\partial u}{\partial x}\right)_{2'} \approx \frac{u_0 - u_2}{\Delta x}, \quad (53)$$

i.e., the numerator represents the absolute deformation of the medium along the  $x$  axis between points 1 - 0 and 0 - 2. The derivatives are related to the median point 1' and 2'. The ratio of the absolute deformation of an element of medium to its length represents the relative deformation of the medium. The product of the relative deformation of the medium (first derivative) with the modulus of elasticity of the material represents nothing other than the stress

$$\frac{\partial u}{\partial x} E = \sigma. \quad (54)$$

Then the second derivative may be considered as the difference in stresses at two neighboring points, which on the basis of Newton's second law is equal to the product of the acceleration and the density (right-hand part of equation (51)). Mathematically the

second derivative with respect to the coordinate axis may be written in the form

$$\frac{\partial^2 u}{\partial x^2} \approx \frac{\frac{u_1 - u_0}{\Delta x} - \frac{u_0 - u_{-1}}{\Delta x}}{\Delta x} = \frac{u_1 + u_{-1} - 2u_0}{\Delta x^2}. \quad (55)$$

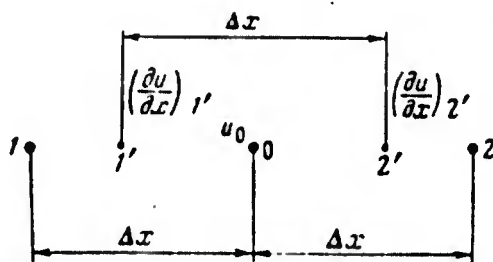


Figure 6. Diagram of a finite difference approximation of the wave equation.

For the one-dimensional case the finite difference approximation is written down in the form

$$\frac{\partial^2 u}{\partial x^2} \approx \frac{u_1 + u_{-1} - 2u_0}{\Delta x^2} \approx \frac{1}{c^2} \frac{\partial^2 u}{\partial t^2}. \quad (56)$$

Analogously for the two-dimensional equation

$$\frac{\partial^2 u}{\partial x^2} + \frac{\partial^2 u}{\partial y^2} \approx \frac{u_1 + u_{-1} - 2u_0}{\Delta x^2} + \frac{u_2 + u_{-2} - 2u_0}{\Delta y^2} \approx \frac{\partial^2 u}{\partial t^2}. \quad (57)$$

For the wave equation in three-dimensional space

$$\frac{\partial^2 u}{\partial x^2} + \frac{\partial^2 u}{\partial y^2} + \frac{\partial^2 u}{\partial z^2} \approx \frac{u_1 + u_2 - 2u_0}{\Delta x^2} + \frac{u_3 + u_4 - 2u_0}{\Delta y^2} + \frac{u_5 + u_6 - 2u_0}{\Delta z^2} = \frac{1}{c^2} \frac{\partial^2 u}{\partial t^2}.$$

In this manner, in the first approximation the continuous wave equation is replaced by finite differences of the displacement values at neighboring points.

In order to establish the analogy of equation (56) with equations describing the passage of a current in electrical circuits, let us consider the electrical networks represented in Figure 7. On the basis of Kirchhoff's first law in correspondence with the equations which determine the voltage, current, energy of a condenser with capacitance  $C$  and a coil with inductance  $L$ , for the typical node point we may write the equation

$$\begin{aligned} U &= \frac{1}{C} \int_{t_1}^{t_2} i dt + K; & U &= L \frac{di}{dt}; & i &= C \frac{dU}{dt}; \\ i &= \frac{1}{L} \int_{t_1}^{t_2} U dt + K; & E &= \frac{CU^2}{2}; & E &= \frac{Li^2}{2}. \end{aligned} \tag{58}$$

where  $C$  is the capacitance,  $L$  is the inductance,  $U$  is the electric potential at the point,  $i$  is the current in the circuit, and  $K$  is the initial charge on the condenser. For the node represented in Figures 7a, b, and c, the following relations are legitimate:

$$\frac{1}{L_1} \int (U_1 - U_0) dt + \frac{1}{L_2} \int (U_2 - U_0) dt = C_0 \frac{dU_0}{dt}; \tag{59}$$

$$\begin{aligned} \frac{1}{L_1} \int (U_1 - U_0) dt + \frac{1}{L_2} \int (U_2 - U_0) dt + \frac{1}{L_3} \int (U_3 - U_0) dt + \\ + \frac{1}{L_4} \int (U_4 - U_0) dt = C_0 \frac{dU_0}{dt}; \end{aligned} \tag{60}$$

$$\begin{aligned} & \frac{1}{L_1} \int (U_1 - U_0) dt + \frac{1}{L_2} \int (U_2 - U_0) dt + \frac{1}{L_3} \int (U_3 - U_0) dt + \\ & + \frac{1}{L_4} \int (U_4 - U_0) dt + \frac{1}{L_5} \int (U_5 - U_0) dt + \\ & + \frac{1}{L_6} \int (U_6 - U_0) dt = C_0 \frac{dU_0}{dt}. \end{aligned} \quad (61)$$

Differentiating all equations with respect to time we obtain

$$\frac{U_1 - U_0}{L_1} + \frac{U_2 - U_0}{L_2} = C_0 \frac{d^2 U_0}{dt^2}; \quad (62)$$

$$\frac{U_1 - U_0}{L_1} + \frac{U_2 - U_0}{L_2} + \frac{U_3 - U_0}{L_3} + \frac{U_4 - U_0}{L_4} = C_0 \frac{d^2 U_0}{dt^2}; \quad (63)$$

$$\begin{aligned} & \frac{U_1 - U_0}{L_1} + \frac{U_2 - U_0}{L_2} + \frac{U_3 - U_0}{L_3} + \frac{U_4 - U_0}{L_4} + \\ & + \frac{U_5 - U_0}{L_5} + \frac{U_6 - U_0}{L_6} = C_0 \frac{d^2 U_0}{dt^2}. \end{aligned} \quad (64)$$

when

$$L_1 = L_2 = L_3 = L_4 = L_5 = L_6 = L$$

the equations are written in the form

$$U_1 + U_2 - 2U_0 = LC \frac{d^2 U_0}{dt^2}; \quad (65)$$

$$U_1 + U_2 + U_3 + U_4 - 4U_0 = LC \frac{d^2 U_0}{dt^2}; \quad (66)$$

$$U_1 + U_2 + U_3 + U_4 + U_5 + U_6 - 6U_0 = LC \frac{d^2 U_0}{dt^2}. \quad (67)$$

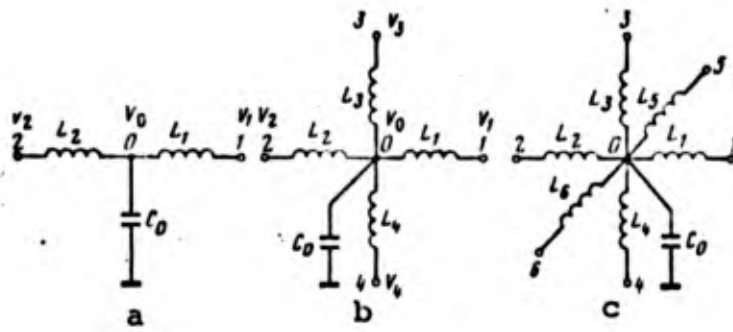


Figure 7. Node points of inductive-capacitive circuits. (a) one-dimensional; (b) two-dimensional; (3) three-dimensional.

Thus the circuits represented in Figures 7a, b, c are the electrical models of the points of the corresponding one-, two- and three-dimensional wave equations, since they describe the same relationships. Equations (56), (57) and (58) are easily transformed into the form (65), (66), and (67), if we set  $\Delta x = \Delta y = \Delta z = h$  and multiply both parts of the equation by  $h^2$ . Then the value  $LC_0$  will be the analog of  $h^2/c^2$ , where  $h$  is the chosen distance between points in the medium.

$$h/c = \sqrt{LC}. \quad (68)$$

The ratio  $h/c$  represents the time for propagation of a wave over the distance  $h$ , i.e., time is modeled with the aid of a corresponding choice of capacitance and inductance. If in the wave equation (51) the second derivative is considered as the ratio of difference in voltage in the medium between two points to the distance between them, then in equations (65), (66) and (67) the difference in potentials at two points in the model has been written on the left-hand side. Specifying the voltage at point 0 (see Figure 7a), measuring the potential at points 2 and 1 and introducing a coefficient of proportionality between the value of the voltage in the model and the displacement of a unit area into a unit length of the medium, we may determine the displace-

ment at two neighboring points in the real medium under study. If we compose a set, i.e., a region composed of separate electrical sections of the network, based on the results of a measurement of the voltage at any node point of the model, one may find the displacement at the corresponding point of the medium. In modeling with the aid of networks of electrical resistances, two approaches to the construction of a model are possible.

The first approach (physical) consists of the creation from the resistances of a network with contours which are geometrically similar to the modeled region. From the nominal values of the resistances of this network a determination is made of the scale factors which make it possible to convert from the values obtained for the electrical quantities to the parameters of the modeling medium.

The second approach (mathematical) consists of the setting up of a differential equation with partial derivatives describing the given process, and also the establishment of boundary and initial conditions. After that from the values of the network function which comes about as the solution of the finite difference equation obtained, a network of resistances is constructed. To sum up the circuit for electrical modeling may be represented in the following manner. A continuous unbroken medium is replaced by a network, either plane or spatial, of elementary discrete resistances, and inductances spread out along the coordinate axes. In each network potentials or currents are fed in to the junction points of the elements (node points), and the potentials which arise at other node points are then the desired quantities. Such a circuit integrates differential equations, and therefore the circuits are called integrators. In Figure 8 the fundamental circuit of an integrator is presented, where it is seen how the initial and boundary conditions are specified in modeling with electrical circuits. In order to measure the difference in potentials a dynamic recording apparatus (oscillograph) is hooked into the nodes of the circuit.

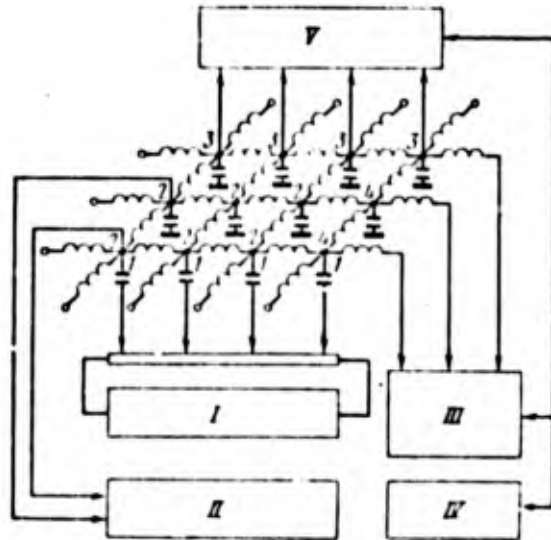


Figure 8. The fundamental circuit of an integrator. (I) - voltage source for establishing initial conditions; (II) - electron oscilloscope or dynamic compensating measuring apparatus; (III) - function generator for providing the boundary conditions; (IV) - device for dividing into periods; (V) - a bank of dischargers for the condensers.

In addition to modeling with electrical circuits, where the operation of the modeled apparatus is based on a direct correspondence between elements which accumulate energy and elements which disperse it -- a discrete equivalent of the prototype -- on the one hand, and electrical resistances, inductances and capacitances on the other hand, it is possible to model with electronic analyzers, in which the elements of the analyzer satisfy mathematical functions in order to obtain a solution. These computing devices are intended for the solution of systems of ordinary differential equations and differential equations in partial derivatives. Besides, in these apparatuses such mathematical functions as summation, subtraction, multiplication, and integration are performed, as well as the formation of arbitrary functions. The basic element of an electronic computing device is the computing amplifier, whose schematic representation is presented in Figure 9.

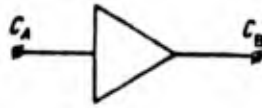


Figure 9. Symbolic representation of the Computing Amplifier.

In the operation of an electronic amplifier as a computing device the elements of feedback  $Z_f$  and input resistance  $Z_i$  are joined in accordance with the schematic shown in Figure 10. Since the current of the amplifier circuit is insignificant, the current  $i_1$  flowing through the input resistance  $Z_i$  is equal to the current  $i_2$  to the feedback resistance  $Z_f$ . The equation for the node A has the form

$$i_1 = i_2 = i, \quad \frac{e_1 - e_A}{Z_i} = \frac{e_A - e_0}{Z_f},$$

but, on the other hand, the voltage  $e_A$  is related to the voltage at the output of the amplifier

$$e_A = -\frac{e_0}{k} \approx 0,$$

where  $k$  is the amplification factor (approximately equal to 15,000), and the voltage  $e_A$  in view of the large amplification factor, may be considered negligible. Consequently, the output voltage

$$e_0 = -\frac{Z_f}{Z_i} e_1.$$

If the feedback resistance  $Z_f$  and the input resistance  $Z_i$  have the same value, then the output voltage  $e_0$  is equal to the negative of the input voltage  $e_1$ . In this case using the circuit under consideration the operation of sign reversal is being accomplished. If one of the two resistances is chosen to be variable, as shown in Figure 10b, then the input voltage may be multiplied by an arbitrary negative quantity which is determined by the ratio

of the feedback resistance to the input resistance in accordance with the expression

$$e_0 = -\frac{R_f}{R_1} e_1.$$

The input of the amplifier may be connected with a large number of input resistances (See Figure 10c). The output voltage in this case is equal to

$$e_0 = -R_f \left( \frac{e_1}{R_1} + \frac{e_2}{R_2} + \frac{e_3}{R_3} + \dots + \frac{e_n}{R_n} \right).$$

Inasmuch as the output voltage is proportional to the sum of input voltages, this circuit is called a "summator" and is used in the summation of two or more quantities. Incorporation of a capacitor  $C_1$  in place of the feedback resistance, as shown in Figure 10d, leads to the following result:

$$e_0 = -\frac{1}{R_1 C_1} \int e_1 dt + K.$$

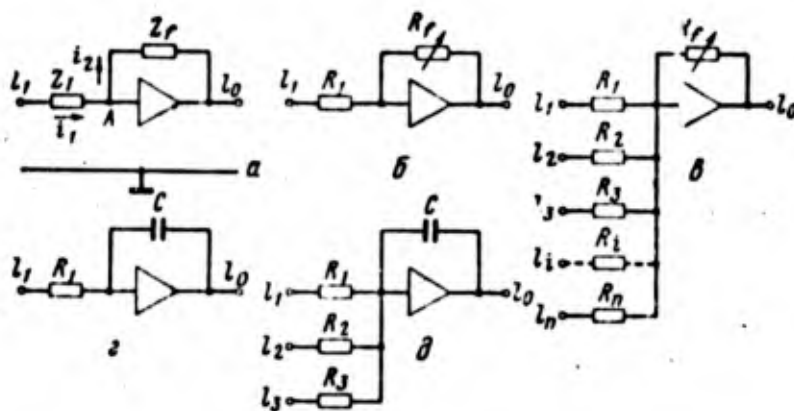


Figure 10. Computing Amplifier. (a) Fundamental computing network; (b) multiplication by a constant; (c) summation; (d) integration; (e) summator with integrator.

Consequently the output voltage is proportional to the negative value of the integral over time of the input voltage. Constant K represents the output voltage at the time  $t = 0$  and determines the initial condition of the voltage up to which the capacitor must be charged prior to the beginning of the computational process. For this purpose a special relay and a constant current source are usually employed. The summation and integration operations may be combined with the aid of a circuit (See Figure 10e), in which the output voltage is equal to .

$$e_0 = -\frac{1}{C} \int_0^{t_1} \left( \frac{e_1}{R_1} + \frac{e_2}{R_2} + \frac{e_3}{R_3} \right) dt + K.$$

The operations of sign change, multiplication by a constant, summation, and integration together with the corresponding input and output devices allow one to solve any systems of ordinary linear differential equations with constant coefficients. For an example let us consider the solution of the wave equation (50) using an electronic analyzer. This equation may be set down in the form

$$\frac{u_1 + u_2 - 2u_0}{h^2} = \frac{1}{c^2} \frac{\partial^2 u_0}{\partial t^2}, \quad (69)$$

$$\frac{u_1 + u_2 + u_3 + u_4 - 4u_0}{h^2} = \frac{1}{c^2} \frac{\partial^2 u_0}{\partial t^2}, \quad (70)$$

$$\frac{u_1 + u_2 + u_3 + u_4 + u_5 + u_6 - 6u_0}{h^2} = \frac{1}{c^2} \frac{\partial^2 u_0}{\partial t^2}, \quad (71)$$

where  $h = \Delta x = \Delta y = \Delta z$ .

Or

$$u_0 = \frac{c^2}{h^2} \iint (u_1 + u_2 - 2u_0) dt^2, \quad (72)$$

$$u_0 = \frac{c^2}{h^2} \iint (u_1 + u_2 + u_3 + u_4 - 4u_0) dt^2, \quad (73)$$

$$u_0 = \frac{c^2}{h^2} \iint (u_1 + u_2 + u_3 + u_4 + u_5 + u_6 - 6u_0) dt^2. \quad (74)$$

Let us take a look at equation (72). The value of  $U_0 = f(t)$  is obtained as a result of a double integration with respect to time of the sum under the integral  $u_1 + u_2 - 2u_0$ . Consequently, the circuit for the node point of the differential analyzer must consist of a summator at the input of which the voltages  $U_1$ ,  $U_2$ , and  $-2U_0$  is fed in, and two 0-integrators. The node point of an electronic analog circuit for modeling the one-dimensional wave equation is shown in Figure 4. At the input of the first integrator (I) (point A, Figure 11) there is fed a voltage, whose value corresponds to the second derivative with respect to time. After integration at the integrator (I) the value of the output voltage corresponds to the value of the first derivative with respect to time. This voltage with the opposite sign (since an integrator reverses the sign upon integration) is fed into the input of the second integrator (II). At the output of integrator II (point B) we have the voltage  $-U_0$ . The voltages  $-2U_0$ ,  $U_1$ , and  $U_2$  are fed into the summator (III), which permits the voltage  $U_1 + U_2 - 2U_0$  to be obtained at the output. The value of this voltage corresponds to the function under the integral in equation (72). Thus, at point A we have the relationship

$$U_1 + \dot{U}_2 - 2U_0 = \frac{h^2}{c^2} \frac{\partial^2 U_0}{\partial t^2},$$

whence

$$U_0 = \frac{c^2}{h^2} \iint (U_1 + U_2 - 2U_0) dt^2.$$

By connecting an oscilloscope or any other recording device to the output of the differential analyzer, one may trace the change in output voltage ( $-U_0$ ) in time  $U_0 = f(t)$ . At  $t = t_1$ ,  $U_0 = U_1$ , but at  $t = t_2$ ,  $U_0 = U_2$ . Since the voltages  $U_1$  and  $U_2$  are proportional to the displacement at points 1 and 2 of the real medium, the change in time of the displacement in the medium between the first and second points is found from the change in output voltage  $U_0 = f(t)$ .

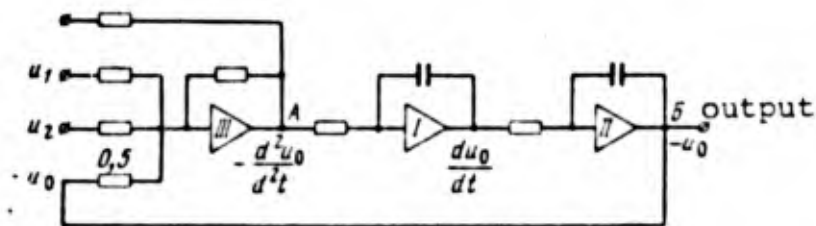


Figure 11. Typical Differential Analyzer Block for Solving a Wave Equation.

In the modeling of complex dynamic processes it is sometimes convenient to combine the electronic analyzers and the circuit devices into one apparatus.

The principle of mathematical modeling which we have just considered makes it possible to solve questions of modeling elastic wave displacements in an absorbing medium. In order to model the parameters of seismic oscillations in an absorbing medium, B. N. Ivakin (1958) employs various models of the medium depending on the mechanism of absorption. An absorbing elastic medium may be represented in the form of an infinite network of infinitesimally small mechanical quadripoles. A macroscopic continuous one-dimensional mechanical model of an elastic medium is shown in Figure 12a; it consists of (to a known degree arbitrary) mechanical impedances  $Z_{10}^m$  and  $Z_{20}^m$ , called respectively the parallel and series arms of the infinites-

imally small mechanical quadripole. For such a model the equation of motion may be written down in operator form

$$\frac{d^2 v}{dx^2} = (q_0^M)^2 v, \quad \frac{d^2 P}{dx^2} = (q_0^M)^2 P, \quad (75)$$

where  $v$  is the displacement velocity;  $P$  is the pressure;  $q_0^M$  is the propagation constant

$$q_0^M = \sqrt{\frac{Z_{10}^M}{Z_{20}^M}} = f(P_x). \quad (76)$$

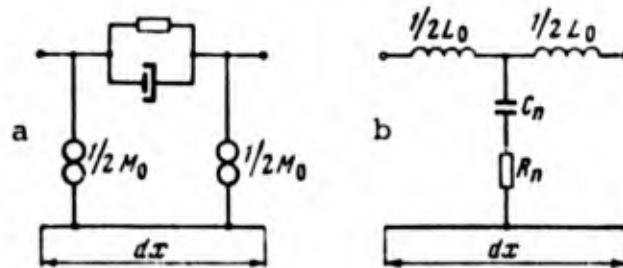


Figure 12. A macroscopic continuous model of an absorbing elastic medium. (a) - mechanical; (b) - electrical.

Consequently the propagation constant of the mechanical model is expressed in simple enough manner in terms of the impedance of the quadripole arms and is a function of the Heaviside operator  $P_x = d/dt$ , if the impedances of the arms are given in operator form. In equation (76) all the quantities are related to the unit of length

$$q_0^M = \frac{q^M}{dx}; \quad Z_{10}^M = \frac{Z_1^M}{dx}; \quad Z_{20}^M = Z_2^M dx. \quad (77)$$

When  $\Delta x \rightarrow 0$  we pass from the mechanical network model over to the macroscopic continuous model. When that happens the wave impedances  $W_{II}^M$  and  $W_I^M$  take the form

$$\frac{P}{v} = W_n^M = W_r^M = \sqrt{Z_{10}^M Z_{20}^M}, \quad (78)$$

where  $P$  and  $v$  are the pressure and displacement velocity at some point in the continuous one-dimensional model.

Thus, for a continuous mechanical model of a non-ideally elastic medium we have in the most general form the following equations.

1. The equation of motion in operator form (75) (written for the displacement velocity  $v$  and for the pressure  $P$ ), where the propagation velocity  $q_0^m$  is expressed in terms of the impedance of the arms of the model  $Z_{10}^m$  and  $Z_{20}^m$  (in accordance with equation (76)).
2. The equation (78) connecting the displacement velocity  $v$  and the pressure  $P$  in a continuous model, coming about as the result of the known relation between the displacement and the mechanical stresses in elastic media.

Comparing the equations (75) and (78) which have been obtained with the corresponding equations of a non-ideally elastic medium, one may determine unambiguously the desired models for the elastic medium. The electrical model of an elastic medium may be obtained if we utilize the first system of electromechanical analogs in the form worked out by G. A. Gamburtsev. In accordance with this system, there exists between the mechanical and electrical quantities the following analogy:

$$P \sim U; v \sim I; H \sim R; m \sim L; k \sim 1/C,$$

where  $P$ ,  $v$ ,  $H$ ,  $m$  and  $k$  are respectively the pressure, displacement velocity, mechanical friction, mass, and rigidity, and  $U$ ,  $I$ ,  $R$ ,  $L$ , and  $C$  are respectively the electrical voltage, current, resistance, self-inductance, and capacitance. In accordance with the first system of analogies we find the electrical analogs (Figure 12b) of the mechanical model. To serve as an example let us consider models of a visco-elastic medium.

Let us write down the equation of motion (Deryagin, 1932) for a visco-elastic medium in the case of a plane longitudinal wave

propagated in the direction of the X axis:

$$\rho \frac{\partial^2 u}{\partial t^2} = (\lambda_B + 2\mu_B) \frac{\partial^2 u}{\partial x^2} + \frac{4}{3} \eta \frac{\partial^2 u}{\partial x^2 \partial t}, \quad (79)$$

where  $\rho$  is the density,  $\lambda_B$  and  $\mu_B$  are the Lamé constants,  $u$  is the displacement of particles of the medium along the X axis, and  $\eta$  is the coefficient of viscosity of the medium. We differentiate equation (79) with respect to  $t$  and denote the displacement velocity of particles of the medium  $v = du/dt$

$$\rho \frac{\partial^2 v}{\partial t^2} = (\lambda_B + 2\mu_B) \frac{\partial^2 v}{\partial x^2} + \frac{4}{3} \eta \frac{\partial^2 v}{\partial x^2 \partial t}. \quad (80)$$

Applying null initial conditions, we put equation (80) into operator form

$$\frac{\partial^2 v}{\partial x^2} = \left( \frac{P_x^2}{a_B^2 + \frac{4\eta}{3\rho} P_x} \right) v, \quad (81)$$

where

$$a_B = \sqrt{\frac{\lambda_B + 2\mu_B}{\rho}}.$$

Comparing (81) and (75), we find the first equation which connects the impedances of the arms  $Z_{10}^m$  and  $Z_{20}^m$  of the desired model with the parameters of the visco-elastic medium:

$$q_{m0}^2 = \frac{Z_{10}^m}{Z_{20}^m} = \frac{P_x^2}{a_B^2 + \frac{4\eta}{3\rho} P_x}. \quad (82)$$

It is assumed that the density of the medium does not affect the wave absorption and that all dissipative losses come as a result of its non-ideal elasticity. Then

$$Z_{10}^M = \rho \cdot M_0 = P_x \rho. \quad (83)$$

Furthermore

$$Z_{20}^M = \frac{a_n^2}{\rho P_x} + \frac{4}{3} \eta = Z_k + H_n, \quad (84)$$

where symbols for the impedances  $Z_k$  and  $H_n$  have been introduced,

$$Z_k = \frac{a_n^2}{\rho P_x} = \frac{k_n}{P_x}, \quad H_n = \frac{4}{3} \eta. \quad (85)$$

The relations between the visco-elastic medium parameters and its mechanical model are found from equations (83) and (85):

$$\rho_0 = M_0, \quad \lambda_n + 2\mu_n = k_n; \quad \frac{4}{3} \eta = H_n, \quad a_D = \sqrt{\frac{k_n}{M_0}}.$$

and the structure of the series arm of the mechanical model is found from equation (84). Starting from the results just obtained and taking account of the fact that in equation (84) the impedances are summed, the elastic impedance  $Z_{k_n}$  and the active impedance  $H_n$  are introduced in parallel fashion and we construct the model of the medium according to Figure 13 (in the electrical model the capacitive impedance  $Z_{C_n}$  and the active impedance  $R_n$  is inserted in series). In Figure 13 the mechanical (a) and electrical (b) models of a visco-elastic medium are represented. In this representation, in accordance with the first system of electromechanical analogs, the relations between the parameters of the visco-elastic medium and the electrical model take the form

$$\hat{\rho} = L_0, \quad \lambda_D + 2\mu_D = \frac{1}{C_n}; \quad \frac{4}{3} \eta = R_n; \quad a_D = \frac{1}{\sqrt{L_0 C_n}}. \quad (86)$$

The equations of motion for the mechanical and electrical models (see Figure 13) are found from the dependencies which determine the value of the arm impedances of the models and from equation (75). In the end we obtain the equations of motion

$$\frac{\partial^2 v}{\partial t^2} = \frac{k_n}{M_n} \cdot \frac{\partial^2 v}{\partial x^2} + \frac{H_n}{M_n} \frac{\partial^3 v}{\partial x^2 \partial t} \quad (87)$$

$$\frac{\partial^2 v}{\partial t^2} = \frac{1}{L_n C_n} \cdot \frac{\partial^2 v}{\partial x^2} + \frac{R_n}{L_n} \frac{\partial^3 v}{\partial x^2 \partial t} \quad (88)$$

which are analogous to the equation for a visco-elastic medium (79). Knowing the arm impedances  $Z_{10}$  and  $Z_{20}$  of the model of a visco-elastic medium, it is not difficult to determine the wave impedance for the model, using relationship (78):

$$W = \sqrt{M_n k_n} \sqrt{1 + P_x \frac{H_n}{k_n}} \quad (89)$$

$$W^a = \sqrt{\frac{L_n}{C_n}} \sqrt{1 + P_x R_n C_n} \quad (90)$$

Using the relationships between the parameters of the medium and the model, we find the value of the wave impedance for a visco-elastic medium:

$$W = \rho a_{11} \sqrt{1 + P_x \frac{4\eta}{3(\lambda_{11} + 2\mu_{11})}}$$

Consequently the given method provides a way to model the absorption of elastic waves in viscous media if the parameters of the model are chosen in the corresponding way.

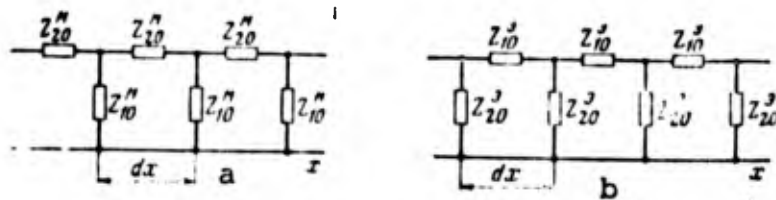


Figure 13. A construction of a section of the model of a visco-elastic medium. (a) - mechanical; (b) - electrical.

Making use of electronic analyzers and vacuum tube devices, it is possible to solve the problems of stress wave propagation in ideally elastic and absorbing media. The spread of a series of problems, soluble with the aid of mathematical modeling, was promoted by the creation of special analyzers. In recent years a series of electronic analyzers and vacuum tube devices have been developed. One example is a computer which solves a system of equations of the sixth degree -- a modeling machine, the coarsest type of modeling device, having 400 operational amplifiers. In order to solve biharmonic equations the model of an analyzer has been worked out. There are also other models that may be used effectively for solving problems connected with elastic wave motions.

#### Fundamentals of Physical Modeling of Crushing and Other Types of Damage to Rock

The process of destruction of rocks is one of the most complex phenomena taking place in an explosion. This complexity helps to explain the large number of works which have been devoted to various questions dealing with damage to friable materials under impulsive loads. Physical modeling plays a special role in investigations of these questions. Theoretical questions concerning the modeling of the processes of crushing and damage to rock as well as methods for laboratory experimentation have been considered in the works of Professor G. I. Pokrovskiy (1957, 1968), Professor O. Ye. Vlasov (1962, 1966), Doctor of Engineering Science G. P. Demidyuk (1960, 1962, 1968) and in other works.

The accumulation of experimental material from the investigation of explosive action under laboratory conditions with models and from the production of industrial explosions has made it possible to establish the basic parameters and the degree of their influence on the destruction process, and to make a series of well-grounded assumptions.

The effect of the design of the charge on the explosive impulse parameters and on the process of destruction of rocks in an explosion was established in the works of academician N. V. Mel'nikov and Doctor of Engineering Science L. N. Marchenko (1960, 1963, 1964). The results of these investigations carry a large significance not only for the development of methods of increasing the beneficial use of explosive energy for crushing, but also for assuring the similitude of the explosive loading in the modeling of explosive action.

The large volume of experiments performed in the explosive works laboratory of the A. A. Skochinskiy Mining Institute under the leadership of L. I. Baron (1962) made it possible to study the particulars of the destruction mechanism and the local distribution of grain-size composition of the shattered material as a function of its strength. The results of the experimental studies are set forth also in the engineering science doctoral thesis of Ye. T. Maksimova (1958).

Questions of the mechanism of explosive action is also dealt with in a series of works by Professor G. P. Demidyuk (1965, 1964) and Professor M. F. Drukovanyy (1965). In the indicated works consideration is given to a question of the effect of the explosive loading parameters on the course of the destruction process, a treatment which allows one to work out methods for guaranteeing similarities in the destruction process for modeling and in nature.

A. N. Khanukayev (1962, 1961), V. N. Mosinets (1969), and Ye. G. Baranov (1969) carried out experiments studying the effect of

stress waves on the destruction process and investigated stress wave parameters in an explosion in several types of rocks at different distances from the charge center, studies which make it possible in a series of cases to establish the similitude conditions for explosive loading.

The investigations just mentioned, along with other works, serve as a groundwork for the development of the following methods for physical modeling of the processes of crushing and other damage to rock:

- 1) The method based on the similitude of elastic wave motions;
- 2) The method utilizing energetic similarity;
- 3) The method of equivalent materials.

A. Modeling of the process of damage to rocks by an explosion by using an elastic model of the medium.

In the majority of cases by destruction or damage we mean destruction of the structure of the material. The maximum tensile stress at which the material still retains its continuity is called the strength. The end result of the destruction process is the crushing or shattering of the material, which is characterized by having grain-size composition. A mean indicator of the intensity of crushing is given by the dimension of an average fragment.

The similitude of elastic wave motions may be used in modeling the destruction processes, if one makes the following assumptions:

- 1) Just before undergoing destruction the material behaves like an elastic material;
- 2) The destruction process proceeds instantaneously, and the intensity of crushing is determined only by the magnitude of the stresses.

One result of the first assumption is the existence of a definite material strength  $[\sigma]$ , up to which the stresses are related to

deformation by a linear dependence. As for all stresses, relation (42) must be satisfied for tensile strength. Therefore, we may write down

$$\frac{|\sigma|_n}{|\sigma|_M} = \lambda_n. \quad (91)$$

The second assumption assumes the absence of a redistribution of stresses during the destruction process and the identity of stresses independently of the dimensions of the model as similitude in the loading is obeyed, i.e., in observance of the condition

$$\frac{\sigma_{\max n}}{\sigma_{\max M}} = \frac{|\sigma|_n}{|\sigma|_M} = \lambda_n. \quad (92)$$

On the model the same quantity of fragments of shattered material will be found as in nature. Use of the method just considered for modeling the destruction process does not cause any difficulties in determining the similitude criteria. The basic difficulties arise in the practical realization of the indicated conditions.

The first difficulty is caused by the necessity of maintaining the definite relationships between the constants of the modeled material, since the velocity, density, and stress scales must satisfy assumption (42). This condition is fulfilled if the durability of the material is proportional to the moduli of elasticity, and the coefficient of proportionality is the same for both nature and the model. As studies have shown, for some tough types of rocks and materials such a proportionality is observed and in a series of cases these difficulties are eliminated. Moreover, in choosing the modeled material it is possible to use the actual material of nature, and then all conditions are satisfied if one neglects the influence of the scale factor on the strength.

Comparatively large difficulties arise in attempting to realize the second assumption. When we take account of the fact that the destruction process lacks a finite interval of time, it is not

possible to avoid redistribution of stresses in the process of crack-formation. Besides, combination of condition (92) with the similitude condition for crushing without supplementary requirements placed on the characteristics of the material leads to contradictory deductions. In order to show the contradiction contained in this assumption without resorting to complex mathematical calculation, let us use a somewhat idealized but a sufficiently easy to understand example. Let us consider the destruction process for two cubes of different dimensions but prepared from the same material (Figure 14). With complete justification we may consider the large cube (with edge  $2a$ ) to be associated with nature, and the small cube (with edge  $a$ ) associated with the model. Let us suppose that under the action of a plane stress wave at all points in nature there arises the same stresses  $\sigma_{On}$ , as a result of which the cube is shattered into 24 approximately equal pieces. If we mentally cut a cube with edge  $a$  from nature, it will be fragmented into approximately three parts. In order to obtain the disintegration which is similar to nature, in accordance with equation (42), it is necessary in the model to create the same stresses ( $\sigma_{OM} = \sigma_{On}$ ). In doing this, in light of the second assumption, we must obtain a similar disintegration, i.e., the model must be fragmented into 24 approximately equal pieces. Thus, we are led to the conclusion that the same volume of one and the same material subjected to the same stresses is crushed into a different number of pieces (3 and 24). This deduction contradicts the initial assumption which says that the process of fragmenting the material is determined only by the value of the maximum stresses. In order to remove this lack of agreement, it is necessary to impose supplementary requirements on the material of the model, requirements which may be established on the basis of the statistical theory of damage.

One should not identify similitude of shattering with similitude of the dimensions of the damage zone. Similitude in the dimensions of the damage zone is related to the modeling of the durability theory problem and not damage theory problems. As is well known,

problems in the theory of durability differ from problems in damage theory in that in problems of the latter type it is required only that answers be found to the question: Is the structure or the continuity of the material preserved under the given loading? In this regard it is absolutely immaterial how the continuity shall be disrupted. In determining the dimensions of the damage zone one should show at what minimum distance from the charge the material retains its continuity. In order to model a similar problem in the theory of durability (conditions (42) and (92)), it is sufficient to preserve similarity in the dimensions of the damage zone. In this case the intensity of fragmentations in nature and in the model may differ substantially. Similarity of the dimensions of the damage zone may be used as the method of indirect determination of the conditions of similar loading in the study of elastic wave phenomena, since it implies similarity in the value of the initial displacement. Considering that the value of the damage zone is proportional to the value of the initial displacement and the modulus of elasticity, and inversely proportional to the value of the fragmenting stresses, we may write

$$r = k u_0(E) / (\sigma).$$

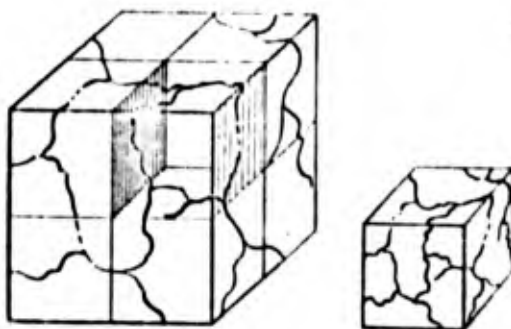


Figure 14. Fragmentation of cubes of different dimensions.

From the similitude condition

$$\frac{u_{on}}{u_{om}} = \frac{r_{II}}{r_M} \frac{|\sigma|_{II}}{|\sigma|_M} \cdot \frac{E_M}{E_{II}},$$

i.e., under conditions (91) and (92),  $u_{on}/u_{om} = \lambda_\ell$  are obeyed. However, employing similitude in the damage zone, we may establish similitude only in the value of the stresses, but this does not indicate similitude in the stress pulse duration, since the stress pulse duration in the material does not affect the dimensions of the damage zone, but influences only the intensity of fragmentation in the media without absorption. Considering the complex dependence of the fragmentation intensity on duration, it is necessary to utilize the results of experimental measurements in order to establish similitude of the duration of loading.

When carrying out laboratory investigations it is necessary to adjust the value of the stresses and the duration of the explosive action in order to have similitude observed in the explosive loading. To a considerable degree the value of the stresses depends on the characteristics of the explosive material, the construction of the charge, and also the time duration of a pressure pulse in the charging chamber as well as on the transformation conditions of the shock wave in the concrete block. Let us find the effect of the separate factors on the value of stresses in an explosion in order to ease the adjustment condition in the performing of laboratory investigations. The value of the maximum stresses depends on the detonation velocity of the explosive material and on the charging density. Up to a well-defined limit (which depends on the acoustic rigidity and the durability of the material) the value of the maximum stresses which occur at the wall of the charging chamber is proportional to the impedance of the explosive material ( $\rho D$ ). An increase in the peak pressure in the charging chamber still does not imply a proportional growth in the maximum stresses

in the rock. In order to obtain a proportionality between these quantities it is necessary to guarantee a corresponding duration of the existence of pressure in the charging chamber.

A pulse of the shortest duration for the same stresses carries the least energies. If the medium is ideally elastic, the value of the maximum stresses for various durations will be the same. In real media upon propagation of the stress pulses a part of the energy is expended in dissipative losses, connected with the non-ideal nature of the medium and with the damage. The dissipative losses depend on the frequency characteristics of the stress pulse. The frequency characteristics of the pulse may be established with the aid of a Fourier transformation. A shorter pulse contains in its spectrum higher frequency oscillations, which are absorbed more intensely. A clear illustration of the damping intensity of various frequency oscillations may be given in the following manner.

We consider a region through which stress waves pass in the block with a frequency  $\omega_0$  and  $2\omega_0$  and with the same initial amplitude  $\sigma_0$  (Figure 15). It is seen in the figure that twice as many wavelengths with frequency  $2\omega$  are enclosed in a transverse section than with  $\omega$ . As shown earlier (according to the data of the work "Physical Acoustics," 1968), the reduction in oscillation amplitude over unit wave lengths for hard materials has a constant value. Let us suppose that in each oscillation the amplitude decreases by a factor of 1.1. Then the oscillation amplitude at the end of the region for a wave with frequency  $\omega_0$  is reduced by  $(1.1)^n$  times (where  $n$  is the number of wavelengths enclosed in the region), and for a wave with frequency  $2\omega_0$  it is reduced by  $(1.1)^{2n}$  times, since the wave accomplishes twice as many oscillations in the region under consideration. In the illustrated example,  $n = 4$ ;  $2n = 8$ . Correspondingly the amplitude in the wave with frequency  $\omega_0$  decreases by 1.46 times, and in the waves with frequency  $2\omega_0$  by 2.14 times. By looking at the peculiarities of the fre-

frequency spectrum of pulses of different durations, it is not difficult to find the difference in their damping. A pulse of duration  $\tau_0$  has a spectral width of

$$B_1 = \frac{1}{\tau_0}.$$

This indicates that in the pulse spectrum all frequencies from zero to  $B_1$  are found. For a pulse duration of  $2\tau_0$ , the spectral width is shortened

$$B_2 = \frac{1}{2\tau_0}.$$

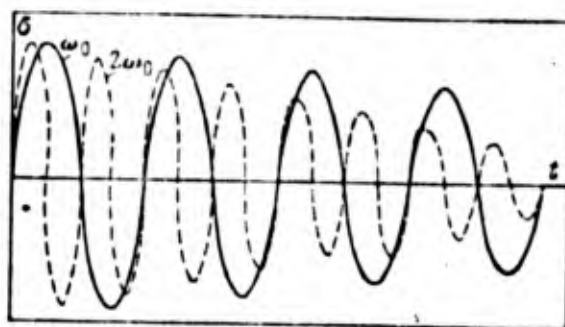


Figure 15. The damping of waves of different frequencies in an absorbing medium.

If we consider the fact that a pulse of longer duration carries also a greater amount of energy, then the amplitude of oscillations of the same frequency in a pulse of longer duration will be considerably greater. Therefore, in the propagation of pulses the amplitudes of oscillation with frequencies from  $B_2$  to  $B_1$ , which are characteristic only of a short pulse, are damped more intensely, but the components with frequencies from 0 to  $B_2$  are nevertheless damped the same, although the initial amplitude of these components are significantly smaller for a short pulse.

Therefore, in the propagation of a short pulse the widths of the spectrum is reduced to the spectral widths of a longer duration pulse, but the amplitude is significantly lower. Consequently a short pulse is damped more intensely owing to the absorption of high-frequency components.

Based on the above damping mechanism for stress waves we are led to the deduction that it is necessary to observe similitude of pulse duration not only for time similitude of elastic wave phenomena, but also for similitude in the value of the maximum stresses, inasmuch as this similitude may not be attained at all points in the model, if similitude is not obeyed in time. A change in the duration of loading may be effected by a change in the construction of the charge. By using charges with air gaps it is possible to increase the duration by a factor of 1.3 to 1.4. A lengthening of the pulse leads to an increase in the damage zone dimensions on account of the reduction in damping of maximum stresses. According to the data of the work of N. V. Mel'nikov and L. N. Marchenko (1964), if charges with air gaps are used the uniformity of fragmentation is also increased, an observation which testifies to the smaller absorption of energy of stress waves in the neighboring zone. The length of the pulse depends also on the number of detonation products formed and on the conditions of their discharge. The number of detonation products formed may be controlled by using composite charges consisting of explosive materials which give off various quantities of detonation products in an explosion. A substantial difference in the quantity of liberated gases characterizes lead azide and mercury fulminate in comparison with other explosive materials (PETN - pentaerythryl tetranitrate, hexogen, tetranitromethylaniline). Furthermore the duration of the discharge depends on the density of detonation product occlusion in the charging chamber. The density of occlusion is determined by the material and the magnitude of stemming. Thus creating a situation of similar loading is a complex

problem, whose solution permits one in the first approximation to establish similitude of the damage zone dimensions. In order to have similitude obeyed more precisely a large volume of preliminary investigations into the effect of various factors on the stress pulse parameters must be performed. In this connection one should mention the very hopeful prospects for exploiting means of creating pulses with specified parameters under laboratory conditions: electrohydraulic impact and electrical breakdown. In both cases the shock wave parameters may be controlled by the value of the voltage and the parameters of the electrical system (capacitance, inductance, etc.). Certain difficulties arise in changing the duration of a voltage pulse. This situation is explained by the fact that after the electrical breakdown the basic energy is consumed in heating the surrounding medium and is not transformed into the energy of a shock wave, a fact which prevents one from obtaining the desired increase in the loading duration. Therefore, increasing the duration of the electrical discharge does not lead to the hoped for increase in loading duration. We should attribute to the deficiencies of this method the emergence of powerful electromagnetic fields in the discharge, complicating the process of working the electronic recording apparatus. The possibilities and the peculiarities of the indicated method are reviewed in a series of works by G. I. Pokrovskiy, N. A. Vlatin, and others. The large amount of attention which has been given to similitude of explosive loading comes about because of the fact that lack of observance of this condition in modeling may lead to erroneous results. In the work by Kucheryavyy et al (1962) the proper attention was not paid to observance of the similitude conditions of explosive loading, particularly in the transition from the volume to the plane model. In this regard it was proposed that one look at the model as a diminutive copy of a layer of the rock cut out mentally and it was considered that similitude in loading was guaranteed automatically. However, in this case the conditions under which the detonation products are discharged are changed in an essential

manner and there is no account taken of the action of the remaining part of the charge on the cut-out layer, a situation which leads to non-identical damage. The results of experimental investigations carried out by O. Ye. Vlasov and S. A. Smirnov (1966) demonstrate this point very well. In exploding a piece of detonation fuse (DF) in a plate of organic glass of thickness 34 mm (the diameter of the fuse was 5.5 mm) the radius of the damage zone amounted to 40 mm. It would seem that by cutting out of such a plate a model of thickness 9 mm and making sure that all other conditions were equal with respect to the geometry of the model, we should obtain the same radius of the damage zone. However, the damage zone radius in the explosion of a plate of thickness 9 mm decreases to 20 mm. The length of the piece of DF in both cases was equal to the thickness of the plate. These experiments testify to the necessity of observing similitude conditions not only in geometrical dimensions and in properties of the medium, but also in the parameters of explosive loading.

One method for using the modeling in the solution of important problems arising in the design of large-scale explosions, based on the similitude of elastic wave motions, was worked out by G. I. Pokrovskiy (1969). In the first approximation it was presumed that the detonations of elements of the medium would be similar in the explosion of two charges, analogous in form and in chemical composition but differing in magnitude, with the same material for nature and for the model, and under the conditions of similar arrangement of the elements of the medium under consideration. For charges of the same shape the volume and weight are proportional to the cube of the linear dimensions

$$Q = kl_0^3, \quad (93)$$

where  $l_0$  is the characteristic dimension;  $k$  is a coefficient accounting for the specific weight of the explosive material, (em) and the shape of the charges.

For a spherical charge

$$Q_{\text{sph}} = \frac{4}{3} \pi \rho_{\text{em}} l_0^3, \quad r = l_0 \quad k = \frac{4}{3} \pi \rho_{\text{em}} \quad (94)$$

From geometrical similarity it follows that the radius vector of the surface of equal stresses is proportional to the charge radius.

$$r = x r_0 \quad (95)$$

From (93) it follows that

$$r_0 = \sqrt[3]{\frac{\bar{Q}}{k}} \quad (96)$$

From (95) and (96)

$$r = x \sqrt[3]{\frac{\bar{Q}}{k}} \quad (97)$$

Denoting

$$x \sqrt[3]{\frac{\bar{Q}}{k}} = k', \quad (98)$$

we obtain

$$r = k' \sqrt[3]{\bar{Q}}, \quad (99)$$

i.e., the dimensions of the characteristic zone of explosive action in the medium varies as the square root of the cube of the weight of the charge. Inasmuch as  $k'$  does not depend on the scale, the value of  $k'$  may be determined in the explosion of small charges and the results of investigation may be incorporated in the design of large-scale explosions, carried out under analogous conditions. Thus the modeling of processes of damage to rock, based on the similitude of elastic wave motion, permits one to study a series of questions which have a large significance in the design of large-scale mass explosions and in the development of methods for enhancing the useful exploitation of the explosive energy for fragmentation.

In modeling damage processes still another difficulty arises, which is caused by the reflection of stress waves from three surfaces owing to the fact that the dimensions of the model are bounded. One method for eliminating the effect of reflective waves on the model is to increase its dimensions. However, such an increase in the dimensions is not desirable, since it complicates the setting up of the experiment and the preparation of models. In the modeling processes which take place in a block of large size, G. N. Kuznetsov (1968) employed a method of stress wave traps. This method provides for setting up special diffusers along the edges of the model, which correspond to the unbounded block in nature (Figure 16). This method is recommended for application in those cases where it is not permissible to prepare a model of such dimensions that from the side corresponding to the unbounded block a reflective stress wave would not arise in the part under investigation during the time over which the process takes place. A stress wave passes across the elongated part of the diffuser, is partially scattered, and after reflection arrives into the model attenuated. If the stress wave has a high intensity, then for a large degree of attenuation of the wave one may employ a diffuser of the

construction shown in Figure 17. In a diffuser of such construction the attenuation of the wave occurs not only on account of geometrical divergence, but also on account of the multiple reflection. A diagram of the path of a reflected wave is shown by dotted lines. Usually after three or four-fold reflection from the surfaces of the plate the intensity of the wave becomes negligible.

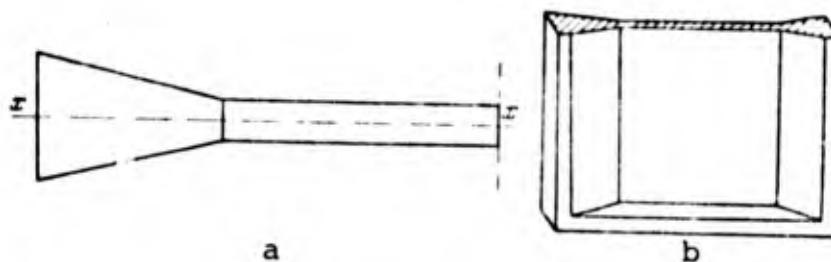


Figure 17 Diagram of a diffuser for reducing the amplitude of a reflected stress wave by means of geometrical divergence. (a) - cross section of the diffuser; (b) - view of the model with the diffuser.

One method for partial elimination of the reflected wave is the use of special attachments. The attachment is prepared from the same material and is cemented to the corresponding edges (Figure 18). A wave propagated from the charge passes through the attachment and is reflected from a free surface. Upon approach of the reflected wave to the point at which the attachment is glued on, a part of the reflected wave is removed and does not enter the model. In arranging for this to happen the strength of the cement must be substantially smaller than the strength of the modeled material in an explosion. In order that the effect of the reflected wave be eliminated entirely, it is necessary to choose the width of the attachment in such a way that it will not be

smaller than half of the blank of the positive phase of the wave, i.e., it is necessary that the condition

$$l > \frac{\lambda}{2} = \frac{c\tau}{2}, \quad (100)$$

be fulfilled, where  $c$  is the velocity of sound in the material, and  $\tau$  is the duration of an explosive pulse in the model.

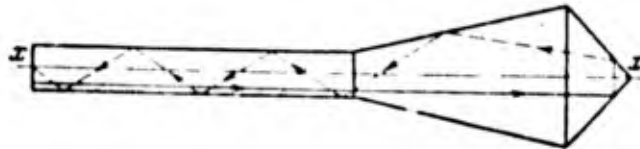


Figure 17. Diagram of a diffuser for reducing the intensity of reflected stress waves owing to geometric divergence and multiple reflection.

Usually the duration of an explosive pulse in the model amounts to tens of microseconds, and in rare cases hundreds of microseconds. For  $\tau = 100$  microseconds and the velocity of sound in the modeled material of 4000 meters/second, the width of the attachment must be no less than 0.2 m. For short pulse duration ( $\tau = 20-30$  microseconds) the width of the attachment may come to about 5-7 cm.

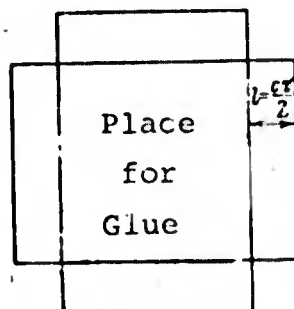


Figure 18. Diagram of an attachment for eliminating the entry of reflected waves into the model.

The chief merit of this method is the possibility of practically complete elimination of a reflected stress wave of any intensity. We must admit that one deficiency is the necessity for providing a reliable height contact between the attachment and the model for each length of the edge. Moreover, for a long duration of loading the dimensions of the attachment may be considerable. Therefore, this method may be applied only for intense pulses of short duration. For intense prolonged pulses it is appropriate to use attachments in conjunction with a diffuser (Figure 19). In this case the penetration of a reflected wave into the block is partially removed by the attachment, and the remaining part is scattered in the diffuser.

Place for Gluing

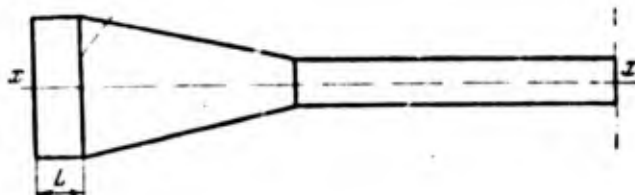


Figure 19. Diagram of the use of an attachment with a diffuser.

#### B. Methods of Modeling Using Energetic Similitude.

Energetic similitude is one of the special cases of thermodynamic similitudes. From the thermodynamic similitude criterion as the most general criterion, all the remaining similitude criteria may be obtained as special cases. Questions relating to thermodynamic similitude are considered in detail in the works of N. A. Nasedkin (1939), G. I. Pokrovskiy and I. S. Fedorov (1957, 1969). The physical essence of thermodynamic similitude is contained in the notion that the change of state of a non-equilibrium closed system proceeds on account of supplied energy and free energy. In order to pass over to

general principles, without stopping to consider special cases, it is proposed that we represent any given system as consisting of a large number of small but macroscopic<sup>1</sup> particles. The state of each particle is represented by a point in some phase state. Thus, the medium is represented by an aggregate of points in some phase space and consideration of the state of the system may be replaced by consideration of the space of the phase space, characterized by density of points,  $\rho_c$ .

The change of state of the system is characterized by a change in the density of points in the phase space. From these premises the thermodynamic similitude criterion is obtained

$$\frac{T \frac{dS_e}{dt} - \left(\frac{\partial E}{\partial V}\right)_T \frac{d}{dt} \left(\frac{1}{\rho_s}\right)}{\frac{dF}{dt}} \rho_s = \mu'(t) \mu'(F), \quad (101)$$

where  $T$  is absolute temperature;  $S_e$  is the system entropy;  $\rho$  is the system density;  $V = 1/\rho_s$  is specific volume;  $E$  is the system energy;  $F$  is the free energy of the system.  $t$  is the present time coordinate.

The right-hand side of the equation (101) represents the density of points in the phase space, corresponding to dispersed energy, and has the dimension of density. In order that similitude be obeyed between two systems it is necessary that the relative densities of points in the phase spaces of these systems be the same for the same moment in time. Proceeding from this condition, the thermodynamic similitude criterion is written down in the form

$$\frac{T dS_e - \left(\frac{\partial E}{\partial V}\right)_T d\left(\frac{1}{\rho_s}\right)}{dF} = \text{idem.} \quad (102)$$

---

<sup>1</sup>By the macroscopic property of an individual particle we understand here the preservation by that particle of the basic properties of the medium.

Thus with the aid of an idealized representation of the system in the form of a phase space with a well-defined density of phase points, the establishment of criteria characterizing the similitude of various systems is facilitated. However it is much simpler to deduce the criterion of thermodynamic similitude if we use another idealized representation of the system.

Representing the system in the form of a large number of phase points, we impart to the aggregate of these points the characteristics of an ideal gas. The change of state of this system will be described by equations characterizing the change of state of an ideal gas. From the gas laws and the laws of thermodynamics it follows that the work done by the gas is equal to the difference between the supplied energy and the change in internal energy of the gas

$$T dS_{\bullet} - \left(\frac{\partial E}{\partial V}\right)_T d\left(\frac{1}{p_{\bullet}}\right) = dA_e. \quad (103)$$

The first term is equal to the supplied energy, and the second is equal to the change in internal energy of the gas. It is clear that the work performed by the ideal gas must characterize the change in free energy of the system

$$T dS_{\bullet} - \left(\frac{\partial E}{\partial V}\right)_T d\left(\frac{1}{p_{\bullet}}\right) = k dF. \quad (104)$$

The left-hand side of equation (104) is proportional to the change in free energy of the system. Equation (104) may be written in the form

$$\frac{T dS_{\bullet} - \left(\frac{\partial E}{\partial V}\right)_T d\left(\frac{1}{p_{\bullet}}\right)}{dF} = k. \quad (105)$$

When we take account of the fact that systems with differing parameters are represented in the form of a phase space, all characteristics of which with the exception of density are constant, the coefficient  $k$  is the scale of conversion from the phase space, to which is imparted the properties of an ideal gas, to the real system. The coefficient  $k$  accounts for the difference in the change of free energy for various systems when the change in energy of the ideal gas would be the same. The similitude criteria of the two systems reduces to an equality between the conversion coefficients, i.e., for similar system  $k_1 = k_2$ .

It is now easy to obtain the thermodynamic criterion for similitude (102). The coefficient  $k$  may be represented in the form of a phase space density function and we arrive at the interpretation given in the works of G. I. Pokrovskiy (1957; 1969). The description of the aggregate of phase points in the form of an ideal gas represents a kind of abstraction which allows one to simplify the mathematical computations. At the basis of this abstraction lies the fact that the laws of conservation of mass and energy are equally valid for a gas as for any other system. Therefore, the deduction of general principles for different systems does not offer any particular difficulties. The expression of one principle is the thermodynamic similitude criterion. A determination of analogous quantities in different systems is considerably more complicated. The use of a thermodynamic similitude criterion is possible if the energy is expressed in terms of parameters which determine the process. Inasmuch as the thermodynamic similitude criterion is general for all processes, N. A. Nasedkin (1939) proposed the following rules for obtaining the similitude criteria for a concrete system.

1. Determine the expressions for the basic thermodynamic functions of a given system: the entropy, free energy, and total energy.
2. Express the functions contained in one system of basic units.

3. Find the differential of the functions of entropy and free energy and the partial derivative with respect to volume of the total energy at constant temperature and substitute them into the expression for the thermodynamic similitude criterion (102).
4. Write down the obtained relation in relative units and find from this the similitude conditions.

Starting from the indicated rules, let us find the similitude criterion for the formation of a crater with an explosion. When the density of the rock does not vary  $\partial/\partial t (1/\rho_s) = 0$ , the similitude criterion (102) may be written down in the form

$$\left| \frac{T dS_e}{dF} = \text{idem.} \right. \quad (106)$$

The change in supplied energy is equal to the change in the energy of the charge

$$T dS_e = dF.$$

The free energy in the gravitational field depends on the lift of the center of gravity of the ejected rock  $H$ . The change in free energy is

$$dF = d(mgH).$$

Expressing the mass of the rock in terms of linear dimensions and the density ( $m = \rho l^3$ ), we obtain

$$dF = d(g\rho l^3 H),$$

where  $l$  is the characteristic dimension,  $\rho$  is the density of rock, and  $g$  is the acceleration of gravity.

From the condition of thermodynamic similitude

$$\frac{T_1 dS_{e1}}{dE_1} = \frac{T_2 dS_{e2}}{dE_2}$$

it follows that

$$\frac{dE_1}{d(g_1 \rho_1 l_1^3 H_1)} = \frac{dE_2}{d(g_2 \rho_2 l_2^3 H_2)} \quad (107)$$

Integrating equation (107), we obtain

$$\frac{E_1}{g_1 \rho_1 l_1^3 H_1} = \frac{E_2}{g_2 \rho_2 l_2^3 H_2} \quad (108)$$

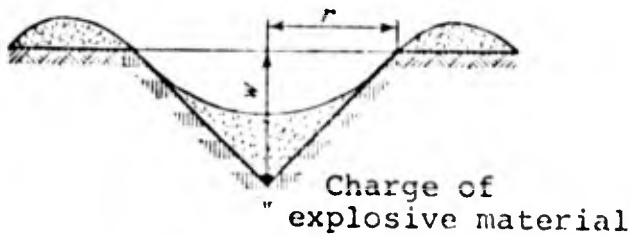
Expressing H in terms of the characteristic dimension  $\lambda$ , we find the similitude criterion

$$\frac{E}{g \rho \lambda^3} = \text{idem.} \quad (109)$$

An identical expression is not difficult to obtain if we use the methods of the theory of dimensionality. In modeling processes of ejection of rock from a crater it is customary to neglect the influence of cohesive forces, atmospheric pressure, and a series of other factors. The basic factors affecting the dimensions of the ejection crater are the force due to the weight of the rock, its density, the energy of the charge, and a quantity describing the deepening action (Figure 20). From the system of determining parameters  $\rho$ ,  $g$ ,  $\lambda$ , and  $E$ , one dimensionless similitude criterion may be set up when there are three basic units of measurement ( $n - r = 1$ )

$$\frac{E}{\rho l^3 g} = \text{const.} \quad (110)$$

From formula (110) it follows that in order to obtain similitude in the form and in the dimensions of the ejection crater the energy of the explosive material, and consequently the weight of the charge, must be proportional to  $\lambda^4$ . In fact,



$$\frac{E_1}{\rho_1 l_1^4} = \frac{E_2}{\rho_2 l_2^4}$$

$$E_1 = \frac{l_1^4}{l_2^4} E_2 = \left(\frac{l_1}{l_2}\right)^4 E_2 = \lambda^4 E_2.$$

(111)

Figure 20. Scheme of ejection crater.

If explosions are produced with the same specific consumption of explosive material, the ratio of energies or the ratio of weights of the charge for various scales of explosions is proportional to the cube of the scale  $E'_1 = q_1 V_1$ ,  $E'_2 = q_1 V_2$ .

$$\frac{E'_1}{E'_2} = \frac{V_1}{V_2} = \frac{l_1^3}{l_2^3} = \left(\frac{l_1}{l_2}\right)^3 = \lambda^3.$$

(112)

Therefore for explosions of various scales with the same specific consumption of explosive material similitude is destroyed in the dimensions of the ejection crater. When the scale of the explosions is increased the specific consumption of explosive material must rise.

When modeling processes in which gravitational forces play a definite role, fulfillment of the similitude conditions is frequently made difficult. In order to simplify the fulfillment of the similitude criteria, the method of centrifugal modeling developed by G. I. Pokrovskiy is used. The basic idea of the method consists of creating high acceleration in order to obtain the capability of preserving similitude conditions for the other parameters. Questions on centrifugal modeling are considered in more detail in the work of G. I. Pokrovskiy and I. S. Fedorov (1969).

## B. The Method of Equivalent Materials

One method for approaching natural experiments is modeling with the use of equivalent materials, i.e., materials whose properties stand in definite correspondence with the physical and mechanical properties of rocks. The method of equivalent materials was worked out by G. N. Kuznetsov (1951, 1969) for the modeling of the occurrence of rock pressure. The similitude equation, which Kuznetsov derived from using equations of mechanical similitude, forms a connection between basic quantities which characterize the mechanical properties of rock and of the equivalent materials:

$$\frac{G_M}{d_M l_M} = \frac{G_n}{d_n l_n} = \text{inv}, \quad (113)$$

where

$$G_M = \frac{F_M}{l_M^2}; \quad G_n = \frac{F_n}{l_n^2}.$$

$G$  is the mechanical characteristic of the rocks (rigidity modulus, tensile strength, etc.);  $F_M$ ,  $F_n$  are forces acting in the model and in nature;  $l_M$ ,  $l_n$  are the characteristic linear dimensions of the model and of nature;  $d$  is the specific weight of the material.

Condition (113) allows one to obtain the similar deformation of the rock and the size of the stresses at the same points in nature and in the model when forces due to the weight have the dominant effect. The similar strength of the materials is based on the fact that shattering of the material of the model and of nature takes place under conditions of similar deformation. Such physical premises make it possible to study by means of the model such things as the size of deformation occurring at the walls and at the roof of the mine site under the action of rock pressure, and the character and dimensions

of the destruction zone. It is not difficult to show that the similitude condition (113) is a special case of the similitude criteria for an elastic medium, when the active forces are determined by the weight of the rock. If the stresses depend on the weight, then they are proportional to  $\ell \cdot d$ , where  $\ell$  is the characteristic dimension.

Then

$$\frac{\sigma_{II}}{\sigma_M} = \frac{l_{II} d_{II}}{l_M d_M} \quad (114)$$

Taking account of the fact that  $\sigma = F/\ell^2$ , i.e., the ratio of force to cross-sectional area, expression (114) may be rewritten in the form

$$\frac{F_{II}}{F_M} = \frac{l_{II}^3 d_{II}}{l_M^3 d_M} \quad (115)$$

Upon consideration of applicability of the similitude conditions of elastic wave motions for modeling damage processes it was shown that

$$\frac{\sigma_{II}}{\sigma_M} = \frac{[\sigma]_{II}}{[\sigma]_M} = \frac{E_{II}}{E_M} \quad (116)$$

where  $[\sigma]$  is tensile strength, and  $E$  is the rigidity modulus

From conditions (114) and (116) it is not difficult to obtain the similitude conditions for the strength and the elastic characteristics of the equivalent materials

$$E_M = E_{II} \frac{l_M d_M}{l_{II} d_{II}} \quad (117)$$

$$[\sigma]_M = [\sigma]_m \frac{l_M d_M}{l_m d_m}. \quad (118)$$

The similitude criteria (117) and (118) may be considered as a special case of condition (113), if we understand by  $G$  the corresponding characteristic of the rock ( $E$  or  $\sigma$ ). Expressions (117) and (118) may be obtained as a special case of the thermodynamic similitude criterion. Without dwelling over the derivation of the formulas, we allude to the work of G. I. Pokrovskiy and I. S. Federov (1969), where the reader may find the indicated computations. The difference in the similitude criteria for static and dynamic problems is determined only by the physical nature of the forces, but mathematically they do not differ in any respect. Actually, on the basis of known physical laws we have

$$\frac{\sigma_M}{\rho_M} = \frac{\rho_M c_M l_M}{\rho_M^2 M_M}.$$

Making use of the accepted designations, we may write

$$\lambda_\sigma = \lambda_\rho \lambda_a \lambda_l.$$

From the theory of dimensionality it is known that

$$\lambda_a = \frac{\lambda_l}{\lambda_l^2}.$$

then

$$\lambda_\sigma = \frac{\lambda_l}{\lambda_l^2} \lambda_\rho = \lambda_\rho \lambda_l^{-1}$$

i.e., the expression  $\lambda_{\sigma} = \lambda_d \lambda_{\ell}$  is identical to  $\lambda_{\sigma} = \lambda_{\rho} \lambda_v^2$ , where  $\lambda_{\sigma}$  is expressed in terms of the scale of the other parameters. Since in dynamics the determining parameters are the density of material, velocity of motion of particles in a wave, and the propagation velocity of the wave, but in statics these parameters are the geometrical dimensions and the specific weight, the scale of the same quantity in statics and in dynamics is expressed in terms of the scale of different parameters.

Professor V. R. Imenitov (1961) is author of the idea of applying the method of equivalent materials to the modeling of the dynamic problems of collapse and discharge of ore. The method is based on the proposition that similar pieces must be arranged in the mass of collapsed rock in a definite manner if the similitude conditions are observed for the forces which are acting. One of the basic conditions for obtaining a similar disposition of the separate pieces of fragmented rock is the crushing of the material of the model into pieces, whose dimensions are geometrically similar to nature. In distributing the pieces of rock in a collapse the determining factors are the gravitational forces; the similitude conditions obtained from these premises are inadequate for attaining similar fragmentations. Therefore, it was proposed to create a model of the medium from geometrically similar pieces of strong material, reinforced by a weak cement. When the explosion takes effect the material of such a model is shattered at the junction points of the pieces. Thus, in the equivalent material we artificially create the same number of crack-formation centers as in nature with the maximum stresses which are created. A change in the maximum stresses in the material of nature leads correspondingly to a change in the number and distribution of zones of reduced strength, these zones being the sources of the destruction of the material.

In a model construction in a similar manner the intensity of fragmentation remains a constant as the stresses are changed within wide limits by virtue of the large difference in strength of the pieces and the cement. Therefore, similitude of the explosive loading is established by starting from similitude of the collapse which is obtained in the model and in nature. The size of the charge of explosive material in the model is determined from the similitude conditions of velocity vectors of motion of particles in the medium (Imenitov, 1961)

$$\lambda_Q = \frac{\lambda_l}{\lambda_k}, \quad (119)$$

where  $\lambda_Q$  is the scale of the weight of the charge;  $\lambda_k$  is the scale of the coefficient describing the effect of the explosive material efficiency, the construction of the charge, the strength of the medium, and the volumetric weight.

For the scale of the charge diameter we propose the function

$$\lambda_D = \frac{\lambda_l^{3/4}}{\sqrt{\lambda_k \cdot \lambda_{d_1}}}, \quad (120)$$

where  $\lambda_{d_1}$  is the scale of the volumetric weight of the explosive material.

With the aid of this method a large number of investigations has been conducted into the character of the distribution of the coarseness of the ore in a collapse and into the conditions of the discharge of the ore using various methods of cutting. The method of equivalent materials is particularly effective in laboratory studies of methods for reducing losses and for reducing the exhaustion of a useful mineral in selective extractions. This method is employed in the works of V. T. Sorokin (1958, 1959) for modeling the ejection crater in an

explosion in mineral rocks, the breaking up of the rock mass, and the dispersion of fragments of various size. Difficulties which are mentioned in the work of V. T. Sorokin (1959) are easily removed if we utilize the dynamic characteristics of the material. For instance, in place of the relationship for the rigidity modulus, for which determination of the value is very difficult, the following identical relationship may be used

$$\frac{E_n}{E_M} = \frac{\rho_n c_n^2}{\rho_M c_M^2}$$

where  $c_n, c_M$  are the stress wave velocities in the material of nature and the model respectively. Determination of the stress wave velocity and the density of the material do not bring forth any special difficulties.

In conclusion we shall mention areas in which the prospects are good for applying the method of equivalent material in the investigation of explosive action. In the literature there is only very scanty information on applying the method of equivalent materials to the investigation of the effectiveness of various methods for controlling the explosive action in the crushing of rock. This is apparently explained by the fact that in preparing a model the particle-size composition of the disintegrated mass is a specified parameter and in the modeling of various methods of explosive operations it does not change. However, this does not eliminate the possibility of studying the effectiveness of various methods of controlling explosive action in rocks using models based on equivalent materials. To this end under actual conditions an explosion is produced with a definite network of bore-hole locations, a complex charge construction and an ordered pattern of explosion. As a result of test probes the form of the broken-up rock in nature and the particle-size compo-

sition of the disintegrated rock mass can be established, and taking account of the geometrical scale the coarseness of material for the model is selected. The size of the charge  $Q_0$  for the model is determined from the similitude condition (119), and after that it is adjusted to obtain a similar form for the broken-up rock. The problem results in the determination of an assemblage of methods for controlling the energy of the explosion, which permits one with minimum expenditure to obtain a highly fragmented rock mass. The crushing of rocks depends on the construction of the charge, the type of explosive material and the density of charging, the diameter of the bore holes, the pattern of explosion, and the delay time. It is also worthwhile to note the high effectiveness of inclined and pair-contiguous bore holes, as well as other methods for controlling the explosive action. Carrying out such a set of investigations under industrial conditions demands a lengthy period of time and entails engineering and organizational difficulties. One should allow for the fact that determining the optimum values for each parameter requires that a whole complex of investigations be carried out. For instance, in order to determine the optimum parameter for the charge construction it is necessary to conduct investigations of the intensity of fragmentation at a different air gap spacing and with a different relationship between the weights of the upper and lower parts of the charge. In order to solve these problems under laboratory conditions, using six parameters it is necessary to change only the construction of the charge in the model, and this will cause a change in the form of the broken-up rock in the model. When the charge is concentrated, in order to obtain the same form of broken-up rock in the model as with a continuous charge  $Q_0$ , one may reduce the weight of the charge for the model or enlarge the network of bore-holes for constant weight of charge.

Reduction of the weight of the charge in the model, which is necessary in order to attain a similar form for the broken-up rock, may be the criterion of effectiveness for the use of explosive energy in fragmentations given the method for carrying out explosive operation under study. For instance, as a result of investigations on the model it has been established that for certain mineral and geological conditions the similar form of the broken-up rock when a dispersed charge is used is attained using a weight of charge 20% less than  $Q_0$ . This indicates that under specified actual conditions one may reduce the specific consumption of explosive material by 20% (a reduction in the weight of charge in a bore-hole or the expansion of the network of bore-holes) while maintaining the same intensity of fragmentation of the rocks. When using models of equivalent materials by a similar method under laboratory conditions one may establish the optimum size of the air gap and the relationship between the weight of the separate parts of the dispersed bore-hole charge, without resorting to laborious industrial experiments. On the basis of analogous investigations other effective methods and parameters for drilling and blasting operations under definite mining and geological conditions may be established. If in using some method for carrying out explosive operations in order to attain a similar form for the broken-up rock one finds it necessary to increase the weight of charge in the model in comparison with  $Q_0$ , this method under the conditions being studied is not efficient and its application will lead to an impairment of crushing.

Determination of the weight of charge, which is necessary in order to obtain a similar form for the broken-up rock in a change of charge construction, type of explosive material and other parameters of explosive operations in the model entails a large amount of laboratory experimentation. In order to cut down the number of investigations under laboratory

conditions it is convenient to utilize a reference or calibrating scale of rock break-ups. A reference scale is created in the following manner. After finding the weight of the charge  $Q_0$ , which assures a similar form of the broken-up rock, for all other identical conditions one produces explosions in the model with smaller ( $0.7 Q_0$ ;  $0.8 Q_0$ ;  $0.9 Q_0$ ) and with larger ( $1.1 Q_0$ ;  $1.2 Q_0$ ;  $1.3 Q_0$ ;  $1.4 Q_0$ ) weights of the charge. For each charge one establishes the form of the broken-up rock which becomes the reference, characterizing the use of explosive energy. Consider for instance the explosion of a dispersed charge with an air gap, as a result of which a form of broken-up rock is obtained which is close to the form found for the explosion of a charge of  $1.1 Q_0$ . Consequently, without correcting the weight of the dispersed charge in the model, using a reference scale one may establish the effectiveness of using explosive energy. By increasing the air gap spacing, we obtain a break-up corresponding to the break-up obtained with the explosion of a charge of continuous construction with weight  $1.2 Q_0$ . By changing in this manner the air gap spacing we find for what size of spacing the form of the broken-up rock will correspond to the largest weight for a continuous charge construction. In light of the geometrical scale this air gap spacing will be optimum under the given conditions. In an analogous manner we determine the optimum values of the other parameters of drilling and blasting operations: the relationship between the separate parts of the dispersed charge, the diameter of the bore-hole, the delay time, the pattern of explosion, etc. The reference scale of the break-up facilitates the performance of laboratory experiments and considerably reduces the number of such experiments.

The modeling method which we have just considered permits, with the aid of equivalent materials, a qualitative evaluation of the effectiveness of application of various methods

for controlling the explosive action in the crushing of rock to be given. However, in this approach one cannot establish a change in the intensity of fragmentation as a function of the applied method. An approximate estimation of the intensity of fragmentation may be realized in the following manner. Under fixed mineral and geological conditions in nature one conducts a series of experimental explosions with a continuous charge construction and with an ordered pattern of explosions consuming various specific amounts of explosive material. If to the charge  $Q_0$  in the model there corresponded in nature a specific consumption of explosive material of  $0.5 \text{ kg/m}^3$ , then it would be necessary to carry out experimental explosions with less ( $0.45 \text{ kg/m}^3$ ;  $0.4 \text{ kg/m}^3$ ;  $0.35 \text{ kg/m}^3$ ) and larger specific consumption ( $0.55 \text{ kg/m}^3$ ;  $0.6 \text{ kg/m}^3$ ;  $0.65 \text{ kg/m}^3$ ;  $0.7 \text{ kg/m}^3$ ). Each specific consumption of explosive material corresponds to a definite charge, which is taken as the reference scale. After each experimental explosion a measurement of the particle-size composition of the disintegrated mass is taken. Having established which reference charge is obtained in identical fashion by the use of some method of controlling the explosive action, it is not difficult to find the change in intensity of fragmentation which is obtained by using this method. In the example considered earlier the use of an air gap in the charge of explosive material made it possible to increase the utilization of explosive energy by 20% in comparison with the continuous charge. In order to determine the intensity of fragmentation in nature using a constant specific consumption of explosive material and a dispersed charge it is necessary to utilize the particle-size composition which was obtained in the case of a continuous charge construction and a specific consumption of explosive material which is 20% higher.

From what has been presented it follows that the possibilities of the method of equivalent materials are far from having been exhausted. The effectiveness of the method of equivalent

materials in modeling is obvious and it is expected to obtain wide dissemination in the investigation of the fragmentation of rocks by explosion.

### Mathematical Modeling of the Processes of Shattering and Crushing

In contrast to physical modeling, for mathematical modeling it is necessary to establish equations describing the processes of shattering and crushing. Because of the complexity and the large number of parameters which determine the process of shattering, there still does not exist a precise mathematical description of this phenomenon. An approximate mathematical description of the crushing process was proposed by Professor O. Ye. Vlasov and Engineering Doctoral Candidate S. A. Smirnov (1962). The indicated work is actually the first and still the only attempt at mathematical modeling of the crushing action of an explosion. In the proposed scheme the process of crushing is arbitrarily divided into three phases: 1) the transmission of energy of the explosion to the surrounding medium; 2) the process of shattering of the medium.

Such a division into phases, makes it impossible to idealize the process of transmission of explosive energy and to determine the distribution of energy in the medium, and after that according to the distribution of energy which is obtained and using as a basis the theory of shattering of a deformable medium it is possible to establish the expected crushing of the rock. In the first phase we use for the material of the model an absolutely incompressible medium. In this case the energy of the explosion is conveyed to the medium instantaneously. By making this assumption we can simplify considerably the computation, since the number of parameters characterizing the medium and the charge is reduced. In particular, for an incompressible medium the parameters of the pressure impulse in the charge chamber have no effect on the distribution of

stresses. The value of the stresses and their distribution in the medium depend only on the overall energy of the explosive material, the form, and the dimensions of the charge. This method permits a solution with a specified degree of accuracy to be found for a series of important problems connected with the fragmentation of rock and the determination of an expected particle-size composition. For the correct evaluation and modeling of phenomena in an explosion let us take a more detailed look at the methodology of modeling, the limits of its applicability, and the errors brought in along with the assumptions taken. As noted by the authors in their work (Vlasov, Smirnov, 1962), the replacement of an actual medium by an incompressible one is the fundamental assumption. Such a model of a medium differs substantially from real rock masses. This model approximates more closely a homogeneous mass with large acoustic rigidity, and having a large modulus of elasticity and a tendency to brittle shattering. In calculating the shattering of such rocks the error caused by the idealization of the medium will be minimal. In rock masses of highly cracked, large-lump construction, in porous rocks, or in rocks of low breaking strength, the error may be considerable and the indicated methods may not always be used. Of all the modeling materials the closest in its properties to the ideal incompressible medium is glass, and if restricted to rocks, monolithic quartzite and jaspilite. From the first assumption, that the nature of the crushing action of the explosion is independent of the parameters of the explosive impulse, complicates both the modeling and the study of the effectiveness of methods for controlling the explosive action, connected with a change in the duration of application of explosive loading. To such methods of controlling the explosive action one should relate the charge construction, the type of explosive material, the stemming and other parameters, which make it possible to redistribute in time the discharge of energy of the explosion. The assumption that all of the

explosive energy is transmitted indicates that with the aid of this model there is no sense of studying methods for increasing the efficiency or performance of the explosion. Therefore, the most reliable results may be obtained by studying the influence of the form of the charge, the density of charging, the specific and overall energy of the charge, and the network of bore-hole placement on the intensity of fragmentation. If we introduce into the equation the corresponding coefficients characterizing the use of explosive energy, then in principle one may solve problems connected with an increase in efficiency of the energy of the charge. Therefore, one of the directions for development of mathematical modeling is the perfection of the indicated method with the goal of applying it to a wider class of problems.

One basic virtue of the model is the identity between the equations obtained and the equations of hydrodynamics, a fact which makes it possible to utilize an electrical model. It is not difficult to show that under the conditions assumed the velocity potential  $\psi$  satisfies the Laplace equation

$$\frac{\partial^2 \psi}{\partial x^2} + \frac{\partial^2 \psi}{\partial y^2} + \frac{\partial^2 \psi}{\partial z^2} = 0.$$

From the condition whereby the energy of the explosion is equal to the full kinetic energy of the medium a relationship is obtained (for the medium with a fixed density)

$$\frac{\rho}{2} \iiint (v_x^2 + v_y^2 + v_z^2) dx dy dz = E_3, \quad (121)$$

which is transformed (according to Green's theorem) into the equation

$$E_3 = -\frac{\rho}{2} \oint \psi \frac{d\psi}{dn} dS, \quad (122)$$

where  $dS$  is a surface element bounding the medium under consideration;  $\psi/dn$  is the derivative with respect to the direction of the interior normal.

At the conclusion of the process of transmission of explosive energy the state of the incompressible medium remains unchanged, and it receives only some initial velocity, representing a function of the coordinates. In the case of a spherical charge of radius  $r_0$  the field of velocities has the form

$$v = \frac{1}{r^2} \sqrt{\frac{r_0 E_0}{2\pi \rho}}, \quad (123)$$

where  $r$  is the distance from the charge center to the point under consideration.

Thus the velocity at which particles of the medium move is determined by its density, energy, and the radius of the charge, as well as distance from the center of the charge to the point under consideration. For another shape of charge (cylindrical or plane) the field of velocities is determined by the same parameters as in the case of a spherical charge; however, the quantities entering into the problem will be related by a different functional dependency. Determining the velocity potential by an analytical means is not always possible. In order to solve the Laplace equation one may employ the method of grids or use electronic analog devices. However, in the given case, in order to determine the velocity potential it is convenient to utilize an electrohydrodynamic analog apparatus. This set-up allows one to construct experimentally the equipotential surfaces.

The theoretical form of an elastical diagram of the set up is shown in Figure 21. The simple method for finding the basic parameter of the process -- namely, the field of velocities

for any form of the charge or system of charges -- underlies the high effectiveness of such a model.

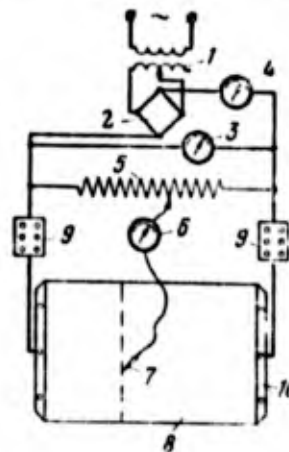


Рис. 21. Принципиальная схема установки ЭГДА

- 1 — трансформатор;
- 2 — выпрямитель;
- 3 — вольтметр;
- 4 — миллиамперметр;
- 5 — потенциометр;
- 6 — нуль-индикатор;
- 7 — зондовый игла;
- 8 — модель;
- 9 — магазин сопротивлений;
- 10 — зажимы тока

Figure 21. Theoretical diagram of the electrohydrodynamic analog apparatus. (1) - transformer; (2) - rectifier; (3) - voltmeter; (4) - milliammeter; (5) - potentiometer; (6) - null indicator; (7) - probing stylus; (8) - model; (9) - resistance boxes; (10) - clamps.

In order to find the interrelationship between the field of velocities and the damage processes a model of an absolutely incompressible medium is unsuitable. Therefore, O. Ye. Vlasov and S. A. Smirnov (1962) took a look at a medium which changes its properties in the process of explosive loading. Such an approach to choosing a model of the medium conforms fully to principle, inasmuch as the characteristics of the medium change continuously during the process of shattering. In the second stage an elasto-plastic medium is employed for the model. On this basis the critical velocity corresponding to the limit of fluidity is determined.

$$v_s = \frac{\sigma_s}{\sqrt{E\rho}}, \quad (124)$$

where  $v_s$  is the critical velocity corresponding to plastic deformation;  $\sigma_s$  is the yield point;  $E$  is the rigidity

modulus of the medium;  $\rho$  is the density of the medium. For brittle shattering taking place by means of breaking apart, we have analogously:

$$v_{ba} = \frac{\sigma_{ba}}{\sqrt{E\rho}}, \quad (125)$$

where  $v_{ba}$  is the critical velocity for breaking apart, and  $\sigma_{ba}$  is the maximum tensile strength.

As we consider the indicated mechanism of damage to the medium several questionable circumstances should be mentioned. In particular, it follows from the presentation of the authors that when the compressing stresses are applied only plastic shattering is possible. However, this contradicts the works of a series of scholars both native (Pokrovskiy, 1967; Pokrovskiy, Fedorov, 1957) and foreign (Kol'skiy, 1963; Louette, 1963), where it is shown that upon application of compressing stresses in the perpendicular direction there arise tangential tensile stresses, which cause the appearance of radial cracks propagating from the center of the charge and typifying brittle shattering. In the work of O. Ye. Vlasov and S. A. Smirnov (1966) it is proposed that brittle shattering is possible only with the reverse motion of the medium (splintering phenomena), when the compressive stresses change their sign to the opposite polarity. In this regard it is to be noted that the fluidity is not a physical constant but depends, apart from everything else, on the velocity of deformation.

Results of investigations by G. Kol'skiy (1963) into the influence of the deformation velocity on the nature of shattering testifies to the fact that for high rates of loading even especially plastic materials are subjected to brittle shattering, i.e., not plastic deformations of the medium which occur, but rather it is radial cracks which appear. In plastic materials

brittle shattering is not observed, since the tangential stresses experience relaxation. The higher the rate of relaxation of tangential stresses, the more plastic is the material. For high rates of loading (of the explosive type) even in plastic materials the tangential stresses do not have time to undergo relaxation, and in connection with this the nature of the damage does not differ essentially from the shattering of brittle materials. The hypothesis of plastic shattering of rocks although it is an arbitrary convenience, nevertheless permits one to solve more simply the problem of determining the average probable dimension of fragment formed in the explosion. By means of not too difficult transformation one obtains the dependency of the dimensions of an average fragment on the critical velocity of plastic shattering and the so-called crushability number

$$a = \frac{v_c \sqrt{3}}{\sqrt{D}}, \quad (126)$$

where  $D$  is the crushability number.

The crushability number represents a quantity depending on the velocity potential  $\psi$ .

$$D = \left(\frac{\partial^2 \psi}{\partial x^2}\right)^2 + \left(\frac{\partial^2 \psi}{\partial y^2}\right)^2 + \left(\frac{\partial^2 \psi}{\partial z^2}\right)^2 + \\ + 2\left(\frac{\partial^2 \psi}{\partial x \partial y}\right)^2 + 2\left(\frac{\partial^2 \psi}{\partial x \partial z}\right)^2 + 2\left(\frac{\partial^2 \psi}{\partial y \partial z}\right)^2. \quad (127)$$

The velocity potential is determined experimentally on the electrohydrodynamic analog apparatus. From the known velocity potentials  $\psi$  at various points it is possible to compute the crushability number and the dimension of an average fragment.

In determining the velocity potential it is necessary to assure a high accuracy for the measurements, since in taking the second derivative, errors compound. There exists methods for measuring  $d\psi/dx$  directly. A detailed description of methods for measuring the potential, as well as the first and second derivatives thereof, is presented in the special literature (Karplyus, 1962). The velocity potential depends on the radius of the charge, its energy and the distance to the center of the charge, and therefore the crushability number also becomes a function of these quantities. For the case of spherical symmetry

$$D = \frac{3r_0 E_1}{\pi \rho r^3}, \quad (128)$$

and the average probable dimension of fragments of rock

$$a = v_0 r^3 \sqrt{\frac{\pi \rho}{r_0 E_1}}. \quad (129)$$

From the formula it follows that the dimension of fragments increases with distance from the charge and decreases with increasing radius of the charge and its energy. From these same premises the dimensions of the crushing zone are obtained

$$r_0 = \frac{4}{\sqrt{2} v_0} \sqrt{\frac{r_0 E_1}{\pi \rho}}. \quad (130)$$

From the known boundaries of the crushing zone and the coarseness of the rock fragments it is possible to find the probable particle-size composition of the damaged part of the mass.

In order to determine the duration of the shattering process it is proposed that the following dependency be employed

$$\tau_p \leq \int_{r_0}^r \frac{dr}{v} \quad (131)$$

For a spherical charge

$$\tau_{max} = \frac{1}{3} \sqrt{\frac{2\tau_p}{r_0 E}} (r_{00}^3 - r_0^3) \quad (132)$$

Formula (131) is obtained under the supposition that the velocity of the advancing front of the shattering action differs very little from the velocity of the motion of particles in the medium. Such an assumption may not be made owing to the fact that the velocity of the shattering front in rocks and in brittle media is an order of magnitude higher than the velocity of motion. In the given case we see the effect of the inapplicability of the assumed mechanism of plastic shattering for the determination of time characteristics of the process. For the action of an explosion in a plastic material or in a liquid, expression (131) may be utilized for determining the time of formation of a cavity of radius  $r$  when the velocity of motion of the walls  $v$  is a variable. However, such a mechanism for the damage is absolutely not typical for rocks and therefore the calculated duration for the process is clearly overstated. To serve as an example let us determine by the proposed method the time for a rock mass to be destroyed under the following conditions:

height of the bench	15 m
depth of the bore-hole	17 m
height of the charge	10 m
weight of the charge	400 kg

density of the rock	$250 \text{ kg}\cdot\text{sec}^2/\text{m}^4$
diameter of the charge	$240 \text{ mm} = 0.24 \text{ m}$
damage radius	$r = 6.25 \text{ m}$

Let us compare these data with the actual time for destruction. On the basis of the proposed dependences in the work (Vlasov, Smirnov, 1962) the time for destruction amounts to  $\tau \leq 400 \text{ msec}$ . According to the data of high-speed motion-picture filming, carried out with the aid of the SKS-1m camera at the Kolomoyevskiy granite quarry, it was found that the shattering process is completed within a time between 30 and 60 msec, since on the photo-recorded frames by 60 msec the rock had not only disintegrated but separate pieces had already begun to fly apart. Although inequality (131) is indeed satisfied, the actual time for shattering is an order of magnitude smaller. Therefore, in the case of hard rock to be excavated the shattering time may not be evaluated according to the proposed formulas even in a first approximation.

As in any other method, the proposed model represents some kind of approximation to the actual process and possesses a number of inadequacies. Nevertheless the method as developed makes it possible to calculate an expected particle-size composition of rock for certain conditions, thus providing a significant contribution to science and furthering the development of methods for predicting the particle-size composition. The mathematical modeling of damage processes must develop by means of the creation of new models for computational purposes and systems on the basis of which the expected particle-size composition of rock may be calculated and effective methods of controlling the fragmentation may be set up. The possibilities of the method proposed by O. Ye. Vlasov and S. A. Smirnov may be expanded significantly if in the equations account can be taken of the conditions for transmission of energy (with the aid of the duty factor for

explosive energy) and if methodologies are worked out for evaluating this factor for various methods of carrying out explosive operations. The methods with the highest prospects are those for predicting the particle-size compositions, based on a choice of a model for the medium which is closer to the actual situation with rocks. A further step in this direction would be the application of statistical methods in the description of the damage process in a medium.

#### The Modeling of Other Phenomena Occurring in An Explosion

In view of the diversity of the use of explosions in the national economy the necessity arises for modeling the various manifestations of its action, such as the question of the rock, the heap of exploded rock mass, its compaction, etc. The modeling of the various factors for explosive action has its own inherent specifics, which stipulate corresponding similitude criteria. In the modeling of the ejection of rock by an explosion the resistance of the air is neglected in a first approximation (Pokrovskiy, Federov, 1969). For a practically attainable degree of accuracy in determining the spot at which the fragments of rock fall (20%), the resistance of the air may be neglected if the following condition is fulfilled:

$$\frac{\eta_a v^1}{r_{n'f}} < 0,2,$$

where  $x_f$  is the maximum distance of flight of the fragments;  $\eta_a$  is the dimensional coefficient of the resistance of air to the motion in flight of the fragments (in the SI system,  $\text{kg/m}^2$ ).

In the motion of any body which has been ejected at an angle  $\alpha$  to the horizontal with an initial velocity  $v$ , the distance of flight is determined by the expression

$$l = \frac{v^2}{g} \sin 2\alpha. \quad (133)$$

The initial velocity of motion, specified by the effect of the explosion may be obtained from the relationship

$$\frac{mv^2}{2} = \eta Q_T, \quad (134)$$

where  $m$  is the mass of the moving fragments;  $\eta$  is the averaging factor for the energy of fragments;  $Q_T$  is the T.N.T. equivalent of the charge.

From equations (133) and (134) it follows that

$$l = \frac{2\eta Q_T}{gm} \sin 2\alpha.$$

If the condition of geometrical similarity is to be fulfilled for the quantity  $\eta$ , the value of  $\sin 2\alpha$  must coincide in both nature and in the model. In this case the characteristics of the charge and the material of the model must satisfy the conditions

$$\frac{m_n}{Q_n} = \frac{m_M}{Q_M},$$

or, taking account of the fact that

$$m_n = \rho_n V_n; \quad m_M = \rho_M V_M \quad \text{и} \quad V_n = \lambda^3 V_M,$$

where  $\rho_n$  and  $\rho_M$  are the densities of the materials of nature

and the model respectively;  $V_n$  and  $V_M$  are the volumes of ejected masses in nature and in the model;  $\lambda_l$  is the linear scale for modeling, then we obtain

$$\frac{\rho_n}{r_n} = \lambda_l^3 \frac{\rho_M}{r_M} \quad (135)$$

For centrifugal modeling the similitude criteria simplifies somewhat (Pokrovskiy, Fedorof 1969)

$$g_n = \lambda_l g_M \quad (136)$$

However, in the case of centrifugation the motion of the fragments of rock ejected by the explosion is altered on account of the Coriolis force. The accelerations which arise because of this change the trajectory of fragments. In the work of G. I. Pokrovskiy and I. S. Fedorov (1969) an estimation is made of the absolute  $\delta$  and relative  $\theta$  of error, with which the model reproduces nature in the case of centrifugal modeling of the process of dispersion:

$$\delta = l^2/2r_k \quad (137)$$

$$\theta = \frac{l}{v} \sqrt{\frac{\lambda_l g}{r_n}} \quad (138)$$

where  $r_k$  is the radius of the periphery describing a body moving under inertial forces in the rotating system of coordinates;  $r_0$  is the radius of the centrifuge.

With a corresponding choice of quantities entering into equations (135) and (136) one may guarantee a specified degree of accuracy in the results obtained. The advantages

of the method of centrifugal modeling consists of the simplicity of the similitude conditions in allowing for air resistance. The velocity of a body moving in air under inertial forces is determined by the equation

$$v = v_0 \exp \left[ - \frac{c_x l \rho_a}{2b\rho} \right], \quad (139)$$

where  $V_0$  is the initial velocity,  $c_x$  is the coefficient of head-on resistance of the body,  $\rho_a$  and  $\rho$  are the densities of air and fragments respectively,  $b$  is the linear dimension of a fragment, measured along the direction of its motion.

From relation (137) it follows that the condition of aerodynamic similitude will be fulfilled when geometrical similarity is observed, i.e.,

$$l_m/b_m = l_n/b_n. \quad (140)$$

In the case where criteria (135) are applied, accounting for aerodynamic resistance in modeling the scattering of fragments is made significantly more complex.

In centrifugal modeling the form of the pile up of rock introduces supplementary requirements: during the free-flight period of the fragments the angle of turning of the centrifuge must be smaller than the angle which is determined by the necessary accuracy of the measurements. This requirement is satisfied when the following relationship is fulfilled

$$l_m/r_T \ll \frac{1}{\gamma}.$$

where  $r_T$  is the radius of rotation of the point under study. The quantity  $\gamma$  is always larger than unity, and its concrete value is determined by the required accuracy of the experiment. If the requirements superimposed by the given relationship onto the geometrical dimensions of the model and the centrifuge are difficult to realize, the necessary accuracy of the experiment may be attained by means of an appropriate correction to the experimental data.

In modeling the compaction of the heap of rock mass the method of centrifugation is that with the highest prospects. The density of the heap when the properties of the rock are specified is determined by the residual kinetic energy of the fragments. Applying the linear dependence of the time resistance of the heap  $\sigma_r$  on its porosity

$$\sigma_r = a - b\varepsilon \quad \text{if} \quad \sigma_r(\varepsilon_{\max}) = 0, \quad \sigma_r(0) = \sigma_{r\max},$$

where  $\varepsilon$  is the porosity of the heap, we obtain

$$\sigma_c = \sigma_{c\max} \left( 1 - \frac{\varepsilon}{\varepsilon_{\max}} \right). \quad (141)$$

equating the kinetic energy of a unit of volume to the work done in compaction of the heap, we obtain

$$\frac{\rho(1-\varepsilon_{\max})v^2}{2} = \frac{\sigma_{c\max}}{2\varepsilon_{\max}} (\varepsilon_{\max} - \varepsilon)^2.$$

Hence

$$\varepsilon = \varepsilon_{\max} - v \left[ \rho \frac{(\varepsilon_{\max} - \varepsilon_{\max}^2)}{\sigma_{c\max}} \right]^{1/2}. \quad (142)$$

The identity of the rock in the model and in nature permits one to obtain a single porosity when the correspondences of velocities of motion of fragments are equated. Considering that the indicated questions have only an indirect relation to the process of shattering, we have limited our discussion to a short statement of the methods for modeling the dispersion of fragments and the compaction of the disintegrated rock mass. These questions are illuminated in more detail in the works of G. I. Pokrovskiy and I. S. Fedorov (1969) and in the works of other authors.

## CHAPTER 3

### THE USE OF STATISTICAL THEORIES OF STRENGTH AND DAMAGE IN THE MODELING OF THE CRUSHING OF ROCK

#### Physical Bases of the Process of Damage

The process of damage or shattering of a material consists in the dispersion of that material under the actions of applied loads. The successes of solid state physics has made it possible to explain the shattering phenomenon by considering the atomic and molecular structure of the substance. The damage process is connected with the existence of a special type of imperfections in the crystalline structure, so-called crystal defects. From a purely geometric point of view defects in actual crystals may be classified according to the number of measurements in which an inelastically distorted region has macroscopic dimensions, whereas in the remaining measurements its dimensions are microscopic, of the order of several interatomic distances. In this case vacant lattice points, atoms imbedded into the interstices, and impurity atoms are considered as zero-dimensional defects, boundaries between crystallites (small crystals of modified form in the polycrystalline mass) and lumps of mosaic structure are considered as two-dimensional defects. Into the category of one-dimensional defects we place chains of vacancies and other zero-dimensional defects, and also special distortions of the structure of an ideal crystal--dislocations (Fig. 22). Displacement of dislocations causes the slippage of atomic layers. There is a difference in edge and screw dislocations in relation to the direction of slippage of atomic layers. If the direction of slip of atomic layers is perpendicular to the boundary between displaced and undisplaced parts of the crystal, the dislocation is considered edge-type (Fig. 23). For slippage parallel to the boundary, the dislocation is called a screw-type (Fig. 24).

The mechanism of formation of micro-cracks and shattering of a medium may be explained on the basis of dislocation theory. The shattering process is considered as consisting of three stages: a) the generation of three slippage (i.e., capable of moving) dislocations; b) the conversion of slippage dislocations into cavity-type dislocations, representing cavities of microscopic dimensions; c) the growth of cracks, formed by the cavity-type dislocations.

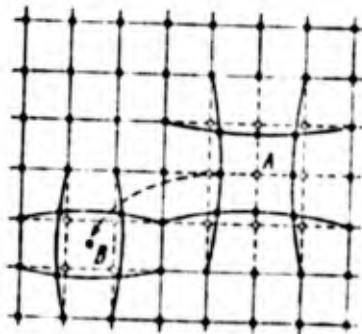


Figure 22. Fundamental point defects: vacancy (A) and imbedded atom (B)

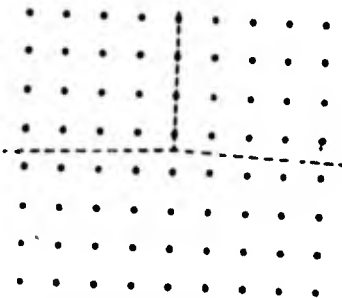


Fig. 23. Edge dislocation.

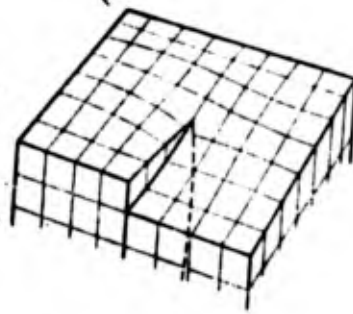


Figure 24. Screw dislocation

The process of conversion of a slippage dislocation into a cavity dislocation is possible only with the aggregation of the former type at some obstacle (a grained boundary, intersection with slippage bands, etc.) and under the condition of obstruction of the sources of dislocation, since the appearance of a large number of dislocations leads to plastic deformation. The motion of an unattached dislocation is connected with a definite frictional resistance  $\sigma_{T,i}$ . Consequently only an effective tangential stress  $\sigma_T - \sigma_{T,i}$  ( $\sigma_T$  is the applied external stress) is acting on the slippage dislocations. But if the process of crack development is made difficult, work is produced by each applied stress  $\sigma_T$ , and not only by  $\sigma_T - \sigma_{T,i}$ , i.e., plastic properties prevail in the material. If the stress due to flow exceeds the stress due to the growth of cracks, the material will shatter in brittle fashion. The criterion for shattering is derived from energetics considerations. The external stress acting on the slippage dislocations causes their drawing together, and in the case of shattering the work produced in this case by external forces must be no smaller than the energy of newly-formed surfaces of fracture.

Molecular theories of strength examine the process of destruction in solid bodies as the rupture of atomic or molecular bonds along some surface. The bond rupture begins at places where

microcracks and other defects in the crystalline structure are localized. According to the kinetic concept, associations of atoms are found at the termini of cracks under special conditions. They are situated at the boundary regions, separating atoms located within the mass, and atoms forming the rupture surface (Fig. 25). A larger reserve of potential energy is concentrated in the surface layer than in the internal layers, and for that reason in order to transfer interior particles to the surface it is necessary to perform a certain amount of work. This work is determined by the energy of the atomic bond in the solid state, i.e., the energy which it is necessary to consume in order to rupture the atomic bond. The rupture of bonds between two atoms in the solid state, accompanied by the formation of two new surfaces, for any type of bond takes place with a transfer of potential energy across a barrier. Qualitatively the existence of a potential barrier becomes clear if we give our attention to the fact that the process of bond rupture is affected by nearest neighbors of particles which emerge onto the free surface. In the process of rupture the distances between particles are increased, and at the termini of cracks they take their maximum values, a fact which corresponds to maximum potential energy. After rupture, particles which form the free surface come closer and the potential energy is reduced. The energy necessary for overcoming this potential barrier in an unstressed substance is available to the particle on account of fluctuations in the energy of thermal oscillations. But in that case the probability of rupture of atomic bond is small because of the large difference in the values of potential energy of particles within and on the surface of the substance. If a load is applied, on account of the concentration of stresses at the termini of the cracks the difference in values of potential energy begins to decrease, and the probability of rupture of atomic bonds

of rupture grows correspondingly. If the probability of atomic bonds exceeds the probability of their recombination the original microcrack begins to grow. The rate of growth of the crack at this stage is a variable and depends on the values of the stresses in regions reaching the end of the cracks. As the stresses increase the energy particles reaches the energy level of the potential barrier, and at that moment the crack begins to grow catastrophically. The velocity of crack propagation reaches its maximum value, which is equal to the velocity of Rayleigh waves, and no longer depends on the values of the stresses.

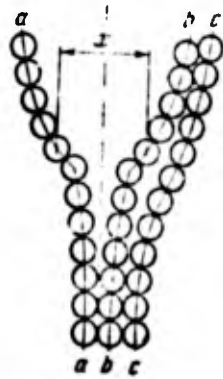


Figure 25. The structure of the terminal region of a crack.

An approach to the description of the damage process which provides very good prospects is based on use of the mathematical apparatus of quantum mechanics, the so-called phonon concept of damage (Barten'ev, Razumovskaya, 1969). In analogy with a quantum of electromagnetic field--a photon, one introduces the concept of the phonon--a quantum of oscillation field in

the crystalline lattice. Regions of stress concentration at apexes and other structural defects become microregions in the phonon spectrum, which differ from the basic phonon spectrum of a substance under load. The loss of energy in these regions on account of bond rupture raises the concentration of non-equilibrium phonons, whose emergence beyond the limits of the region is made more difficult. It is only in the direction of crack growth that the "interior" non-equilibrium phonon may proceed with sufficient ease. In this manner the region of overstress may be considered as a semi-transparent resonator, emitting oscillations with definite frequencies in chosen directions. The gradual development of a phonon concentration of damage makes it possible for one to establish the connection between physical and mechanical theories of strength.

In mechanical theories of strength the criteria of damage are formulated as conditions for stability of cracks within the framework of the theory of elasticity. There are two approaches to the solution of this problem: the energetic and the force approach.

The theory of A. A. Griffiths (1920, 1924) and the numerous modifications of this theory associated with the names A. Snekal (1922), K. Wolf (1923), G. P. Irvin (1948), O. Ye. Orovan (1950), and others are based on the energetic methods for describing the process of damage. A. A. Griffiths postulated the existence of crack-type defects in unstressed bodies. When a load is applied at places where these defects are localized a concentration of stresses occurs. At the site of a crack having the form of an ellipse, the stresses are concentrated on the atomic bonds at the apexes of the crack. The value of the stresses is computed as the maximum stress  $\sigma_{\max}$  in a plane with an elliptical indentation which is subjected to the effect of an average tensile stress  $\sigma$ .

$$\sigma_{\max} = 2\gamma \left( \frac{l_e}{r_e} \right)^{1/2}, \quad (143)$$

where  $l_e$  is the length of the major semi-axis of the ellipse, and  $r_e$  is the radius of curvature at the ends of the major semi-axis.

In actual cracks the value of  $r_e$  is of the order of interatomic distances. Distances of this order cannot be considered finite in investigations based on concepts of continuous media. As  $r_e$  approaches zero the stresses at the termini of cracks become infinitely large. As the length of a crack increases each of the bonds in turn receives the stress of the initial bond, and the work expended in stretching and rupturing these bonds is converted into surface energy in the planes of rupture. This work is accomplished through the applied external forces or as a result of the lasting energy of the system. The potential energy of an elastic body containing a crack may be divided into three components: a) the energy of elastic deformation of the whole body after deducting the part next to the crack; b) the energy of elastic deformation connected with a crack  $E_e$  and owing its existence to that crack; c) the surface energy  $E_s$  of the crack which has been formed.

The first component of energy exerts only an indirect influence and may be omitted in the consideration of an energetic balance of the propagating crack. The condition for growth of a given crack consists in the fact that as the dimensions of the crack increase there need not be an increase in the free energy of the substance. In this case the parameters of the critical non-equilibrium state are found from the condition

$$\frac{\partial (E_e - E_s)}{\partial l} = 0, \quad (144)$$

where  $l$  is the length of the crack.

The theory of Griffiths calls upon the presence of microscopic cracks and defects in the crystalline lattice to explain the paradoxical fact that the theoretically calculated strengths of the material is many orders of magnitude higher than the actual strength that is determined from mechanical experiments. A determination of the critical stress reduces a determination of the rate of liberation of elastic energy  $dE/dl$ . Using the solution of Inglis (1913) or the value of stress at the terminus of a crack, Griffiths calculated the critical values of the destructive stresses for the conditions of a plane deformation

$$\sigma_{cr} = \sqrt{\frac{2E\gamma_0}{\pi(1-\nu)l}}, \quad (145)$$

where  $E$  is Young's modulus,  $\gamma_0$  is the surface energy density,  $\nu$  is the poisson ratio and for the plane stressed state

$$\sigma_{cr} = \sqrt{\frac{2E\gamma_0}{\pi l}}. \quad (146)$$

B. Ya. Pines, starting from the theory of dimensionality and similitude obtained an expression for the critical stress in the case of volume stress state

$$\sigma_{cr} = \frac{3}{2} \sqrt{\frac{E\gamma_0 l}{S_{cr}}}, \quad (147)$$

where  $L$  is the linear dimension of the body;  $S_{cr}$  is the area of the crack.

A. R. Sak, employing the energetic model of Griffiths, calculated critical stresses for a brittle substance, weakened by a disc-shaped macroscopic crack, and subjected at infinity

to an elongation by uniform stresses  $\sigma$

$$\sigma_{cr} = \sqrt{\frac{\pi E \sigma}{2(1-\nu)S}}, \quad (148)$$

where  $S$  is the area of a crack.

Ya. I. Frenkel' (1952) noticed the contradiction between Griffiths' hypothesis regarding the existence of microcracks in the unstressed state and the equation of energy balance which had been applied, this equation not allowing for the existence of cracks in an unstressed state. Formally this contradiction may be reduced to the existence of one extremum point on the curve  $U(l)$  (Fig. 26) (when  $\sigma = \text{constant}$ ), corresponding to maximum energy, i.e., to an unstable state of the substance. In modifications of Griffiths' theory, using the expanded energy balance equation, this deficiency is removed (Fig. 27).

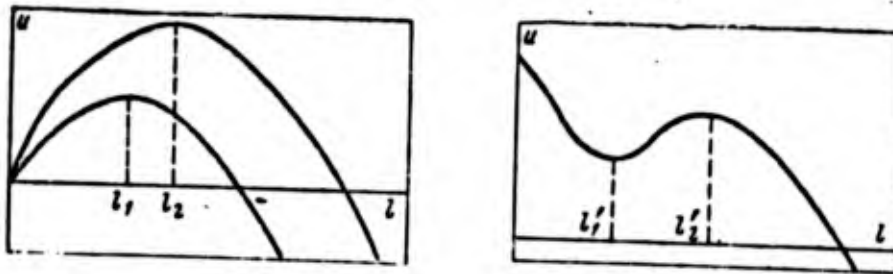


Fig. 26. Dependence of potential energy on the length of a crack according to the theory of Griffiths.

Fig. 27. Dependence of potential energy on the length of a crack in modifications of Griffiths' theory.

A serious objection must be made to the elliptical form of a crack which is assumed in the Griffiths' theory. P. A. Rebinder and Ya. I. Frenkel' believed that in crystalline substances actual microcracks must have pointed ends, in which the radius of curvature is equal to zero. This corresponds to the notion whereby surfaces separated by a crack approach gradually up to a separation equal to the crystalline lattice concept. From the geometric point of view every solid body may be considered as being pierced or permeated in all directions by a system of cracks with atomic widths. However, from the dynamic point of view these gaps may be cracks in the case where distances between atoms, although it is in some limited part of the sample, become greater in size by an order of magnitude or higher in comparison with normal distances. Formally the length of a crack becomes infinitely large, but in practice one considers that a crack ends at that point where the distance between its edges becomes equal to double the value of the normal interatomic distance. Starting from such an idea of the development of a crack, one may estimate the value of surface energy, having found the dependence of the force of interaction between oppositely lying regions of the crack walls on the distance between them. Such an evaluation has up to the present time offered only a rather theoretical interest, inasmuch as difficulties arise in the experimental determination of quantities which enter into the equation.

Subsequent modifications of the theory of Griffiths preserve the basic concepts of energy balance, but supplementary factors, the value of which became apparent, were taken into account in these modifications. In the energy balance equation a correction was introduced which represents the energy dissipated in the plastic deformation. Using the values of the surface energy which are ordinarily taken, cracks which may cause damage under normal stresses must be too large and may not exist previous to this in the unstressed state. In order to overcome

this difficulty, one introduces into the equation of energy balance a local elastic energy, by means of which the assumption of local concentration of stresses at the apex of cracks is taken into account.

One of the widely adopted modifications of Griffiths' theory considers four component energies, determining the growth of a crack:

1. The surface energy of a crack, proportional to its length.
2. The energy of the applied stress field, proportional to the square of the applied stresses and to the square of the crack length.
3. The energy of plastic deformation, depending on the crack length, the applied stress and the fluidity of the material.
4. The energy of local concentration of stresses, for which damage begins (ordinarily this is taken to be proportional to  $\log l$ ).

The condition for propagation of a crack does not differ from that formulated by G. R. Irvin (1948) and O. Ye. Orovan (1950) in the theory of quasi-brittle damage which made use of a different method for accounting for the energy of plastic deformation. They assume Griffiths' formula to be valid if in the place of  $\gamma$  one substitutes the so-called surface energy  $\gamma_{ef}$ , which represents the sum of the actual surface energy and the energy of plastic deformation. The Irvin-Orovan theory in which a relatively simple method for accounting for the energy of plastic deformation is employed, has substantially broadened the range of application for the Griffiths theory.

The equations of energy balance considered above describe the state of a system when the stress is lower than critical

value and when the system possesses only a potential energy. When the stresses exceed this value, the system possesses both potential and kinetic energy. N. F. Mott (1948) made use of a dimensionality analysis to obtain an expression for the kinetic energy of a moving crack.

$$W_k = k \rho l^2 v^2 \left( \frac{\sigma}{E} \right)^2, \quad (149)$$

where  $\rho$  is the density of the material;  $v$  is the propagation velocity of the crack;  $k$  is a dimensionless factor;  $\sigma$  is the tensile stress.

Supplementing the equation for energy balance with the expression for kinetic energy, and considering that the remaining terms maintain the same form as in the static problem, Mott found the propagation velocity for a crack

$$v = \left[ \frac{\pi(1-v^2)}{k} \right]^{\frac{1}{2}} \left( \frac{E}{\rho} \right)^{\frac{1}{2}} \left( 1 - \frac{l_*}{l} \right), \quad (150)$$

where  $l_*$  is the critical length of a crack.

As the crack grows, to a proportional degree its velocity approaches the limit

$$v_0 = \left[ \frac{\pi(1-v^2)}{k} \right]^{\frac{1}{2}} \left( \frac{E}{\rho} \right)^{\frac{1}{2}}. \quad (151)$$

From this relationship it is seen that the limiting velocity of a propagating crack comprises a definite part of the longitudinal wave velocity. Numerous experiments carried out by various authors allow one to come to the conclusion that the limiting propagation velocity of cracks is equal to the Rayleigh wave

velocity, i.e., it amounts to approximately 0.6 of the longitudinal wave velocity. A series of authors (Bikerman, 1946; Broberg, 1960) view with some doubt the applicability of the theorem concerning a minimum potential energy to the actual damage process. The surface energy of a substance is really free energy and not potential energy, as introduced by Griffiths. In order to form a new surface free energy it is not necessary to fulfill the condition of isothermality. In the general case, if, upon heating, the surface area of the sample increases, then according to the Le Chatelier principle any increase in this area by other means leads to a drop in temperature at the surface. It has been experimentally proved that the temperature of a newly formed surface is lower than the temperature of internal points of the sample, and there exists an irreversible thermal flux from internal points to external points of the substance. Thus the damage process can no longer be looked at as consisting of a series of quasi-equilibrium states; in the light of what has just been said it must be treated as an essentially irreversible process. Let us utilize the second law of thermodynamics which includes the theorem of minimum potential energy in implicit form. According to the law of the conservation of energy

$$dE = dQ - dA, \quad (152)$$

where  $E$  is the internal energy of the system,  $Q$  is the amount of heat received by the system, and  $A$  is the work performed by the system. Let us write down the second law of thermodynamics in the form

$$dQ = TdS - dq, \quad (153)$$

where  $T$  is the absolute temperature,  $S_e$  is the entropy of the system, and  $Q$  is the dissipated energy (the uncompensated heat according to Clausius).

Inasmuch as we are dealing with mechanical phenomena, it is convenient to express the internal energy  $E$  in terms of the Helmholtz free energy

$$F = E - TS_e, \quad (154)$$

whence

$$dq = -dF - dA - S_e dT > 0. \quad (155)$$

In accordance with the calculations of Griffiths the gain in free energy upon an increase in crack length by  $dl$  is equal to

$$dF = \gamma_l dl, \quad (156)$$

where  $\gamma_l$  is the surface energy of a crack, related to a unit length. The gain in elastic energy amounts to

$$dW_e = -2k\sigma^2 l dl, \quad (157)$$

where  $k$  is a constant. Then the dissipated energy becomes equal to

$$dq = -(\gamma_l - 2k\sigma^2 l) dl - S_e dT > 0. \quad (158)$$

If the term  $S_e dt$  is small, then by neglecting it we return to the Griffiths' theory. However, this is justified only for temperatures close to absolute zero.

The thermodynamic approach to damage phenomena makes it possible to illuminate certain theoretical sides of this process in a new way. In practical calculations the Griffiths' theory retains its validity as before, inasmuch as the non-isothermality of the process is automatically taken into account in the experimental determination of specific surface energy  $\gamma$ .

I. I. Bikerman (1964) proposed a new criterion for damage. Subjecting to criticism the energy balance equation in Griffiths' theory, which is based on a balance of the energy of deformation and the increase in surface energy of a crack, he connects damage with a favorable distribution of the energy of deformation alone. A crack may propagate in the case where a reduction in deformation energy around the critical region is greater than that required for an elastic deformation of the critical region prior to rupture. In contrast to Griffiths' theory it is assumed that the energy expended in the damage process is converted mainly into heat, and not into the surface energy of a crack. Formulas for calculation, obtained on the basis of this hypothesis, are identical to formulas from the Griffiths' theory, but in place of the specific energy in the latter, the specific work of damage plays a part, a quantity which has a different physical meaning.

I. V. Kraggs proposes that the critical conditions for damage be evaluated from the local energy of the stress in a region which includes the crack. He supposes the damage to be a quantum (discontinuous) phenomenon. The rupture of atomic bonds takes place within the limits of a surface of area  $S_z$  in a small interval of time  $\Delta_t$ . Since the crack cannot propagate with a velocity exceeding that of longitudinal elastic waves  $C$

the energy of a new surface must be concentrated in a region whose boundary is removed by no more than a distance of  $a = c\Delta t$  from the edges of the crack. The crack is formed only in the case where

$$\iiint_{(V)} w_e \, dr \, dy \, dz \geq 2S_e \gamma, \quad (159)$$

where  $w_e$  is the energy of elastic deformations of a unit of volume. The integration in formula (159) is performed over the region of concentration of elastic deformation energy  $c\Delta t$ . Two new parameters,  $S_e$ , and  $a$ , enter into expression 159. Let us determine their physical meaning. Let us suppose that an ideal crystal is damaged by a uniaxial tensile stress  $\sigma_0$ . This stress will be equivalent to the theoretical forces of adhesion, referred to a unit of area corresponding to a plane of the crystal. Criterion (159) is transformed into the form

$$\left[ \frac{\sigma_0^2}{E} \right] 2S_e a > 2S_e \gamma, \quad (160)$$

and thus

$$a = 2\gamma \frac{E}{\sigma_0^2}. \quad (161)$$

We note that expression (161) signifies only a necessary condition for damage. However, in principle, it may be applied as a sufficient condition as well. The value of  $S_e$  depends on the internal structure of the medium being damaged and has the order of magnitude of the average cross-sectional area of a grain or a crystal.

Although the hypothesis of damage being considered here

differ in their physical meaning and in the method of analysis, damage effects and formulas for calculation obtained on their basis agree in form with the computational formulas from the modified Griffiths' theory.

The essence of the force approach to a description of the damage process consists in a replacement of interparticle adhesion forces, acting in the dead-end part of a crack, by some external forces. This makes it possible to utilize the methods of the mathematical theory of elasticity and the model of a continuous medium in the calculations, and the problem of crack propagation is formulated as a force problem in the mechanics of a deformable body. G. I. Barenblatt (1961) proposed a theoretical scheme for solving problems on the ultimate equilibrium of brittle bodies with macro-cracks. At the root of this scheme lie the hypotheses of independence of the terminal region of a crack, the smallness in size of the terminal region in comparison with dimensions of the crack itself (the conditions of macroscopicity), and the finiteness of stresses in the dead-end portion. However, the given computational scheme is not satisfactory for the description of microcrack behavior, since in a series of cases microcracks exert a quite significant influence on the strength properties of a solid body.

In the works of M. Ya. Leonov and V. V. Panasyuk (1959, 1961, 1968) a new model for calculation ( $\delta_k$ -model) was proposed, providing the capability for studying in a single-plan the equilibrium state of a solid body weakened with both micro- and macro-cracks. In the case of macroscopic cracks the  $\delta_k$ -model of a brittle body leads to the same results as the G. I. Barenblatt scheme (1961). The basic hypothesis in the construction of this model is an assumption about the nature of the dependence of interparticle forces on distance: if the distance between

opposite sides of a crack does not exceed some constant for a given material whose value is  $\delta_k$ , the forces of attraction between them are equal to a constant value  $\sigma_0$ ; but if the distance between opposite sides of the cracks is greater than  $\delta_k$ , they are equal to zero. The condition for crack propagation within the framework of this scheme is the relationship

$$2u_n(l_0, l, q_*) = \delta_k, \quad (162)$$

where  $u_n$  is the normal component of the displacement vector of points on the sides (shores) of the crack;  $l_0$  is the characteristic linear dimension of the region of the initial crack;  $q_*$  is a parameter characterizing the external load.

The value of the limiting load  $\sigma_{cr}$  for a specified initial crack length  $l$  within the framework of the  $\delta_k$ -model is determined as

$$\sigma_{cr} = \frac{2}{\pi} \sigma_0 \arccos \left\{ e^{-\frac{l_0}{2l} k} \right\}, \quad (163)$$

where  $k$  is a constant equal to  $1/\pi E$  for a plane stressed state equal to  $(1-\nu_2)/\pi E$  for a plane deformation. For  $l_0$  much greater than  $\delta_k$  expression (163) turns into the familiar formula of Griffiths, and for  $l_0$  approaching zero,  $\sigma_{cr}$  approaches  $\sigma_0$ , i.e., a plate with a crack of zero length has the strength of a defectless plate. Thus, the problem of damage in a solid body reduces to the study of crack propagation in deformable bodies using methods of the linear theory of elasticity.

Advances in mathematical statistics made it possible to apply some of the methods of this science to an investigation of the damage process (Bolotin, 1965; Volkov, 1954; 1960). The

basic idea of the statistical theory of strength is the construction of an original model of the medium that permits one to apply the methods of statistics in describing the process of damage. The model of a quasi-isotropic crystalline body is chosen in the form of a single-phase system of crystals, contained in a volume  $\omega_v$  and bound to each other by adhesion forces. The size of the volume  $\omega_v$  is chosen with a reckoning such that comparability is assured between the results of calculations carried out for a uniform medium and the results of experimental measurements of the stresses and deformations in the case of a polycrystalline body. To serve as a physical analog of a mathematical point we introduce the volume  $V$ , which is small in comparison with the dimensions of the total sample, but which at the same time contains a large number of atoms or molecules, whereby a  $\omega_v$  is much greater than  $V$ .

In accordance with the views of M. V. Yakutovich (1961) the sole cause for the formation of microcracks is the action of breaking apart under the influence of normal tensile stresses. In the case of complex stressed states only the normal component of the tensile stress is considered. This makes it possible to consider from a single point of view all types of macroscopic damage. The process of macroscopic damage within the scale of volumes  $V$  begins with stresses which are smaller than the resistance to damage of the polycrystalline material. Calculations show that even with a null stress in a cross-section of the volume  $\omega_v$  in some part of the cross-sections volumes  $V$  there exist stresses greater than the critical stress for breaking apart  $\sigma_{cr}$ . Consequently, in accordance with the single mechanism for damage in the solid state, there come to exist microscopic cracks. The relative number of damaged volumes  $V$ , in which microcracks have appeared in response to uniaxial tensile strength  $\sigma$ , is equal to

$$n = \frac{1}{2} - \frac{1}{\sqrt{\pi}} \int_0^{\frac{\sigma}{\sigma_{cr}}} e^{-t^2} dt, \quad (164)$$

where

$$y = \frac{\sigma_p - \sigma}{\sqrt{\theta}}$$

( $\sigma_p$  is the average resistance to damage of the crystals of polycrystalline material;  $\theta$  is the coefficient of normal distribution of volumes  $V$  in values of the stress). With an increase in external loading the number of microscopic cracks grows rapidly, reaching some critical value. After that there occurs a consolidation or coalescence into one macroscopic crack occupying a volume which is typically a  $\omega_v$ . The condition for attaining the critical number of microcracks for any type of stressed type is equivalent to the equation

$$n = n_k, \tag{165}$$

where  $n_k$  is a constant for a given material, which does not depend on the nature of the stressed state of the solid material in the volume  $\omega_v$ . This constant is equal to the relative number of cracks in volumes  $V$  which is sufficient for macroscopic damage. Not all volumes  $\omega_v$  are laced by damage, including macroscopic damage, but only some part of them. In this connection, the more brittle the material is the smaller this part will be, since in such a material a microcrack will be more dangerous than in a plastic material. With brittle macroscopic damage in separate microscopic volumes the damage may be viscous. The proportion of microscopic volumes of brittle and viscous damage, determines the nature of macroscopic damage. In the process of plastic deformation in similar volumes of viscous damage, the resistance to damage changes at a level with the change in geometric form. As the deformation increases there is observed a general tendency for the shear strength to increase

and for the cohesive strength in a direction perpendicular to the slippage plane to decrease. However, in some cases true tensile strength increases with a growth in the value of plastic deformation or remains constant. In the general case under the influence of an external stress both elastic and plastic deformations rise in a damaged substance. Out of a total number  $N$  of volumes of type  $V$  a part of them,  $N_e$ , will deform elastically and a part  $N_p$  in a plastic fashion. The total number of microcracks up to the moment of macroscopic damage is

$$m = m_e + m_p, \quad (166)$$

where  $m_e$  is the number of microcracks formed upon damage in elastically deformed volumes  $V_y$ ;  $m_p$  is the number of microcracks formed as a result of damage in elastically deformed volumes  $V_p$ . The relative number of microcracks up to the moment of damage will be

$$n_k = \frac{m}{N} = \frac{N_e}{N} \frac{m_e}{N_e} + \frac{N_p}{N} \frac{m_p}{N_p} = (1 - p) n_{y_e} + p n_p, \quad (167)$$

where  $P = N_e/N$  is the relative number of elastically deformed volumes  $V_p$ , or the probability of the elastic state;  $N_p$  is the relative number of microcracks in elastically deformed volumes  $V_p$ ;  $n_e$  is the relative number of microcracks in elastically deformed volumes  $V_e$ . From this one may obtain the criteria for brittle and viscous damage in the statistical theory of strength:

a) in the case of brittle damage

$$n_k = n_e, \quad (168)$$

b) in the case of viscous damage

$$n_k = n_p. \quad (169)$$

In the works S. D. Volkov and other authors the numerous applications of the statistical theory of strength are reviewed as to the manner in which they verify the correctness of the basic assumptions and other aspects of the theory and its advantages over more engineering-oriented theories of strength, as a single unique theory both with respect to the mechanism of damage and with respect to the condition for strength which is common for all types of stressed states. The statistical theory of strength may be successfully utilized in the study of the damage process in rocks.

Actual media, in particular rocks, possess complicated structures. Mathematical models of media, even when their plastic and relaxation properties are taken into account, do not fully describe all the peculiarities of behavior of an actual medium under the action of high impulsive loads. The use of the concept of a continuum is already by itself an approximation especially in the case where destructive stresses are exceeded. Therefore, at the present time an analytical description of the damage process in rocks is not possible. Only qualitative ideas exist regarding the essence of phenomena which take place in damage. This explains the phenomenological character of theories of damage in rocks. They belong to the same category as the classical theories of strength, i.e., to the category of mechanical theories of strength.

A description of the damage process in an explosion using a solid state model similar to the Griffiths' model was first introduced by Professor M. V. Machinskiy (1936), who proposes that "the wave passes through strong places in the rock leaving no trace; as it passes through 'weak' places the beginning of cracks emerge." Supposing that one knows the pressure at every point in the block is a function of time, the distribution law of crack nuclei as a function of strength, the velocity of

motion of crack apexes as a function of pressure, and the distribution pattern of weak points (centers of crack formation) within the body, M. V. Machinskiy obtained theoretical dependences relating the parameters of the explosion, and the number and average volume of the fragments that were formed. For a long time the absence of methods for determining the "weak" places in the block prevented M. V. Machinskiy's theory from being used for finding quantitative dependences which were suitable for practical calculations. Taking account of these experimental difficulties, M. V. Machinskiy noted the relation of the theory under consideration to the theory of a series of more general processes. Therefore, "experimental verification of these more general processes along with confirmation of agreement between the actual results of the process and the processes indicated above may serve as a criterion for the correctness for the proposed theory."

Experimental investigations carried out at the A. A. Skochinskiy Institute of Mining Affairs. (Sorokin, 1959) and in the Institute for Geotechnical Machinics of the Ukrainian SSR Academy of Sciences testify convincingly to the fact that the process of shattering begins in zones of reduced strength. Further investigations showed that the density of crack-formation centers is a function of the stresses. The distance between a zone of lowered strength and the rate at which cracks develop determine the time parameters of the damage process, i.e., the time for shattering to take place is a function of the stresses.

Over the last few years in addition to a study of the qualitative picture of shattering, experimental investigations have been conducted which examine the process of damage and the rate at which cracks develop as an important physical

and mechanical characteristic of rocks. G. Kol'skiy (1963) studied the conditions of brittle shattering on the basis of experimental data. As a result of these studies he came to the conclusion that the brittleness of a material depends on the rate at which a load is applied and on the physical and mechanical properties of the rocks. However, up to the present time there exists no generally accepted theory of shattering, for which reason various methods for calculating the fragmentation of rocks have been proposed.

One of the first attempts at calculating the particle-size composition of an exploded rock mass was the work of O. Ye. Vlasov (1958), which was considered in detail in the preceding chapter. In the work of A. N. Khanukavev (1962) the determining influence of the acoustic rigidity of rocks on the nature of shattering is proved convincingly on the basis of copious experimental material. In the case of hard excavated rock possessing a high acoustic rigidity, crushing is conditioned by the stress wave parameters. It is proposed that the number of splintered fragments for these rocks be determined from the expression

$$N_k = \frac{\sigma_{\max}}{[\sigma]}, \quad (170)$$

where  $N_k$  is the number of strips formed in the rock by the stress wave;  $\sigma_{\max}$  is the maximum pressure at the wave front of the stress wave,  $[\sigma]$  is the ultimate tensile strength of the rock,

The indicated dependence naturally cannot be used for describing damage effects produced by a compression wave. An analogous form may be obtained by using the statistical theory of

strength for a uniform distribution of cracks over the whole volume of damaged medium and the impossibility of simultaneous growth of two or more cracks. The deviation of the results of the calculation from the experimental data is explained by the nature of the assumptions made.

Recently in the works of Doctor of Engineering Science G. P. Demidyuk, the concept of the intensity of shattering on the energy reserve of the explosive material being exerted on a unit volume of the rock being shattered has received development. This permits wider use of the method of energy modeling employing the thermodynamic criteria of similarity.

In utilizing the similarity criteria for elastic wave motions in order to model the destructive action of an explosion no account is taken for the effect of piston action of the gaseous products of the explosion on the shattering process. An indirect confirmation of the influence of piston action of the gaseous detonation products on the damage process is rendered by an evaluation of the damping of tangential stresses causing the development of radial cracks. The tangential stresses, arising in the explosion of cylindrical charges may be approximately determined from the formula

$$\sigma_t = p \frac{(r_a^2/r^2) + 1}{(r_a^2/r_0^2) - 1}, \quad (171)$$

where  $\sigma_t$  is the value of tangential stresses in the rock at point  $r$ ;  $p$  is the pressure in the charge chamber;  $r_a$  is the radius of the shattered zone;  $r_0$  is the radius of the charge cavity;  $r$  is the distance of the point where stresses are determined from the axis of the charge. An analysis of equation (171) shows that with increasing separation from the charge center the tangential stresses diminish quite rapidly. If

they were the only reason for the development of cracks, the damaged volume would be insignificant. However, owing to the high pressure in the charge chamber, the gases penetrate into cracks formed in the wall of the blast hole and exert pressure on the walls of the cracks. As a result of this high tensile stresses develop at the termini of a crack facilitating further growth of the crack. As a consequence, the piston action of gaseous explosion products favors the increase in terminal length of the cracks being formed and has practically no effect on the number of cracks.

As the result of an analysis of the present state of the theory of damage it has been established that in shattering the block of rock may be considered as a medium with non-uniformities and microcracks, to which the basic assumptions of the of strength of Griffiths and the statistical theory of damage may be applied.

#### Basic Mechanisms of the Process of Damage (Shattering)

In sufficiently large volumes of a substance the effect of microcracks, dislocations, and displacements of atoms averages out to some mean value. One may consider that the microcracks are uniformly distributed over the whole volume under study, and even over its elementary parts (sufficiently large in order for the condition of uniform distribution of defects to be fulfilled). The damage process is determined by the physical, the mechanical, and the structural properties of the medium and by the parameters of the stress field. Let us take a look at the basic mechanisms or regularities of the damage process. The mechanism of damage consists in the growth and coalescence of cracks which are found in the medium. Quantities which characterize the capacity of the cracks to grow will be called the crack parameters. Included in their number will be the

dimensions of the crack, their orientation in space, the radius of curvature at the apex of the crack, etc. The number of parameters which determine fully the behavior of a crack upon application of a load we will take as equal to  $n$ . The value of the parameters will change as we pass from one crack to another in a discrete manner. But the aggregate of parameters forms a continuous system. This means that the parameters of any separate crack may take on any value (here we take no notice of possible correlations between them). Thus, the crack parameters may be represented in the form of points in an  $n$ -dimensional space. The aggregate of all possible values of the parameters, by virtue of the continuity of their variation, forms some simply connected region  $V$  in the  $n$ -dimensional space. The number of cracks  $n_c$  in a fixed volume as the medium (without limiting the generality of our discussion it may be considered as a single number) possessing parameters  $\alpha_1, \dots, \alpha_n$ , lying in a region of  $n$ -dimensional space  $\Delta V$ , is determined in the following manner:

$$N_c = \int_{(\Delta V)} f(\alpha_1, \dots, \alpha_n) \prod_{i=1}^n d\alpha_i, \quad (172)$$

where  $\prod_{i=1}^n \alpha_i$ , is an element of the  $n$ -dimensional volume;  $f(\alpha_1, \dots, \alpha_n)$  is the differential distribution function.

The differential distribution function characterizes the rule for distribution of cracks according to the values of their parameters. The concrete form of this function depends on the properties and the structure of the medium under consideration. It specifies the probability that any crack chosen in a random fashion will have parameters lying within the limits of

$$(\alpha_1, \dots, \alpha_n) - \left[ (\alpha_1, \dots, \alpha_n) + \prod_{i=1}^n d\alpha_i \right].$$

In order that the crack might begin to propagate in the case of a concrete form for the stressed state, its parameters might satisfy definite conditions. Mathematically this means that the parameters of the propagating cracks must lie inside some region  $\Delta V$  of the parameter values. The dimensions of this region are determined by the nature of the stress field, i.e., by the form of the function  $\sigma_{jif}(r, t)$  [ $\sigma_{jif}(r, t)$  is a tensor describing the dynamic field of the stresses]. Consequently, the form and dimensions of the region  $\Delta V$  will be a function of the stress tensor:

$$\Delta V = \Phi[\sigma_{ij}(r, t)]. \quad (173)$$

The dependence of the boundaries of region  $\Delta V$  on  $\sigma_{ij}(r, t)$  may be represented in the form

$$F[a_1, \dots, a_n, \sigma_{ij}(r, t)] = 0. \quad (174)$$

Relation (174) represents the condition for growth of cracks. It is a necessary but not a sufficient condition for fragmentation, since does it not include kinetic characteristics of the process but only force characteristics.

The number of cracks which have lost their stability in  $N_t$  will be determined by the equation

$$N_t = \int_{\Delta V} f(a_1, \dots, a_n) \prod_{i=1}^n da_i = \int_{\sigma_{ij}} f(a_1, \dots, a_n) \prod_{i=1}^n da_i. \quad (175)$$

the kinematic condition for fragmentation will consist of the requirement that values of  $\sigma_{ij}(r, t)$  within the course of an interval of time  $\tau$  should not fall within the region  $W$  of the values  $\sigma_{ij}$ ,

$$\sigma_{ij} \in \Pi \quad \text{when} \quad t_1 \leq t \leq t_1 + \tau, \quad (176)$$

where  $t_1$  is some fixed moment in time. The value of the time interval  $\tau$  is a complicated function of the crack parameters, the number of cracks, the value of the stresses, and the physical properties of the medium.

$$\tau = F(a_1, \dots, a_n, b_1, \dots, b_m, \sigma_{ij}, N_\tau), \quad (177)$$

where  $b_1, \dots, b_m$  are elastic constants of the medium.

Relations (174) and (176) represent a necessary and sufficient condition for shattering and may be taken to be a generalized criterion of fragmentation. The dependencies thus obtained are quite general. They characterize only that general quality which is inherent in any form of damage to any material. Naturally these dependencies are not sensitive to a series of important qualitative aspects of the actual form of damage, by which one type is distinguished from another. The peculiarities of brittle shattering of rock is considered below.

#### The Mechanism of Crushing of Rock By Explosive Action .

The destruction or shattering of rock under the action of explosive loads represents a complex non-stationary process. The phenomenon is complicated by the structural peculiarities of rocks, which in most cases are anisotropic nonhomogeneous systems. Interruptions in the continuity, stratification of the structure, and inhomogeneity of the physical and mechanical properties make an accurate solution of the problem impossible given the present level of development of this science. Any notion on the mechanism of destruction in rocks have basically only a qualitative nature. The high pressure of gases formed

in the explosion inside the charge chamber acts on the walls of the chamber and cause them to move and deform, an effect which propagates in the form of waves with a velocity determined by the physical and mechanical properties of the medium. In a region enveloped by wave action, the massive exists in a stressed state. If the stresses exceed some value which is characteristic for a given region, the cracks which are found there begin to grow and the volume becomes divided into parts by a spatial network of cracks. The value of the critical stress depends on the type of stressed state, the dimensions of cracks, and the region under consideration and on the average is equal to the mechanical strength of the material. The scatter of values of the critical stress is not large and fluctuates within limits determined by the scale of the effect. The maximum velocity of growth of cracks is determined by the physical and mechanical properties of the material. According to theoretical calculations it is equal to the velocity of a Rayleigh wave. But the velocity of crack propagation does not immediately attain its maximum value. The time taken by the velocity of a crack to reach its maximum (or a value close to it) depends on the level of the stressed state, decreasing sharply with an increase of stress. Since the velocity of crack propagation is a finite quantity, the length of time during which the stress field exists in a given region has a substantial effect on the damage process in addition to the level of the stressed state. The minimum time necessary for destruction of a given volume is determined by the velocity of crack propagation and the density of sites of their origin. When the velocity of cracks reaches its maximum value the value of the stresses no longer exerts any influence over the velocity of crack propagation. The density of sites where cracks have originated is a quantity which is quite sensitive to the stress. This is explained by the fact that cracks of smaller dimensions, the probability of

whose existence in the solid state is larger than that of cracks of larger dimensions, are exposed as the stresses are increased. Therefore, as the value of the stresses rises the minimum time for damage decreases on account of shortening of the path covered by cracks up to the time of their coalescence. For very high stresses the solid state passes over into a quasi-liquid state and in the processes of shattering plastic deformations begin to play the principle role, i.e., the mechanism of damage itself changes. Nevertheless these phenomena have small practical significance in explosive operations with excavated rocks, since the radius of this zone does not exceed 3 to 5 charged radii. The process of shattering of a solid block especially in distant zones, continues for a rather long time (in terms of the temporal characteristics of the explosion) and the stressed state of these regions is determined by the interference between the reflected and direct waves. The stresses in the reflected wave depend in their magnitude and their size on the condition of reflection existing at the boundary of the load. By changing these conditions one may control the quality of crushing of the rock and the size into which the exploded rock mass is broken up.

The majority of rocks contain numerous cracks, the number, orientation, and density of which depends on the physical and mechanical properties of the rock and the actual mineral and geological conditions of their occurrence. The mechanism of damage of blocks of cracked rocks subjected to the action of explosive loads have their peculiarities which set them apart to a significant degree from the mechanism of crushing of monolithic media. In weak rocks, i.e., rocks with a developed system of fine cracks, the pressure of the products of explosive decomposition on the charge cavity falls more rapidly than in monolithic rocks, on account of the penetration of compressed gases into the cracks. The stress field is less intense and is

characterized by a high degree of damping of the stresses in proportion to increasing distance from the charge. This comes as a consequence of absorption of energy of a stress wave as it passes through the cracks. A significant part of the energy of the stress field is thereby transferred into kinetic energy of moving fragments. Shattering caused by the action of a stress wave is in this case insignificant and the principle role is played by the piston action of the gaseous products of detonation. In blocks which have been divided into separate structural units by coarse, sparsely distributed cracks, the only lump which is intensely fragmented is that in which the explosion cavity was situated and the remaining part of the shattered block represents structural units which are disconnected by virtue of the crack which exist there. Consequently, the particle-size composition of the exploded rock mass will be determined by the structural elements of the spatial network of cracks in a significant portion of its total.

A more efficient use of the energy accumulated in the field of stresses formed in the explosion is possible if the following conditions are fulfilled. First of all conditions must be created which prevent a substantial opening of cracks. The intensity of the stress field diminishes to the least degree in the presence of only tightly closed cracks or cracks with a width that does not exceed the absolute deformations of the block in the region where a crack is localized. Secondly, the block must not move as a single unit. This means that the field of velocities of the block must have a gradient which is different from zero. In this case there arises a supplementary mechanism for transmitting energy into the distant zones of the block which is being shattered. The essence of the idea consists in the collision of moving pieces of rock. A series of such impacts causes a stressed state to obtain in the remote parts of the block, and a part of the kinetic energy is once more transformed into energy in the stress field. All the conditions

enumerated above are fulfilled in the case of an explosion in a compressed medium. In this case the conditions for explosion play a decisive role in the damage process. A qualitative analysis of the process of shattering permits one to separate out three basic factors which effect the quality of the disintegrated rock mass: the parameters of the stress pulse, physical and mechanical properties of the rock being shattered, and the explosion conditions. When mining operations are being conducted under actual conditions the physical and mechanical properties of the rock turn out to be fixed quantities and a variation in the intensity of fragmentation of the rock may be attained through a modification of the stress pulse parameters and the explosion conditions. The characteristic which underlies these factors are the parameters of the stress field.

To serve as a mechanical model of the rock mass we choose an isotropic homogeneous medium which contains a large number of irregularly arranged cracks. Let us suppose that the system of cracks does not possess a preferential orientation. The sizes of the cracks being considered must obey  $L_i$  much less than  $L_g$ , where  $L_i$  and  $L_g$  are the linear dimensions of the cracks and the block respectively. If there exists in the block of rock cracks with dimensions of the order of  $L_g$ , then the block may be considered as the aggregate of separate fragments. For each of the similar individual units all previously stated assumptions remain in force.

Let us consider the shattering of an elementary volume. We will consider as elementary the smallest volume of rock which possesses properties similar to the properties of the block with the exception of the peculiarities connected with the scale effect. The stressed state which causes damage in the elementary volume will at the same time be the condition for fragmentation of the block. Let us assume that in the medium a plane wave is propagating with an amplitude which exceeds the shattering stress.

The energy of a deformed homogeneous isotropic body is determined in the following manner:

$$E_e = \frac{1}{2} \int \sigma_{ij} \epsilon_{ij} dV = \int \left[ -\frac{\nu}{2E} \theta^2 + \frac{1+\nu}{2E} \epsilon_{ij} \epsilon_{ij} \right] dV, \quad (178)$$

where  $\theta = \sigma_{ii} = \sigma_{11} + \sigma_{22} + \sigma_{33}$  --the first invariant of the stress tensor;  $\sigma_{ij}$  are components of the stress tensor.  $\epsilon_{ij}$  are components of the deformation tensor.

To serve as a characteristic quantity of the stressed state we shall choose the effective stress  $\sigma_{ef}$  which is determined by the equation

$$\frac{\sigma_{ef}^2}{2E} = \left[ -\frac{\nu}{2E} \theta^2 + \frac{1+\nu}{2E} \epsilon_{ij} \epsilon_{ij} \right] \quad (179)$$

assuming that the components of the stress tensor do not change significantly within the confines of the elementary volume, we obtain

$$E_e = \frac{\sigma_{ef}^2}{2E} \Delta V, \quad (180)$$

where  $\Delta V$  is the elementary volume.

The crack parameters differ as to their role in the process of fragmentation. Let us take a look at the distribution of principle crack parameters: the dimensions and the orientation of cracks in space. If the cracks do not have a preferred direction (a representative feature of the distribution of micro-cracks), then the distribution of number of cracks in the various directions may be considered uniform to a sufficient degree of accuracy. The formation of cracks in unstressed material takes place under the control of numerous factors. The distribution of random magnitudes which are under the influence of a rather large number of independent (or almost

independent) factors, the effect of each of which is insignificant, approaches a normal distribution in agreement with the limiting theorems of the theory of probability (Bolotin, 1965; Gnedenko, 1961). The assumption of independence for the crack parameters eliminates the possibility of taking account of interactions between them. An account of the mutual influence of propagating cracks is exceedingly complex and up to the present time has not been accomplished. However, it is obvious that the effect of interaction between cracks on their development diminishes with an increase in the rate of application of the load. From this point of view, introducing an assumption about the independence of parameters of the growing cracks in the case of shattering by explosive loads is fully justified. An account of the interacting of cracks may be related both to a change in the parameters of the normal distribution as well as to a completely different distribution law. Consequently, we will consider that the number of cracks in a unit of volume of rock obeys the normal distribution law in areas.

$$dn = n_0 e^{-\beta S} dS, \quad (181)$$

where  $n_0$  is a constant characterizing the structure of the substance;  $\beta$  is a constant factor which has the dimension of inverse area.

The quantity  $\beta$  depends on the physical and mechanical properties of the rock and determines its strength. Even with uniform loading in actual substances the stress fields contain local inhomogeneities. At the termini there occurs a concentration of stresses depending on the crack dimensions. When the value of these stresses reaches a certain value, called the critical stress, the crack begins to grow with a finite velocity (i.e., the process of crack development becomes irreversible). Sometimes this value of the critical stress is identified with

the theoretical strength of the material. Such an identification is erroneous. The theoretical strength is the greatest possible quasi-elastic force in an ideal defectless lattice under conditions of uniform steady deformation. The critical stress is the maximum quasi-elastic force under special conditions at the apexes of a crack. The first quantity is a constant of the material but the second varies not only from crack to crack but also for a given crack throughout the process of its growth. In the calculation formulas we must insert precisely the critical stresses, not the theoretical strength.

The connection between the applied stresses and the dimensions of a crack, where the concentration of stresses at the boundary of that crack attains the critical value, is found from formula (147). If the applied load creates stress fields in the material with a value of  $\sigma_{cr}$ , then all cracks with an area  $S$  greater than or equal to  $S_{cr}$  begin to grow. The number of such propagating cracks is determined in the following way:

$$N = n_0 \int_{S_{cr}}^{\infty} e^{-\beta S} dS = \frac{\sqrt{\pi} n_0}{2\beta} [1 - \Phi(S_{cr})] = \frac{\sqrt{\pi} n_0}{2\beta} \operatorname{erfc}(\beta S), \quad (182)$$

where)

$$\frac{2}{\pi} \int_0^{S_{cr}} e^{-\beta S} d(\beta S) = \Phi(S_{cr}),$$

◆  $(S_{cr})$  is the probability integral.

The atomic-molecular theory of structures does not permit an unlimited decrease in the dimensions of cracks. Arguments based on the concentration of a continuous medium cease to be correct when the dimensions of the region are reduced to distance on the order of atomic dimensions. A series of investigators (Barenblatt et al, 1967; Berry, 1958) confirmed the presence of some characteristic linear dimension  $l_0$  in every material. Thus, Berry (1958) in his attempt to establish the

applicability of the usual theory of cracks for polymethylmethacrylate (an inorganic glass) and polystyrene discovered that when the dimensions of the initial cracks were reduced to some tenths of a millimeter the destructive stress (contrary to the theory) ceases to depend on the length of the crack. Berry concluded that cracks of such lengths arise in a material in a natural manner (there were none in an unloaded material). Analogous results were obtained on nylon and introesters. The linear dimensions  $l_0$  for these materials lay between 0.05 and 1 mm. G. I. Barenblatt et al. (1967) on the basis of a theoretical analysis of the mechanism of fluctuational damage came to the conclusion that there exists cracks of a constant length  $\delta$ , arising in a natural manner in an unloaded material which originally did not have cracks. This quantity agrees in size with  $l_0$ . Thus,  $l_0$  will be the minimum length of cracks which are capable of forming a spatial network under practically realizable loads. In order for cracks of smaller dimensions to grow a longer time is necessary than that necessary for a body to be damaged by cracks developing from a disruption of continuity of more substantial dimensions. When the spatial network of cracks forms these stresses in the damaged volume become vanishingly small and further growth of the crack comes to a stop.

Let us determine the average distance between growing cracks under the condition of their uniform distribution throughout the volume of the sample. We will consider that each growing crack is located in the center of a cube with edge  $A$ , so that

$$V = Na^3; \quad a = \sqrt[3]{\frac{V}{N}}, \quad (183)$$

or for unit volume

$$a = N^{-\frac{1}{3}}.$$

substituting the value of N into formulas (183) and expression (182), we obtain

$$a = \left\{ \frac{23}{V \pi n_0 [1 - \Phi(S_{cr})]} \right\}^{\frac{1}{3}}. \quad (184)$$

the mean distance between propagating cracks

$$b = \left\{ \frac{163}{V \pi n_0 [1 - \Phi(S_{cr})]} \right\}^{\frac{1}{3}}. \quad (185)$$

Let us calculate the time required for the coalescence of growing cracks. The distance covered by a crack consists of two terms, corresponding to two stages of growth. The length of a crack at a moment in time  $t$  may be written down in approximately in the following form:

$$l_t = \frac{1}{2} l_0 v_{max} + v_{max} (t - t_0), \quad (186)$$

where  $t_0$  is the time taken by the crack to reach maximum velocity  $v_{max}$  and  $t$  is the overall time taken by the shattering process to develop.

Formula (186) is derived on the basis of the assumption that growth in the crack velocity is a linear function of time. The quantity  $l_t$  changes with a variation in the level of the stressed state. Experimental studies into the time dependence of strength (Zhurkov, 1958; 1959) permit us to approximate the dependence of the time taken by a crack to reach maximum propagation velocity in the form

$$t_0 = \tau e^{-k\sigma} \rho (\sigma - \sigma_{001}), \quad (187)$$

where  $k$  and  $\tau$  are constants which depend on the physical and

mechanical properties of the material;  $\sigma_{\text{saf}}$  is the so-called safety stress, i.e., that stress at which the probability of growth of a crack is equal to the probability of its closing up  $p(\sigma - \sigma_{\text{saf}})$  is the  $\sigma$  function (step);  $p(\sigma - \sigma_{\text{saf}}) =$   
 $\begin{cases} 1 & \text{when } \sigma - \sigma_{\text{saf}} > 0 \\ 0 & \text{when } \sigma - \sigma_{\text{saf}} \leq 0. \end{cases}$

The overall time for shattering of a unit of volume

$$t = \frac{1}{v_{\text{max}}} \left( \frac{163}{a_0 \sqrt{\pi}} \right)^{\frac{1}{3}} \left[ 1 - \Phi \left( \frac{1}{9} L \frac{E\gamma}{\sigma^2} \right) \right]^{\frac{1}{3}} - \frac{c}{2} e^{-k\sigma} p(\sigma - \sigma_{\text{saf}}). \quad (188)$$

An analysis of expression (188) showed that even when the stress approaches infinity the shattering time remains finite, and when  $\rho = 0$  then  $t \rightarrow \infty$ . This agrees with the behavior of actual materials.

The intensity of fragmentation of rocks by explosive action depends on a number of factors. However, their effect on the nature of crushing is not equivalent. The basic factors which determine the particle-size composition of the exploded rock mass are the values of stresses arising in the rock block at the time of explosion, the duration of existence of a stress state and the physical and mechanical properties of the rock mass. The properties of the rock mass under practical conditions are quantities which are specified and invariable. Consequently, the crushing process may be controlled only through an alteration of the first two factors. In the general case, the stressed state is fully determined by the six components of the stress tensor. For definite forms of the stressed state, there exists completely unambiguous relations between the tensor components. The stress fields which are formed in the explosion of a spherical and cylindrical charges constitute the object of our interest. By virtue of the specifics of the stress distribution in such fields, their intensity may be characterized by one component--the value

of the maximum primary stress.

The shape of the stress impulse is an integral characteristic quantity of the stress and the duration of its existence. From the state of the stress impulse we understand the form of the curve  $\sigma(t)$ . Thus, the shape of the stress impulse characterizes the particular way in which the value of the stress varies with time.

Let us take a look at the typical shape of stress impulse arising in a medium at the time of explosion (Fig. 28). The segment of the curve  $ab$  characterizes the forward front of the wave, segment  $bc$  characterizes the rear front. The amplitude, i.e., the maximum stress in the impulse is  $\sigma_{\max}$ . Segment  $ac$  along the time axis is equal to the overall duration of the impulse. The time taken for maximum stress to be reached is determined by segment  $at_m$ . The ratio of the value of the maximum stress to the time for it to be reached,  $\sigma_{\max}/t_m$  determines the slope of the forward front of the impulse.

A study of the mechanism of fragmentation makes it possible to determine the influence of each stress pulse parameter on the particle-size composition of the exploded rock mass. The amplitude of the stress impulse  $\sigma_{\max}$  is controlled by the number of cracks opening in a unit of volume (182). The density with which the opening cracks are arranged determines the possible dimension of an average fragment. Consequently, by varying the amplitude of the stress pulse one may regulate the linear dimensions of the fragment. The relation between these quantities is given by formula (185). Relationship (185) determines only the possible dimension of an average piece  $b$ . In fact, by the duration of the stressed state is not long enough, the growing cracks are not able to coalesce, i.e., to form a spatial network. In this case, the dimension of an average fragment grows on account of an increase in the specific gravity of the coarse fractions. Pieces of large dimensions will retain their large number of cracks, while not evolving towards coalescence with

their neighbors. The cracks which exist will lower the strength of the pieces of rock, though this strength may be sufficient to guarantee the integrity of individual structural units.

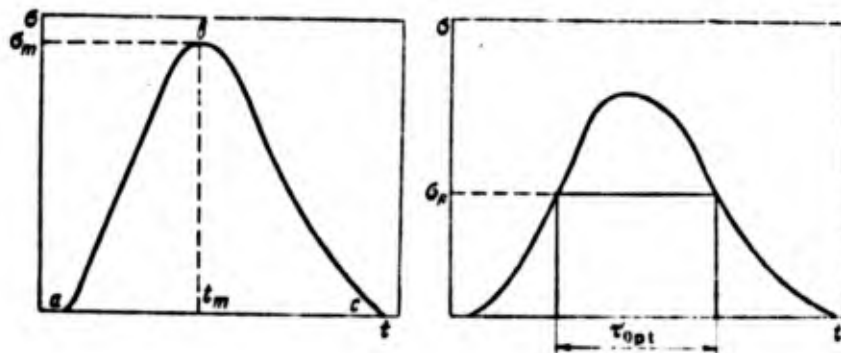


Fig. 28. Shape of the stress impulse arising in a medium upon explosion.

Fig. 29. Optimum of stress impulse of rectangular shape.

In order that all cracks opening under a stress  $\sigma$  should unite it is necessary that the duration of the stressed state should be no less than some quantity  $t_{op}$ . The value of this quantity depends on the average distance between crack-formation centers and on the propagation velocity of the cracks. Inasmuch as the number of crack generation sites and the rate of their evolution in a certain material depend on the value of the stress, the necessary interval of time  $t_{op}$  will be a complicated function of the stress. The nature of this dependence is described by equation (188).

The shape of actual stress impulses is such that the maximum stress is attained only at one point on the curve  $\sigma(t)$ , i.e.,

the duration of the stressed state when there is a normal stress equal to  $\sigma_{\max}$ , is equal to 0. Consequently, cracks whose dimensions are critical at  $\sigma(t) = \sigma_{\max}$  cannot form a spatial network. The nature of fragmentation in this case is determined not by  $\sigma_{\max}$  but by some quantity  $\sigma_R$ . The value of  $\sigma_R$  is found from the condition that the time during which the stressed state exists with  $\sigma$  greater than or equal to  $\sigma_R$  is equal to  $t_{\text{op}}$ . A similar consideration of the crushing process leads to the idea of an optimum impulse of rectangular form. A stress impulse is considered sufficient for crushing of a medium to a specified coarseness of the fragment if the optimum impulse is accommodated inside it or can be inscribed within (Fig. 29). The rectangular shape of the optimum stress impulse is only a first approximation. It will be correct when the condition holds that the shattering stress does not decrease in the process of crack growth. However, fulfillment of this condition is not mandatory. In the process of development of a crack its dimensions increase and, consequently, the value of the critical stress decreases in accordance with (147). When we take account of this effect the shape of the optimum impulse takes the form of a curved trapezoid abcd (Fig. 30). Curve bc is described by the equation

$$\sigma = K_0 t^{-\frac{1}{2}}, \quad (189)$$

where

$$K_0 = \frac{2}{3} (E\gamma l)^{\frac{1}{2}} v_{\max}^{-\frac{1}{2}}.$$

The value of the stress  $\sigma$  from equation (189) is the minimum stress which is necessary for normal growth of cracks opening up under a stress  $\sigma(t)$ . When the stress  $\sigma(t)$  increases to a value  $\sigma_1$  growth of cracks having a smaller dimension begins.

In order to support their growth all succeeding values of the stress must lie above the curve bc, located along the curve  $\sigma(t)$  up to the point  $\sigma_i$ . An average fragment with an edge  $b_i$  will correspond to the optimal stress impulse, constructed on the basis of this curve. Thus, to every point on the forward front of an actual impulse  $\sigma_i$  lying within the interval  $[\sigma] \leq \sigma_i \leq \sigma_m$  (where  $[\sigma]$  is the limit of brittle rupture) there will correspond some curve  $\sigma(t)$ . The aggregate of these curves forms a parametric family

$$\begin{aligned} \sigma_i(t) &= K_0 (t - t_i)^{-\frac{1}{2}} & \text{where } t \geq t_i, \\ \sigma_i(t) &= \sigma(t_i) & \text{where } t = t_i. \end{aligned} \quad (190)$$

For sufficient impulse duration in the exploded rock mass all fractions up to  $b_{\min}$  inclusively will be present ( $b_{\min}$  is the dimension of a fraction corresponding to the amplitude value of the stress in the impulse).

Actual stress impulses, as a rule, have a tendency toward reduction of the duration of existence of the stressed state with an increase in the stress. Owing to this fact, cracks which arise under high stresses are not able to coalesce because of the negligibly short duration of their existence. The geometrical locations of the ends of optimal impulses of rectangular form may be represented in the form of the following analytical function

$$t = B [\operatorname{erfc}(u\sigma^{-2})]^{-\frac{1}{2}}, \quad (191)$$

where

$$B = \left( \frac{16\beta}{n_0 (V\lambda)} \right)^{\frac{1}{2}} \frac{1}{v_{\max}}; \quad u = \frac{1}{9} LE\gamma.$$

The limiting propagation velocity does not depend on the value of the stress. Consequently, neglecting the initial period of crack

development, the crack velocity may be taken to be independent of stress. In this case the optimal duration is determined only by the stress at the forward front of the optimal impulse and does not depend on the way in which the stress beyond that front changes. Because of this situation the value of the duration of an optimal impulse of rectangular form will coincide with the duration of an optimal impulse of any other shape. Graphically, the impulse duration will be found from the abscissa of the point of intersection of curve  $\sigma_i(t)$  with the straight line  $t = t_1$ , where  $t_1$  is the abscissa of the point of intersection of the upper boundary of the rectangular impulse with a curve ab (Fig. 31). Keeping in mind that the evolution of a crack is characterized by some value of the initial period  $t_n$  during the course of which the stress must be maintained constant, we are led to the conclusion that the optimal impulse must obey the condition

$$\sigma_i(t) = \sigma_{max} \quad \text{when} \quad t_1 \leq t \leq t_1 + t_n' \quad (192)$$

Condition (192) indicates that the optimal impulse must have a flat value. As the amplitude of an optimal impulse is increased  $t_n$  diminishes according to an exponential law in agreement with dependence (187). Accounting for relationship (192) allows for some increase in stress in an optimal impulse, though this effect will be noticeable only for stress values lying near in the neighborhood of  $\sigma_R$ .

In Fig. 31 the shape of an optimal impulse is depicted, where all features of the variation of the impulse parameters in the shattering process are taken into account. The minimum stress in an impulse  $\sigma_k$  is not equal to zero. The value of  $\sigma_k$  will be determined in general by the value of  $b$ , i.e., the average distance between crack formation centers. In the limit  $\sigma_i$  must be such as to assure the growth of cracks with dimensions  $b_i$ .

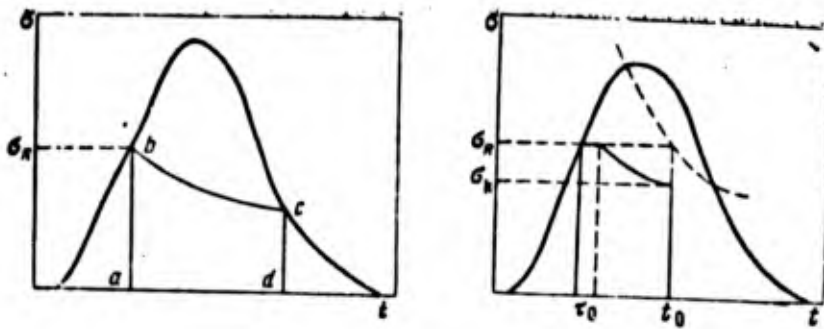


Fig. 30. A trapezoidal optimal stress impulse.

Fig. 31. Construction of an optimal stress impulse.

The size  $\sigma_k$  may be found from the relationship

$$\sigma_k = \frac{2}{3\beta} \sqrt{LE\gamma}. \quad (193)$$

As the stresses  $\sigma_k$  increase the dimensions of the zone of repulverization must grow. To obtain a uniform crushing it is necessary to lower the value of the stresses (up to a certain limit) and increase the impulse duration.

#### Prediction of the Particle-Size Composition of an Exploded Rock Mass.

The particle-size composition of a shattered body is determined by the density of crack generation sites, which form a spatial network. Cracks for which the duration of load application turned out to be insufficient for them to coalesce do not have much of an effect on the dimension of fragments, but they may lower the strength of the pieces considerably.

When a stress impulse is propagated in a medium its parameters change. Owing to geometrical dispersion and dissipated losses its amplitude decreases and the duration increases. The rules by which the yield of fraction varies according to zone is determined from these phenomenon. The near-zone is characterized

by intense fragmentation, but the dimension of an average fragment rises in proportion to the distance of removal from the center of explosion. Inasmuch as the shape of a stress impulse changes continuously as it propagates in the rock mass, the criteria obtained are, generally speaking, local. However, when the laws by which the stress pulse changes are considered they may also give an integrated evaluation of the nature of the crushing. The maximum stresses in an impulse are some function of the distance  $\sigma_{\max}(r)$ . As has been noted above, the quality of crushing is determined not by  $\sigma_{\max}$  but by some value  $\sigma_R$ , whose duration of existence is greater or equal to  $t_{op}$ . Assuming that  $\sigma_R$  follows the same law of decrease with distance as  $\sigma_{\max}(r)$ , we obtain

$$\sigma_R(r) = k_p \sigma_{\max}(r), \quad (194)$$

where  $k_p$  is a proportionality factor. The proportionality factor  $k_p$  for a given rock will depend only on the length of the impulse in time, and for a fixed initial shape of impulse will be a constant quantity. The size of an average fragment  $b$  will be determined by the equality

$$b(r) = \left( \frac{163}{V \pi \mu_0} \right)^{\frac{1}{3}} \left[ 1 - \Phi \left( \frac{1}{\psi} \frac{EL_T}{k_p^2 \sigma_{\max}^2} \right) \right]^{-\frac{1}{3}}. \quad (195)$$

The quantity  $b(r)$  has a probabilistic character. Using this quantity one may determine the average dimension of a fragment in the zone bounded by radii  $R_n - ct_{op}/2$  and  $R_n + ct_{op}/2$ , according to the formula

$$b_n = \frac{1}{ct_{op}} \int_{R_n - \frac{ct_{op}}{2}}^{R_n + \frac{ct_{op}}{2}} b(r) dr. \quad (196)$$

The propagation velocity of the stress field  $c$  is always larger than the velocity of cracks  $v$ , and therefore the dimensions of the zone under consideration is always larger than the dimensions of pieces. The zone dimensions will not remain constant when  $r$  is changed. With an increase in distance to the explosion center the value of the  $\sigma_R(r)$  will decrease, and as a consequence of that  $t_{op}$  will rise, as will the zone dimensions as a result. With the aid of relationship (196) one may obtain the integrated characteristics of the particle-size composition of the exploded rock mass.

The particle-size composition of the exploded rock mass may characterize the size of an average fragment. Let us calculate the value of this quantity starting from the theoretical plan we have adopted. The shattered volume is divided into a series of zones with centers at the points  $R_n$  and with variable widths  $ct_{op}$ . The size of an average piece in each zone is determined in accordance with formula (196). The volume of a zone in which pieces of dimension  $b_n$  are formed will be equal to

$$V_n = 2\pi H c t_{op} n_n \quad (197)$$

where  $H$  is the height of a scarp

The quantity  $V_n$  is the statistical weight of fragments of dimension  $b_n$  in the overall volume of a shattered mass. Then the average dimension of a fragment of the whole exploded rock mass is determined by the relation

$$l = \frac{\sum_{n=1}^N b_n t_{op} n_n}{l^3} \quad (198)$$

or, after substitution of (196) into (198),

$$b = \frac{2}{L^2} \sum_{n=1}^N R_n \int_{R_n - \frac{c'_{sp}}{2}}^{R_n + \frac{c'_{sp}}{2}} h(r) dr, \quad (199)$$

where  $L$  is the line of least resistance, and  $N$  is the total number of zones.

The difficulty in practical utilization of the relationships (199) consists in the complexity encountered in finding the surface energy  $\gamma$  and the parameters of normal distribution. For ideally brittle crystalline bodies the value of  $\gamma$  may be determined from the approximate formula

$$\gamma = \frac{E a_0}{20}, \quad (200)$$

where  $a_0$  is the interatomic distance ( $a_0 \approx 2.4 \text{ \AA}$ ).

However, purely brittle shattering is an idealization. Even in materials which in practice are considered brittle, at the end of a propagating crack there is a region of plastic deformation. The consumption of energy in plastic deformation increases by factors of a hundred and a thousand (up to  $10^8 \text{ erg/cm}^2$ ) in comparison with values calculated from formula (200). For a wide class of rocks under conditions of explosive loading,  $\gamma$  changes within a narrow range of values and, once it is determined for one rock, may be employed as an approximation in other cases.

In view of the absence of reliable methods for determining the fracturing of rock blocks, especially in the case of closed or microscopic cracks which are invisible to the unaided eye, the determination of the parameters of the normal distribution of cracks from their dimension using a direct method is not

possible at the present time. In a first approximation this problem may be solved by appealing to the results of statistical tests on rock samples. The damage of a sample in this case is determined by the crack of maximum dimension. The totality of results of these tests amounts to some distribution of the maximum values of crack lengths. In the work (Bolotin, 1965) asymptotic formulas are presented for the characteristics of the normal distribution of maximum values in the case of large values of  $n$

$$X_{nn} = a + \sigma \sqrt{\ln n}, \quad \sigma_{nn} = \frac{\sigma}{\sqrt{6 \ln n}}, \quad (201)$$

where  $x_{nn}$  and  $\sigma_{nn}$  are respectively the mathematical expectation value and the standard deviation of the distribution of maximum values;  $a$  and  $\sigma$  are the mathematical expectation value and standard deviation of the distribution of all values;  $n$  is the number of tests.

Solving equation (201) with respect  $a$  and  $\sigma$  we obtain

$$a = X_{nn} - \sqrt{6} \frac{\sigma_{nn} \ln n}{\pi}, \quad \sigma = \frac{\sigma_{nn} \sqrt{6 \ln n}}{\pi}. \quad (202)$$

In this way the normal distribution may be obtained in the form

$$f(x) = \frac{1}{\sigma \sqrt{2\pi}} e^{-\frac{(x-a)^2}{2\sigma^2}}. \quad (203)$$

The value of  $\bar{X}_{nn}$  and  $\sigma_{nn}$  are determined from the results of statistical experiments as

$$\bar{X}_{nn} = \frac{1}{n} \sum_{i=1}^n d_i, \quad \sigma_{nn} = \sqrt{X_{nn}^2 - (\bar{X})^2}, \quad (204)$$

where  $(\bar{X})^2$  is the mean square of the values of  $d$ . In testing the samples for strength we obtain several values for the

shattering stresses. The dimensions of a crack causing damage to a sample may be calculated by the formula

$$d = \frac{\pi E \gamma}{2s^2(1-\nu^2)} \quad (205)$$

The proposed method permits one to determine the crack distribution function from the dimensions within samples. In making the transitions to the rock blocks it is necessary to take into account the scale factor, i.e., the reduction in strength of the sample with an increase in its dimensions. This dependence is expressed by the relationship

$$[\sigma_V] = \frac{[\sigma_{V_0}]}{V_{rel}^2}, \quad (206)$$

where  $[\sigma_V]$  is the strength of a sample of volume  $V$ ;  $[\sigma_{V_0}]$  is the strength of a sample of volume  $V_0$ ;  $V_{rel}$  is the relative volume  $V/V_0$ ;  $\beta$  is a coefficient characterizing the strength properties of the shattered material. Then the maximum crack dimensions in the samples will be connected by the relationship

$$d_V = d_{V_0} V_{rel}^{2\beta} \quad (207)$$

and the distribution law transforms into the form

$$f_V(x) = \frac{1}{\sigma_{V_0}^{2\beta} V_{rel}^{2\beta}} e^{-\frac{(x-d_V)^2}{2\sigma_{V_0}^{2\beta}}}, \quad (208)$$

where  $d_V$  is the maximum crack dimension in samples of volume  $V$ ; and  $d_{V_0}$  is the maximum crack dimension in samples of volume  $V_0$ .

Choosing a volume which is sufficiently large (such that the homogeneity condition is fulfilled) we obtain the distribution

function for the number of cracks in the rock block. The presence of a system of coarse cracks with an expressed preferential direction, arising from the effect of geological factors, violate the condition of isotropicity and demands a special accounting. This special calculation may be carried out directly owing to the considerable dimensions of cracks of this type. Therefore, when we determine the distribution function using the indicated method, it is in principle possible, knowing the explosive impulse parameters, to predict the particle-size composition of the exploded rock mass.

#### Principles of Modeling and the Destructive Effect of an Explosion.

Modeling the explosive effect in general, i.e., modeling whole aspects of this phenomenon, is at the present time not possible. This is a result of both the limited knowledge of the separate processes taking place in an explosion and of the possibility for incompatible similitude conditions to arise. Therefore, as was shown in the preceding chapters, one usually models one of several aspects of the explosive action, which lead to success in some one engineering application of explosions. The accuracy of similitude modeling depends primarily on the correctness of the choice of basic factors determining the course of the process, and on the degree of influence of factors not taken into account. Therefore, a thorough analysis of the shattering mechanism is necessary in order to establish reliable criteria for modeling the crushing action of an explosion. In the finding of the dependence of the average fragment on the stress field parameters, the piston action of the explosion was not taken into account. Consequently, the additional mechanisms of fragmentation, arising in the movement of the block and in the collision of moving fragments, were discarded. In the case of shattering of solid excavated rock the contribution of these factors to the overall extent of shattering is insignificant. It is with these rocks that the sphere of applicability of the

relations obtained is bounded.

The investigations that were carried out on the crushing mechanism made it possible to establish criteria for modeling the destructive action of an explosion. We will consider equality between the number of crack generation sites in the model  $N_m$  and the number of such sites in the object under study  $N_n$  to be the similitude criterion for crushing of the material.

$$N_n = N_m. \quad (209)$$

This assertion is equivalent to the assumption of equality of the number of fragments of disintegrated mass in both cases. The number of crack generation sites in a unit of volume in the model and in nature will be connected by the relationship

$$n_{vm} = \lambda_1^3 n_{vn}, \quad (210)$$

where  $\lambda_1$  is the geometric scale of the modeling.

Utilizing relationship (182) we obtain

$$\frac{\sqrt{\pi}}{2\beta_m} (1 - \Phi(\beta_n S_n^*)) = \frac{\sqrt{\pi}}{2\beta_n} (1 - \Phi(\beta_n S_n^*)). \quad (211)$$

The dispersion in the distribution of a number of cracks in nature and in the model do not differ significantly, and therefore one may consider, approximately  $\beta_n = \beta_m$ . In consideration of this assumption, expression (209) transforms into the form

$$\Phi(\beta S_m^*) = \Phi(\beta S_n^*). \quad (212)$$

From this it follows  $S_m^* = S_n^*$ , i.e., the minimum areas of the opening cracks must be equal in nature and in the model. Using relations (145) and (200), we obtain

$$S_m^* = \frac{\pi E_M^2 h}{40(1 - \nu_M^2) \sigma_M^2} \quad (213)$$

Accounting for the fact that  $\nu$  varies within narrow limits and that the strength of a material in the first approximation is proportional to the elastic modulus, i.e.,  $[\sigma_R] \sim E$  (Khanukaev, 1962), expression (209) may be transformed into the form

$$\frac{|\sigma_R|_m^2}{\sigma_m^2} = \frac{|\sigma_R|_n^2}{\sigma_n^2}$$

or

$$\frac{\sigma_m}{|\sigma_R|_m} = \frac{\sigma_n}{|\sigma_R|_n} \quad (214)$$

Values of the stresses in actual media are complicated functions of the relative distances. Relation (214) in explicit form is written down in the following way:

$$\frac{\sigma_{op}}{|\sigma_R|_n} \int_0^{R_n} \psi_n(r_n) dr_n = \frac{\sigma_{im}}{|\sigma_R|_m} \int_0^{R_m} \psi_m(r_m) dr_m, \quad (215)$$

where  $R_n$  and  $R_m$  are the relative radii of the shattering zone for nature and for the model respectively.

In the special case where dissipative losses in the material are absent but the shape of the charge in nature and in the model are the same instead of the geometrical divergence reaching a state of identity, these similitude criteria simplify:

$$\frac{\sigma_{op}}{[\sigma_R]_r} = \frac{\sigma_{im}}{[\sigma_R]_m} \quad (216)$$

The conditions presented appear as necessary but not sufficient conditions in the modeling of the shattering process. This is because from the same number of generation sites, cracks may develop with different velocities, a situation which causes similitude in fragmentation to be violated. Let us denote the distance between crack generation centers in nature and in the model as  $a_n$  and  $a_m$  respectively. The time taken for damage in nature and in the model is determined from the ordinary kinematic relationship, in which both the distances between crack-formation centers and the velocities of crack growth may vary with distance from the center of the charge

$$[t_R]_n = \frac{a_n}{v_{cr,n}}, \quad [t_R]_m = \frac{a_m}{v_{cr,m}}, \quad (217)$$

where  $[t_R]_n$ ,  $[t_R]_m$  are the times for damage in nature and in the model respectively;  $v_{cr,n}$ ,  $v_{cr,m}$  are the velocities of crack growth in nature and in the model.

The ratio of the damage time in nature to that in the model was

$$\frac{[t_R]_r}{[t_R]_m} = \frac{a_n}{a_m} \cdot \frac{v_{cr,m}}{v_{cr,n}} \quad (218)$$

The condition

$$a_m = \frac{a_n}{\lambda_1} \quad (219)$$

is valid for nature and for the model where  $\lambda_1$  is the geometric scale.

From (218) and (219) we obtain

$$\lambda_1 = \frac{[t_R]_n}{[t_R]_m} = \lambda_1 \frac{v_{cr,n}}{v_{cr,m}}, \quad (220)$$

where  $\lambda_t$  is time scale in modeling the damage process. In the general case  $\lambda_t$  is a function of the relative distance.

From the criteria obtained it follows that similar fragmentation may be obtained by two means: 1) by choice of a material for the model with corresponding physical and mechanical properties for specified impulse parameters in nature and in the model, i.e., by selecting appropriate strength properties and velocity of crack development; 2) by creating the appropriate stress impulse in the model for a specified impulse in nature and with similitude in the physical and mechanical properties of the materials of nature and the model.

## CHAPTER FOUR

### EXPERIMENTAL METHODS FOR DETERMINING THE CHARACTERISTICS OF THE SHATTERING PROCESS<sup>1</sup>

#### Measurement of the Stress Field Parameters and Deformation Parameters In an Elastic Medium Under Explosive Conditions

Observance of similitude in explosive shock loading when modeling the explosive effect is sometimes coupled with a requirement for finding the change in stresses and deformations in time at the most characteristic points. The solution of this problem is made difficult because of the rapid change in stresses with time, the short duration of the stressed state, and the large values of the maximum stresses. Mechanical methods for measuring these qualities have been developed, in which the simple and ingenious experiment with a measuring rod proposed by Hopkinson (Hopkinson, 1914) in 1914 serves as the basis; this method was used by him in order to determine the change in time of pressures which arise in explosions and mechanical shocks with high velocities. The pressure which was to be measured was applied to one of the ends of a uniform steel rod, so that a compression wave was created which propagated with a constant velocity (if we neglect the effect of dispersion)

$$c = \sqrt{\frac{E}{\rho}} \quad (221)$$

where  $E$  is the elastic modulus of the material of the rod, and  $\rho$  is the density of the rod material. The stress wave, having reached the free end of the rod, is reflected as a longitudinal wave (under the assumed conditions the rod itself does not cause any distortion in the wave). At subsequent moments in time the stress in any cross section of the rod is determined as the sum of the stresses in the incident and the reflected waves. Near the free end the rod is cut and the surfaces of the cut are ground and joined together. The incident wave passes through the joint without changing; the end part of the rod will remain in contact with the main part of the rod for as long as the

---

<sup>1</sup>This chapter was written jointly with Engineer S. N. Rodak

tensile stress caused by the reflected wave does not exceed the compressive stresses of the incident wave at the point of contact. In this case the end part separates from the main part of the rod and flies off. The momentum of the part which has separated may be found with the aid of a ballistic pendulum. If the cross sectional area of the end part is  $S$ , its length is  $l$  and the stress in the wave is  $\sigma$  then the momentum

$$I_d = \int_0^{\frac{2l}{c}} S \sigma dt. \quad (222)$$

Proceeding in this fashion and taking end parts of various lengths it is possible to obtain the momentum for various intervals of time. This experiment does not render it possible to determine the shape of the curve  $\sigma(t)$ , since the moment of time corresponding to the beginning of the various time integrals are not known, but one may always find the duration of the impulse  $\tau$  and the maximum value of the stresses  $\sigma_{\max}$

$$\tau = \frac{2l_0}{c}, \quad (223)$$

where  $l_0$  is the length of the end part for which the main part of the rod remains in a state of rest.

In order to determine  $\sigma_{\max}$  the end parts are taken to be very short so that the moment of time  $2l/c$  will correspond to the time at which maximum stresses are reached. Then the momentum is found in the following way:

$$I_d = \frac{2S\sigma_{\max} l}{c} \quad (224)$$

or

$$I_d = \rho S l v_{T.0}, \quad (225)$$

where  $v_{T.0}$  is the velocity with which the separating part moves.

Equating (224) and (225), we obtain

$$\sigma_{max} = \frac{\rho c v_{T.0}}{2}. \quad (226)$$

For longitudinal elastic waves

$$J_{max} = \rho c v_{max}, \quad (227)$$

where  $v_{max}$  is the maximum value of a velocity with which particles move in the wave. Consequently, from (226) and (227)

$$v_{T.0} = 2v_{max}. \quad (228)$$

When a stress wave undergoes normal reflection from a free surface, the mass velocity of points on the surface is equal to  $2v_{max}$ ; therefore the velocity of separation  $v_{T.0}$  of the very short end part is equal to the maximum velocity, which is then communicated to the free end by the stress wave.

Using Hopkinson's method Reinhart and Pearson developed two methods for measuring the propagation velocity of stress waves in metals during explosive shock loading, the first method (Fig. 32) consists in a disc being attached to a massive cylinder (plate) serving as a "time measurer" (the end part in the Hopkinson rods), and this disc being separated from the cylinder whenever the stresses at the surface of the contact become zero; the velocity of separation of the disc was measured by spark photography. From the data obtained for discs of various thicknesses, it was possible to reconstruct the dependence of the stresses on time at the rear surface of the plate (cylinder). A modification of

this method (Fig. 33) consists in drilling out a cylindrical depression in the rear side of the plate, in this pit several discs of various thicknesses were placed. This reduced the number of experiments and, furthermore, made it possible to measure those stresses which were sufficiently high to cause "splintering off" of the thin discs due to the effects of the waves reflected from the free surface of the discs. The duration of the effect from the stresses, measured by Reinhart, was of the order of 10 microsec., and the maximum stresses for steel plates amounted to  $7.5 \times 10^4$  kgf/cm<sup>2</sup>, which is 5-6 times higher than the critical breaking stresses of the material.

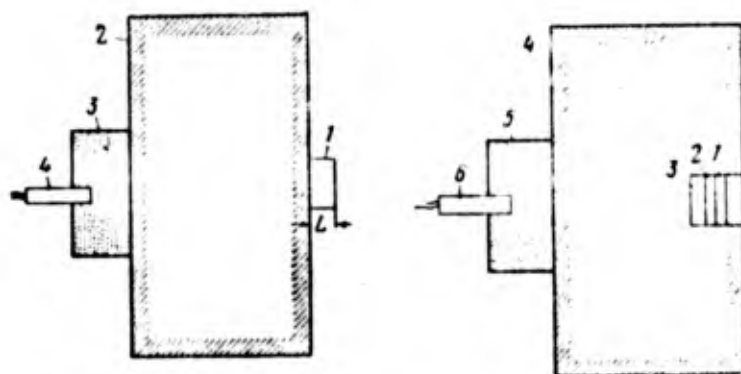


Fig. 32. Apparatus for determining experimentally particle velocities with one disc.

1 - disc; 2 - cylinder; 3 - explosive charge; 4 - detonation cap.

Fig. 33. Apparatus for determining experimentally particle velocities with several discs.

1, 2, 3 - discs; 4 - cylinder; 5 - explosive charge; 6 - detonation cap.

In the second series of experiments, Reinhart and Pearson employed the impression method for determining the velocities of particles of the rear surface of the plate. Let us denote by  $S$  the area of the contact between the disc and the plate, by  $l$  the thickness of the disc, and by  $t$  the time counted from the moment of arrival of the stress wave front at the rear surface of the disc. At the moment  $t = 0$  particles on the platform  $S$  begins to move with a velocity equal to the velocity of particles located in the neighborhood of the platform  $S_0$ . The difference in the bulk velocities in these two regions will be maintained until the time  $t = 2l/c$ , when the contact is broken owing to the arrival of the longitudinal wave at the point of contact between the disc and the plate. If the material of the plate behaves in plastic fashion, this difference in velocities leads to a residual impression or dent in the surface of the plate. When elastic deformations are absent the depth of the impression will be equal to

$$h = \int_0^{\frac{2l}{c}} v dt, \quad (228a)$$

where  $h$  is the depth of the impression of the disc.

Thus, by using discs of various thicknesses it is possible to find the dependence of particle velocity on time. The agreement in the experimental results obtained by these two methods is satisfactory.

The degree of development of high speed photography allowed us to make successful use of this technique in studying the process of shattering of solid bodies by impulsive loads. Photographic methods made it possible to study the displacement of a point on the surface of the sample or model as well as propagation of the stress wave front (by the photoelasticity method and the shadow method).

Two methods are used for studying the movement of points on the surface of the sample: a continuous record of the motion, obtained by means of rapid photography by using cameras with a drum or by mirror scanning; or, a continuous record is obtained by using a light source which produces flashes of very short duration. The difficulties which arise in applying photographic methods of investigation are attributable to the short duration of the phenomenon, the very small displacements, the high values of the propagation front velocity, and the necessity for careful synchronization of the beginning of operation of the illumination source with the beginning of the effect to be studied.

In recent years the practice of measuring non-electrical quantities using electrical methods has received increasingly wide use in the recording of displacements, stresses, or deformations in stress waves. Changes in the dynamic and kinematic characteristics of a medium as a wave passes through the medium correspond to a change in the parameters of electrical capacitances or voltages. Inductance and capacitance-type sensors for measurement of displacements, resistance sensors for measuring the relative deformation, and piezoelectric pick-ups for measuring voltages have found wide use in laboratory and industrial investigations.

A capacitance-type sensor is realized as a flat condenser, one plate of which is the surface of the sample to be studied, and the other of which is an insulated conductor (Fig. 34). In response to impulse loads the surface of the sample moves, whereas the insulated conductor remains at rest. The translation of the surface of the sample causes a change in the capacitance, which is transformed into a variation of the potential difference, recorded in time with the aid of a cathode ray oscilloscope. The change in capacitance of the sensor is a function of the system geometry and of the corresponding complements of surface displacements, averaged over the area of the insulated conductor. Fig. 35 shows the arrangement used by G. Kol'skiy (1963) for studying stresses

which were developed in the shattering of rods made of sodium glass, polystyrene, and plexiglass. Determining the way in which the displacement of the end of the rod depends on time enables one to calculate the shape of the compression pulse arriving at the end of the rod. In practice this is related to a numerical differentiation of the curve representing the dependence of displacement on time. One may measure the various complements of surface translation as a function of the geometrical shape of the sensor (see Fig. 34).

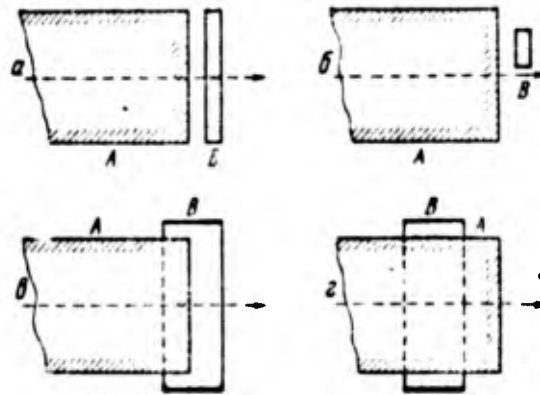


Fig. 34. Capacitive elements for measuring the surface displacements in pulsed stress waves

a- grounded rod; b- insulated disc or cylinder for measuring the following:

- a- the average displacement of the rod end,
- b- the average displacement of the bounded region of the end plane;
- c- the longitudinal displacements of the circumference of the end plane,
- d- the radial displacements averaged over the length.

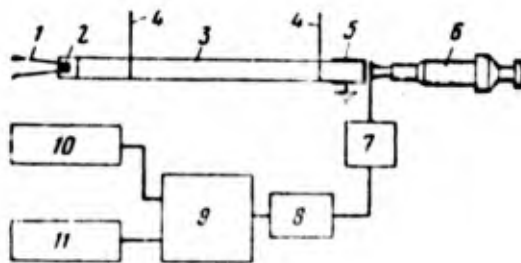


Fig. 35. Experimental setup for determining the displacement of the end plane of the rod.

- 1- Ignition wire;
- 2- Explosive charge;
- 3- Rod;
- 4- Hangers (suspension);
- 5- Condenser;
- 6- Micrometer head;
- 7- Voltage feed source;
- 8- Amplifier;
- 9- Cathode ray oscilloscope;
- 10- Photocell;
- 11- Oscillator.

Strain gauges of various type for measuring deformation. The most widely used type of resistance strain gauge consists of a thin wire with high electrical resistance, laid out in such a

way that it forms a system of parallel loops, connected in series. The lattice which is formed in this way is attached between layers of thin paper. At the time of use the sensor is cemented to the sample over its entire area. If this fastening is satisfactory from the mechanical point of view, the deformation of the sample at the point of contact is equal to the deformation of the sensor. In the case of a deformation that consists of an elongation in the direction of the sensor axis the length of the wire will increase and its diameter will decrease. This leads to a rise in the resistance of the wire, and consequently in the total resistance of the sensor also. A compression deformation leads to a reduction in the sensor resistance. It has been found experimentally that with a uniform static loading the increase in electrical resistance is directly proportional to that component of the deformation which lies in the direction of the axis of the sensor winding.

(229)

$$\frac{\Delta R}{R} = \alpha \frac{\Delta l}{l},$$

where  $R$  is the sensor resistance prior to deformation;  $\Delta R$  is the increase (or decrease) of resistance upon deformation;  $l$  is the total length of the undeformed wire of the sensor;  $\Delta l$  is the size of the deformation of the sensor in the direction of the winding axis;  $\alpha$  is the sensitivity factor of the sensor. The quantity  $\alpha$  depends basically on the material of the wire of the sensor and in most cases is equal to a constant, close to 2. For some experiments it is sufficient to take the value of the sensitivity as given by the manufacturer (e.g. on the name plate), but for more accurate measurements it is necessary to calibrate the sensor. In dynamic loading the value of the sensitivity factor of the sensor may differ from the value obtained in a static calibration, since the mechanical behavior of the wire and of the paper pad in the fastening material may be different in both cases. Moreover, with

dynamic loads the deformations may differ noticeably in the location of the base line. In this case the measurement error is determined by the size of the gradient of the deformation.

R. M. Davis (1961) has carried out an estimation of the error which arises due to nonuniformity of deformation at the point of contact. Let us suppose that the sensor is attached to a rod, along whose axis Ox longitudinal stress waves are propagated with a velocity c without dispersion. The sensor is oriented such that its axis is parallel to Ox so that in the undeformed state it is located between the points  $x = 0$  and  $x = l$ . If  $\epsilon$  is the deformation at the point with abscissa  $x$  at the moment in time  $t$ , then the total increase  $\Delta l$  in the length of the sensor at the moment  $t$  will equal  $\int_0^l \epsilon dr$  under the condition that there is no difference in the static and dynamic behavior of the sensor, and from (229) we obtain

$$\frac{\Delta l}{l} = \frac{\alpha}{l} \int_0^l \epsilon dr. \quad (230)$$

For plane stress waves

$$\epsilon = f(x - ct) \quad (231)$$

and equation (230) takes the form

$$\frac{\Delta l}{l} = \frac{\alpha}{l} \int_0^l f(x - ct) dx. \quad (232)$$

For an infinite series of monochromatic sinusoidal waves with wave length  $\lambda$  and period T

$$\epsilon = \epsilon_{\max} \sin \frac{2\pi}{\lambda} (x - ct), \quad (233)$$

where  $\epsilon_{\max}$  is the maximum value of the relative deformation.

From equation (232) it follows that

(234)

$$\frac{\Delta R}{R} = \alpha \epsilon_{\max} \frac{\sin\left(\frac{\pi l}{\lambda}\right)}{\frac{\pi l}{\lambda}} \sin\left(\frac{2\pi t}{T} - \psi\right).$$

where  $\phi = \pi l/\lambda$  is the phase angle.

From equations (233) and (234) it is seen that the amplitude and phase will be distorted if the condition  $l/\lambda \ll 1$  is not fulfilled. The analysis of the measurement error may be extended to stress pulses of different forms. For a pulse during which the deformation at a given point on the rod rises instantaneously from zero to some maximum value  $\epsilon_{\max}$ , and afterwards falls exponentially,

(235)

$$\frac{\Delta R}{R} = \alpha \epsilon_{\max} \cdot \frac{c^0}{l} \left(1 - e^{-\frac{t}{\theta}}\right),$$

where  $\theta$  is a constant representing the time necessary for the deformation at the given point to decrease from the maximum value  $\epsilon_{\max}$  to the value  $\epsilon_{\max}/e$ .

The effect of the length of the sensor on the value of  $\Delta R/R$  turns out to be twofold: a) the initial growth will not be instantaneous, since the leading front of the pulse approaches the length of the sensor over a finite time  $l/c$ ; b) the maximum values of  $\Delta R/R$  will be smaller than  $\alpha \epsilon_{\max}$ , since at the moment when the effect of the pulse has propagated across the whole length of the sensor, the average value of the stresses will be less than their

maximum value. The method of measuring deformation with strain gauges has two essential shortcomings: 1) the finite length of the sensor limits its resolution capacity with rapidly changing deformation; 2) the resistance sensor measures deformation only on the surface of a sample. In accounting for the effect of dispersion for stresses changing rapidly in time it is difficult to connect these deformations with the average stresses over a cross section. Peterson sought to reduce dispersion by using two resistance sensors, cemented at right angles to each other and forming two arms of a bridge system. The indicated method increases somewhat the accuracy of the data obtained, but it does not fully eliminate the difficulties of using wire-type strain gauge sensors for measuring impulsive loads.

Piezoelectric sensors of various types may be employed for recording stresses within a sample. The most promising one's are ceramic sensors made of barium titanate and lead zirconate-titanate. Piezoelectric sensors made from the indicated materials are distinguished by their considerable mechanical strength ( $[\sigma_R]=2000 \text{ kgf/cm}^2$ ) and high sensitivity ( $3-8 \cdot 10^{-6} \text{ CGSE/dyne}$ ). It is easy to prepare sensors of any required dimension and shape from these materials. Applicable barium-titanate sensors are intended for registering stresses perpendicular to the working surface of the sensors. In order to eliminate the effect of other complements of the stress sensor the sensor is placed inside a special band. The calibration of a piezosensor is carried out in the following manner. The sample, placed between the two electrodes of a holder, is subjected to compression using a press (Fig. 36). Measurement of the quantity of electrical charge arriving at the faces of the sample when the load is quickly removed, performed with a ballistic galvanometer

(236)

$$Q = C_0 \epsilon_0$$

where  $C_b$  is the ballistic constant of the galvanometer and  $\alpha_g$  is the deflection of the galvanometer.

The piezoelectric modulus is determined as

(237)

$$d = \frac{I}{S} = \frac{Q'S}{F.S} = \frac{z_i C_b \alpha_g}{F} ,$$

where  $I$  is the electrical polarization in the direction of mechanical compression of the sample;  $\sigma$  is the mechanical stress;  $F$  is the force acting on the sensor;  $S$  is the working area of the sensor;  $d$  is the piezoelectric modulus of the sensor.

Investigation of the dependence of the piezomodulus on the size of the impulsive load is carried out on a calibration stand (Fig. 37), on which the sensor is tightly pressed to the surface of a massive steel cube with the aid of special band. Impact is accomplished with a steel ball suspended by a thread. From the angle of deflection of the ball and the duration of the impact (the impact duration is measured using a cathode ray oscilloscope) one calculates the maximum force of the impact

(238)

$$F = \frac{2m}{\Delta t} \sqrt{2gR_H(1 - \cos \alpha)} ,$$

where  $m$  is the mass of the ball;  $\Delta t$  is the duration of the impact;  $R_H$  is the sum of length of the thread and the radius of the ball;  $\alpha$  is the angle of deflection of the thread. By varying the angle of deflection of the thread and the weight of the ball, it is possible to control the force of the impact throughout a wide range.. The electrical charge arising at the electrodes of the sensor upon impact is equal to

(239)

$$Q = CU .$$

where  $C$  is the capacitance of the sensor,  $U$  is the potential difference at the faces of the sensor as recorded by the oscilloscope.

Expressing the value of the charge in terms of the piezomodulus of the sensor and the force acting upon it

$$Q = Fd. \quad (240)$$

we obtained from (239) and (240)

$$d = \frac{C^2 U}{F}. \quad (241)$$

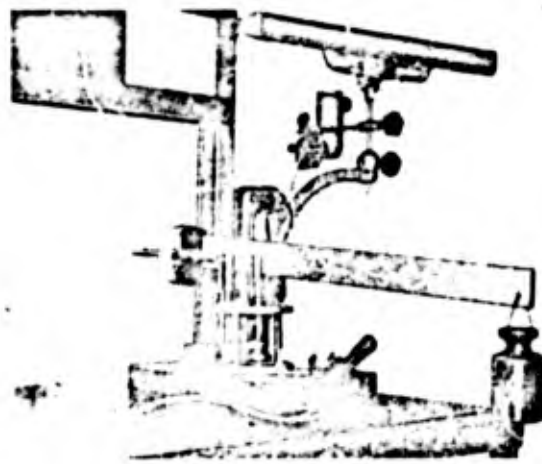


Fig. 36. Overall view of the press for calibrating sensors



Fig. 37. Overall view of the calibration stand.

The investigations are conducted by varying the dynamic load between the limits of 100 and 1500 kgf/cm<sup>2</sup>. The results of a measurement of the piezoelectric modulus under the influence of various values of the load are shown in Fig. 38. The drawing shows that within the range studied the piezomodulus does not depend on the value of the load.

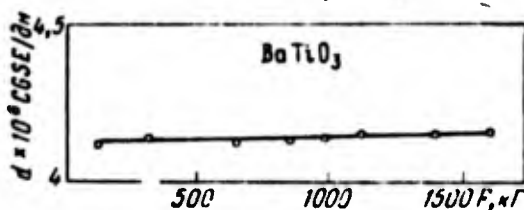


Fig. 38. Dependence of the piezomodulus on barium-titanate sensors on the size of the impulsive loading

In order to measure stresses in an explosion the piezo-sensors with their leads are placed in forms for preparation of models, into which the substance of the model is afterwards poured in the liquid state. The leads must be soldered to the working surfaces of the sensor with a low-temperature solder in order to avoid partial or complete depolarization of the piezo-ceramic. After hardening has occurred the sensors are placed inside a solid body in which the stresses will be measured when the stress waves pass through. Under natural conditions, at definite distances from the charge chamber, special blast holes are drilled, through which the sensors are oriented and fastened, and afterwards these holes are filled in with a cement solution. After the cement has hardened the stresses which occur when the charge is exploded may be measured. When the stresses are measured in a medium whose conductivity is higher than the conductivity of the sensor, the latter must be carefully insulated. In the opposite case the medium will shunt the sensor, and this is unavoidably reflected in the accuracy of the readings. As an insulating material one uses a coating of epoxy resin. When a stress field is developed in the medium there acts upon the sensor a force

$$F = \sigma S, \quad (242)$$

where  $\sigma$  is the value of the normal stresses, and  $S$  is the area of the working surface of the sensor. In response to the force on the surfaces of the sensor an electrical charge  $Q$  appears, whose value is determined according to the formula (240).

From (241) and (240) we obtain

$$\sigma = \frac{CU}{dS}, \quad (243)$$

where  $C = C_1 + C_2 + C_3 + C_4$  is the capacitance of the measuring system ( $C_1$  is the capacitance of the piezosensor,  $C_2$  is the capacitance of the conductive wires,  $C_3$  is the capacitance of the oscilloscope plates, and  $C_4$  is an additional capacitance).

Recording of the signals is carried out using cathode ray oscilloscopes. In order to check the accuracy of the measurement of stresses using piezosensors, a series of experiments were conducted. In the center of the ring a charge of explosive material (100 mg PETN, pentaerythretril tetranitrate) was fastened, and around the circumference piezoelectric sensors were arranged. The piezosensors and the explosive charge were covered with a impermeable film. As the explosion took place measurements of the pressure at the front of the shock wave in the water were taken. The stresses, as registered by the sensors, were calculated according to formula (243). In Table 2 values for the maximum stresses at the wave front in water are computed at distances of  $20r_0$  and  $30r_0$  ( $r_0$  is the charge radius) for an explosion of 100 mg of TETN. For the same distances the maximum pressures  $P_{\max}$  for an underwater explosion were computed from the formula (Yakovlev, 1961)

(244)

$$P_{\max} = B \left( \frac{Q}{r} \right)^{1.13}$$

where  $P_{\max}$  is the maximum pressure at the point; B is a constant factor (for TNT,  $B=533$ ); Q is the weight of the explosive charge; R is the distance at which the pressure is measured.

In accordance with the principle of energetic similarity the value of the coefficient  $B_i$  for other types of explosive

material may be computed using the approximate dependence (245)

$$P_i = \gamma_i B,$$

(246)

$$\gamma_i = \frac{q_i^{\frac{1.13}{3}}}{q_T} = \left(\frac{q_i}{q_T}\right)^{0.376},$$

where  $q_i$  is the specific energy of the given explosive material in kcal/kg,  $q_T$  is the specific energy of TNT, i.e.,  $q_T=1000$ kcal/kg.

For dimensionless distances expression (244) transforms into the following

$$P_{max} = \frac{11700}{\bar{r}^{1.13}} \gamma_i. \quad (247)$$

For the indicated charge of TETN we obtain

$$P_{max} = \frac{1680}{\bar{r}^{1.13}}, \quad (248)$$

where  $\bar{r}$  is the relative distance.

Table 2. Calculated and Experimental Values for the Maximum Stresses In An Explosion of 100 mg of TETN In Water.

Relative distance	Experimental value, kgf/cm <sup>2</sup>	Calculated value, kgf/cm <sup>2</sup>	Relative distance	Experimental value, kgf/cm <sup>2</sup>	Calculated value, kgf/cm <sup>2</sup>
20	52,0	56,7	30	37,5	36,0
20	57,2	56,7	30	33,5	36,0
20	56,9	56,7	30	35,3	36,0

From the data of Table 2 it follows that the results of the calculations and the experimentally found values of  $P_{max}$  differ by 8-10%.

In the second series of experiments the measurement error caused by an uncontrolled variation in the properties of the sensors was studied. For this purpose, plates made of resin of diameter 210 x 210 x 16 mm were prepared. The diameter of the blast hole was made equal to 5 mm, and for the explosive material TETN was used, the weight of the explosive charge amounting to 500 mg. The trigger was a suspension of lead oxide, and initiation took place simultaneously along the whole core of charge. The piezosensors were arranged around a circumference of radius 50 mm. The computation of stresses, as registered by the sensors, was carried out according to the given formula (248). The results of the investigation are presented in Table 3.

The data of Table 3 show that the scatter in the indications of various sensors does not exceed 5%. The next step was verification of the piezoelectric sensor indications by comparing them with data obtained by an electro magnetic method. For this purpose the rods were prepared from three materials: cement, resin, and hypo-sulfite. Piezosensors and electromagnetic wire sensors were set up at distances of 30, 60, and 90 mm. Comparison of the results of stress measurements of the time of explosion using the two methods showed that the relative error comes to 5-10%. Therefore, the piezoelectric sensor made from barium titanate may be used for measuring stresses in a medium which is subjected to an explosion. In measuring the stresses with piezosensor it is necessary that the duration of the measured signal be at least one order of magnitude lower than the time constant RC of the measuring system. This circumstance limits the range of application of piezosensors to short-time reactions.

Capacitance sensors made of barium titanate are conveniently used for recording stress impulses of long duration. The principle of their operation consists of the change in

Table 3. Results of Stress Measurements With Piezoelectric Sensors.

Plate	Sensor number	Stress, kgf/cm <sup>3</sup>	Average value of stress measurements, kgf/cm <sup>2</sup>	Relative error, %
1	1	316	322	-1.8
	2	327		+1.5
	3	306		+5.0
2	1	342	336	+1.7
	2	338		+0.6
	3	329		-2.0
3	1	324	326	-0.6
	2	332		+1.8
	3	321		-1.5

permittivity, and consequently also the capacitance, in response to mechanical stresses. In order to record stresses with the capacitance sensors, the circuit depicted in Fig. 39 was employed. This circuit consists of a voltage oscillator, composed of a 6K7 vacuum tube  $L_1$ ; the emf taken from coil  $L_3$  is fed to the amplifier  $L_2$ , a 6K7 vacuum tube, to the anode of which is connected a discriminator circuit  $L_4 C_7 C_8$ , tuned to the nominal frequency of the oscillator (1MHz). The resonant circuit  $L_5 L_6 C_9 C_{10}$  is tuned to the same frequency. In the frequency of the oscillator changes there appears at the output of the discriminator a voltage which is proportional to the change in capacitance of the sensor. The size of the electrical signal is registered on a cathode ray oscilloscope. An RC-filter  $R_6 R_7 R_8 C_{13} C_{14} C_{15}$  is connected at the output of the discriminator, permitting the induction of high frequency to be reduced to a significant degree. The capacitance sensor is hooked into the oscillator circuit through capacitor  $C_2$  using a RK-101 cable. Since in the process of operation the sensor is subjected only to impulsive loads, any method for calibrating the sensor using a static pressure is unsuitable, since whenever a pressure acts on the sensor for a prolonged

period an irreversible change in its parameters is observed. The method of calibrating capacitance sensors using impulsive loads is analogous to the method of calibrating piezoelectric sensors using an impact. Determination of the value of the stresses occurring in the medium at the time of explosion is performed in line with the formula

(249)

$$\sigma = \frac{\Delta V}{\beta S},$$

where  $\Delta V$  is the size of the voltage change at the sensor in response to the pressure,  $\beta$  is the sensitivity of the sensor, and  $S$  is the area of the working surface of the sensor.

Capacitance sensors were used for recording stresses arising in the medium when explosive charges were set off in blast holes and boreholes, i.e., in experimental investigations under artillery range and industrial conditions. The installation, arrangement, and installation in blast holes for the purpose of measurements are the same as the tests using piezoelectric sensors.

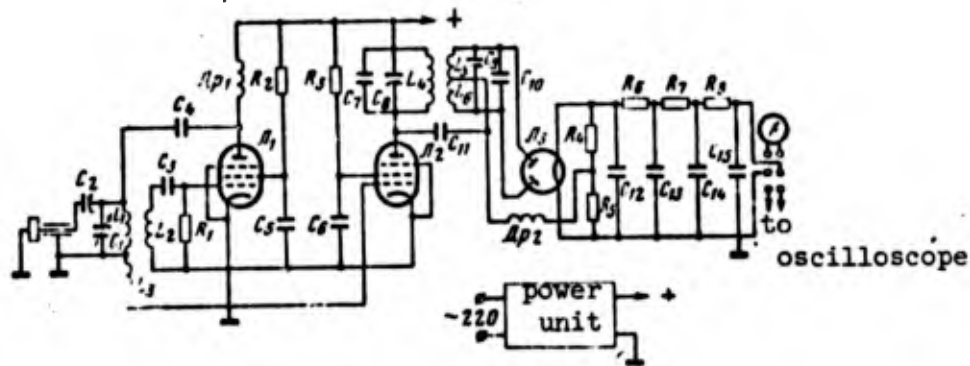


Fig. 39. Diagram of a Capacitance Converter.

The electromagnetic method of measuring stresses is based on the appearance of an induced emf in a conductor moving in a magnetic field. According to the law of electromagnetic induction the size of the emf induced in the wire is determined by the expression

$$E = B \cdot l \cdot v \sin \alpha, \quad (250)$$

where  $E$  is the value of the emf induced in the wire;  $B$  is the magnetic induction;  $l$  is the length of the wire;  $v$  is the velocity of the wire in the magnetic field;  $\alpha$  is the angle which the wire makes with the magnetic field lines. For known values of  $E$ ,  $B$ ,  $l$ , and  $\alpha$  one may determine the velocity of the wire. For the purpose of the sensor usually one used a constantine or copper wire of diameter 0.08 mm. Either the sensor had been previously constructed into a shape for preparation of the model and then the unhardened material of the model was poured in to fill it, or the sensor was cemented tightly to the body which was to be studied. Thus, in the explosion the velocity of the sensor coincides with the translational velocity of particles of the medium and is easily found from relationship (250). Measurements are performed using a special magnetic apparatus and cathode ray oscilloscopes. The size of the magnetic field and its homogeneity for various gaps between the pole pieces of the magnet were determined using magnetic induction measuring devices IMI-2 and IMI-3. Having found the maximum bulk velocity  $v_{\max}$  in the explosion, let us calculate the value of the maximum stresses arising in the medium according to the formula

$$(251)$$

$$\sigma_{\max} = \rho \cdot v_{\max}^2$$

where  $\sigma_{\max}$  is the maximum stress in the medium occurring in the explosion,  $\rho$  is the density of the material, and  $c$  is the propagation velocity of longitudinal elastic waves in the given medium. Placing the sensors at various distances  $r$  from the explosive charge, it is not difficult to establish the dependence  $\sigma=f(r)$ .

The indicated methods enable one to determine the stresses and deformation which occur in a medium at the time of explosion with a sufficient degree of accuracy. The main shortcoming in the method which has been considered is the necessity of creating special cavities for setting up the sensors. In order to eliminate to some degree the distortion of the stress field which is caused by the creation of cavities for the sensors, it is necessary to select a composition of cementing material which differs very little in its properties from the rock of the surrounding masses.

#### Optical Methods for Recording the Damage Process in an Explosion

Optical methods of investigation enable one to determine both the kinematic and the dynamic characteristics of the shattering process. An important advantage of such methods over others is the possibility of making a complex study of the damage phenomenon, i.e., a simultaneous recording of factors having an effect on various aspects of the phenomenon. In view of the short time duration of processes taking place in an explosion, high speed surveying cameras are used, and these are classified into two groups. To the first group belong cameras which enable one to make discrete frame recordings of the action, as the result of which a series of sequential frames are formed on film. Cameras of the second group are intended for rapid continuous photographic recording of the process in which an evolved image is obtained without being divided into frames.

In terms of the features of their construction cameras of the first group are divided into three types. To the first type of surveying cameras, which are close to the ordinary motion picture film apparatus, belong high speed cameras with discontinuous motion of the film, obtained with the aid of a skip pull-down mechanism. The frame frequency range of such cameras is 250-300 frames/sec. Cameras of the second type, with so called optical compensation, allow frame frequencies up to approximately 12-15 thousand frames/sec to be obtained. In these cameras the film moves discontinuously during the picture taking, and the optical image is shifted to the same side and with the same speed in the course of time during which each successive frame is exposed, as a result of which the possibility of practically eliminating smearing of the film is realized. The very widely used high speed motion picture camera SKS-1 belongs to this class of camera and is distinguished by a number of important features of merit. To the third type belong multi-objective surveying cameras in which the image is formed on successive frames with the aid of a series of identical optical systems, functioning one after the other. The frame frequency realized with these cameras may go as high as several tens of millions of frames per second.

In surveying cameras of the second group - high speed photo registering devices - a continuous relative translation of the optical image along a photographic layer takes place, as a result of which the image is developed. The time-development velocity in such cameras reaches 4000 m/sec.

The most acceptable cameras existing at the present time for the purpose of studying explosive processes are the SKS-1 and the SFR cameras. The frame frequency range of these cameras makes it possible to utilize them for studying the velocity of detonation

of explosive charges, the nature of the motion of ejected rock mass, the development of stress fields in models made from optically active materials, the velocity of crack formation, and other kinematic characteristics of the processes under study.

The SFR apparatus (Fig 40) permits one to record a process with a frame frequency of from 2,500 to 2,500,000 frames/sec. Photographic recording is accomplished on a motionless film with the aid of a rotating mirror. The maximum velocity of image development on the film is 3,750 m/sec. In the case of such a high frame frequency an intense illumination of the photographed object is necessary for normal exposure of the film. The duration of illumination in this case must not exceed the period of rotation of the mirror in the camera in order not to obtain double exposure of the image. Such a requirement is satisfied by flash lamp sources, for instance flash lamps of type ISSh-100-2, ISSh-300, and ISSh-500. The lamps operate on the principle of a capacitor discharge through discharge electrodes. The brightness of the lamp is as high as  $10^7$  stilb and even higher. The duration of the luminance under normal conditions of operation of the lamp depends on the capacitance of the condenser and may be controlled within wide limits from 500 to 1,500 microseconds. In order to operate the flash lamp a supplementary circuit is assembled (Fig. 41) which performs the function of supplying a high voltage (3000-3,500V) to the electrode. The discharge in the lamp is excited by the voltage fed to the ignition electrode. At the proper moment in time a voltage pulse is applied to this electrode of such a magnitude that a discharge takes place between it and the cathode. The ionization of gas in the lamp leads to an electrical breakdown of the main discharge gap. In order to record the process it is necessary to make these three factors coincide in time: the working position of the mirror, the beginning of the event to be examined, and the beginning of the flash of the flash lamp. In Fig. 41 the scheme for synchronizing the flash of the flash lamp with the explosion and the

operating position of the mirror is shown. Prior to the beginning of the picture taking condensers  $C_1$  and  $C_2$  (see Fig. 41) are charged to a voltage of 3.5 kV. The voltage from the condensers is fed to the electrode of pulse lamp 1 and the discharge gap. To serve as the discharge gap another ISSh-100-2 flash lamp is used, but it has no illumination function. The voltages to which condensers  $C_1$  and  $C_2$  are charged are selected in such a way that no spontaneous discharge takes place through the lamp. The circuits of the capacitors  $C_1$  and  $C_2$  are isolated, and this permits one to charge each capacitor independently of the other. The flash lamp is connected into the discharge circuit of the first of these. A connection is made into the discharge circuit of the second condenser through the discharge gap 5 using a thin constantine filament, soldered between current - carrying wires. The constantine thread passes through a layer of the initiating explosive material (usually lead azide). When the mirror of the camera takes its operating position corresponding to the beginning of recording of the process, the generator of the triggering pulse delivers a high-voltage pulse with an amplitude of 50 kV. This pulse arrives at the divider 6 and from here it is fed to the igniting electrode of the bias lighting lamp and the discharge lamp. As the pulse arrives at the igniting electrodes of the lamp a spark jumps between the cathode and the igniting electrode, and this causes the discharge of the capacitors  $C_1$  and  $C_2$  to take place in the lamp. As condenser  $C_1$  discharges a flash occurs in the flash lamp, and as condenser  $C_2$  discharges the explosive charge explodes. Since the high-voltage synchronizing pulse is delivered at the initial moment of the operating position of the mirror, a strict coincidence is maintained relating the time of the explosion, the beginning of the flash in the bias lighting lamp, and the beginning of the operating position of the mirror. When the capacitance of condenser  $C_1$  is 100  $\mu\text{f}$  the duration

of the flash in the ISSh-1.00-2 lamp amounts to 500 microseconds. This duration is not sufficiently long for the recording of processes with a frame speed of less than 125,000 frames/second. The duration of luminescence of the flash lamp may be increased by two methods: 1) by increasing the capacitance of condenser  $C_1$ ; 2) by incorporating an inductance  $L$  into the discharge circuit of condenser  $C_1$ .



Fig. 40. Overall view of the SFK apparatus.

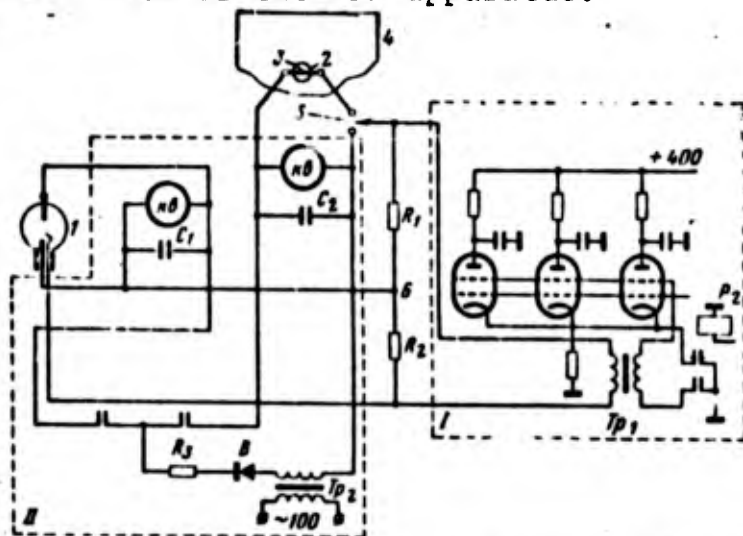


Fig. 41. Circuit for synchronizing the flash of a flash lamp with an explosion by means of the rotating position of the mirror.  
 1- flash lamp; 2- explosive charge; 3- constantine bridge; 4- model;  
 5- discharge gap; 6- ohmic voltage divider.

In the first case the increase in the luminescence duration is caused by the increase in the electric charge in the previous discharge current, and in the second case it is caused by the decrease in the discharge current when there is no change in the magnitude of the electric charge. The first method is the preferred one since the brightness in the flash in the lamp remains constant. Utilization of the second method leads to a decrease in the flash brightness, a fact which has an effect on the quality of the film recordings obtained.

If a recording is made of the indications of a different kind of sensor installed on the model and this registration is made on a cathode ray oscilloscope in parallel with the photographic recording of the process, then it is necessary to synchronize in time the start-up of the oscilloscope with the instant of the explosion. In order to assure synchronization an induction coil is placed in parallel with the transformer winding of the initiating pulse generator. At the time of delivery of the initiating pulse an emf is induced in the coil whose magnitude is controlled by the number of windings on the coil. The voltage pulse which is induced in the winding of the coil is used as a starting signal, guaranteeing simultaneity of the explosion and the start-up of the oscilloscope.

In modelling a series of problems (short-time delayed-action explosions, inter-borehole delayed action) the necessity arises for delaying the explosion of one charge relative to the explosion of the other. Considering the fact that in the study of damage processes in models of small dimension the time scale amounts to  $\lambda_t = 100-500$ , it is necessary to create delays counted in tens and hundreds of microseconds. Explosions of two charges having a difference in time may be attained by using a constantine filament of various diameters for the initiating charges. In the case of

series correction of such filaments a delay in the explosion is obtained which depends on the relationship between the filament diameter and the value of the current in the circuit. In Fig. 42 the delay of the explosion of the charge of explosive material is shown as a function of the diameter of the constantine bridge. The delay time is determined in regard to the explosion of a charge initiated by a constantine bridge of diameter 0.03 mm. The delay time of the explosion depends on the circuit parameters: the resistance, the voltage on condenser  $C_2$ , the length of the material, and the diameter of the wire. By changing these parameters one may obtain the necessary delay time. In the study of the simultaneous explosion of several charges it is necessary that the material, the length and the diameter of the wires of the triggering filaments be the same. In the investigation of the simultaneous explosion of several charges the series connection of incandescent bridges is not always acceptable, since failures possible. Therefore, in the explosion of more than two charges it is expedient to use parallel connections of triggering bridges.

The most common optical scheme for studying the shattering process is shown in Fig. 43. Condenser 3 converts the light flux coming from flash lamp 4 into a parallel light beam which, after passing through the model 2, falls upon the objective of the SFR 1 camera. With the aid of the objective an image of the object is formed in the plane which intersects the center of the reflecting face of the mirror. At some distance from the mirror along the arc of the surrounding enclosure a series of lenses are set up, which sequentially project the image of the object on to a high-sensitivity film.

Using high speed photographic recording one may establish the propagation mechanism and parameters of stress waves in the material of the model during an explosion. For this purpose it pays to employ the optical polarization method for measuring the

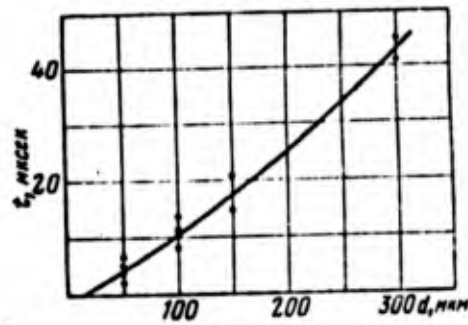


Fig. 42. Dependence of delay time of the explosion on the diameter of the constantine bridge wire.

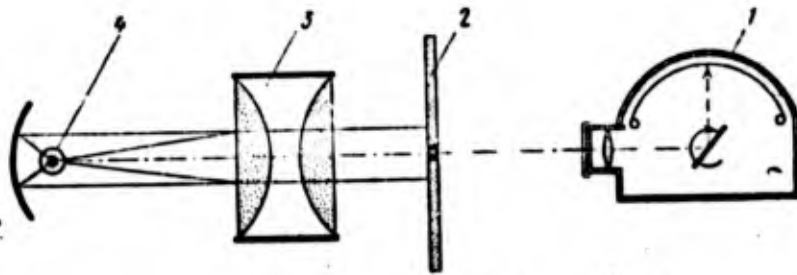


Fig. 43. Optical scheme for studying the damage process by SFR (High speed photographic recording).

stresses, this method being based on the capability of a number of transparent isotropic materials to exhibit double refraction of light under the influence of voltages. The elastic-optical effect, quantitatively expressed in terms of the order of the isochrome, may be considered as a function of two variables: the specific elongation and the normal stress. However, within the

limits of elasticity, these quantities are proportional to each other, so that when using the optical method both the stress and the deformation are measured. The optical method, in contrast to other methods, permits one to measure the stress at all points of the model under study. When using other methods it is sometimes rather difficult to obtain a representation of the distribution of stresses over the whole object in order to determine accurately the points of maximum stresses. In order to study the stress fields occurring in an explosion in models made of optically active materials, a polarization apparatus is used in combination with the SFR. To serve as the polarizers one often employs artificially prepared polaroids. They consist of two pieces of glass glued together with a film in between them. The film contains crystals of herapathite, which possess the property of double refraction. The simplest polarization set up consists of a light source (reliably monochromatic) and two cross polaroids, called the polarizer and the analyzer, between which the model is placed (Fig. 44). As a result of the investigation it was established that the band factor for an elastic material does not depend on the nature of the loading, and the results of calibration using static loads may be used in interpreting the dynamic stress fields.

For the recording of more protracted processes occurring under natural conditions, as for instance the shifting of a block due to an explosion or the dispersion of fragments, one uses the SKS-1 surveying camera. In view of the large overall time duration of the frame in the given case such a careful synchronization is not necessary as when using the SFR camera. The frame frequency of the SKS-1 camera is regulated within the limits of from 150 to 4,000 frames/sec when the total number of frames is 3,900.

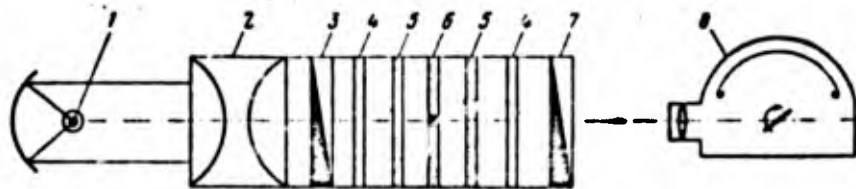


Fig. 44. Abstract diagram of the optical apparatus for studying dynamic stress fields.

1- flash lamp; 2- condenser; 3- polarizer; 4- quarter-wave plates; 5- protective glass; 6- model made of optically active material; 7- analyzer; 8- SFR motion picture camera.

Application of modern methods of photographic recording enable one to establish the basic regularities of the shattering process in both transparent and opaque materials.

#### Methods for Determining the Velocity of Crack Development

The shattering of rocks by impulsive loads is to be viewed as a process of formation, growth, and amalgamation of cracks. One of the characteristics of the process, namely the velocity of crack development, enters as a determining parameter into the similitude criteria for modelling the destructive action of an explosion. Methods for measuring the velocity of crack development in response to impulsive loads may be divided into three groups: methods using high speed photography, ultrasonic methods, and electrical methods.

High speed photography in conjunction with the shadow method of Teppler and the method of the double reflection of light from the surface of shattering (Kol'skiy, 1963) permits one not only to determine the velocity of crack development in optically transparent materials, but also to investigate stresses at the front of the propagating cracks.

Kh. Shardin and V. Shtrut (1937) established the constant maximum velocity of shattering in glass with the aid of a motion picture apparatus with multiple flashes, which makes it possible to obtain frame exchange rates from  $10^5$  to  $10^6$  per second as well as good resolution. Ordinarily when using an apparatus with multiple flashes one studied processes in transparent materials only, but using light reflected from a plane surface one may in principle study the velocity of crack development in opaque materials. The front of the propagating crack is usually visible with simple illumination of the transparent plate by point flashes without any supplementary optical design. The domestic ultra high speed photographic recording system SFR (Dubovik, 1964) makes it possible to investigate the process of crack development in transparent plates.

In order to investigate the shattering process within an opaque material one uses the ultrasonic method (Kerkhof, 1953; 1956), which is based on utilization of the Walner lines that form in response to transverse waves. The surface of shattering is modulated by a standard, continuously radiated, transverse ultrasonic wave of frequency  $10^6 - 10^7$  Hz. When there is interaction with these waves the front of the crack deviates and forms trenches or steps, which are observed as lines on the surface of fracture. The direction of the deviation of the cracked front is determined by the phase of the ultrasonic oscillation, and in the course of one period one trench and one step is formed. The distance between neighboring steps depends on the path traversed by a crack over a period of time equal to the period of oscillation

of the ultrasonic wave. For a constant frequency of oscillation the distance between neighboring steps is determined only by the velocity of crack propagation. Thus the surface of shattering is imprinted with time markings from which it is possible to find the velocity of crack propagation. Taking account of the small distances between steps (for a crack velocity of 1000 m/sec and an ultrasonic oscillation frequency of  $10^7$  Hz the distance between steps will come to 0.1 mm), and also the very deviation of the crack front, the shattering surface, modulated by ultrasonic radiation, is studied with the aid of the ordinary shadow microscope or the interference microscope. In making use of the ultrasonic method the chief difficulties are related to the transmission of transverse waves into the sample to be studied. In the original variation of this method the source of ultrasonic waves was immersed in water along with the sample. Subsequently two new adaptations were worked out (Kerkhof, 1956). In the first adaptation one uses an ordinary quartz crystal cut along the x axis to serve as the radiator (Fig. 45); this crystal conveys the energy of the longitudinal waves into a water converter, enclosed in a rubber membrane. When the membrane is in contact with the sample, the sound enters into the sample just as if the whole sample were immersed in water. The water also serves as a cooling liquid, which circulates around a closed system through the pipe K under the action of a small pump. This method makes it possible to transmit the ultrasonic wave to the rubber - sample surface at angles of incidence from 0 to  $40^\circ$ . With such angles of incidence of the longitudinal wave in the sample transverse waves of sufficient intensity are formed.

The sound converter depicted in Fig. 46 consists of a composite oscillator which generates transverse waves. In order to excite the transverse waves one uses a quartz crystal, cut along the y axis. At a frequency of  $5 \cdot 10^6$  Hz the thickness of the



Fig. 45. Diagram of an ultrasonic radiator for introducing longitudinal waves into solid samples through a water cushion.

$Q_x$  - quartz crystal, cut along x axis; G - rubber membrane; W - water; K - pipe for water cooling; U.S. - radiated longitudinal wave

Fig. 46. Transverse ultrasonic wave radiating device.

$Q_y$  - quartz crystal, cut along y axis; A - composite oscillator with aluminum; K - water cooling channel;  $U_1 S_1$  - radiated transverse wave.

crystal is 0.3 mm and therefore it may be very easily damaged. In order to avoid damaging the crystal it is fastened to a support made of aluminum whose thickness is 10 times greater than the wavelength of the transverse waves. Owing to the intense heating during operation the composite oscillator is cooled with water passing through the channel K. Using such a device one may transmit transverse waves directly into the sample being tested, but only in a direction perpendicular to the surface. In introducing a wave into the sample when using this adaptation various schemes are possible, whose essence is made clear in Fig. 47.

The shortcoming of the ultrasonic method is the considerable complexity entailed in making contact between brittle radiators and the sample under conditions of sufficiently high ejection velocity of the sample fragments. The complexity involved in carrying out the experiment imposes a limitation on the practical utilization of the ultrasonic method for measuring the velocity of crack development in rocks.

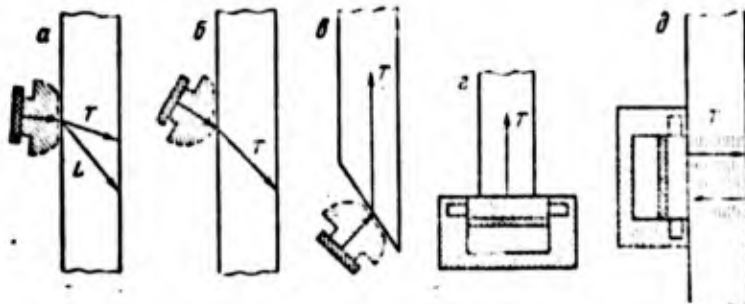


Fig. 47. A scheme for introducing waves into the sample.

a- simultaneous introduction of a longitudinal L and a transverse T wave; b- introduction of a transverse wave with full reflection of the longitudinal wave in the radiator, c- introduction of a transverse wave along the axis of a rod using a water radiator, d- introduction of a transverse wave using a composite oscillator; e- introduction of standing transverse waves.

In a number of cases Wallner lines were formed by the interaction of the crack front with the transverse elastic oscillations which arise under conditions of shatter, the so-called Wallner waves. These oscillations, whose frequency may go as high as  $10^{10}$  or  $10^{11}$  Hz, occur in the shattering of the region with a disrupted structure. In order to determine the velocity of crack development it is necessary to establish the frequency of the

Wallner waves which occur in the process of shattering. From the Waller lines on the shear surface in accordance with the approach which has been described one can determine the velocity of crack development. Such a methodism may be successfully applied to the investigation of crack kinetics in metals, some rocks in plexiglass (organic glass), etc. In plexiglass the roughness of the surface of shattering may be so significant that it is possible to get along without a microscope in the investigation. In the case of large crack velocities the Wallner line method cannot be employed owing to the growth of the number of centers which radiate waves and the complexity of the shattering surface.

In order to investigate the velocity of crack development in opaque materials and in rocks, electrical methods are widely used, which consist in the fixation of current carrying lines drawn on the surface of the samples at the moment of rupture. To serve as the signal lines one uses a glued-on wire or a foil or layers of metal obtained by vacuum deposition, Aquadag, silver paste, graphite preparation VKGS-0 (TU-35-X11-329-61) (Danchev, 1960; Drukovanyy, 1967; Kucheryavyy et al., 1962; Smirnov, 1967). The many existing schemes for making the measurement have a number of deficiencies and require a critical approach in choosing the types of signal lines and recording apparatus to be used. The accuracy and reliability of measuring the velocity of crack development depends in turn on the property of the material in the signal line, which must satisfy the following requirements: 1) minimum lag or persistence, i.e., the capability of fixing with high accuracy the moment of passage of the top of the growing crack; 2) the technology of drawing signal lines must not affect the properties of the rocks. These requirements determine the most important properties of the material of the line: high adhesion capabilities, brittleness, and strength, not exceeding the strength of the rock.

Determining the velocity of crack development in rock using glued-on wires or foils is carried out in the following manner (Kucheryavyy et al., 1962). Thin wires or strips of foil depending on the shape of damage front are glued on in the form of straight lines, concentric circles, or semicircles on the sample or model to be studied. The moment of explosion of the charge is fixed with a special sensor. The MPO-2 oscilloscope with a time marker at 100 Hz is used as the recording apparatus. The maximum frame velocity for recording the process on photographic film is 5000 mm/sec. Cracks propagating from the charge disrupt the current carrying ring, and the moment of the rupture is fixed with the aid of a MPO-2 oscilloscope. Knowing the distance between the rings, it is easy to compute the velocity of crack development from ordinary kinematic relationships. Using a thin wire or foils to function as the signal lines is the source of a number of shortcomings. The adhesive joint does not have sufficient brittleness, and the signal line, connected with the rock by a viscous layer of cement, may rupture not at the top of the passing crack, but far away from it as a result of the separation of the sides of the crack. Moreover, in the rupture of the wire plastic deformations occur while most of the rock is shattering in brittle fashion. Experimental investigations have established that wire-type sensors, attached to a block undergoing shattering, will rupture not at the moment at which cracks are passing through them but after the cracks have opened up to some size. Under experimental conditions on the artillery range after the explosion of blast-hole charges, cracks were found at the bottom which had opened up to some size but the wire crossing them turned out to be unbroken.

In the work of V. V. Smirnov (1967) the nature of the rupture of signal wires made of constantine wire, aluminum foil, and colloidal

graphite preparation VKGS-0 (TU-35-XII-61) was soundly established. In Fig. 48 microphotographs of regions of a sample of soapstone (magnification 60x) with signal lines made from a wire of diameter 0.05 mm are given. For a crack width of 0.06 mm (Fig. 48a) the wire undergoes a rupture which was preceded by considerable plastic deformation, and closer to the top the crack caused no damage to the signal wire (Fig. 48b). Tests with lines made of aluminum foil gave the same results. Apparently, the signal lines made of wire and foil cannot give precise information on the moment of passage of the top of a crack. Investigations conducted by the authors of a group of works (Drubovanny, 1965, 1967; Smirnov, 1967) lead us to the conclusion that in order to record the velocity of cracks in rocks the most acceptable signal lines are those made from silver paste (kontaktol) and thinly dispersed graphite. The paste consists of colloidal silver and epoxy cement (5 parts silver and 1 part cement), alabaster (plaster of paris), cement (4:1), and it possess a high conductivity, a fact which makes it possible to use it for conductive rocks of the iron ore type, where the graphite preparation is unsuitable. Silver paste and graphite preparation have good adhesion properties, and the lines drawn on the surface of samples, after a brief drying at room temperature, have low strength and high brittleness. In Fig. 49 a microphotograph of a region of a sample at the top of a crack at rest (separation of the sides 0.015 mm; magnification 135x) is shown. And the nature of the rupture illustrates convincingly the suitability of graphite preparations for use in the role of signal lines. Verification of the rupture of signal lines made of silver paste was carried out on glass plates. The velocity of crack development was determined by two methods: from the time of rupture of the signal lines and from the frames of the photographic recording (frame frequency 625,000 frames/sec). The values of the crack development velocity, all determined in the same region but by different methods, did not differ by more than 5%. One of the advantages of the indicated method is the simple technology for drawing lines of the desired thickness on any kind of surface. In measuring the

velocity of crack development in various materials the feasibility of using one or another type of recording device is determined by the assumed velocity of crack movement, typical of the dimensions of the sample, and by the speed with which the process is recorded.

In the majority of known schemes for measuring crack velocity cathode ray oscilloscopes are employed. Let us take a look at the schemes which are most widely utilized.



Fig. 48. Microphotographs of a sample and signal lines after passage of a crack

Width of the crack: a- 0.06 mm; b- 0.03 mm (60X)



Fig. 49. Microphotographs of a sample with lines drawn on with graphite preparation after passage of a crack of width 0.015 mm (135X)

The simplest scheme is the one introduced in the work of M. F. Drukovanyy (1967). According to this scheme (Fig. 50) the voltage from a signal line is fed to the plates of an OK-17 (C1-24) oscilloscope. BAS-100 batteries are used as the feed source. As the line ruptures the potential on the oscilloscope plates changes, and this causes a deflection of the beam on the screen. For rocks with high conductivity (for instance, iron ore) the resistance of 2-5 kohm is shunted by a resistance  $R_1$  of the order of several megohms in order to obtain a higher discontinuity in voltage as the signal line is ruptured. Start up (triggering) of the oscilloscope is performed by a piezoelectric sensor, which is situated directly on the explosive charge. The diagram shows switching of two signal lines to one oscilloscope. The oscilloscope traces obtained permit one to determine the velocity of crack movement.

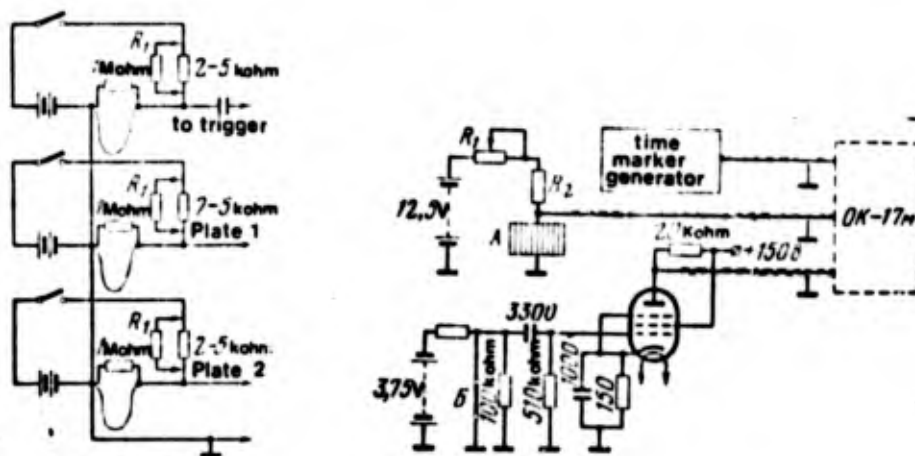


Fig. 50. Electrical circuit for determining the time of rupture of the current-conducting sensors.

Fig. 51. Measuring circuit for determining the velocity of crack development with a OK-17M oscilloscope.

In the works of V. V. Smirnov (1967) for velocity measurement several constant current half-bridge circuits are proposed whose measuring arms are signal lines connected in parallel (Fig. 51). Rupture of the lines by the top of a passing crack leads to a discontinuous rise in voltage, which is fed to the input of the oscilloscope. It has been experimentally established that the optimum voltage necessary for feeding the half-bridge is of the order of 5-10V. In this connection it is convenient to take the sweep trigger signal from the signal being measured in view of the large amplitude of the automatic triggering signal of the device. In order to trigger the oscilloscope at the moment of crack formation a system is built up operating on the principle of interruption of continuity. At the time of rupture of a current-conducting line by the crack which has been formed, a signal of small amplitude from the external feed source is enhanced by a pulse amplifier and fed to the trigger input of the OK-17M oscilloscope. The electrical measuring scheme for the case just described is shown in Fig. 51, where A is the signal line and B is the triggering sensor. With the aid of resistors  $R_1$  and  $R_2$  one chooses the size of the beam deflection for signal lines switched in and switched out (modelling of the rupture) within the limits of the linear part of the amplitude characteristics. The trigger signal pulse amplifier is built around a 6Zh9P pentode. Recording of the velocity of crack propagation by the scheme developed here may be realized for various means of damage of the sample and using any period of cathode ray oscilloscope which has a high signal level for automatic triggering and a signal voltage in the regime of independent triggering up to 50 v.

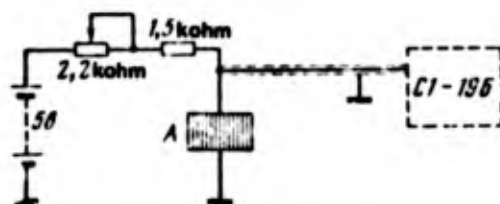


Fig. 52. Measuring circuit for determining the velocity of crack development with a S1-19b oscilloscope.

The S1-19b oscilloscope has a number of advantages over the OK-17M: a significantly larger (up to 50 mm) beam deflection along the vertical axis within the linear portion of the amplitude characteristics, a fact which makes it possible to increase the number of signal lines and to raise the accuracy of the measurement; a low level of triggering signal within the regime of automatic triggering; wider amplification limits for constant current. Utilization of the S1-19b oscilloscope made it possible to improve the measuring circuit (Fig. 52): the independent triggering system was removed, the reliability of the measuring scheme was enhanced, and the signal lines were brought close to the contact zone of the instrument with the sample. A low voltage was fed to the measuring half-bridge as a result of which the accuracy of measurement was improved. By modelling the rupture of current-carrying lines of various resistances using a variable resistance of  $R=2.2$  kohm the beam deflection in the linear range of amplitude characteristics is found.

In the explosive mechanics department of the Institute for Geological Engineering Mechanics of the Ukrainian SSR Academy of Sciences studies were carried out on the velocity of crack development in various materials and in rocks using silver paste for the signal lines and with the electrical circuitry shown in Fig. 50. It was found that in the rupture of the signal line a coherent order was not observed. First of all ring I may rupture from the charge, and after that rings III, II, IV, etc. During investigation of shattering of glass models using SFR it was found that cracks arise simultaneously at various distances from the center of the explosion (Fig. 53). Such lack of coherence and, at first glance, haphazard behavior is easy to explain if, in our consideration of the shattering process, we start from the hypothesis of M. V. Machinskiy concerning the existence of "weak points". The number of crack generation sites is not a fixed quantity for a given material. When the magnitude of the applied

stress is made larger the number of cracks appearing increases, and the length of an elementary crack decreases (Regel; 1956).

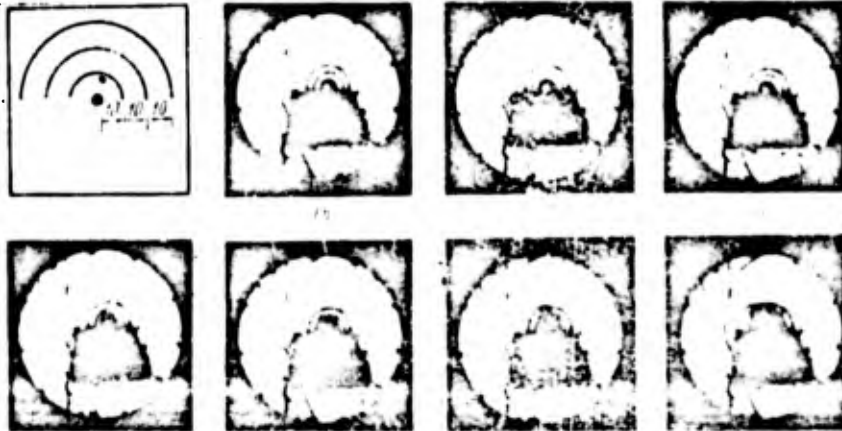


Fig. 53. Shattering process in a glass plate (in microseconds)

In considering the process of shattering, it is necessary to distinguish the velocity of development of a single crack and the propagation velocity of the shattering front. In the experiment the velocity of crack development was determined from the known distance between neighboring signal lines and the time of rupture of these lines.

(252)

$$v_{rp} = \frac{r_{n, n+1}}{|t_n - t_{n+1}|},$$

where  $r_{n, n+1}$  is the distance between the  $n$ th and  $(n+1)$ st signal lines (accounting for the width of one line);  $t_n, t_{n+1}$  are the moments of rupture of the  $n$ th and  $(n+1)$ st signal lines respectively.

The mean velocity of shattering is found from the known distance between the first and the last signal lines and from the time of rupture of the first ( $t_{\min}$ ) and the last ( $t_{\max}$ ) rings

(253)

$$v_R = \frac{r_k - r_1}{t_{\max} - t_{\min}},$$

where  $r_1$  is the distance from the charge center to the first line, and  $r_k$  is the distance from the charge center to the last line.

These methods have made it possible to study crack velocity in the rocks of the Krivoy Rog open pit iron ore mines, open pit mines of the Dokuchayevskyy flux-dolomite Kombinat, the granite quarries of Krivoy Rog, Kremenchug, the Vinnitskyy region and in other quarries and mines. Rock samples of approximately cubic shape with edge length of 30-40 cm were extracted directly at the quarry. A blast hole was drilled in the sample, and around it on the side of the line of least resistance through 5-15 mm a semi-circle was drawn out of silver paste. Ammonite V-3 was used as the explosive material. The specific consumption of explosive material was 600 g/m<sup>3</sup>. The results of measurement of the velocity of crack development in some rocks are shown in Table 4. The mean velocity of shattering and the velocity of crack development were measured also directly in the block with explosions of blast-hole charges. The approach toward making the measurements was not in any way different from that described. The results of the crack development velocity measurement in the massif are given in Table 5.

Table 4

Characteristics of the Shattering Process of Outsized Blocks of Rock By Means of Explosion of Ammonite V-3 Charges (Specific Consumption of Explosive Material 600 g/m<sup>3</sup>)

Sampling site	Rock	Crack development rate, m/sec	Average destruction rate, m/sec
New Krivoy-Rog Mining and Concentration Kombinat	Martite-magnetite chert	230	780
Central Mining and Concentration Kombinat	Carbonate-magnetite chert	295	920
	Magnetite chert	85-100	330-390
Inguletskiy Mining and Concentration Kombinat	Chloritic shale	580-670	985-1050
Gnivan'skiy granite quarry	Gray, small-granular granite	210-230	555-820
Dokuchayevskiy flux-dolomite Kombinat, dolomite mine	Dolomite	450	1210

Table 5

Velocity of the Shattering Process In Explosion of Blast-Hole Charges in a Block

Place where experiment was conducted	Rock	Crack development rate, m/sec	Average destruction rate, m/sec
Dokuchayevskiy flux-dolomite Kombinat, Dolomite mine	Gray limestone	300-340	1200-1310
Krivoy Rog, Kolomoyevskiy granite quarry	Granite	130	700-800
	Diabase	245	1000-1200

Methods for Determining the Distribution of Zones of Reduced Strength in Model Materials and in Rocks

Experimental determination of the distribution of reduced strength zones with regard to the degree to which they represent a hazard is of paramount importance in statistical theories of damage. The basis of similarities in the use of statistical theories of damage is the equality of the number of microcracks opening in a unit of relative volume. Experimental determination of the distribution of reduced strength zones makes it possible to realize the physical modelling of crushing processes on a strict scientific basis. Since by a zone of reduced strength we usually mean regions with decreased adhesive forces, the main part of the similar zones is comprised of places where continuity is disrupted, i.e., cracks. Existing methods for determining the degree of crumbling or fracturing of rock blocks are based mainly on consideration of visible cracks. Direct, reliable methods for finding closely joined or microscopic cracks at the present time do not exist, in spite of the fact that it has been recognized that

the defects determine in large part the nature of shattering in monolithic rocks. One of the indirect methods for finding the number of weak spots is the simultaneous determination of the propagation velocity of individual cracks  $v_{cr}$  and the shattering front  $v_R$ . Then the number of crack generation sites is found from the relationship

(253a)

$$n_l = \frac{v_R}{v_{cr}}$$

where  $n_l$  is the number of crack generation sites along the direction  $l$ . Knowing the total number of cracks in the chosen region, it is easy to determine the number of generation sites in a unit of volume  $n_0$ .

In order to determine experimentally  $n_0=f(\sigma)$  from the material under study a rod of diameter 20 mm was prepared, in which wire sensors were arranged at definite distances (5-8 mm) perpendicular to the axis. The diameter of the sensor was 0.03 mm and the length was 20 mm. In rods made of rock, openings were drilled ( $d=0.7 - 1.0$  mm) in which wire sensors were set and cemented. If self-hardening mixtures (cement, gypsum, etc.) or low-melting materials (rosin, hyposulphite, sulphur, etc.) were used for preparing the rod, then the sensors were set in shape before pouring the material. The rod prepared with sensors was placed inside a detachable covering made of non-magnetite steel (Fig. 54), which prevented intermixing of the disintegrated material and scattering of the fragments. On the free end of the rod a washer was installed, on which explosive charge (1), creating a plane shock wave, was placed. The rod in its covering (3) was situated between the pole pieces of a strong permanent magnetite. Upon explosion of the charge, the sensors (2) installed on the rod enabled the value of the maximum velocity of particle movement in the shock wave to be determined. The emf induced in the sensor was registered on S1-29 oscilloscopes. Some typical oscilloscope

tracers are shown in Fig. 55. As a result of an analysis of the oscilloscope traces the size of the maximum velocity of motion was established and in the acoustic approximation the value of the maximum stresses were calculated (Fig. 56). Following the explosion, the covering of non-magnetite steel was dismantled in such a manner that the distribution of particle sizes in the composition of fragments formed at various regions of the rod was preserved. Knowing the value of the maximum stresses and the particle-size composition of the fragmented material in a region, one may determine to a first approximation the dependence  $n_0 = f(\sigma_{\max})$ .

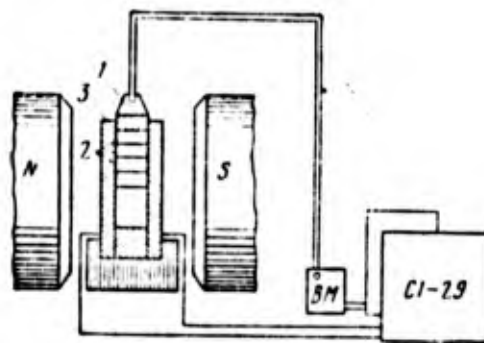


Fig. 54. Experimental scheme for determining the specific number of crack generation sites as a function of the value of stresses in various materials.

In some transparent material, for instance in rosin, a direct determination of the frequency of cracks being formed in various zones is possible. In order to do this a transverse cut of the rod is made in the plane of every sensor (Fig. 57), from which the number of cracks being formed at various distances from the charge is determined. In Fig. 57 it is seen that the number of cracks at large distances from the charge decreases in connection with

a decrease in  $\sigma$ . Using a longitudinal cut

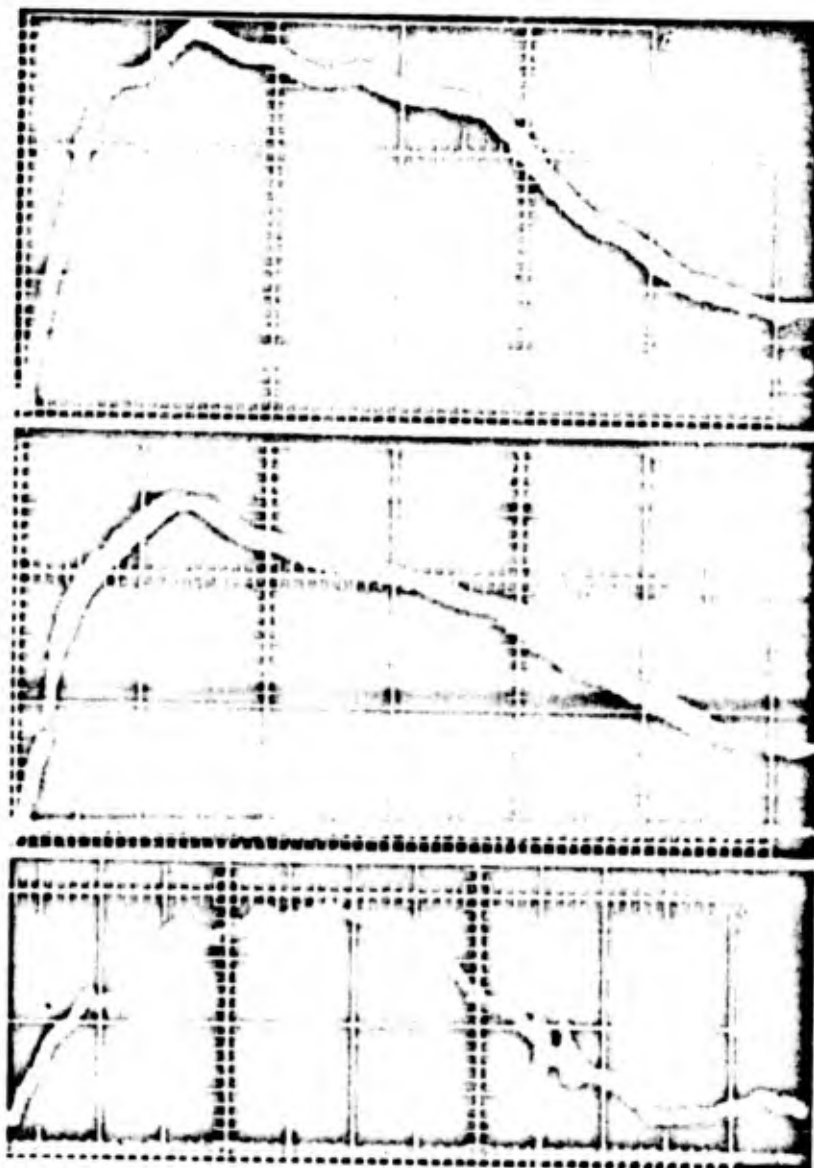


Fig. 55. Typical oscilloscope traces of a stress pulse in a rod in the zone of intense crushing at the following distance from the charge (in mm) a - 8, b - 16, c - 24.

of the rod (Fig. 58) it is possible to trace very clearly the change in number of crack formation centers

in various regions of the rod and to establish the dependence  $n_0 = f(\sigma_{\max})$ .

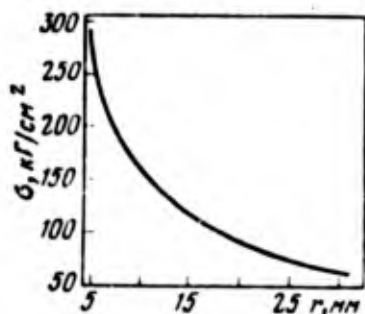


Fig. 56. Variation in the value of the maximum stresses in a rod as a function of distance.



Fig. 57. Transverse sections of a rod in the zone of intense crushing at the following distances from the charge (in mm) a - 8, b - 16, c - 24.



Fig. 58. Longitudinal section of a disintegrated rod.

The nature of the change in value of  $\partial n / \partial \sigma$  for various materials has its peculiarities, caused by the structure of these materials. For instance, hyposulphite in contrast to rosin has a crystalline structure. The process of shattering for small stresses usually begins along cleavage planes, where the adhesion forces are considerably less than binding forces in the crystal and the dimensions of defects in the cleavage region are frequently considerably greater. Such a structure in hyposulphite explains the smaller number of crack formation centers in comparison with rosin for small relative stresses (Fig. 59), since shattering takes place only along cleavage planes. The number of crack formation centers in a unit of volume depends on the crystallization condition and in every case it must be determined by experimental means. The decrease in  $\partial n / \partial \sigma$  in the range  $\sigma_{\max} / [\sigma]_R = 3-7$  is explained by the difference in the strengths of the crystals and of the joints between them, and the value of  $\sigma_{\max} / [\sigma]_R$  for which one again observes an increase in  $\partial n / \partial \sigma$  characterizes the ratio of the crystal strength to the strength of the joint between the crystals. After the strength of the crystals themselves is exceeded one observes a sharp increase in the centers of crack formation on account of the exposure of defects in the crystalline lattice. Theoretically,  $n_0 = f(\sigma)$  must rise sharply with an increase in stresses, though for small distances between the cracks there is a substantial effect of redistribution of stresses near the moving crack, which leads to a reduction in  $\partial n_0 / \partial \sigma$ . A further

increase in  $\partial n_0 / \partial \sigma$  with an increase in stresses must be observed in the shock wave, leading to evaporation of the material. An analogous dependence holds also for dolomitized limestone (Fig. 60, curve 1). For granite the difference in strength of the various components of the minerals is more clearly expressed. At first one observes a sharp increase in the number of weak points owing to the shattering of the minerals with less strength (mica, feldspar). After that an increase in stresses has little effect on the number of weak points as long as the strength of quartz is not exceeded. The nature of the curve depends on the ratio of the strengths of the minerals included and their composition ratio.

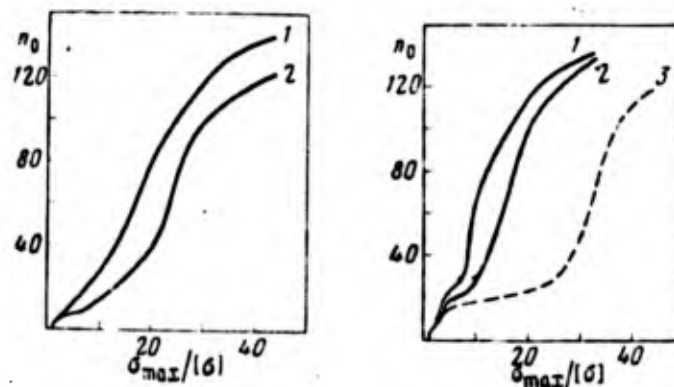


Fig. 59. Nature of the change in specific number of crack generation sites as a function of the relative stress

1- for rosin; 2- for hyposulphite.

Fig. 60. Nature of the change in specific number of crack generation sites as a function of the relative stress

1- for granite; 2- for dolomitized limestone; 3- for a hypothetical rock block.

Even for different dimensions of a sample of the same rock  $[\sigma]_R$  is different. Particular distinctions in the nature of shattering are observed in the block. The block is usually broken by a system of microcracks, many of which may be tightly closed and invisible to the unaided eye. For relatively small stresses these cracks begin to open, damaging the separate region.

Therefore, one observes in the block a redistribution of stresses at the time of shattering. In the block the tendency toward reduction of  $\partial n_0 / \partial \sigma$  must be more strongly expressed than in granite, since the difference in strength of the crack filler, in the adhesion forces in closely joined macrocracks, and in the strength of the material is very large. Therefore, in Fig. 60 (curve 3) the assumed dependence is shown for the block.

The number of crack generation sites depends on the distribution of weak points in the material being studied and on the value of the stresses. Knowing the nature of the change in number of crack generation sites with stress, it is possible to determine indirectly the parameters of the desired distribution. The function  $n_0(\sigma)$  is determined from an analysis of the particle size composition of the damage medium within limited regions. The dimensions of these regions are found from the conditions stipulating that the change in stresses within these limits is negligible.

The methods which have been set forth make it possible to study the distribution of zones of reduced strength in various modelling materials and in rocks as well as to employ the dependences obtained in modelling the destructive action of an explosion. An analysis of the experimental data obtained attests to the fact that the distribution of weak points in the materials studied agrees with the normal distribution law in the majority of cases.

## CHAPTER FIVE

### PARAMETERS OF THE SHATTERING PROCESS<sup>1</sup>

#### Physical and Mechanical Properties of Rocks and Modelling Materials

One of the main factors ascertaining the nature of the shattering process is the physical and mechanical properties of the medium. The most important of these are: the elastic characteristics of the medium, its strength and the velocity of crack propagation. In order to model the crushing process it is necessary to study the basic physical and mechanical properties of the rocks and modelling materials and the effect they have on the shattering. The nature of propagation and reflection of elastic waves determines the structure of the stress field arising in the block at the time of explosion and, consequently, exerts an important influence on the process of shattering of rocks. One of the fundamental characteristics of the process, along with the laws of absorption, reflection, and refraction, is the velocity of propagation of an elastic wave. The velocity of waves in a sufficiently broad region does not depend on the oscillation frequency (i.e., the wavelengths) and is unambiguously connected with the elastic modulus of the material. Several methods exist for determining the propagation velocity of elastic waves. All of these, except for resonance methods, are based on a measurement of the time taken for a wave to travel over a known distance. In order to measure the time of passage of an ultrasonic wave one uses devices of two classes. In devices of one of these classes one records the moment of arrival of a passing elastic wave, and in devices of the other type one fixes the time of arrival of the reflected wave. All remaining differences are contained in the technique of measurement.

---

1. This chapter has been written jointly with engineer V.P. Bilokon.

Determination of the velocity of wave propagation by the resonance method is based on the phenomenon of resonance. For a known length of the sample and a known frequency of first resonance (the fundamental tone) the value of the velocity is obtained from the relationship

(254)

$$c = \frac{l_r \omega}{4\pi}$$

where  $c$  is the propagation velocity of longitudinal waves;  $l_r$  is the length of the sample (rod),  $\omega$  is the cyclic resonance frequency.

In the Institute for Geological Engineering Mechanics of the Ukrainian SSR Academy of Sciences measurements were carried out on the velocity of wave propagation in rocks of Krivoy Rog, the Dokuchayevskyy flux-dolomite Kombinat, , the Balaklavskyy Ore Administration and in modelling material-rosin and hypersulphite. The wave propagation velocity was determined by two methods: the ultrasonic method, based on the measurement of propagation velocity of ultrasonic signals, and the explosive method, consisting of the measurement of propagation velocity of an explosive stress in the impulse. In order to determine the propagation velocity of dilatational elastic waves by the first method the ultrasonic device UZP-62 was employed. This device is intended for the measurement of propagation time of an ultrasonic pulse in various materials. It is equipped with two interchangeable ultrasonic heads (sensors), one of which serves as an oscillation source and the other as a receiver. In measuring the propagation velocity of ultrasonic radiation in a solid material an acoustical contact must be mounted between the sensors and the medium of interest, the contact being realized in the following way. On parallel faces of the rock sample selected for measurement, two planes are

grounded, located opposite each other. Their dimensions must be slightly larger than the area of the end surface of the ultrasonic sensors. The planes are lubricated with commercial vaseline and the ultrasonic heads are pressed against them.

In the elastic medium several types of waves arise and are propagated: dilatational waves (longitudinal waves), flexural waves, shear waves (transverse waves), Rayleigh surface waves, and purely transverse surface waves (Love waves). In order for flexural waves, surface waves, and purely transverse surface waves to develop in the samples it is necessary to satisfy a series of special conditions, and they do not arise in the case of the method which has been described above for exciting ultrasonic oscillations in the sample. Transverse waves do not arise directly at the point of contact of the ultrasonic head with the sample, but in reflection from the free surface a part of the longitudinal wave (depending on the angle of reflection) are transformed into transverse waves. The ultrasonic receiver determines only the moment of entrance of longitudinal waves, since their velocity is larger than the propagation velocity of the transverse waves.

Furthermore, the transverse wave may arrive at the ultrasonic receiver after reflection from lateral surfaces of the sample at the moment that the longitudinal wave is propagating directly from the radiator.

The conditions for propagation of a longitudinal wave in an infinite block and in a rod are different; the wave propagation velocities are also not the same in the two cases.

The ratio between the wave velocities in the rod and in the block depend on the Poisson coefficient

(255)

$$\frac{c_{\text{rod}}}{c_{\text{block}}} = \sqrt{\frac{1-\nu-2\nu^2}{1-\nu}}$$

- where  $C_r$  is the velocity of longitudinal wave propagation in the rod;  $C_b$  is the velocity of longitudinal wave propagation in the block.

The shape of the rock samples and the material samples being studied were made to approximate the shape of a cube. In order that the propagation velocity of the ultrasonic pulse in the sample correspond to the propagation velocity of the longitudinal wave in the block, it was necessary to satisfy the inequality

(256)

$$\frac{\lambda}{r_0} \leq 1,$$

where  $\lambda$  is the ultrasonic wavelength;  $r_0$  is the radius of the base of the sample. In this case the lateral surfaces do not introduce distortion into the reckoned time of arrival of the longitudinal wave. The propagation velocity of longitudinal waves is computed from the formula

(257)

$$C_w = 10^3 \frac{l_0}{t},$$

where  $l_0$  is the base of the measurement (length of the sample) in mm, and  $t$  is the time for passage of a wave in microseconds. Besides the ultrasonic method for determining the velocity of an elastic wave in the rock samples the method of explosive loading was used. The propagation of an elastic wave in this case proceeds in the following way: explosive charge-triggering piezoelement - sample - receiving piezoelement. The piezoelement made of Rochelle salt was cemented to the polished end of the rock samples. Afterwards one end of the sample was subjected to the effect of the explosion of a charge of PETN of weight 200 mg, which was triggered by a suspension of lead azide (10 mg). Recording of the time

taken for the wave to cross the distance between the triggering and the receiving piezoelements was accomplished using an OK-17M oscilloscope. On the basis of the data obtained the average velocity of the stress wave was determined. Each type of rock was represented by five samples. The dimensions of their faces fluctuated within the limits 60-120 mm. The results of measurement of the wave propagation velocity by both methods are shown in Table 6. An analysis of the results obtained showed that the values of the wave propagation velocities obtained by the explosive method are, as a rule, somewhat larger than the values of the velocities obtained by the ultrasonic method. The reason for this difference in velocities lies in the fact that near the charge a shock wave is formed.

The velocity of the shock wave is a variable quantity, depending on the stress at the wave front, but it always remains larger than the velocity of the elastic stress wave.

In order to determine the other elastic constants measurement was made of the propagation velocity of elastic waves in rods made of rock employing the ultrasonic method. The length of the rods exceeded the wave length of the ultrasonic radiation by a factor of 4 or 5. The results of the experiments carried out in Table 6 enable one to determine the elastic modulus of the rocks

$$E = (c_{cr})^2 \rho \quad (258)$$

and the Poisson coefficient

$$\nu = \frac{1}{4} \left[ \left( \frac{c_{cr}}{c_M} \right)^2 - 1 + \sqrt{\left( \frac{c_{cr}}{c_M} \right)^4 - 10 \left( \frac{c_{cr}}{c_M} \right)^2 + 9} \right] \quad (259)$$

where  $\rho$  is the density of the material, which is determined by a method in which the volume of water displaced by a sample of known mass is measured. The data obtained fully characterized the elastic properties of the rocks and the modelling materials.

TABLE 6

Sampling Site	Rock	Density of rock, g/cm <sup>3</sup>	Velocity of longitudinal wave in block, m/sec		Velocity of longitudinal wave in rod, m/sec (ultrasonic method)	Elasticity Modulus kgf/cm <sup>2</sup> ·10 <sup>-5</sup>	Poisson Coefficient
			Ultrasonic Method	Explosive Method			
Krivoy Rog, New Krivoy Rog Mining and Concentration Kombinat	Martite-magnetite red banded chart	4.60	6080/5740	6150/5550	5400/5125	15.5/13.50	0.27
	Carbonate-magnetite chart	4.12	5630/7315	6500/7240	5910/6530	16.2/19.70	0.27
	Semi-oxidized martite-magnetite chart	5.222	6880/6520	6700/6200	6090/5775	22.1/20.90	0.28
	Biotite-chloritic shale	2.95	5980/5510	5500/5100	5440/5010	8.9/7.60	0.28
	Non-oxidized martite-magnetite chart	3.46	- /7000	7050/6050	- /6250	- /15.10	0.27
	Chloritic shale	3.23	2850/2755	2370/2180	2590/2500	2.22/2.04	0.25
Krivoy Rog, Central Mining and Concentration Kombinat	Nonconditioned Hematite-martite chart	3.22	4650/5020	5100/4670	4150/4480	6.14/7.26	0.27
	Hematite-martite chart	3.89	5230/4500	6200/5500	4670/4020	9.57/7.03	0.27
	Oxidized hematite	4.70	6210/5660	6190/4950	5550/4980	16.4/13.50	0.27
Krivoy Rog, Central Mining and Concentration Kombinat	Martite-ferromica jaspilite chart	4.22	6590/5280	6300/5700	5875/4720	16.37/10.51	0.27
	Quartz-mica shale	3.09	6000/3560	5900/3960	5450/3237	9.43/3.32	0.25
	Magnetic shale	3.28	5500/5000	5500/5050	4780/4350	8.92/7.34	0.30
	Hematite-martite shale	3.19	6250/5180	6000/5050	5570/4625	11.13/7.64	0.27
	Silicate-magnetite shale	3.29	5700/4970	5750/4900	5130/4475	9.71/7.28	0.26
	Quartz-micaceous shale with non-mined cl. rt intercalations	2.19	6890/4770	6330/5000	6310/4020	16.95/6.80	0.24
	Carbonate-magnetite chart	2.44	5760/4630	5020/4400	4740/4170	6.03/4.67	0.26
Balaklavskoye Mine Management	White marble-type limestone	2.71	5940	6300	5160	5.61	0.30
	Rose marble-type limestone	2.78	6750	6200	5875	7.06	0.30

TABLE 6 (Cont'd)

Sampling Site	Rock	Density of rock g/cm <sup>3</sup>	Velocity of longitudinal wave in block, m/sec		Velocity of longitudinal wave in rad, m/sec (ultrasonic method)	Elasticity Modulus kgf/cm <sup>2</sup> ·10 <sup>-5</sup>	Poisson Coefficient
			Ultrasonic Method	Explosive Method			
Dokuchayevskiy flux-dolomite Kombinat							
Dolomite Mine	Dolomite	2.66	5800/5360/5130			7.2	0.28
	Dolomite-type limestone	2.62	4800/5760/4210			4.88	0.29
	Dolomite	2.49	6120/5830/5415			8.0	0.28
Central	Blended gray limestone	2.50	5890/5800/5115			6.95	0.33
	Bituminous thin grained limestone	2.54	6200/6100/5440			8.04	0.29
	Medium-grained gray limestone	2.66	6180/6320/5475			8.12	0.30
Eastern Mine	Blended gray and bluish-gray limestone	2.66	6180/6200/5377			8.12	0.30
Eastern Dolomite Mine	Dolomite	2.70	5380/4800/4675			6.05	0.28
Modeling Material	Rosin	1.10	2200/2280/2150			0.52	0.14
	Hyposulphite	1.70	4070/4190/3750			2.78	0.24

Remarks. Numerator represents longitudinal wave velocity in parallel to stratification, and the denominator represents the velocity perpendicular to the stratification. In the case of one value, the data coincide.

The uniaxial compressive strength may serve as the characteristic strength of a rock. Tests on the uniaxial compression (Crushing) are the most widely used laboratory methods for the general evaluation of the strength properties of rocks. The strength criterion determined in these experiments is the temporary resistance to uniaxial compression  $[\sigma_R]$ , i.e., the maximum value of the compressing stress experienced by the rock at the moment of destruction of the sample. There exists a series of All-Union State Standards establishing requirements for samples intended for the determination of the tensile resistance to crushing. In the work of L. I. Baron (1962) it is noted that the shape, ratio of the sides, diameter of the base, and dimensions of the samples have a strong influence on the value of the tensile resistance to compression. The use of various elastic pads (gaskets) or greases in the testing of the samples reduces the value of the tensile resistance. In order to perform the tests on samples of rock and modelling materials one prepares tubes with edge dimensions of 50 and 65 mm, with six samples in each series of models. In the tests the force of crushing of the sample is determined, from which the strength of the material is found:

(260)

$$[\sigma_R] = \frac{F}{S},$$

where  $F$  is the force at which the sample is shattered and  $S$  is the cross-sectional area of the sample.

The main difficulty in carrying out large-scale tests for crushing is the preparation of regularly shaped samples. In this connection Professor M. N. Trotod'yakonov (the younger) and V. S. Voblikov at the A. A. Skochinskiy Institute for Geological Affairs have worked out a simple method for determining the tensile resistance to crushing in irregularly shaped samples, which is at the same time convenient for large-scale testing

of rocks. This method was also applied to the determination of  $[\sigma_R]$  of rocks. Its essence consists of the following. Irregularly shaped samples are selected for the tests, with the length of the edges not different from each other by more than a factor of 1.5. All of them have about the same volume (in the given experiments this was about  $100 \text{ cm}^3$ ). In the press the force  $F_H$  at which the sample is destroyed was established. The value of the stresses at which shattering of an irregularly shaped sample takes place is computed from the formula

$$[\sigma_R]' = F_H \left( \frac{\gamma_k}{P_a} \right)^{\frac{2}{3}}, \quad (261)$$

where  $[\sigma_R]'$  is the tensile resistance to crushing of irregularly shaped samples, in  $\text{kgf/cm}^2$ ;  $P_a$  is the weight of the sample, in g;  $\gamma_k$  is the apparent specific (volume) weight of the rock, in  $\text{g/cm}^3$ ;  $F_H$  is the force of crushing of irregularly shaped samples, in  $\text{kgf}$ .

For a series of rocks there exists the following relationship between the values of the tensile resistance to crushing of regularly and irregularly shaped samples

$$[\sigma_R]' = 0,19[\sigma_R]. \quad (262)$$

Making use of this relationship, one may easily pass over to the results which are obtained for the same rocks in tests of regularly shaped samples. Fifteen samples of each type of rock were subjected to testing. In the calculation the maximum value of the force at the point of shattering of each sample was used. For all tests of the rocks the average value of the shattering force was computed. From the known value of the tensile resistance to compression, the hardness coefficient of these rocks was calculated according to the scale of M. M. Protod'yakov,  $f = [\sigma_R]/100$ .

Tests were conducted for rocks from Krivoy Rog, Dokuchayevskiy flux-dolomite Kombinat and several quarries of construction materials. The results of the experiments are presented in Table 7.

Table 7

## The Hardness Characteristics of Rocks and Modelling Materials

Sampling Site	Rock	Bulk Density, g/cm <sup>3</sup>	Breaking Stress Under Compression, kgf/cm <sup>2</sup>	Tensile Stress According to M. M. Protod'yakov
New Krivoy Rog, Mining and Concentration Kombinat	Red-banded martite magnetite chart	4.60	1500	16
	Low-content carbonate-magnetite chart	4.12	1370	14
	Semi-oxidized martite-magnetite chart	5.22	1400	15
	Diotite-chloritic chart	2.95	795	8
	Non-oxidized martite magnetite chart	3.46	1690	17
Jaspilars Mining and Concentration Kombinat	Chloritic shale	3.23	1080	11
	Noncondensate chart	3.22	1470	15
	Semi-oxidized chart	3.59	1420	14
	Oxidized chart	4.70	1540	15
Central Mining and Concentration Kombinat	Silicate-magnetite chart	3.29	1620	10
	Magnetite chart	3.28	1490	15
	Dense hematite-martite chart	3.19	1420	14
	Carbonate-Magnetite chart	2.44	1040	10
	Extracted hematite-martite chart	2.44	1350	13-14
	Martite-ferromicaceous jaspilite chart	4.22	1590	16
	Quartz-micaceous shale with intercalations lacking chart	2.19	1041	10
Central Mining and Concentration Kombinat	Quartz-micaceous shale	3.09	750	8
	Balaklava			

Reproduced from  
best available copy.



Table 7 (cont.)

Sampling Site	Rock	Bulk Density, g/cm <sup>3</sup>	Breaking Stress Under Compression kgf/cm <sup>2</sup>	Tensile Stress According to M. M. Protod'yakov
Western Kadykov Mine	White marble-like limestone	2.71.	680	7
" "	Rose marble-like limestone	2.78	954	9-10
Osilerakh Mine	Rose marble-like limestone	2.51	765	8
	Vinnits Region			
Samchin Quarry	Fine-grained gray granite	2.74	720	7
Onivan'skiy Quarry	Coarse-grained gray granite	2.57	1050	11
	Donets Basin			
Dokuchayev Flux-Dolomite Kombinat				
Eastern Dolomite Mine	Dolomite	2.70	1170	12
Dolomite Mine	"	2.49	835	8
	"	2.66	1055	11
Dolomite Mine	Dolomized limestone	2.62	1055	10-11
Central Mine	Fine small-grained bituminous limestone	2.11	956	10
	Middle-grained limestone	2.66	1088	11
	Middle-grained and blended limestone	2.50	1011	10
Eastern Mine	Blended gray and bluish-gray limestone	2.66	1075	11
Modelling Materials	Rosin	1.10	15 27	
	Hyposulphite	1.70	39 59 82	

## Characteristics of Explosive Loading

The way in which the charge of explosive material performs in the medium depends on the pressure pulse in the charge chamber. The pressure impulse is characterized by a function of the change of pressure in time  $p(t)$ , and its magnitude is determined by the formula

$$I = \int_0^{\tau} p(t) dt, \quad (263)$$

where  $p(t)$  is the change in pressure on the charge plane and  $\tau$  is the time over which the excess pressure acts on the wall of the charge cavity.

The maximum pressure of the gaseous detonation products is determined as

$$p_{\max} = \rho_{\text{ex}} D v_{\max}^2, \quad (264)$$

where  $\rho_{\text{ex}}$  is the density of the charge of explosive material;  $D$  is the velocity of detonation;  $v_{\max}$  is the maximum (initial) velocity of motion of particles at the front of the forming shock wave. For an ideally detonating explosive charge

$$v_{\max} = \frac{D}{k_i + 1}, \quad (265)$$

where  $k_i$  is the index of isentropic expansion of detonation products.

From equation (264) and (265) for high explosives ( $k_i=3$ ) it is readily found that

$$p = \frac{1}{4} \rho_{\text{ex}} D^2. \quad (266)$$

The mean pressure of detonation products in the charge chamber is equal to half of the pressure at the front of the detonation wave

$$p = \frac{1}{2} \rho_{ex} D^2. \quad (267)$$

Expression (266) may give unsatisfactory results if the velocity of detonation is smaller than the steady-state velocity for a given explosive material, a circumstance which occurs in actual bore-hole charges of industrial explosive materials when inert impurities are present in them. In this case it pays to resort to a more rigorous analytical calculation or to an experimental determination of the detonation pressure.

In order to determine the parameters of waves arriving at a discontinuity of the medium, one uses the dependences between the characteristics of the detonation and shock waves in the medium adjacent to the detonating explosive material. The pressure at the front of the shock wave in the medium is determined by the dependence

$$p_{sh} = \rho_m D_v v, \quad (268)$$

where  $p_{sh}$  is the pressure at the shock wave front;  $\rho_m$  is the density of the medium;  $D_v$  is the velocity of the shock wave;  $v$  is the velocity of motion of particles at the shock wave front.

The coefficients  $\rho_{ex} D$  in equation (264) and  $\rho_m D_v$  in equation (268) denote the ratio between the jump in pressure and the sudden change in bulk velocity at the shock wave front and have the dimensions of impedance.

In the case of normal incidence of the detonation wave at the charge-medium interface, the relationship connecting the pressure in the medium with the detonation pressure is determined by a ratio of impedances

(269)

$$P_{sh} = p \frac{2}{1 + \frac{\rho_{ex} D}{\rho_m D_v}}$$

The parameters of shock waves arising through an explosion in several materials are presented in Table 8. In a more precise form the dependence (269) has the form (Atchison et al., 1962; Nichols, Duval, 1966)

(270)

$$P_{sh} = p \frac{1 + N}{1 + N \frac{\rho_{ex} D}{\rho_m D_v}}$$

Here

(271)

$$N = \frac{\rho_1 (v + w)}{\rho_{ex} \cdot D}$$

where  $\rho_1$  is the density of detonation products, and  $w$  is the velocity of sound in the detonation products. Expression (271) represents the ratio of the impedance of explosion products to the impedance of the explosive material. The value of  $N$  may be determined with the aid of a graph (Fig. 61) with  $Z = (\rho_{ex} D) / (\rho_m D_v)$  varying within the range from 0.4 to 1.

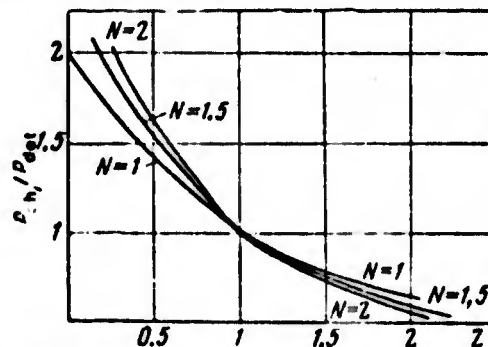


Fig. 61. The dependence of the ratio of pressure on the ratio of acoustic stiffnesses for various values of  $N$ .

The value of  $N$  differs very little from unity. The ratio of impedances can in fact be determined in this manner only where the detonation wave moves perpendicularly to the boundary line (normal incidence). Under actual conditions the detonation wave moves in the charge parallel to the wall of the charge chamber. In this case one should take into account, along with the value of  $N$ , the angles of the incident, the reflected, and the refracted waves. A study of the laws of propagation of shock waves in solid and liquid media presents a very complex problem. Therefore, experimental methods for investigating the behavior of rocks under the action of intense shock waves takes on a special role. The main characteristic feature distinguishing the condensate state from the gaseous state and determining the behavior of solid and liquid bodies under compression by shock waves is the strong interaction of atoms (or molecules) with each other. The radius within which interatomic forces can act is quite limited. It is of the order of the dimensions of the atoms and molecules themselves. The interaction forces have a dual character. On the one hand the atoms attract one another, but on the other hand with closer approach the atoms repel one another as a result of the interpenetration of each other's electronic shell. With strong compression of the condensate material a huge internal pressure builds up inside it, even in the absence of heating, only because of the repulsive forces of the atoms. The existence of this pressure of non-thermal origin determines the basic features of the behavior of solid and liquid bodies under compression by shock waves. In shock waves of very large amplitude a vigorous heating of the material occurs, leading to the appearance of a pressure connected with thermal motion of the atoms (and electrons), which is called "thermal" in distinction to the elastic or "cold" pressure, caused by the forces of repulsion. In strong shock waves (with pressures higher than a million atmospheres) pressures of both types are comparable with each other. In less powerful waves,

with a pressure on the order of hundreds of thousands of atmospheres and lower, elastic pressure predominates. A shock wave with a similar jump in pressure at the front is "weak" and differs little from an acoustic wave: it propagates with a velocity close to the speed of sound, the density of material at the wave front increases by no more than 10%, and the velocity behind the front is 10 times smaller than the velocity of wave propagation (Zel'dovich, 1966).

Table 8

Shock Wave Parameters at the Charge-Medium Interface with Normal Incidence (Explosives - Tetryl:  $\rho_{ex} = 1.665 \text{ g/cm}^3$ )

Medium	$D$ , m/sec	$p$ kbar	$D_v$ , m/sec	$v_m$ , m/sec	$p_c$ , kbar	$p_c/p_D$	$c_m$ , g/cm <sup>3</sup>	$Z = \frac{c_{ex} D}{c_m D_v}$
Plexiglass	6772	200.29	5510	1947	126.59	0.632	1.18	1.734
	6771	196.70	5612	2035	119.91	0.615	1.18	1.678
	6598	181.91	5109	1879	119.91	0.618	1.18	1.698
	6648	192.98	5598	2005	132.45	0.687	1.18	1.676
Aluminum	6711	196.7	7067	1281	252.31	1.283	2.787	0.567
	6546	187.11	7279	1140	292.13	1.560	2.787	0.537
	6565	188.28	6955	1198	232.22	1.233	2.787	0.564
	6516	187.11	6696	1005	187.55	1.002	2.787	0.584
Copper	6565	188.28	4978	679	297.11	1.580	8.80	0.250
	6648	192.98	5086	751	336.13	1.742	8.80	0.217
	6516	187.11	5115	790	357.68	1.911	8.80	0.211

Remarks. The detonation pressure is calculated from the formula  $p_D + 4.157D^2\rho_{ex}(1 + 0.543\rho_{ex} + 0.193\rho_{ex}^2) \cdot 10^{-6}$  ( $p_D$  - in kbar;  $D$  in m/sec;  $\rho_{ex}$  - in g/cm<sup>3</sup>).  $D$  is the detonation velocity;  $p$  is the pressure at the detonation wave front;  $D_v$  is the shock wave velocity;  $v_m$  is

the bulk velocity of particles of the medium;  $p_c$  is the pressure at the shock wave front;  $z$  is the ratio of acoustic stiffnesses of the explosive material and the medium.

The elastic components  $p_x$  and  $E_x$  depend only on the density of the material  $\rho$  or the specific volume  $V_y = 1/\rho$  and are equal to the total pressure and the specific internal energy at absolute zero temperature (these are sometimes called "cold" pressure and energy). In considering the behavior of a solid substance undergoing a change in volume, we will have in mind cubic compression (and expansion) of the body, while paying no attention to effects connected with the anisotropy of the elastic properties, shear deformation, strength properties, etc., which appear at comparatively small pressure. The elastic pressure is related to the potential energy by the relationship

$$p_x = \frac{dE_x}{dV_y}, \quad (272)$$

which has a natural mechanical sense (the increase in energy is equal to the work of compression) and may be considered as the equation of an isotherm or adiabatic curve of cold compression. The curve  $p_x(V_y)$  is shown schematically in Fig. 62. At the point  $V_y=V_0$  the elastic pressure is equal to zero, with compression of the body the pressure rises rapidly, and with elongation it becomes negative. The negative side of the pressure corresponds to the physical fact that for expansion of a body from zero volume, corresponding to a mechanical equilibrium at  $T=0$ ,  $p=0$ , a tensile force must be applied to the body. Theoretical calculations of the cold compression curves  $p_x(V_y)$  or  $E_x(V_y)$  in practically attainable ranges of compression and pressure are based on a quantum mechanical consideration of interatomic interaction. In a number of cases satisfactory agreement is obtained with experimental data on compressibility (Gombash, 1951).

The laws of conservation of mass, momentum, and energy fluxes at the shock wave front have their usual meaning, irrespective of the aggregate state of the material through which the wave is propagated. Dropping the index for quantities characterizing the state of the material behind the wave front, let us write down the laws of conservation of mass and momentum in the form

$$\frac{v_y}{V_{0y}} = \frac{D}{(D-v)}, \quad (273)$$

$$p = \frac{Dv}{V_{0y}}. \quad (274)$$

Eliminating  $v$  from (273) and (274), we obtain

$$p = \frac{D^2}{V_{0y}} \left(1 - \frac{v_y}{V_{0y}}\right). \quad (275)$$

To serve as the third, energetic, relation let us take the equation of the adiabatic curve with  $p_0=0$

$$E - E_0 = \frac{1}{2} p (V_{0y} - V_y), \quad (276)$$

The total energy acquired by one g of material as a result of shock compression, equal to  $p(V_{0y} - V_y)$ , is distributed equally between the kinetic  $v^2/2$  and internal  $E-E_0$  energies (in a system of coordinates where undisturbed matter is at rest). The change in internal energy is the sum of the changes in elastic energy and thermal energy. In Fig. 63 the adiabatic curve of cold compression  $p_x(V_y)$  is shown as well as the Hugoniot curve  $p_H(V_y)$  which is located above the former since the full pressure behind the front is the sum of the elastic and the thermal pressure. The elastic energy  $E_x$  acquired by the matter is numerically equal to the area of the curvilinear triangle OBC, cross-hatched with horizontal lines ( $E_x = \int_{V_y}^{V_{0y}} p_x dV_y$ ).

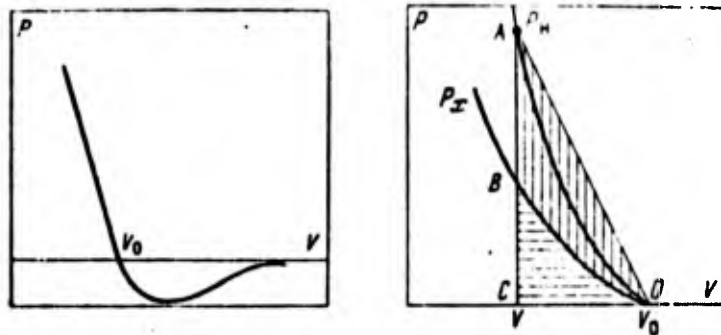


Fig. 62. Curve of the elastic pressure as a function of specific volume.

Fig. 63. Cold compression adiabatic and Hugoniot curves  $P, V$  - graph for shock compression and cold compression of the material;  $P_H$  - Hugoniot curve;  $P_x$  - curve of cold compression.

The total internal energy  $E$ , in accordance with equation (276) is equal to the area of the triangle  $OAC$ ; the difference of the areas hatched with vertical lines also constitutes the thermal energy of the matter which is subjected to shock compression.

The laws of conservation of mass and momentum (273) and (274) provide a connection between four parameters at the shock wave front: the propagation velocity of the shock wave through undisturbed matter  $D$ , the sudden change in the bulk velocity  $v$ , equal to the velocity of motion of the compressed matter with respect to the undisturbed matter, the pressure  $p$ , and the specific volume  $V_y$  (or the density  $\rho = 1/V_y$ ). Thus the problem of finding all mechanical parameters of the shock wave front is reduced to an experimental determination of any two of them, in particular, the kinematic parameters which are the most accessible for measurements - the velocity  $D$  and  $v$ .

The Effect of Stress Waves in Gaseous Detonation Products on the Process of Rock Shattering.

The shock wave in dying out degenerates into an elastoplastic stress wave and this in turn is transformed into an elastic wave of seismic oscillations. In conformity with the nature of these waves we divide the zones of explosion action in the medium into a near zone (buckling zone), a central zone (radial crack zone), and a far zone (elastic oscillation zone).

In the near zone the medium is repulverized and recompact. Some investigators believe that the medium behaves in this zone not as solid state but as liquid. In this connection allusion is usually made to the fact that the pressure in the shock wave is

many times greater than the strength of the rock. Attempts to describe theoretically the processes, taking place in the buckling zone have met with no particular success owing to the absence of a sufficient volume of experimental data on the behavior of the material.

In his consideration of the action of stress waves in rocks, Reinhart (1966) notes that one must keep in mind the difference of motions in the spherical, cylindrical, and plane symmetry cases: for instance, when no damping is present the shape of the plane component does not change, but the shape of the other components do vary. In Fig. 64 the shapes of two cylindrically diverging waves as calculated by Sel'berg are shown; one of these is described at the initial moment as a step function, and the other by an exponential function. The shape of the waves become indistinguishable after a dislocation at some distance from the charge, in the given case equal to 10 times the radius of the bore-hole. The consequence of this initial shape of the stress wave has relatively little significance. Rodionov (1969) also makes note of the fact that the dissipation of energy in the near zone leads to a "forgetting" of the initial conditions by the developing process, a situation which is reflected in the law of energetic similitude, in accordance with which the parameters of the shock waves arising in the explosion are determined only by the total separated energy and do not depend on the density of the explosive material, the detonation velocity, or anything else.

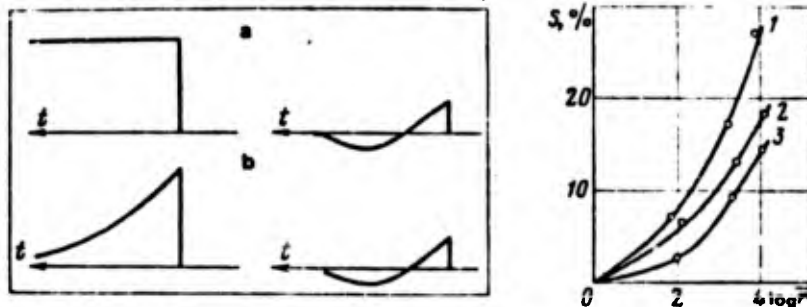


Fig. 64. Nature of the change in radial stress in a diverging cylindrical wave, described by a step function (a) and by an exponential function (b)

Fig. 65. Plot of the change in relative energy content as a function of distance for argillaceous aleurite (1), limestone (2), and marble (3)

In the work of Ye. G. Baranov and V. Ya. Klapovskiy (1969) the dependence of the change in relative integrated energy loss of the wave, on distance and on the physical and mechanical properties of the rock was established experimentally. It was shown that for a constant weight of charge of the same explosive material the maximum values of energy in the wave are observed for argillaceous aleurite, after that for limestone, and finally the least for marble. The largest values of energy correspond with the highest particle velocities behind the front, and the time of existence of positive wave phase and deformation (Table 9). From the plots of  $S_{11} = f[\lg(r)]$ , presented, it follows that for explosive loading the largest relative integral energy losses are observed for argillaceous aleurite and the least for marble (Fig. 65). Analogous regularities were obtained as a result of experimental investigations carried out in the explosive mechanics department of the Institute for Geotechnical Mechanics of the Ukrainian SSR Academy of Sciences. Besides, it was shown that in the same material damping of the shock wave created by various types of explosives does not proceed uniformly and depends on both the value of the stresses and on the duration of the detonation impulse (Table 10). The most representative example of this observation is the damping of a shock wave arising from the explosion of a charge of lead azide. The value of the maximum translation velocity at the charge - medium contact amounts to 1350 m/sec, at a distance of 5 mm it diminishes to 635 m/sec, and at a distance of 10 mm it has diminished to 135 m/sec. This can be explained by saying that the pulse duration is small by virtue of the small specific energy of the lead azide for high peak pressures. Naturally, in the near zone for large expenditures of energy on the repulvarization of the material the value of stresses in the shock wave falls more drastically. As the stress wave passes through the medium a large number of cracks appear, and their further growth is prolonged on account of the piston action of the gases (Demidyuk, 1968). The role of the piston action of the explosion may be fairly closely estimated on the basis of experimental data obtained in an underwater explosion.

The energy of the shock wave in water, which is analogous to the shock wave energy in solid bodies, and the pulsation energy of a gas bubble, which is analogous to the energy of heaving and displacement of the medium in an explosion in rocks, together comprise the largest part of the energy of the explosion. Comparison of the total of these works with the theoretical total satisfactorily characterizes the transmission of explosive energy into the surrounding medium. Up to 50% of the energy of the explosive material is dissipated in the piston action, whereas only 15% of the energy is transferred into the shock wave or the stress wave (Sedvin, 1962). In an explosion in rocks the piston action of the detonation products is difficult to estimate, since no pulsations similar to the pulsations of a gas bubble in an underwater explosion, having any kind of a measurable amplitude, were noted. Following from laboratory investigations of the process of destruction and displacement of a model under the action of an explosion - using the high speed motion picture method - it was established that the detonation products of the charge not only produced a displacement of the fragmented mass, but also take part directly in the process of crack formation. The gaseous detonation products, penetrating into the cracks, facilitate the growth of the latter because of the wedging action. In Fig. 66 motion picture frames are shown which describe the process of shattering of a cylindrical model made of plexiglass of diameter 140 mm and height 200 mm with a TETN charge of weight 2 g. The initial velocity of the inrush of gases through the cracks amounts to 600-700 m/sec, which serves as an indirect confirmation of the high pressure of gases penetrating into the forming cracks.

It is necessary to separate out the following factors from all of those influencing the nature of the pressure change in the charge cavity: the type of explosive; the design, size, and

length of the charge; the quality of the stemming.

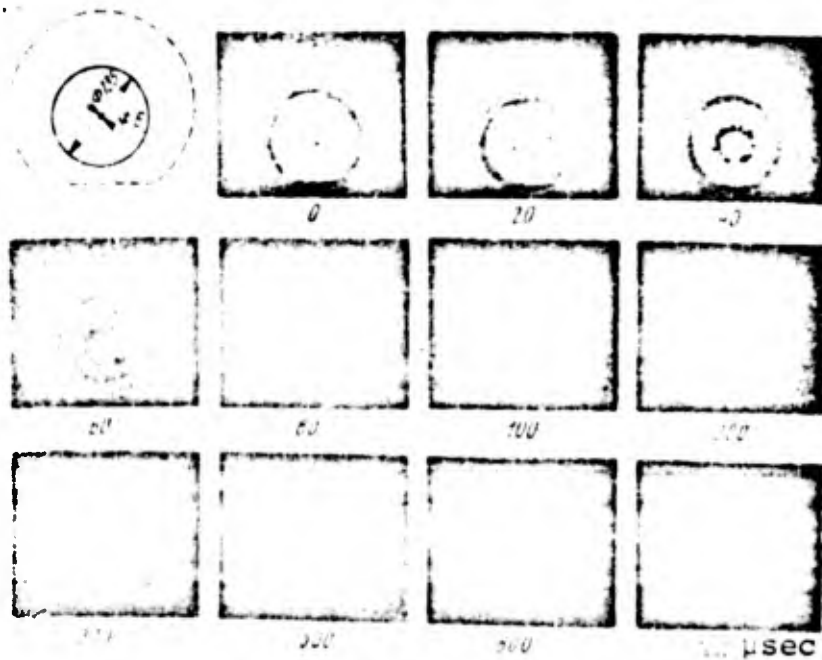


Fig. 66. Motion Picture Frames of the Destruction of a Model Made of Plexiglass

Table 9. Experimental Parameters for Plane Shock Waves.

Relative distance, r	Velocity v of particles behind the shock wave, km/sec	Velocity D <sub>v</sub> of shock wave, km/sec	Pressure at wave front p·10 <sup>-3</sup> , kgf/cm <sup>2</sup>	Period of existence of wave t, μsec	Density of material at wave front, g/cm <sup>3</sup>	Compressibility, p/p <sub>0</sub>	Energy at wave front, E·10 <sup>-6</sup> , kg-m/m <sup>2</sup>	Current value of wave energy E·10 <sup>-6</sup> , kg-m/m <sup>2</sup>	Relative integral energy loss S <sub>11</sub> of wave
<b>Argillaceous aleurite</b>									
1,00	1,507	3,262	88,7	18,36	3,29	1,85	25,55	25,55	0
1,97	1,430	3,107	79,6	19,27	3,25	1,84	25,55	22,67	0,113
3,01	1,292	2,772	61,6	21,60	3,18	1,79	25,55	17,07	0,332
5,02	0,791	1,986	29,3	30,16	2,94	1,66	25,55	12,02	0,529
<b>Limestone</b>									
1,00	1,182	3,954	114,4	10,53	3,42	1,42	14,85	14,85	0
2,03	1,109	3,792	102,9	11,01	3,39	1,41	14,85	13,07	0,119
3,00	1,035	3,628	91,9	11,50	3,35	1,39	14,85	11,38	0,231
4,25	0,910	3,418	78,6	12,21	3,31	1,37	14,85	9,39	0,368
<b>Marble</b>									
1,00	1,023	5,400	152,1	6,75	3,31	1,21	10,92	10,92	0
1,98	0,999	5,388	148,2	6,77	3,31	1,22	10,92	10,43	0,045
2,98	0,930	5,250	134,4	6,95	3,28	1,21	10,92	9,04	0,172
4,00	0,873	5,115	123,4	7,11	3,25	1,20	10,92	7,97	0,270

Table 10. Shock Wave Parameters in Rosin Rods.

Type of explosive charge	Density of charge, g/cm <sup>3</sup>	Velocity of detonation, m/sec	Maximal displacement velocity in shock wave, m/sec						
			In charge	At charged medium contact	r = 5 mm	r = 10 mm	r = 15 mm	r = 20 mm	r = 25 mm
TETN	0,80	4500	1050	845	482	321	292,0	182,0	101,0
	1,00	5200	1270	1270	507	370	340,0	237,0	—
Lead azide	1,67	5200	—	1350	635	135	84,5	46,5	33,8
	1,00	4200	—	—	170	101	—	33,8	25,2
Tetryl	0,80	4400	530	420	210	147	91,0	52,5	31,5
Phlegmatizer hexogen	1,00	350	845	510	203	152	—	48,5	—
	0,80	2500	530	340	127	—	50,0	30,0	25,0

The characteristics of the detonation process that depend on the type of explosive material determine the value of the maximum pressure and the rate of its accretion. The rate of loading depends on the detonation velocity and on the state of dispersion of the explosive material. Thinly dispersed explosives are characterized by a narrow zone of chemical reaction and rapid growth of pressure. Granulated explosives have a more even pressure buildup. From the point of view of the wave theory of damage, it is necessary to utilize an explosive material with a high density and detonation velocity in order to assume the maximum transmission of explosive energy to a rock with high acoustic stiffness. However, increasing the potency of an explosive material is accompanied by a disproportionate rise in its cost. Therefore, in using an explosive material with a low detonation velocity one should strive to increase the share of the action attributed to the gas piston effect in the process of shattering (Demidyuk, 1968).

On the basis of a large volume of experimental work by Academician N. V. Mel'nikov and Dr. of Engineering Science L. N. Marchenko (1960; 1963), the theoretical bases were worked out for choosing the most appropriate design for the core charge and for choosing a method of calculating the air gap parameters when using core and concentrated charges under various geological and mining conditions for the working of mine and non-mine deposits. The essence of this method consists of the creation of air gaps along the length of the core charge, a procedure which leads to a lowering of the maximum pressure in the charge chamber and a raising of the profitable use of energy of the explosion. For a continuous construction of a core charge the pressure depends only on the type of explosive material. For the charge construction with air gaps the pressure at the first moment after detonation is distributed nonuniformly along the length of the bore-hole. Afterwards it equalizes somewhat and then its maximum value is determined not only by the type of explosive but also by the ratio of the volumes of explosive material and the air gaps. For this case the effect of the explosion products on the medium subject to explosion is increased, and this promotes a more effective shattering of the medium.

The stemming, weight, and length of the core charge has no effect on the value of maximum pressure in the charge chamber, but to a significant degree it influences the time over which the detonation products act on the bore-hole walls. The stemming plays a substantial role in the blasting of monolithic rocks, since in this case there takes place mainly a leakage of gases through the stemming. In heavily cracked or crumbling rock the stemming has less of an effect on the parameters of the pressure impulse because of a rather significant leakage of gases through the cracks in the walls of the bore-hole.

The weight of the charge in the bore-hole is determined by the length of the core of explosive material and by the diameter, and this situation influences the duration of the emission process

and the time characteristics of the explosive impulse. Increasing the length of the charge core for constant charge diameter leads to a lengthening of the time of explosive action.

By using a charge design with air gaps, an explosive material with progressively increasing pressure, a method of intra-bore-hole retardation, and an explosion in a compressed medium, it becomes possible to enhance the role of the piston action of gases in the process of shattering mineable rocks and to raise the efficiency of using the explosive energy.

#### Energetic Characteristics of the Shattering Process in Impact and in Explosion.

One of the factors which conditions the process of shattering is the energy transmitted to the medium being damaged. The fragmenting of solid bodies must naturally depend on some energetic characteristics, among which are the specific energy content of the shattering for impulsive loads and the efficiency of use of the explosive energy. By specific energy content of shattering we need the work expended in forming a unit of new surface

$$q_y = \frac{A}{S_H}, \quad (277)$$

where  $q_y$  is the specific energy content of shattering;  $A$  is the work expended in crushing;  $S_H$  is the area of newly formed surface.

In determining  $q_y$  the dimensions of the samples and the nature of the load must be chosen in such a way that the effect of random factors is reduced to a minimum.

However, the specific energy content of shattering cannot be fully characterized by the crushability of the rock. A different fraction of the explosive energy is transmitted to the medium depending on the physical and mechanical properties of the rock,

and therefore for the same specific energy content of shattering a different quality of crushing will be obtained. Energy losses may be characterized by the efficiency of use of explosive energy, i.e., by the ratio of the energy going into the fragmentation to the total energy of the explosive material. The efficiency of use of explosive energy depends on many factors: the physical and mechanical properties (elastic constant of the medium, value of the shattering stresses, number of zones of reduced strength, and velocity of crack development), the type of explosive material, the density of charging, etc., a situation which makes theoretical determination of the efficiency very difficult. Tentative experimental values of the efficiency of use of explosive energy may be determined as the ratio of specific energy content of shattering of a given rock to the value of the energy content of shattering in an explosion for definite conditions and parameters of the explosive operations. The latter quantity is the quantity of energy of the explosive material, related to a unit of newly formed surface

$$q_e = \frac{E_{ex}}{S_H}, \quad (278)$$

where  $q_e$  is the energy content of shattering in the explosion;  $E_{ex}$  is the energy escaping in detonation of the explosive;  $S_H$  is the quantity of newly formed surface. Then the efficiency of use of explosive energy is expressed as

$$\eta = \frac{q_y}{q_e} 100\%. \quad (279)$$

The quantity of specific energy content of shattering was determined by the method of L. I. Baron (1962). For this purpose

10 samples were gathered for each rock, each sample being in shape close to a cube and having the same weight, approximately equal to 50 g. The samples were shattered using a falling weight on the usual impact testing machine. The mass of deformed weight was 21.4kg, and the height of the fall was 0.934m. The work expended in shattering the sample amounted to 20 kg-m. The particle-size composition of the shattered sample was determined by the sieve analysis method. The disintegrated material of the samples was sifted through #10, 7, 5, 3, 2 and 1 screens and each fraction was weighed. The amount of total newly formed surface was computed from the formula

$$S_n = \frac{6}{\gamma} \sum_{i=1}^m \frac{Q_i}{d_i} - S_0, \quad (280)$$

where  $m$  is the number of fractions;  $Q_i$  is the average linear dimension of pieces of a given fraction;  $\gamma$  is the specific gravity of the rock under study;  $S_0$  is the initial surface of the sample.

In this manner the quantities entering into expression (280) have been determined and the quantity of specific energy content of shattering has been calculated for each type of rock (Table 11). A determination of the energy content of shattering in an explosion was carried out for each definite case. For this purpose the energy of the explosive material and the area of newly formed surface was calculated. The value of  $q_e$  was computed from formula (278). From the known values of the energy content upon impact and upon explosion, the efficiency of use of explosive energy was determined (see Table 11). An analysis of the experimental data obtained shows that for the majority of rocks the efficiency of use of explosive energy varies within the limits 10-20%. This efficiency has a tendency to increase for monolithic homogeneous rocks. The experimental investigations which were performed make it possible to determine the parameters of the shattering process and to utilize them in modelling the effect of explosions.

Table 11

## Energetic Characteristics of the Shattering of Rocks and of Modelling Materials.

Sampling Site	Rock	Specific energy content of shattering kgf/cm <sup>2</sup>	energy content in explosion kgf/cm <sup>2</sup>	Efficiency of use of explosive energy %
Dokuchayev Flux-Dolomite Kombinat				
Dolomite mine	Dolomite	0.043	0.212	20.0
	Dolomized limestone	0.055	0.250	14.0
Eastern Dolomite Mine	Dolomite	0.049	0.254	19.3
Central Mine	Bituminous fine-grained limestone	0.042	0.201	20.8
	Middle-grained limestone	0.044	0.260	17.0
	Blended limestone	0.039	0.298	13.1
Eastern Mine	Blended gray limestone	0.044	0.272	16.2
Palaklava				
Western Kadkov Mine	Dokuchayev Flux dolomite Kombinat	0.038	0.345	11.1
	Rose marble-like limestone	0.046	0.276	16.6
Psilerakh Mine	Dokuchayev flux-dolomite Kombinat	0.0374	0.325	11.5
Vinnits Region				
Sapchin Quarry	Coarse-grained granite	0.037	0.400	9.3
Gnivan'skiy Quarry	Fine-grained granite	0.045	0.33	13.6

Table 11 (cont.)

Sampling Site	Rock	Specific energy content or shattering, kg/cm <sup>2</sup>	Energy content in explosion kg/cm <sup>2</sup>	Efficiency of use of explosive energy %
Krivoy Rog				
New Krivoy Rog Mining and Concentration Kombinat	Bed-banded martite magnetite chart	0.091	0.880	10.3
	Low-content carbonate-magnetite chart	0.074	0.750	10.0
	Martite-magnetite chart	0.063	0.610	12.2
	Biotite-chloritic chart	0.059	0.500	11.7
Central Mining and Concentration Kombinat	Silicate-magnetite chart	0.043	0.410	10.4
	Magnetite chart	0.048	0.410	11.6
	Hematite-martite chart	0.047	0.410	11.3
	Carbonate-magnetite chart	0.039	0.230	16.9
	Martite-ferromagnetic jaspilite chart	0.110	0.630	17.5
	Quartz-micaceous shale	0.054	0.385	14.0
	Chloritic shale	0.064	0.378	17.0
Ingulets Mining and Concentration Kombinat	Oxidized hematite chart	0.102	0.430	23.0
Kolomoyskiy Quarry	Granite	0.042	0.240	17.5
	Diabase	0.065	0.296	21.8
Artemovsk				
Artemsol' Kombinat	Rock Salt	0.005	0.018	29.6
Modeling Materials	Kosin	0.005		
	Hyposulphite	0.010		

Reproduced from best available copy.

## Chapter Six

### EXPERIMENTAL INVESTIGATIONS OF THE SHATTERING PROCESS IN MODELS AND IN NATURE

#### Modelling the Shattering Process with Models of Various Materials

Experimental confirmation of the applicability and reliability of similitude criteria obtained on the basis of the statistical theory of damage were carried out under laboratory and industrial conditions. The laboratory experiment has the advantage that it allows one to reduce the affect of random factors, to determine with high accuracy the properties of the materials and to construct explosive loading parameters for computation purposes. From the criteria obtained on the basis of the statistical theory of damage, it follows that similar fragmentation may be attained by two means: (1) by choice of a model material with corresponding physical and mechanical properties for given impulse parameters in nature and in the model, i.e., by choosing corresponding strength properties and velocity of crack development; (2) by creating the corresponding stress pulse in the model for specified physical and mechanical properties of the materials of nature and of the model and for specified stress pulse parameters in nature. Besides these similitude criteria, in order to compute the scales of the models one uses the similarity of elastic wave motions, in order to indicate the common features and peculiarities of the various methods of modelling.

To serve as the modelling materials rosin and hyposulphite were chosen. The explanation of the choice of these materials is that they are uniform with respect to structure, they undergo brittle shattering under impulsive loads, and models may be easily

prepared from them since they possess a low temperature of melting. The technology of preparing models from rosin and hyposulphite specifies heating of the material to the melting temperature (for rosin to  $110^{\circ}\text{C}$ , for hyposulphite to  $60^{\circ}\text{C}$ ). The pasty mass is poured into metal dismountable forms, to which sensors and a paper tube for placement of the explosive charge are attached. The models were prepared in the form of cubes with dimensions  $200 \times 200 \times 200$  mm and  $300 \times 300 \times 300$  mm. The depth of the blast-hole which was used was equal to half the height of the block, the diameter of the blast-holes was 8 mm for the smaller cubes and 12 mm for the larger cubes. In order to measure the stress, piezoelectric sensors are used, which are placed at various distances from the center of the blast-hole at the depth of placement of the explosive charge, with the working surface toward the charge. The methods for making the measurement and the formulas for calculating the stresses when using piezoelectric sensors were presented in Chapter four. From the oscilloscope traces obtained stress-time plots for various relative distances were constructed. The reflected wave is not recorded by the sensors, inasmuch as the tensile strength at the point of sensor-medium contact is vanishingly small. In the given case, in order to model the crushing process it is sufficient to follow the shape of the forward-travelling wave, and the parameters of the reflected wave automatically satisfy the similitude condition, owing to similarity of the form of the models. Together with the measurement of stresses one determines the particle-size composition of the exploded blocks using the sieve analysis method. In pieces with the largest edge greater than 30 mm three linear dimensions are measured and the surface is computed as the surface of a parallelepiped. For pieces with linear dimensions smaller than 30 mm the following fractions are separated: 30-20; 20-10; 10-7; 7-5; 5-3; 3-1 mm; less than 1.0 mm. The amount of newly formed surface is

determined by formula (280). In finding the size of an average fragment  $d_{av}$  one uses the technique of L. I. Baron (1960):

$$d_{av} = \frac{\sum_{i=1}^n d_i w_i}{\sum_{i=1}^n w_i} \quad (281)$$

where  $d_i$  is the average dimension of the  $i$ -th piece or the  $i$ -th fraction in cm;  $w_i$  is the weight fraction of the  $i$ -th fraction or the  $i$ -th piece, in per cent.

Variation of the explosive impulse parameters is accomplished by changing the various constructions of the charge, the types of explosive material (PETN, tetryl) and the value of the specific consumption of explosive material.

Let us take a look at the technique and the results of modelling by means of a choice of corresponding material of the model. To serve as the starting data we take the characteristics of the material of nature, the geometric scale, and the change in value of maximum stresses with distance for the materials of the model and of nature. It is necessary to determine for which properties of the model material similitude of the particle-size composition of the disintegrated mass can be guaranteed. In the example under consideration we use  $\lambda_1 = 1.5$  and we take rosin for the material of nature. The characteristics of the material of nature (rosin block 3) and of the charge are presented in Table 12. From the data of the experimental tests a plot of  $\sigma_{max} = f(r)$  is constructed (Fig. 67, curve 1). Let us find what conditions must be satisfied by the model material in order that the particle-size composition of this material after the explosion be similar to the particle-size composition of the material of nature for a given change in maximum stresses with distance (see Fig. 67, curve 2). From the similitude condition of the shattering zone the strength characteristics of the model material are determined. In nature the value of the maximum stresses at a distance of  $70\bar{r}_{OM}$  is equal to

the strength of the material. Consequently, in order to obtain similar dimensions for the shattering zone, it is necessary to choose a model material such that its strength be equal to the value of maximum stresses at a distance of  $70\bar{r}_{OM}$ . From the plot (see Fig. 67, curve 2) it follows that the strength of the model material must be equal to  $\sigma_{\max}/r = 70 = [\sigma_R]_M = 35 \text{ kgf/cm}^2$ . By fulfilling this condition it is possible to obtain a similar dimension for the shattering zone in the model. In order to obtain a similar particle-size composition for the disintegrated material it is necessary that for any relative distance the number of crack-formation centers in a unit of relative volume be the same, i.e.,

$$n_{0M}^* = n_{0N}^* \quad (282)$$

Table 12

Characteristics of Model Materials and Charges\*

Number of blocks	Material	Dimensions of the lumps, mm	Density of the material, g/cm <sup>3</sup>	Velocity of sound, m/sec	Shattering stresses for compression, kgf/cm	Specific consumption of explosive material, mg/kg
3	Rosin	300 × 300 × 300	1.1	2100	20	56
9	Hyposulfite	200 × 200 × 200	1.7	3000	35	180**
8	Rosin	200 × 200 × 200	1.1	2120	27	80
38	Hyposulfite	200 × 200 × 200	1.7	4050	45	250

\* In the experiment TETN was used for the explosive

\*\* The charge was in an air gap

Condition (282) is a direct consequence of (210), except that the number of crack formation centers is related to a unit of relative volume instead of absolute volume. The function  $n_{ON}^* = f(\sigma_{\max N}/[\sigma_R]_N)$  was established by experimental means (see Fig. 68, curve 1), using the approach laid out in the fourth chapter. For a distance of  $r = 5$ :

in nature  $\frac{\sigma_{\max N}}{[\sigma_R]_N} = \frac{8000}{20} = 40, \quad n_0^* = 130;$

in the model  $\frac{\sigma_{\max M}}{[\sigma_R]_M} = \frac{1800}{35} = 51.$

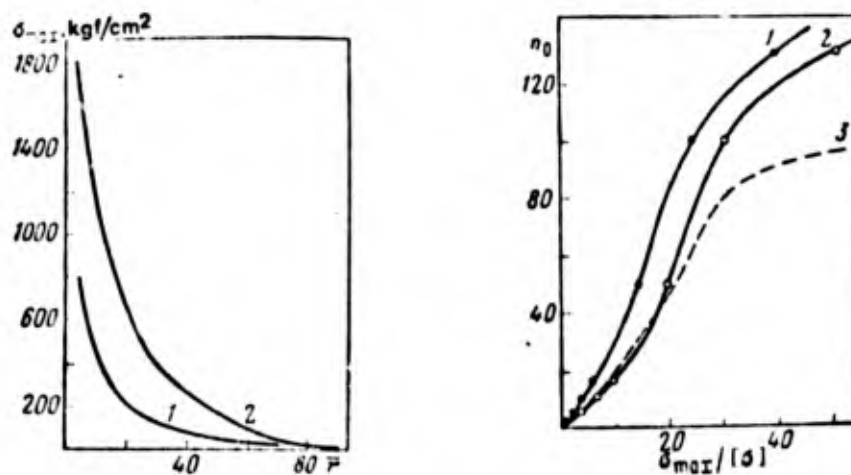


Fig. 67. The change in maximum stresses with distance  
1- for rosin; 2- for the model material

Fig. 68. Dependence of the number of crack formation centers in a unit of relative volume on the value of the stresses  
1- for the material of nature (rosin); 2- for the material of the model (calculated), 3- for hyposulphite

In accordance with condition (282), for this relationship  $n_{OM}^* = 130$ . Thus, we determine the coordinates of point 1, characterizing the material of the model in the system of coordinates  $n_0^*, \sigma_{\max}/[\sigma_R]$ . Having found the coordinates of the other points, we may obtain the dependence  $n_{OM}^* = f(\sigma_{\max M}/[\sigma_R]_M)$ .

For a distance of  $\bar{r} = 10$ :

$$\text{in nature } \sigma_{\max N} / [\sigma_R]_N = 500/20=25$$

From the plot (see Fig. 68, curve 1) it follows that  $n_{0N} = 100$  and for the model  $\sigma_{\max M} / [\sigma_R]_M = 1200/35=34$ . From condition (282) for this relationship  $(\sigma_{\max M} / [\sigma_R]_M) n_{0M}$  must be equal to 100.

Analogously for  $\bar{r} = 20$ :

$$\text{in nature } \sigma_{\max N} / [\sigma_R]_N = 250/20=12.5$$

From the plot (see Fig. 68, curve 1)  $n_0^* = 50$ .

For the model  $\sigma_{\max M} / [\sigma_R]_M = 700/35=20$ . In accordance with the similitude condition for the relation  $\sigma_{\max M} / [\sigma_R]_M = 20$ ,  $n_{0M}^* = 50$ .

For  $\bar{r} = 30$ :

$$\text{in nature } \frac{\sigma_{\max N}}{[\sigma_R]_N} = \frac{120}{20} = 6, \quad n_{0N}^* = 18;$$

$$\text{in the model } \frac{\sigma_{\max M}}{[\sigma_R]_M} = \frac{400}{35} = 12, \quad n_{0M}^* = 18.$$

For  $\bar{r} = 40$ :

$$\text{in nature } \frac{\sigma_{\max N}}{[\sigma_R]_N} = \frac{90}{20} = 4,5, \quad n_{0N}^* = 10;$$

$$\text{in the model } \frac{\sigma_{\max M}}{[\sigma_R]_M} = \frac{270}{35} = 8, \quad n_{0M}^* = 10.$$

For  $\bar{r} = 50$ :

$$\text{in nature } \frac{\sigma_{\max N}}{[\sigma_R]_N} = \frac{60}{20} = 3, \quad n_{0N}^* = 5;$$

$$\text{in the model } \frac{\sigma_{\max M}}{[\sigma_R]_M} = \frac{180}{35} = 5, \quad n_{0M}^* = 5.$$

For  $\bar{r} = 60$ :

$$\text{in nature } \frac{\sigma_{\max N}}{[\sigma_R]_N} = \frac{30}{20} = 1,5, \quad n_{0N}^* = 2;$$

$$\text{in the model } \frac{\sigma_{\max M}}{[\sigma_R]_M} = \frac{90}{35} = 2,5, \quad n_{0M}^* = 2.$$

For  $\bar{r} = 70$  in nature and in the model the maximum strength of the material is reached and therefore we assume provisionally that  $n^* = 0$ . If the stress is greater than the strength, then  $n$  is greater than 0. Joining the points by a smooth curve we obtain the graphical dependence which characterizes the material of the model (Fig. 68, curve 2). The similitude of the intensity of crushing (similitude of particle-size composition) will be attained if for a specified manner in which the maximum stresses change, the material of the model will satisfy the dependence  $n^*_{OM} = f(\sigma_{\max M} / [\sigma_R]_M)$ , shown in Fig. 68, (curve 3). As a result of tests on a number of materials it was established that the material which has the characteristics closest to the calculated ones is hypsulphite (see Table 12, lump 9). In Fig. 68 (curve 3) the dependence  $n_0 = f(\sigma_{\max} / [\sigma_R])$  is shown. In the region of values of  $\sigma_{\max} / [\sigma_R]$  from 1 to 25 the characteristics of the material agree closely with the calculated ones. For  $\sigma_{\max} / \sigma_R > 25$  a substantial deviation from the required characteristics is observed. This is explained by the fact that for large stresses (exceeding by a factor of 25 to 30 the maximum strength) the dimensions of the particles which are formed tends to a constant value and depends only slightly on the value of the stresses and the strength of the material. Consequently, for such stress in a unit of absolute volume the number of particles being formed and the number of crack formation centers is approximately the same for all materials. A unit of relative volume for nature is  $\lambda_\ell^3$  times greater than a unit of volume for the model. Therefore, with a geometrical scale of modelling  $\lambda_\ell \neq 1$ , in a unit of relative volume (for large values of  $\sigma_{\max}$ ) there will be a different number of crack formation centers by virtue of the difference in absolute values of the volumes. Such a difference in the calculated and actual properties of the material leads to the situation where for scales of modelling  $\lambda_\ell \neq 1$  it is not possible to obtain similitude in the dimensions of particles of the pulverized zone, and for large geometrical scales ( $\lambda_\ell \geq 100$ ) it becomes

difficult to have similitude obeyed in the yield of fine fractions (less than 100 mm in nature). If one is given not only the rule by which  $\sigma_{\max}$  changes with distance from the center of the charge but also the nature of the change in stresses in time at various points of nature and of the model, then the time scale is established from the relationship between the pulse durations at similar points. From the given velocity of crack development in nature and from the known time scale from condition (220), we determine the required velocity of crack development at a specified point of the material of the model. If, for instance, the relationship between the durations of stress pulses of nature and of the model  $\lambda_t = 2.0$ , and at a distance of  $\bar{r} = 5$  the velocity of crack development in nature  $v_{\text{cr}} = 1100 \text{ m/sec}$  (Fig. 69, curve 1), then at this distance the velocity of crack development in the model must be

$$V_{\text{cr.M}} = (\lambda_e / \lambda_t) v_{\text{cr.N}} = (1.5/2) 1100 = 825 \text{ m/sec}$$

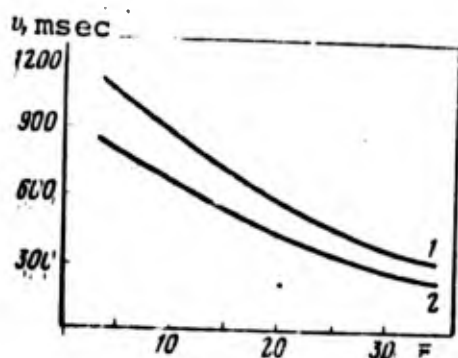


Fig. 69. The velocity of crack development as a function of relative distance from the explosion center

- 1- calculated for the model;
- 2- for the material of nature.

It is desirable to take into account the fact that the time scale is a function of the relative distance. In calculating the pulse duration at various distances it is necessary to find

the corresponding value of  $\lambda_t$ . In Fig. 69 (curve 2) the required law for the crack development velocity in the model material is shown as a function of the relative distance under the condition that  $\lambda_t = 2.0$  and that it not depend on  $r$ . Consequently, in order to obtain identical shattering the material of the model must satisfy still one other condition: for a specified rule for the change in maximum stresses the velocity of crack development must correspond to the calculated velocity. Naturally, it is difficult to select a material which satisfies simultaneously all these requirements. Therefore, in choosing a model material only the corresponding function  $n_0^* = f(\sigma_{\max} M / [J_R]_M)$  to the calculated characteristics was controlled. After the explosion the particle-size composition of the fragmented material was tested. Results of the measurement are shown in Table 13.

Table 13

Particle-size composition of fragmented material in nature and in the model

Block 3 (Nature)		Block 9 (Model)		Block 3 (Nature)		Block 9 (Model)	
Dimensions of fractions, cm	Yield of fractions, %	Dimensions of fractions, cm	Yield of fractions, %	Dimensions of fractions, cm	Yield of fractions, %	Dimensions of fractions, cm	Yield of fractions, %
10x7x6	6,4	8x4x4	5,8	3-1,5	26,1	2-1	27,6
10x5x5	5,4	8x4x3	4,8	1,5-1,0	9,0	1-0,5	9,2
8x5x4	3,4	7x3x3	3,2	1,0-0,7	8,1	0,7-0,5	8,0
8x4x4	4,0	6x3x3	3,0	0,7-0,5	3,7	0,5-0,3	3,5
7x5x3	4,8	5x3x2	5,0	0,5-0,3	2,9	0,3-0,2	3,0
6x4x3	2,6	5x3x1	2,6	0,3-0,2	1,5	0,2-0,1	4,8
6x4x2	5,3	4x3x2	6,1	Mean 0,2	6,4	Mean 0,1	4,9
4,5-3,0	8,0	3-2	8,5				

From the data of Table 13 it follows that the particle size composition obtained in the model is very close to the composition in nature (taking account of the geometrical scale), with the exception of the fine fractions. This circumstance is explained by the deviation of the properties of a real material from the calculated characteristics for high stresses and by the fact that the charge used for the model has an air gap, thus contributing to a reduction of the dimensions of the zone of repulverization.

Let us take a look at the requirements which must be produced in the material of the model in order that the similitude criteria of elastic wave phenomena be obeyed. As was shown earlier, in having similitude of elastic wave phenomena observed one can obtain only similitude of the damage zone. Inasmuch as the parameters of explosive loading are specified, it is necessary to choose the strength of the material to be equal to the value of the maximum stresses at the boundary of the zone which is similar to the damage zone in nature. Moreover, it follows from the similitude condition of elastic wave motions that

$$\sigma_{\max N} / \sigma_{\max M} = \rho_N C_N^2 / \rho_M C_M^2$$

The ratio of  $\sigma_{\max N} / \sigma_{\max M}$  is not required to be a constant for similar points in nature and in the model, so that for a given loading it is necessary that the density of the material  $\rho_M$  or the velocity of sound  $C_M$  be variable. Only in this case may the similitude conditions of elastic wave phenomena be satisfied. When making use of equivalent materials for similar points the ratio  $\sigma_{\max} / [\sigma_R] = \text{idem}$  must be observed.

For a specified loading this condition may be fulfilled in the case where the strength of the material of the model will be found as a function of distance from the center of the charge, since from the calculation presented above it follows that for a constant strength of material of the model the condition  $\sigma_{\max}/[\sigma_R]$  is not fulfilled. However, even when the strength is variable and the condition  $\sigma_{\max}/[\sigma_R] = \text{idem}$ , is observed, similar particle size composition may be obtained only in the case where the curves  $n_0^* = f(\sigma_{\max}/[\sigma_R])$  for nature and for the model coincide. Then at similar points the number of crack formation centers in a unit of relative volume will be the same.

Thus, from the similitude condition of elastic wave motion one cannot establish similitude of the particle size composition. When using the method of equivalent materials, similar particle size composition may be obtained only in the special case where the model material in which, along with fulfillment of the condition  $\sigma_{\max}/[\sigma_R] = \text{idem}$ , the number of crack formation centers in a unit of relative volume for nature and for the model are the same for  $\sigma_{\max}/[\sigma_R] = \text{constant}$ . Similitude criteria for the process of shattering of rocks in an explosion, obtained from the statistical theory of damage, are more general, since the similitude criteria used in the method of equivalent materials follows from these as a special case. However, the method under consideration for attaining similar crushing by means of choosing material with specified characteristics is very complicated when it comes to practical realization. Therefore, it is more expedient to employ a different method for solving the problems of obtaining similar crushing.

To serve as our initial data let us take the physical and mechanical properties of the materials of nature (rosin) and of the model (hyposulphite) (see Table 12, blocks 8 and 38) and the

stress pulse in nature for a distance of  $\bar{r} = 7.5$  and  $\bar{r} = 15$  (Fig. 70, 71, curves 1 and Table 14).

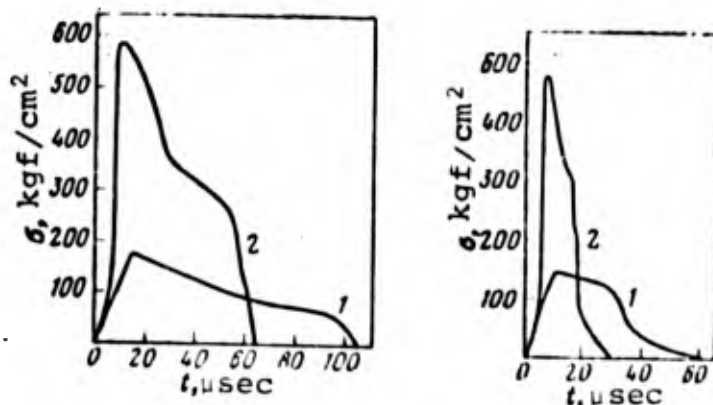


Fig. 70. Change in stress with time at a distance  $\bar{r} = 7.5$   
1- in nature; 2- calculated for the model

Fig. 71. Change in stress with time at a distance  $\bar{r} = 15$   
1- in nature; 2- calculated for the model

The change in maximum stress as a function of relative distance from the center of explosion is given in Fig. 72 (curve 1). It is necessary to construct a stress pulse for the model which assures crushing identical to nature. From the plot (see Fig. 72) we determine the value of maximum stress in nature  $\sigma_{\max N}$ . For the distance  $\bar{r} = 7.5$ ,  $\sigma_{\max N} = 200 \text{ kgf/cm}^2$ . The ratio

$$\sigma_{\max N}/[\sigma_R] = 200/27 = 7.4.$$

From the plot (Fig. 73) we find that for such a value of relative stresses  $n_0^* = 28$ . For  $n_0^* = 28$  in the model it is necessary to create relative stresses such that  $\sigma_{\max M}/[\sigma_R]_M = 13$ . Knowing the strength of the model material, we determine the required value of the maximum stresses at a distance of  $\bar{r} = 7.5$ . For  $[\sigma_R] = 45 \text{ kgf/cm}^2$ ,  $\bar{r} = 7.5$   $\sigma_{\max} = 13.45 \text{ kgf/cm}^2 = 585 \text{ kgf/cm}^2$ .

Table 14

Experimental values of stresses in a rosin lump (nature)

relative distance in front of center of explosive charge, $r = r_0/r$	Stresses (kgf/cm <sup>2</sup> ) appearing during impact in different moments of time (μsec) from priming moment											Magnitude of maximum stresses, kgf/cm	Time for reaching maximal stresses, μsec	
	5	10	20	30	40	50	60	70	80	90	100			110
4,0	0	220	305	215	242,0	233	187	169,0	122,0	65,5	18,7	0	150	17,6
8,5	0	0	152	181	155,0	129	116	103,0	90,6	77,6	72,2	0	181	30,4
15,0	0	0	0	69	131,0	128	79	44,4	11,0	10,0	0	0	138	32,0
20,0	0	0	0	0	32,3	118	86	43	22,0	0	0	0	124	51,9

Table 15

Calculated values of stresses in a hyposulphite lump (model)

Relative distance in front of center of explosive charge $r = r_0/r$	Stresses (kgf/cm <sup>2</sup> ) calculated for different moments of time (μsec) from beginning of initiation										Magnitude of maximum stresses, kgf/cm <sup>2</sup>	Time for reaching maximal stresses, μsec
	5	10	20	30	40	50	60	70	80	90		
4,0	0	1470	1000	720	540	320	220	87	20	0	1470	10,0
8,5	0	0	50	520	470	340	270	100	0	0	580	17,7
15,0	0	0	0	60	350	60	0	0	0	0	480	33,4
20,0	0	0	0	0	180	20	0	0	0	0	265	37,5

In a similar manner the stresses at the remaining points in the model are found. From the computed values we construct the dependence of the change in maximum stresses with distance from the charge center for the model (see Fig. 72, curve 2). In modelling the damage process the time scale is determined in order to synthesize the time characteristics of the desired pulse. The time scale is computed from the dependence of the velocity of crack development on the relative distance to the charge center (see Fig. 74). For a distance of  $\bar{r} = 7.5$  the velocity of crack development in nature  $v_{TP.N} = 1100$  m/sec, the velocity of cracks in the model  $v_{cr.M} = 750$  m/sec, and the geometric scale  $\lambda_l = 1$ . In accordance with dependence (220)

$$\lambda_t = 1 \cdot \frac{700}{1100} = 0,64.$$

The time scale for other typical points of the model are computed in an analogous way. The data of the computations are presented in Table 15, and the constructed pulses for the model are shown in Fig. 70 and 71 (curve 2).

In order to create the necessary pulse in the model, PETN was used for the explosive material (specific consumption 250 mg/kg). The particle size composition of the exploded blocks is shown in Table 16. From the oscilloscope traces obtained in the explosion for the distances  $\bar{r} = 7.5$  and  $\bar{r} = 15$  in the model, plots of the change in stress with time were constructed (Fig. 75). The small difference in dimensions of the fractions obtained is explained by the fact that there are discrepancies in the calculated and constructed pulses.

Experimental investigations carried out on blocks of various dimensions for the same and for different materials of nature and of the model were also performed under laboratory conditions.

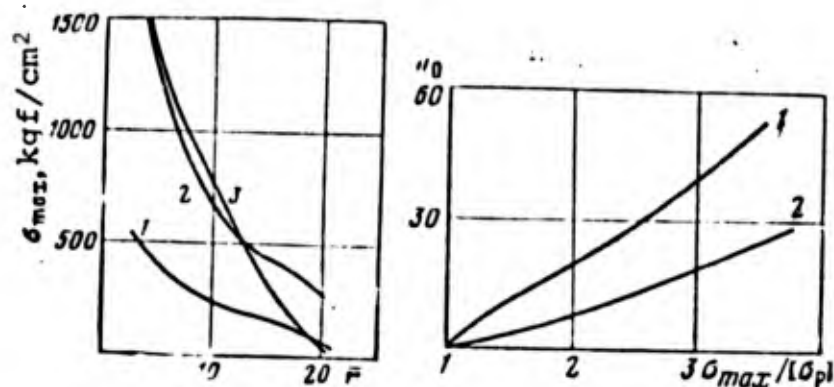


Fig. 72. Change in maximum stress as a function of the relative distance:

1- for nature (block 8); 2- calculated for the model; 3- experimental for the model (block 38)

Fig. 73. Dependence of the specific number of crack generation sites on the relative stress for rosin (1) and hyposulphite (2)

The characteristics of some of the models and charges used are shown in Table 17.

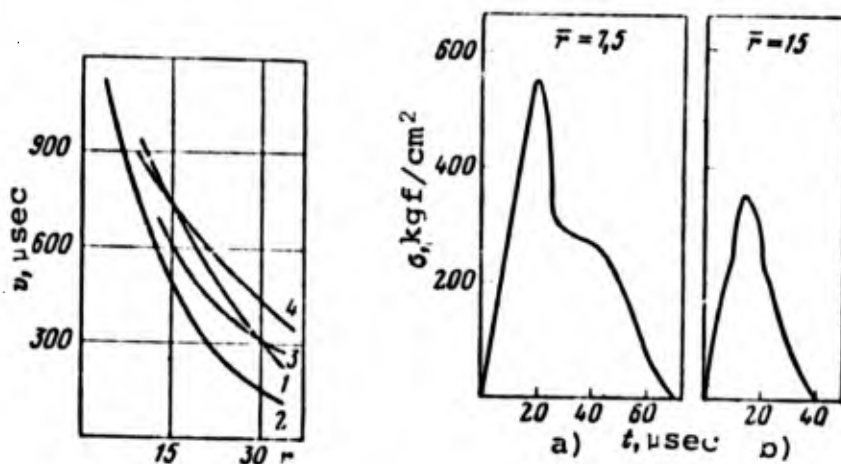


Fig. 74. Change in velocity of crack development with distance for rosin (1), hyposulphite (2), granite (3) and dolomitized limestone (4)

Fig. 75. Variation of stresses in time for a hyposulphite block at the distances

a -  $\bar{r} = 7.5$ ; b -  $\bar{r} = 15$

From the data of the table it follows that lump 10 of rosin should be used in the capacity of nature. Modelling was accomplished by various means.

The model, represented by block 14, was prepared from the same material, but differs in dimensions. Furthermore, in this model a dispersed charge was used, thus making it possible to create calculated parameters of the pulse for a smaller specific consumption of explosive material (50 mg/kg instead of 56 mg/kg). The model represented by block 33 had the same dimensions as in nature, but it was made from hyposulphite. The model was also shattered by a dispersed charge with a 1:2 weight ratio of the parts of the charge. The smaller charge was placed in the upper part of the bore-hole. The size of the air gap was 15 mm. The calculated parameters of the stress pulse (Table 18) were determined by the method which has been described. They differ somewhat from the actual values (Table 19), a fact which is explained by the complexity of creating a specified pulse. In order to obtain a pulse with characteristics close to the calculated ones, several identical models with various types of explosive material, specific consumption, and charge construction are exploded. From these the model is chosen in which the stress pulse parameters are close to the calculated ones. The results of testing the particle size composition are presented in Table 20. The dimensions of the fractions of the particle size composition of block 14 are referred to nature by taking account of the geometric scale of modelling (i.e., multiplied by the geometric scale  $\lambda_g = 1.5$ ). From the data of Table 20 it follows that by using a charge with an air gap it became possible to obtain more uniform crushing in comparison with the continuous charge in block 37, notwithstanding the smaller specific consumption of explosive material. Analogous results were obtained for other blocks as well.

Table 16

Particle size composition of the exploded lumps

Dimensions of the fractions, cm	Block 8		Block 38		
	Yield of fractions, %	Average weight of fractions, g	Dimensions of fractions, cm	Yield of fractions, %	Average weight of fractions, g
6×5×4	2,6	220	8×3×2	0,6	85
5×3×2	1,1	90	5×3×2,5	2,7	350
5×3,5×1,5	0,8	70	5×2×2	0,6	85
			6,5×2,5×1,5	0,7	100
4,5×3×2	2,6	220	4,5×2,5×2	2,7	350
3-2	6,9	580	3,5×2,5×2	5,0	635
2-1	22,7	1920	3-2	7,4	1070
			2-1	30,6	3800
1-0,7	12,8	1080	1-0,7	9,7	1230
			0,7-0,5	9,6	1225
0,7-0,5	13,8	1170	0,5-0,3	7,9	1000
0,5-0,3	15,6	1320	0,3-0,2	6,8	870
0,3-0,2	8,0	680	0,2-0,1	7,9	1000
0,2-0,1	7,2	610	0,1	7,9	1020
0,1	5,9	500			
	$d_{cp} = 1,06$		$d_{cp} = 1,11$		

Table 17

Characteristics of laboratory explosions\*

Number of Block	Material	Dimensions of blocks, mm.	Density of material, g/cm <sup>3</sup>	Velocity of sound, m/sec.	Shattering stresses, kgf/cm <sup>2</sup>	Construction of charge	Specific consumption of explosive material, mg/kg
10	Rosin	300×300×300	1,1	2100	15	Continuous	84
14	"	200×200×200	1,1	2100	15	Dispersed	50
33	Hyposulphite	300×300×300	1,7	4000	60	"	125
16	Rosin	200×200×200	1,1	2100	20	Continuous	112
27	Hyposulphite	200×200×200	1,7	4000	40	Dispersed	105
19	Rosin	200×200×200	1,1	2100	20	Continuous	56
24	Hyposulphite	200×200×200	1,7	4000	50	"	125

Footnote. In block 16 tetryl was used for the explosive material, and in the remaining cases PETN.

Table 18

Calculated values of the stresses in the model

Number of block	Relative distance to charge center, $\bar{r} = r_0/r$	Stresses (kgf/cm <sup>2</sup> ) calculated for various moments of time (microseconds) from priming time														Value of the maximum stresses kgf/cm <sup>2</sup>	
		0	5	10	20	30	40	50	60	70	80	90	100	110	120		130
14p	5	0	1150	957	960	810	570	290	0	0	0	0	0	0	0	0	1150
	14	0	0	0	0	390	280	320	390	290	260	135	100	60	0	0	390
33p	5	0	0	900	1600	1300	1000	670	320	0	0	0	0	0	0	0	1840
	14	0	0	0	260	350	480	570	670	570	420	340	260	200	100	0	640
19p	10	0	0	0	180	260	320	420	330	250	180	140	80	0	0	0	420
	20	0	0	0	0	40	52	70	100	140	120	105	72	63	20	0	170
16p	7.5	0	0	0	280	420	340	260	290	115	60	0	0	0	0	0	420
	15	0	0	0	0	50	100	140	120	95	70	50	30	0	0	0	170
	20	0	0	0	0	30	50	67	80	83	67	52	40	30	22	0	85

Table 19

Experimental values of the stresses in shattered blocks

Number of block	Relative distance to charge center, $\bar{r} = r_0/r$	Stresses (kgf/cm <sup>2</sup> ) calculated for various moments of time (microseconds) from priming time													Value of the maximum stresses kgf/cm <sup>2</sup>	
		10	20	30	40	50	60	70	80	90	100	110	120	130		
10	5	1000	915	1000	820	640	460	270	120	0	0	0	0	0	0	1150
	14	0	370	230	190	350	390	250	210	150	160	115	100	70	0	390
14	5	930	930	650	430	320	270	190	125	90	60	40	0	0	0	980
	14	0	270	300	270	340	240	130	150	150	80	60	30	0	0	340
33	5	930	1100	830	620	450	375	250	130	100	60	40	60	0	0	1100
	14	0	270	300	320	400	440	400	370	315	270	200	150	100	0	490
27	7.5	0	520	570	680	830	440	320	230	140	90	50	0	0	0	830
	15.0	0	80	110	135	140	190	175	120	95	70	50	0	0	0	190
	21.0	0	0	30	45	90	130	140	145	100	60	50	30	0	0	145
16	7.5	0	260	390	340	220	190	130	65	0	0	0	0	0	0	390
	15.0	0	0	52	140	140	110	90	70	40	20	0	0	0	0	140
	20.0	0	0	35	60	69	75	55	48	40	35	20	10	0	0	75
24	10.0	0	315	870	930	720	580	290	135	0	0	0	0	0	0	990
	20.0	0	0	27	75	120	83	50	33	20	0	0	0	0	0	120
19	10.0	0	190	220	250	350	290	190	120	80	65	0	0	0	0	340
	20.0	0	0	15	23	30	45	67	53	45	35	24	15	0	0	70

Particle size composition of shattered blocks

Table 20

Block 10 (nature)		Block 14 (model)		Block 33 (model)			
Yield of fractions							
cm	%	cm	%	cm	%		
12×7×3	1,3	8×8×6	6,3	8×5×4	1,0		
9×4×3	2,0	6×5×5	3,9	6×5×2	3,0		
7×6×3	2,0	6×4×3	1,9	6×5×2	1,0		
7×6×6	0,7	5×3×3	2,8	5×3×2	5,0		
6×5×2	2,0	5×2×2	2,0	4×3×2	3,4		
5×3×2	9,9	4×3×2	2,0	4×4×4	8,2		
3-2	3,9	3-2	7,3	3-2	10,0		
2-1	21,2	2-1	21,6	2-1	19,8		
1-0,7	11,2	1-0,7	12,1	1-0,7	12,2		
0,7-0,5	11,6	0,7-0,5	11,8	0,7-0,5	10,0		
0,5-0,3	11,9	0,5-0,3	11,6	0,5-0,3	8,1		
0,3-0,2	6,4	0,3-0,2	6,4	0,3-0,2	6,1		
0,2-0,1	6,5	0,2-0,1	6,2	0,2-0,1	6,3		
0,1	4,5	0,1	4,3	0,1	3,2		
Block 27 (nature)		Block 16 (model)		Block 19 (model)		Block 24 (nature)	
12×7×3	1,0	7×5×3	1,0	10×7×7	7,8	8×5×2	1,9
8×4×3	1,7	6×4×2	3,3	9×6×4	3,5	5×4×3	8,0
6×3×2	1,8	5,5×4×2	1,0	5×5×5	3,4	7×3×2	6,6
5×3×2	2,0	4×3×3	1,9	5×4×3	6,4	5×3×2	5,0
6×3×2	2,6	4×3×2	2,1	5×3×3	3,6	4×2×2,5	5,8
5×2×2	3,7	—	—	4×2×2	2,0	—	—
3-2	3,6	3-2	1,7	3-2	9,0	3-2	12,2
2-1	25,3	2-1	24,6	2-1	25,3	2-1	21,8
1-0,7	11,0	1-0,7	11,1	1-0,7	11,0	1-0,7	10,5
0,7-0,5	10,8	0,7-0,5	12,2	0,7-0,5	8,6	0,7-0,5	6,8
0,5-0,3	11,6	0,5-0,3	12,8	0,5-0,3	8,5	0,5-0,3	7,8
0,3-0,2	9,2	0,3-0,2	6,2	0,3-0,2	3,7	0,3-0,2	3,6
0,2-0,1	7,7	0,2-0,1	8,0	0,2-0,1	4,8	0,2-0,1	4,2
0,1	4,0	0,1	5,1	0,1	2,4	0,1	2,9

Thus, by varying the physical and mechanical properties of the materials and the parameters of the explosive impulse it is possible to obtain crushing in the model which is identical to nature. Investigations of methods for controlling the explosive action in models permit one to set up the required characteristics of the stress pulse in the block in order to obtain the specified fragmentation. Moreover, according to how the stress field parameters are changed in the model, it is possible to obtain a quantitative estimate of the effectiveness of the methods under study for controlling the energy of the explosion.

## Determination of the Necessary Parameters of the Stress Pulse in a Rock Block in Order to Obtain a Given Degree of Crushing.

In order to model the shattering process in explosions in quarries it is necessary to determine the value of constants characterizing the properties of the rock and the parameters of the stress pulse. Physical constants of some rocks and modelling materials obtained as a result of some pertinent studies were presented in the preceding chapter. In modelling the shattering process of large volumes of rock it is necessary to take account of the effect of the scale factor on the strength of the rock in the block, and special studies have been carried out for this purpose. For the investigation samples of cubic shape having various dimensions (5 x 5 x 5 cm; 10 x 10 x 10 cm; 15 x 15 x 15 cm; 20 x 20 x 20 cm) were selected and the value of the shattering compression stresses was determined. As a result of the experiments it was found that the increase in linear dimensions of a sample greater than 15 cm has little influence on the strengths of limestone and granite. The strength of the sample when the dimensions are 15 x 15 x 15 cm is taken to be the characteristic strength of the material in succeeding calculations. This strength is substantially different from the strength of the 5 x 5 x 5 cm sample which was referred to in Chapter five, and which was used to determine the strength coefficient of Protod'yakonov. The main difficulty in the investigations turns out to be the creation of a stress field with the specified parameters in the block. Since the physical and mechanical properties of the rock may vary over a wide range, there is a special significance to the question concerning methods for controlling the energy of the explosion. Experimental studies were conducted with an eye toward establishing the effect of the specific consumption, type of explosive material, the stemming and the construction of the charge on the quality of fragmentation of the rock mass. Preliminary studies were carried out on outsized blocks, and from the final results of the explosions an evaluation of the effectiveness of

various methods was performed. Separate experiments of this nature were conducted also in the exploding of bore-hole charges on a scarp.

The next step in the investigation was the measurement of the stresses which arise at various points of the block during the explosion. These experiments made it possible to make a quantitative evaluation of the influence of various factors on the stress field parameters, with which one then finds it possible to create the required impulse. Under laboratory conditions definite particle size composition of the model shattered by the explosion and definite stress field parameters are obtained. The dependencies obtained and the results of the laboratory experiment were utilized in the calculation of stress pulse parameters in nature which assure similar crushing of the rock mass. The required stress pulse was created by an appropriate choice of the specific consumption, type of explosive material, and charge design. In order to record the stress field parameters capacitance sensors made of barium titanate were used, and bore-holes were drilled along the line of least resistance to a depth of the level of the charge center in order to locate the sensors in the block. The sensors were insulated in order to avoid short-circuiting of the coverings. In the bore-hole the sensor was oriented in such a way as to fix the radial component of stress. In order to eliminate any affect from the tangential stress component on the operation of the sensor the latter was placed in a rubber clip or ring. The bore-hole was filled with a cement solution whose strength (after hardening) was close to the strength of a rock sample whose dimension was 200 mm. The choice of this strength for the cement assured the stable registering of the value of stresses during the course of each process of shattering of the block, inasmuch as the cement did not shatter earlier than the rock. Testing of the particle size composition after explosion was carried out by the method of oblique-angled photoplanimetry, developed by L. I. Baron (1960). As a result of experiments under

industrial conditions a full corroboration was made of the dependences and similitude criteria which were obtained for modelling the shattering process.

In order to model the process of shattering a bench a model of a bench was prepared out of rosin with the scale 1:75 (model 1). Charges of PETN were placed in channels (models of the bore-holes), and the weight of the charges was determined from a calculation showing that the specific consumption of explosive material amounted to 100 mg/kg (the specific consumption of explosive material is taken in the calculation as 1 kg of the weight of the material being broken up). After the explosion the disintegrated mass was sifted on screens and its particle size composition was determined. With the aid of piezoelectric sensors the stress pulse parameters were recorded at various distances from the center of the charge. After the oscilloscope traces were interpreted plots were constructed of the change in value of maximum stresses as a function of distance (Fig. 76)

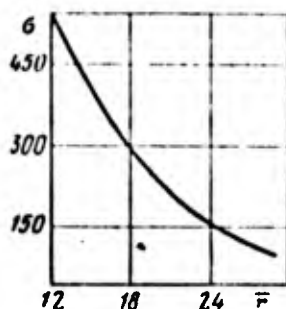


Fig. 76. Change in value of maximum stresses with distance from the charge center in a model made of rosin

1- for granite; 2- for limestone

Characteristics of the rocks of the Kolomoyevskiy granite quarry and of the model material are presented in Table 21. The strength of granite is shown for blocks of dimensions 20 x 20 x 20 cm. This strength is two to three times smaller than the strength according to Protod'yakov, which is determined on the basis of cubes of smaller dimensions. The range of variation of the crack development velocity is wider for hyposulphite and rosin than for

granite and limestone, a fact which is explained by the larger interval of change in the value of relative stresses. In order to obtain similarities in the particle size composition, it is necessary to provide for validity of the condition whereby the number of forming cracks in a unit of relative volume of the model and of nature is the same. The dependence of the distribution of centers of reduced strength on the value of the stresses is shown for rosin and for hyposulphite in Fig. 73, and for granite and limestone in Fig. 77. From the existing experimental data and from the plots let us determine the stress field parameters for a given block of rosin, and also the distribution of weak points, as a function of relative distance. The results of the computations are presented in Table 22. On the basis of these data the necessary values of maximum stresses in the scale of stresses as a function of relative distance are established.

Table 21

Characteristics of materials of the model and of the block

Material	Velocity of longitudinal waves, m/sec	Rate of crack development, m/sec	Density, g/cm <sup>3</sup>	Modulus of elasticity, kgf/cm	Uniaxial compression strength, kgf/cm <sup>2</sup>
Rosin	2200	100-1000	1,1	$52 \cdot 10^3$	20
Hyposulphite	4000	70-1400	1,7	$2,72 \cdot 10^4$	30
Granite	5500	130-200	2,7	$8,1 \cdot 10^5$	420

In making the computations one should take account of the change in the values of relative volume with variation of the scale of modelling. Plots in Figs. 73 and 77 are composed with a scale of modelling 1:100. For a different scale of modelling (1:m) it is necessary to relate the number of weak points to a unit of volume, which is taken in constructing the graph of Fig. 77, and in this regard the calculated number of weak points must be

increased by a factor of  $(100/m)^3$  and the quantity  $\sigma_{\max}/[\sigma_R]$  must be determined for

$$n_0 = k_0 \left( \frac{100}{m} \right)^3 \quad (283)$$

Analogous calculations were carried out for the model made of hyposulphite. The scale of modelling is taken as 1:50. A plot of the change in maximum stresses as a function of distance in this explosion is presented in Fig. 78 the results of the computations are shown in Table 22.

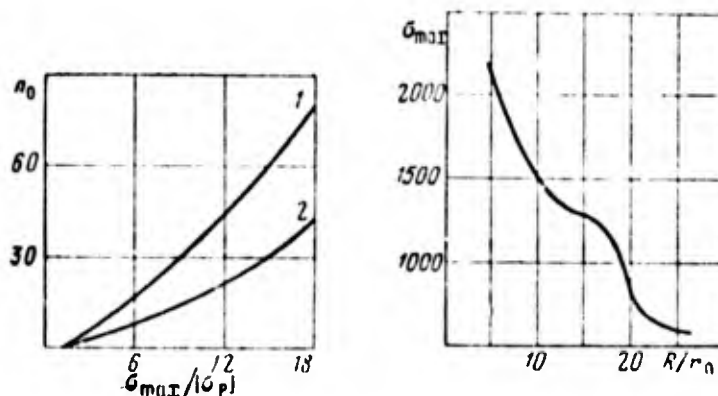


Fig. 77. Dependence of the number of crack formation centers in a unit of relative volume for granite and for limestone

Fig. 78. Change in the value of maximum stresses as a function of distance in a block of hyposulphite

The next step in the construction is a determination of the scale of time characteristics of the explosive impulse. As follows from formula (20), the scale of time may be different depending on the law according to which the velocity of cracks changes with distance for nature and for the model. Using the values of crack development velocities in rosin, hyposulphite and granite (Fig. 74),

let us compute the scale of time as a function of distance (Fig. 79).

Table 22

Calculated characteristics of the stress field

Material being shattered	Relative distance (referred to the charge radii) $r = r/r_0$	Relative value of the maximum stresses	Number of weak points in a unit of relative volume	Value of maximum stresses,
Rosin	5	6	100	1200
	10	50	90	1000
	15	45	80	1000
	20	20	60	500
	30	9	30	150
Hyposulphite	5	20	30	1000
	10	6,2	15	496
	15	3,75	5	300
	20	2,5	2	200
	30	1,0	1	80
Granite	5	5/5	240/240	2400/2400
	10	4,0/3,5	144/120	1680/1470
	15	3,2/3,0	52/40	1320/1250
	20	2/1,8	20/16	840/750
	30	1,5/1,3	10/8	630/580

Footnote. In the numerator are the calculated values for the model made of rosin, in the denominator are the values for the model made of hyposulphite.

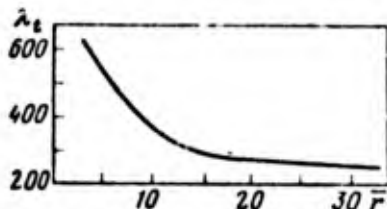


Fig. 79. Change in the time scale with distance to the charge center

From the data of the table it follows that the value of the maximum stresses calculated from the results of modelling with hyposulphite and rosin differ somewhat, in which connection the particle size composition of the shattered blocks contains a deviation from similitude. Owing to the fact that it is exceedingly difficult to generate the required law of changes in stresses with any accuracy, it pays to attain stress pulse parameters in

nature such that the value of maximum stresses lies in the interval of values calculated from the results of experiments on the models. In this case one may obtain a particle size composition which is close to the calculated one. The probability of deviation from similitude is greater for the coarse fractions that are created by macrocracks and structural features of the blocks that are not taken into account in the modelling. Using the stress and time scales, plots of the calculated stress pulse in the block are constructed. In generating the calculated stresses in the block one should expect to obtain a similar particle size composition of the rock mass. In constructing plots of the change in stresses in nature at various relative distances one uses the graphs of the stresses in the model with the stress and time scales taken into consideration. From Table 22 for the relative distance  $\bar{r} = 5$  the stress scale amounts to  $\lambda_\sigma = 1.75$ . According to the graph (see Fig. 79) the time scale for a distance of  $\bar{r} = 5$  is  $\lambda_t = 550$ . From the plot of stresses for the model (Fig. 80), constructed on the basis of experimental oscilloscope traces, the characteristic points are determined. For the moment of time  $t_{1M} = 6$  microseconds and for the stress corresponding to that time,  $\sigma_{1M} = 1200 \text{ kgf/cm}^2$  in the model, we must have in nature

$$t_{1N} = \lambda_t t_{1M}, \quad t_{1N} = 6 \cdot 10^{-6} \cdot 550 = 3,3 \cdot 10^{-3} \text{ sec} = 3,3 \text{ msec},$$

$$\sigma_{1N} = \lambda_\sigma \sigma_{1M} = 1200 \cdot 1,75 = 2100 \text{ kgf/cm}^2.$$

Analogously for the moment of time  $t_{2M} = 20$  microseconds and  $\sigma_{2M} = 480 \text{ kgf/cm}^2$

$$t_{2N} = \lambda_t t_{2M}, \quad t_{2N} = 20 \cdot 10^{-6} \cdot 550 = 11 \cdot 10^{-3} \text{ sec} = 11 \text{ msec},$$

$$\sigma_{2N} = \lambda_\sigma \sigma_{2M} = 480 \cdot 1,75 = 840 \text{ kgf/cm}^2$$

etc. From the data of the computations the required stress pulse in the block for  $\bar{r} = 5$  (Fig. 81) is constructed.

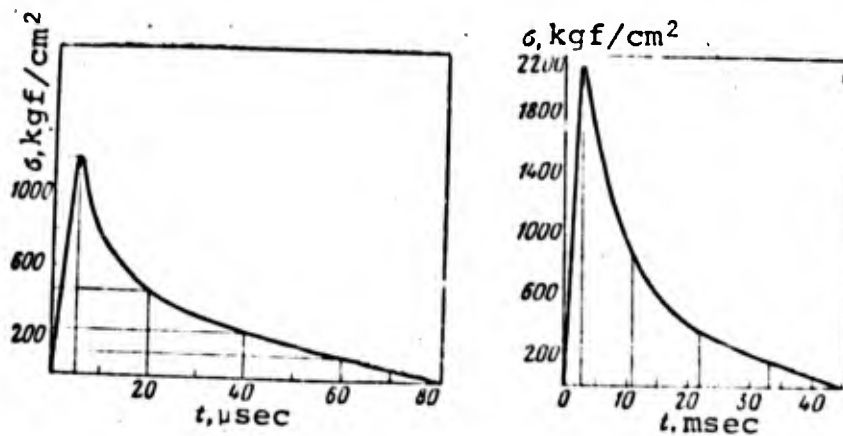


Fig. 80. Change in stresses with time at a distance  $\bar{r} = 5$  in a model made of rosin

Fig. 81. Calculated pulse in the block at a distance  $\bar{r} = 5$  in order to obtain the required degree of crushing.

From the same table and graph we determine the time and stress scales: for  $\bar{r} = 15$ ,  $\lambda_t = 300$ ;  $\lambda_\sigma = 1.5$ ; for  $\bar{r} = 30$ ,  $\lambda_t = 270$ ,  $\lambda_\sigma = 3.5$

Using the same scales the required stress pulse parameters at the indicated distances in nature ( $\bar{r} = 15; 30$ ) are established. In order to create the required stress pulse parameters in the block a series of experimental explosions were carried out under industrial conditions.

#### Investigation of the Quality of Crushing of Rocks in an Explosion by Generating Calculated Parameters of the Stress Pulse.

Industrial experimental explosions were conducted in which the characteristics of the stress field for various parameters of the bore-hole network, various specific consumptions, types of explosive material, and designs of the charge were recorded, and the results enabled one to obtain stress field parameters close to the calculated ones. In granite of the IV category (Kolomoyevskiy granite quarry) stress field parameters close to

the calculated ones were obtained using ammonite #6 for the explosive material. The specific consumption amounted to 500g/m<sup>3</sup> for the explosion of charges with air gaps.

The parameters of the bore-hole network:

line of least resistance	7.5 m
distance between bore-holes	5 m
bore-hole diameter	220 mm
length of air gap	2.2 m
ratio of the rate of the upper to the lower charge	1:3
height of the stemming	2.5 m

Seventeen bore-holes were exploded simultaneously. After the explosion the particle size composition was measured using the method of oblique-angle photoplanimetry. The distribution of fractions is characterized by the following numbers

1500-750 $\mu\text{m}$ . . . . .	20.5%	220-150 $\mu\text{m}$ . . . . .	12.1%
750-550 $\mu\text{m}$ . . . . .	15.0%	150-75 $\mu\text{m}$ . . . . .	12.2%
550-370 $\mu\text{m}$ . . . . .	14.5%	< 75 $\mu\text{m}$ . . . . .	7.0%
370-220 $\mu\text{m}$ . . . . .	18.7%		

The distribution of fractions in the rosin model

20-10 $\mu\text{m}$ (1500-750 $\mu\text{m}$ ) * . . . . .	18.8%	3-2 $\mu\text{m}$ (220-150 $\mu\text{m}$ ) . . . . .	9.9%
10-7 $\mu\text{m}$ (750-550 $\mu\text{m}$ ) . . . . .	15.4%	2-1 $\mu\text{m}$ (150-75 $\mu\text{m}$ ) . . . . .	13.7%
7-5 $\mu\text{m}$ (550-370 $\mu\text{m}$ ) . . . . .	17.3%	< 1 $\mu\text{m}$ . . . . .	6.2%
5-3 $\mu\text{m}$ (370-220 $\mu\text{m}$ ) . . . . .	18.7%		

\* The fractions corresponding to nature are indicated inside the parenthesis.

In comparing the particle size composition of nature and of the model we see that the results exhibit reasonably good agreement. The small deviation is explained by the fact that the stress pulse in nature differs slightly from the calculated pulse. The distribution of fractions in the block of hyposulphite is also close to the distribution obtained in nature (Table 23).

Table 23

Particle-size composition of the model (hyposulphite) and of nature (granite)

Dimensions of fractions, mm (model)	Corresponding dimensions of fractions, mm (nature)	Yield of fractions, % (nature)	Yield of fractions, % (nature)
> 33	> 150	0,2	—
30-20	1500-1000	15,4	47,7
20-10	1000-500	15,7	18,0
10-7	500-350	14,0	14,4
7-5	350-250	17,2	18,3
5-3	250-150	13,2	12,4
3-2	150-100	13,7	10,8
2-1	100-50	7,6	5,4
< 1	< 50	3,0	3,3

In the Dolomite mine (Donets region) in September 1968 an experimental explosion was conducted. The rocks consisted of dolomitized limestones. Granulite AS was taken as the explosive material, with a specific consumption of 420 g/m<sup>3</sup>. The line of least resistance was 8.0 m, the distance between bore-holes was 7.5 m, and the diameter of the bore-holes was 220 mm. The charge was dispersed, the length of the air gap was 2.5 m, and the ratio of the weight of the upper charge to the lower charge was 1:2.

The length of stemming was 3.0 m. Ten bore-holes were exploded at the same time. The particle-size composition of the explosion in nature and of the shattered model of hyposulphite (scale 1:50; explosive material TETN; specific consumption 200 mg/kg;  $[\sigma_R] = 40 \text{ kgf/cm}^2$ ) is shown in Table 24.

Table 24

Particle size composition of the shattered model (hyposulphite) and shattered nature (dolomitized limestone).

Dimensions of fractions, mm (model)	Corresponding dimensions of fractions, mm (nature)	Yield of fractions, % (model)	Yield of fractions, % (nature)
18-16	900-800	—	0.9
16-14	800-700	1.4	1.8
14-12	700-600	2.1	3.2
12-10	600-500	3.1	3.9
10-8	500-400	4.7	5.1
8-6	400-300	6.8	6.2
6-4	300-200	8.5	8.7
4-2	200-100	49.3	45.2
2	100	21.8	25.0

A comparison of the particle size composition in nature and in the model permits us to conclude that the results are in good agreement. The experiments which were carried out indicated that the similitude criteria which were employed make it possible to guarantee identity of the particle size composition in nature according to the results of investigations on the model.

## REFERENCES

- Авершин С. Г.** Возможность аналитических исследований проявления горного давления и область их целесообразного применения. Математические методы в горном деле, ч. II. Новосибирск, Изд-во Сиб. отд. АН СССР, 1963.
- Албурев П. М., Геронимус В. В.** и др. Теория подобия и размерностей. Моделирование. Изд-во «Высшая школа», 1968.
- Албурев П. М., Минькович Л. М.** Основы теории подобия и моделирования. Новосибирск, Изд-во Сиб. отд. АН СССР, 1965.
- Александров А. И., Журков С. И.** Явление хрупкого разрыва. М.—Л., Изд-во ГТТИ, 1933.
- Аляев П. П.** Механизм хрупкого разрушения металлов.— Сб. «Атомный механизм разрушения». Металлургия, 1963.
- Андерсон О. Л.** Критерии Гриффитса при разрушении стекла. Сб. «Атомный механизм разрушения». Металлургия, 1963.
- Андреев К. К., Белов А. Ф.** Теория вязкопластичных веществ. Оборонгиз, 1960.
- Давиденко Т. Ц., Давидов В. И.** Влияние радиального зазора на величину напряжений, образованные взрывом в породе.— Сб. «Механика горных пород». Изд-во «Недра», 1966.
- Атчисон Т. С., Хартер С. Д., Давидов В. И.** Сравнение двух методов оценки скорости вязкопластичных веществ.— Сб. «Разрушение и механика горных пород». Гостехиздат, 1962.
- Афонин В. Г.** и др. Влияние параметров вязкого течения на сейсмический эффект взрыва.— Сб. «Взрывное дело, № 62/19». Изд-во «Недра», 1967.
- Байкоцуров О. А., Кориско А. Ф., Каражанов Л. Д.** Опыт моделирования процесса дробления крепких руд взрывом.— Известия вузов, 1966, № 5.
- Балдин А. В., Койлов В. Г.** Эквивалентные материалы для моделирования действия взрыва в крепких горных породах. М., Изд. ИГД им. А. А. Скочинского, 1965.
- Баранов Е. Г., Владовский В. Е.** Оценка энергоемкости горных пород при взрыве.— Физико-технические проблемы разработки полезных ископаемых, 1969, № 5.
- Баренблатт Г. И.** Математическая теория равновесных трещин, образующихся при хрупком разрушении.— Прикладная механика и техническая физика, 1961, № 4.
- Баренблатт Г. И.** О некоторых оценках для удельной поверхности трещин, образующихся при динамических воздействиях на твердое тело.— Прикладная механика и техническая физика, 1964, № 4.
- Баренблатт Г. И., Ентов В. М., Саламанк Р. М.** О кинетике распространения трещин.— Инженерный журнал, 1967, № 1.
- Барон Л. И.** Кусковатость и методы ее измерения. Изд-во АН СССР, 1960.

- Барон Л. П.** Об акустической жесткости как критерии сопротивляемости горных пород разрушению (дроблению) динамическими нагрузками.— Сб. «Варианное дело, № 67/24». Изд-во «Недра», 1969.
- Барон Л. П.** и др. Определение свойств горных пород. Гостортехиздат, 1962.
- Баррет Ч. С., Хопкинс В. К., Грайт П. Дж.** Современное состояние задачи исследования разрушения.— Сб. «Атомный механизм разрушения». Металлургиядат, 1963.
- Бартевич Г. М., Радумовская Л. В.** Критическая прочность и критическое напряжение разрушения твердых тел.— Докл. АН СССР, 1960, 133, № 2.
- Бартевич Г. М., Радумовская Л. В.** Фононная концепция разрушения твердых тел.— Физико-химическая механика материалов, 1969, № 1.
- Баум Ф. А., Ставицкий К. П., Шелтер В. П.** Физика взрыва. Физматгиз, 1959.
- Бекленин А. В.** Мера и единица физических величин. Физматгиз, 1963.
- Беленко Ф. А., Гаск Ю. В., Друковский М. Ф.** Применение сверхскоростной фотографии для изучения напряжений при взрыве заряда в горном массиве.— Известия высшей школы, Горное дело, 1961, № 3.
- Богданович А. С., Дурченко В. П.** Таблица международной системы единиц. Изд-во Харьковского государственного университета, 1969.
- Бодаль П. Т., Пригорский П. П.** Измерение деформаций и напряжений методом оптически чувствительных покрытий.— Сб. «Проблемы прочности в машиностроении», вып. 8, 1962.
- Болотин В. В.** Статистические методы в строительной механике, Гостройиздат, 1965.
- Брорберг К. Б.** Ударные волны в упругой и упруго-пластической среде. Гостортехиздат, 1959.
- Бусленко П. П.** и др. Метод статистических испытаний (метод Монте-Карло). Физматгиз, 1962.
- Бурдун Г. Д.** Единицы физических величин. Стандартгиз, 1963.
- Веников В. А., Пылов-Смолинский А. В.** Физическое моделирование электрических систем. М.— Л., Гребнергоиздат, 1956.
- Веников В. А.** Теория подобия и моделирование применительно к задачам электроэнергетики. Изд-во «Высшая школа», 1966.
- Врховин С. П.** О статистических методах в механике горных пород.— Сб. «Вопросы горного давления». Изд-во АН СССР, 1962.
- Вртинский Н. М.** Прочность микронеоднородных хрупких тел со статистическим распределением дефектов типа трещин.— Физико-химическая механика материалов, 1968, 4, № 4.
- Власов О. Е.** Основы теории варьана. Гостортехиздат, 1958.
- Власов О. Е., Смирнов С. А.** О моделировании действия варьана.— Сб. «Варианное дело, 59/16». Изд-во «Недра», 1966.
- Власов О. Е., Смирнов С. А.** Основы расчета дробления горных пород действием варьана. Изд-во АН СССР, 1962.
- Волков С. Д.** Единая статистическая теория прочности твердых тел.— Журнал технической физики, 1953, XXIII, вып. 7; 1954, XXIV, вып. 12.
- Волков С. Д.** Статистическая теория прочности. Машгиз, 1960.
- Гарбер Р. П., Ендлин Н. А.** Физика прочности кристаллических тел.— Ученые физические наук, 1960, 70.
- Гертегорин С. А.** Прибор для интегрирования дифференциальных уравнений.— Прикладная физика, 1925, 2, вып. 3—4.
- Гертегорин С. А.** Об электрических сетках для приближенного решения уравнений Лапласа.— Прикладная физика, 1929, 4.

- Глушкo И. М.* Введение в кибернетику. Изд-во АН УССР, 1964.
- Гюденко Е. В.* Курс теории вероятностей. Физматгиз, 1961.
- Гомбан П.* Статистическая теория атома и ее применение. ИЛ, 1951.
- Голкин Г.* Динамические неупругие деформации металлов. Изд-во «Мир», 1964.
- Градштейн И. С., Рыжик И. М.* Таблица интегралов, сумм, рядов и произведений. Физматгиз, 1962.
- Григорин С. С.* Некоторые вопросы математической теории деформирования и разрушения горных пород.— Прикладная математика и механика, 1967, 31, вып. 4.
- Губкин С. П., Добровольский С. И., Бойко В. М.* Фотопластичность. Изд-во АН СССР, 1957.
- Гутенмагер А. П.* Электрические модели. Изд-во АН СССР, 1949.
- Гурман А. А.* Распространение теории подобия на случай среды с переменными физическими свойствами. Изв. Казахского филиала АН СССР. Алма-Ата, 1946, № 1 (25).
- Гурман А. А.* Введение в теорию подобия. Изд-во «Высшая школа», 1963.
- Давлес И. С., Пирков И. М., Ветдревский В. П.* О скорости распространения трещин в вязкой среде при вариве. Изд. Ин-та горного дела. Уральский филиал АН СССР, Свердловск, 1960, вып. 7.
- Дебонс Р. М.* Волны напряжений в твердых телах. ИЛ, 1961.
- Демидок Г. П.* Пути увеличения кусковатости при варивной отбойке подземных ископаемых.— Сб. «Варивные работы». Гостортехиздат, 1960.
- Демидок Г. П.* О механизме действия варива и свойствах варивчатых веществ.— Сб. «Варивное дело», № 55/12». Изд-во «Недра», 1964.
- Демидок Г. П.* О потенциальной энергии как критерии оценки промышленных варивчатых веществ.— Сб. «Варивное дело», № 57/14». Изд-во «Недра», 1965.
- Демидок Г. П.* К вопросу о критериях оценки варивных свойств ВВ для горных пород. Финансо-технические проблемы разработки подземных ископаемых, 1967, № 1.
- Демидок Г. П.* О параметрах ВВ в связи с проектированием варивов с заданной степенью дробления.— Сб. «Варивное дело», № 65/22», Изд-во «Недра», 1968.
- Демидок Г. П., Смирнов С. А.* О методике лабораторного моделирования варива. Новое в дроблении горных пород варивом.— Сб. «Варивное дело», № 50/7», Гостортехиздат, 1962.
- Джонг Ней чи, Кензи Г. А.* Единое рассмотрение цилиндрических и сферических упругих волн методом характеристик.— Прикладная механика, 1966, № 4.
- Драбавский В. А., Фридман И. В.* Влияние трещин на механические свойства конструкционных сталей. Металлургияиздат, 1960.
- Дружинин И. П.* Метод электрогидродинамических аналогов и его применение при исследовании фильтрации. Госэнергоиздат, 1956.
- Друковский М. Ф., Козир В. М.* О механизме разрушения горных пород действием варива и управлением им.— Сб. «Варивное дело», № 57/14», Изд-во «Недра», 1965.
- Друковский М. Ф., Козир В. М., Мачина И. П.* О моделировании разрушения горных пород действием варива.— Сб. «Варивное дело», № 57/14», Изд-во «Недра», 1965.
- Друковский М. Ф.* и др. Экспериментальные исследования скорости развития трещин.— Машеткин А. А., Горный журнал, 1967, № 7.

- Друкославский М. Ф.** и др. Критерий подобия при моделировании процесса разрушения твердых тел действием взрыва. — Физико-технические проблемы разработки подземных пещераемых, 1968, № 3.
- Дубовин А. С.** Фотографическая регистрация быстропотекающих процессов. Изд-во «Наука», 1964.
- Дерягин Б.** Затухание сейсмических и акустических волн и его зависимость от частоты. — Журнал геофизики, 1932, № 3—4.
- Журков С. П., Нардусов Б. П.** Временная зависимость прочности твердых тел. — Журнал технической физики, 1958, XXIII, вып. 10.
- Журков С. П., Савицкий А. В.** К вопросу о механизме разрушения твердых тел. — Докл. АН СССР, 1959, 129, № 1.
- Замесов Н. Ф.** Применение теории подобия и размерности при моделировании процессов дробления пород взрывом. Сб. «Проблемы механизации горных пород». Изд-во АН СССР, 1963.
- Зельдович Я. Б., Коминзон А. С.** Теория детонации. Гостехиздат, 1955.
- Зельдович Я. Б., Розар Ю. П.** Физика ударных волн и высокотемпературных гидродинамических явлений. Изд-во «Наука», 1966.
- Зиневель А. А.** Логическая модель как средство научного исследования. — Вопросы философии, 1960, № 4.
- Златин Н. А.** и др. Исследование разрушения стекла при электроионизационном пробое. — Труды VIII сессии Научного совета по народнохозяйственному использованию взрыва. Киев, изд-во «Наукова думка», В. 9.
- Иванкин В. П.** Подобие упругих волновых движений. Изв. АН СССР, серия геофиз., 1956, № 11, 12.
- Иванкин В. П.** О моделировании волновых сейсмических волн. — Изв. АН СССР, серия геофиз., 1958, № 7.
- Идельсон Н. И.** Теория потенциала с приложениями к теории фигуры Земли и геофизике. ОНТИ, 1936.
- Именитов В. Р., Ковалев Н. А., Уралов В. С.** Моделирование обрушения и выноса руды. М., Изд. МГУ, 1961.
- Карлаев А.** Моделирующие устройства для решения задач теории поля. ЦИ, 1962.
- Карякин П. П., Бастов К. П., Киреев П. С.** Краткий справочник по физике. Изд-во «Высшая школа», 1962.
- Киричев В. Л.** О подобии при упругих явлениях. — Журнал Русского физико-химического общества, 1874, № 6, отд. 1, ч. физическая.
- Киричев М. В.** Теория подобия. Изд-во АН СССР, 1953.
- Киричев М. В., Копылов Н. К.** Математические основы теории подобия. Изд-во АН СССР, 1949.
- Кобринский Н. Е.** Математические машины непрерывного действия. Гостехиздат, 1954.
- Покер Э., Филдс Л.** Оптический метод исследования напряжений. ОНТИ, 1939.
- Кольский Г.** Волны напряжений в твердых телах. ЦИ, 1952.
- Кольский Г.** Разрушение под действием волн напряжений. — Сб. «Атомный механизм разрушения». Металлургиядат, 1963.
- Коробейников В. П., Мельникова Н. С., Рязанов Е. П.** Теория точечного взрыва. Физматгиз, 1961.
- Коттрелл А. Х.** Теоретические аспекты процесса разрушения. — Сб. «Атомный механизм разрушения». Металлургиядат, 1963.
- Коттрелл А. Х.** Дислокации и пластическое течение в кристаллах. — Сб. «Атомный механизм разрушения». Металлургиядат 1963.

- Козл Р.* Подводные взрывы. ИЛ, 1950.
- Крылов А. И.* Собрание трудов. 7. Изд-во АН СССР, 1936.
- Крылов А. И.* Собрание трудов. 8. Изд-во АН СССР, 1950.
- Кузнецов В. Д.* Поверхностная энергия твердых тел. ГИТТЛ, 1954.
- Кузнецов Г. И.* и др. Исследование проявлений горного давления на моделях. Гостехиздат, 1951.
- Кузнецов Г. И.* и др. Моделирование проявлений горного давления. Л., изд-во «Недра», 1968.
- Кузьмин В. А., Пил В. П.* Скорость роста крупки трещины в стекле и каолине. — Сб. «Некоторые проблемы прочности твердого тела». Изд-во АН СССР, 1959.
- Курок В. Т.* Принципы алгоритмизации и построения управляющих машин. Киев, Гостехиздат УССР, 1963.
- Кусерский Ф. И., Дрыковский М. Ф., Гаек Ю. В.* Короткозамедленное варяние на катках. Гостехиздат, 1962.
- Лавриш В. А., Мамбетов Ш. А.* Скорость развития трещин в образцах горных пород. — Прикладная математика и техническая физика, 1965, № 6.
- Ландау Л. Д., Лисниц Е. М.* Механика сплошных сред. Гостехиздат, 1962.
- Леонев М. Я., Панисюк В. В.* — Прикладная механика, 1959, 5, № 4, 391.
- Леонев М. Я., Панисюк В. В.* — Докл. АН УССР, 1961, 2, 165.
- Лурт Н., Вилл Х. Л.* Хрупкое разрушение и течение текучести. — Сб. «Атомная механика разрушения». Металлургия, 1963.
- Максимова Е. И.* Моделирование процесса взрывного разрушения. — Сб. «Вопросы горного дела». Углетехиздат, 1958.
- Мачинский М. В.* Теория расчета заряда. — Сб. «Взрывное дело». ОНТИ, 1936, № 26, 27.
- Мельников Н. В., Марченко Л. Д.* Рациональная конструкция заряда как метод увеличения полезной работы взрыва. — Горный журнал, 1963, № 4.
- Мельников Н. В., Марченко Л. Д.* Конструкции заряда и апертуры взрыва. Изд-во «Недра», 1965.
- Мельников Н. В., Марченко Л. Д., Кудряшов В. С.* Методы повышения коэффициента полезного использования энергии взрыва. Изд. ЦД АН СССР, 1960.
- Морова В. Е.* Математическое моделирование в научном познании. Изд-во «Мысль», 1969.
- Мосинц В. П.* Энергетические и корреляционные связи процесса разрушения пород взрывом. Фрунзе, Изд-во АН КиргССР, 1969.
- Москальский И. П.* О моделировании первой основной задачи плоской теории упругости для многосвязных областей. — Прикладная математика и механика, 1955, 19, № 3.
- Мушкетер И. П.* Некоторые основные задачи теории упругости. Изд-во «Наука», 1966.
- Надан А.* Пластичность и разрушение твердых тел. ИЛ, 1954.
- Назаров Г. А.* О механическом подобии твердых деформируемых тел (к теории моделирования). Ереван, Изд-во АН АрмССР, 1965.
- Назаров И. П.* Производственный эксперимент и его роль в познании. Соц-эктн, 1962.
- Наседкин И. А.* Термодинамическая теория подобия и ее приложения к моделированию почв и грунтов. Автореф. канд. дисс. М., МГУ, 1939.
- Насонов И. Д.* Моделирование горных процессов. Изд-во «Недра», 1969.

- Нестеркин Ю. Е., Соловьев Р. И.** Методы скоростных измерений в галлодинамике и физике плазмы. Изд-во «Наука», 1967.
- Никольс Г. Р., Демаль В. П.** Влияние акустической жесткости на волны напряжений, образование парового и горючей породе. — Сб. «Механика горных пород». Изд-во «Недра», 1966.
- Осипов В. Г., Дробышев Е. К., Ушаков Е. В.** Микромеханизм разрушения Сб. «Пластическая деформация металлов». Изд-во «Наука», 1964.
- Павлов В. А., Якубович М. В.** Природа вязкого разрушения металлов. — Докл. АН СССР, 1951, 77, № 1.
- Павловский Н. П.** Теория движения грунтовых вод под гидротехническими сооружениями и ее основные приложения. М. — Изд., 1922.
- Падурков В. А., Антипенко В. А.** О подобии при моделировании действия варьера. Тезисы докладов и сообщений на научно-техническом совещании по бурно-варьерным работам. Сборник 3, М., Изд. ИГД им. А. А. Скочинского, 1965.
- Панасюк В. В.** — Докл. АН СССР, 1960, 9, 1185—1189.
- Панасюк В. В.** Предельное равновесие хрупких тел с трещинами. Киев, изд-во «Наукова думка», 1968.
- Петрахов Г. П.** О моделировании процессов распространения сейсмических волн. — Сб. «Вопросы динамической теории распространения сейсмических волн». Изд-во ИГУ, 1964, вып. 7.
- Покровский Г. П.** Варьер. Изд-во «Недра», 1967.
- Покровский Г. П., Федоров Н. С.** Действие удара и варьера в деформируемых средах. М., Промстройиздат, 1957.
- Покровский Г. П., Федоров Н. С.** Центробежное моделирование в горном деле. Изд-во «Недра», 1969.
- Подмарев Г. Л.** Моделирование. Воен. издат, 1963.
- Пузьев Г. Е.** и др. Электрическое моделирование задач строительной механики. Киев, Изд-во АН СССР, 1963.
- Пушкова Я. М., Давыдов В. С., Бетандурские В. К.** К вопросу трещинообразования в прочной среде при варьере. Труды V сессии Ученого совета по народнохозяйственному использованию варьера. Фрунзе, изд-во «Илим», 1965.
- Райнгарт Д. С.** Действие полей напряжений в горных породах. Сб. «Механика горных пород». Изд-во «Недра», 1966.
- Райнгарт Дж. С., Нирсон Дж.** Поведение металлов при импульсных нагрузках. ИЛ, 1958.
- Раздатовский Х. А., Демаль В. П.** Упрочность при интенсивных кратковременных нагрузках. Фрунзе, 1961.
- Резель В. Р.** К вопросу о законе роста трещины в процессе разрушения твердых тел. — Журнал технической физики, 1956, 26.
- Рудников В. П.** К вопросу о изменении эффективности удара в твердой среде. М., В. Д. ИГД АН СССР им. А. А. Скочинского, 1962.
- Рудников В. П.** О значении кривых соотношений в исследовании механического действия варьера в твердой среде. М., Изд. ИГД им. А. А. Скочинского, 1969.
- Росси В. Д.** Константы вариационных полей для горной промышленности. Углетехиздат, 1961.
- Седов Л. Д.** и др. Оценка вариационных свойств ВВ методом подводного варьера. — Сб. «Разрушение и механика горных пород». Госгортехиздат, 1962.
- Седов Л. Д.** Методы подобия и размерности в механике. Изд-во «Наука», 1965.

- Смирнов В. В.* Метод измерения скорости развития трещины в образцах горных пород при ударном нагружении. — Физико-технические проблемы разработки полезных ископаемых, 1967, № 4.
- Соболев Н. Д.* О природе начального разрушения. — Журнал технической физики, 1957, XXVII, вып. 10.
- Сорокин В. Т.* Методика моделирования действия варива в эквивалентных материалах. Автореф. канд. дисс. М., МГУ, 1958.
- Сорокин В. Т.* Моделирование действия варива в эквивалентных материалах. Изд. МГУ, 1959.
- Суханов А. Ф.* Предпосылки теории дробления пород варивом. — Сб. «Вопросы теории разрушения горных пород действием варива». Изд-во АН СССР, 1968.
- Тетсатовиди И. М.* Электрическое моделирование. Физматгиз, 1959.
- Уралов В. С.* Моделирование действия варива при разрушении горных пород. М., Изд. ИГД им. А. А. Скочинского, 1964.
- Успехи научной фотографии. М. — Л., Изд-во АН СССР, 1957.
- Федерман А. О.* О некоторых общих методах интегрирования уравнений с частными производными первого порядка. Разд. 9, СИБ., — Изв. СИБ. Политехнического института, 1944, 16, вып. 1.
- «Физическая акустика», т. III, ч. Б. Динамика решетки. Под редакцией У. Малона. Изд-во «Мир», 1968.
- Филиппов В. К.* Направление распространения трещины, образующихся при разрушении крепких пород варивом. — Сб. «Варивное дело, № 47/4». Гостехиздат, 1961.
- Финк К. и Рорбинг А.* Измерение напряжений и деформаций. Машиизд, 1961.
- Френкель И. И.* Теория обратных и необратимых трещин в твердых телах. — Журнал технической физики, 1952, 22.
- Фришман И. Б.* Единая теория прочности металлов. Оборонгиз, 1952.
- Хануков А. И.* Энергия волн напряжения при разрушении пород варивом. Гостехиздат, 1962.
- Хануков А. И., Баранов Е. Г., Мостниц В. И.* Экспериментальные исследования процесса разрушения пород варивом. Фрунзе, Изд-во АН Киргизской ССР, 1961.
- Хестин Г. Л.* Рациональные оптические активные материалы поляризации-оптического метода исследования напряжений. — Изв. высшей школы, Машиностроение, 1958, вып. 4.
- Чубаров С. И.* Изучение распространения сейсмических волн методом моделирования. Автореф. канд. дисс. М., Изд. МГУ, 1954.
- Чудакос А. Д.* Электрические моделирующие сетки и их применение. Изд-во «Энергия», 1968.
- Шардин Х.* Исследование скорости разрушения. — Сб. «Атомный механизм разрушения». Металлургия, 1963.
- Шкляков Е. М.* О едином механизме разрушения и единой (нормальной) прочности металлов. — Журнал технической физики, 1952, 22, вып. 10.
- Штофц В. А.* О роли моделей в познании. Изд-во МГУ, 1962.
- Иколев Б. С.* Гидродинамика варива. М., Судпромиздат, 1961.
- Якутович М. В.* Теория пластической деформации. Металлургия, 1961.
- Benbow J. J., Roessler F. C.* Experiments on Controlled Fractures. — Proc. Phys. Soc., 1957, 70.
- Berry J. M.* Fracture Process in Polymeric Materials. — J. Polymer Sci., 1958, 50.

- Bertrand I.** Note sur la similitude en mécanique.-- J. Ecole polytechn., 1848, cahier 32.
- Birkman J. J.** The Criterion of Fracture.-- SPE Trans., 1964, 4, N 4.
- Broberg K. B.** The Propagation of a Brittle Crack.-- Arkiv fys., 1960, 18.
- Broberg K. B.** On the Speed of a Brittle Crack.-- Trans. ASME, 1964, N 3.
- Buckingham I.** On Physically similar Systems. Illustrations of the Use of Dimensional Equations.-- Phys. Rev., 1914, ser. 4, 4.
- Bucky P. B., Taborli R. V.** Effect of Immediate Roof Thickness in Longwall Mining as Determined by Barodynamic Experiment. -- Trans. Amer. Inst. Mining and Metall. Engrs. Coal Div., 1938, 130.
- Clark A. B. J., Irwin G. R.** Crack Propagation Behaviours. -- Exper. Mech., 1966, N 6.
- Cloutier G. J.** Crushable Materials Energy Absorbers at Very High Impact Velocities. -- J. Spacecraft and Rockets, 3, 1966, N 4.
- Cotterell B.** Velocity Effects in Fracture Propagation. -- Appl. Mater. Res., 1965, 4, N 4.
- Craggs J. W.** Fracture of Solids. N. Y., 1962.
- Fayol H.** Notes sur les mouvements de terrain provoques par l'exploitation des mines.-- Bull. Soc. Industr. Min., 1885.
- Fosse C.** Etude de la pression de choc produite par un explosif dans un matière solide.-- Explosifs, 1968, 21, N 4.
- Griffith A. A.** The Phenomenon of Rupture and Flow in Solids. -- Philos. Trans. Roy. Soc., 1920, A221.
- Griffith A. A.** Theory of Rupture. -- Proc. First Internat. Congr. Appl. Mech. Delhi, 1924.
- Griffith J. E., Baldwin W. M.** Failure Theories for Generally Orthotropic Materials. -- Development Theory and Applied Mechanics, 1. N. Y., Plenum Press, 1963.
- Gurney H. C.** The Study of Cracks.-- Mining Engr., 1966, N 67.
- Harris C. C.** On the Role of Energy in Communication: a Review of Physical and Mathematical Principles.-- Trans. Inst. Mining Metallurgy, March Marsh 1966, 675.
- Hapkinson B. A.** A Method of Measuring the Pressure Produced in the Detonation of High Explosives or by Impact of Bullets.-- Philos. Trans. Roy. Soc., 1914 A213.
- Inglis C. E.** Stresses in a Plate due to the Presence of Cracks and Sharp Corners.-- Trans. Inst. Naval Architects, 1913, 55.
- Irwin G. R.** Fracture of Metals. Cleveland, ASM, 1948.
- Jaeger J. C.** Fracture. Melbourne, 1965.
- Kerkhof F.** Analyse des sprüden Zugbrüches von Gläsern mittels Ultraschall.-- Naturwissenschaften, 1953, 40.
- Kerkhof F.** Proc. 3-rd Internat. Congr. High-Speed Photography, London, 1953, 194.
- Krafft, J. M., Irwin G. R.** Crack-Velocity Considerations. -- Fracture Toughness Testing and Applications. Philadelphia, Pan Amer. Soc. Test. and Mater., 1965.
- Kromm B.** Zur Ausbreitung von Stosswellen in Kreislochscheiben.-- Z. angew. Math., 1948, 28, N 4.
- Miller M. H.** The Effect of Stresses Wave Duration on Brittle Fracture. -- Internat. J. Rock Mech. and Mining Sci., 1966, N 3, 3.
- Mott N. F.** Fracture of Metals; Theoretical Considerations.-- Engineering, 1948, 165.

- Drowan O. E.* Fatigue and Fracture of Metals. N. Y., Wiley, 1950.
- Rinchart J. S.* On Fractures Caused by Explosions and Impacts.— *Quart. Colorado School Mines*, 1960, 55, N 4.
- Sack R. A.* Extension of Griffith's Theory of Rupture to Three Dimensions.— *Proc. Phys. Soc.*, 1946, 58.
- Schardin H., Struth W.* Neuere Ergebnisse der Funkenkinematographie.— *Z. techn. Phys.*, 1937, 18.
- Selberg H. J.* Transient compression waves from spherical and cylindrical cavities.— *Arkiv-fys.*, 1952, 5, N 7.
- Smekal A.* Technische Festigkeit und molekulare Festigkeit.— *Naturwissenschaften*, 10, 1922.
- Vadovic F.* Fenomenologicka hypotese pevnosti.— *Sbornik vedeckych prací Stroiniky fakulty Slovenskej vysoke školy technickej*, Bratislava, 1963, 3.
- Weiss V., Yukawa S.* Critical Appraisal of Fracture Mechanics.— *Fracture Toughness Testing and Applications*, Philadelphia, Pan Amer. Soc. Test. and Mater., 1965.
- Wolf K.* Zur Bruchtheories von A. Griffith. — *Z. angew. Math. und Mech.*, 1923, 3.